AD_____

Award Number: DAMD17-00-1-0546

TITLE: Statistical Methods for Analysis of NF Clinical Data

PRINCIPAL INVESTIGATOR: Harry Joe, Ph.D.

CONTRACTING ORGANIZATION: The University of British Columbia
Vancouver, BC, Canada V6T 1Z3

REPORT DATE: August 2004

TYPE OF REPORT: Final

PREPARED FOR: U.S. Army Medical Research and Materiel Command
Fort Detrick, Maryland 21702-5012

REPORT DOCUMENTATION PAGE

Form Approved
OMB No. 074-0188

1. AGENCY USE ONLY (Leave blank)	2. REPORT DATE	3. REPORT TYPE AND DATES COVERED
	August 2004	Final (1 Aug 00 - 31 Jul 04)

4. TITLE AND SUBTITLE
Statistical Methods for Analysis of NF Clinical Data

5. FUNDING NUMBERS
DAMD17-00-1-0546

6. AUTHOR(S)
Harry Joe, Ph.D.

7. PERFORMING ORGANIZATION NAME(S) AND ADDRESS(ES)
The University of British Columbia
Vancouver, BC, Canada V6T 1Z3

E-Mail: harry@stat.ubc.ca

8. PERFORMING ORGANIZATION REPORT NUMBER

9. SPONSORING / MONITORING AGENCY NAME(S) AND ADDRESS(ES)
U.S. Army Medical Research and Materiel Command
Fort Detrick, Maryland 21702-5012

10. SPONSORING / MONITORING AGENCY REPORT NUMBER

11. SUPPLEMENTARY NOTES

12a. DISTRIBUTION / AVAILABILITY STATEMENT
Approved for Public Release; Distribution Unlimited

12b. DISTRIBUTION CODE

13. ABSTRACT (Maximum 200 Words)

This project describes research in statistical methods that has been useful for statistical modelling and analysis of clinical data from NF1 and NF2 subjects. The statistical methods are classified into the areas:
(a) estimation of familial correlation for different types of data,
(b) assessment of multi-hit mutation models for incidence of tumours.

Accomplishing the project required development of some new statistical theory, as well as non-trivial computer programming to implement the new and existing theory. One new statistical inference method for familial data is composite likelihood. This method is intended in general for situations in which a multivariate probability is too time consuming to compute because of numerical integrations; for the NF data, this situation occurred when the family size exceeded 4 to 6 (the lower bound on family size depends on the actual multivariate probability).

Clinical data exist in many formats including binary, categorical, count, and continuous information. Also common are censored data (e.g., only a lower bound is known for some measurements). One goal of the project was the creation of a software package for familial data analysis for different types of data, such as binary, count, and right-censored survival data. The modules based on composite likelihood were the most recent additions to the package.

14. SUBJECT TERMS
Familial associations, genotype-phenotype correlation, multi-hit mutation models

15. NUMBER OF PAGES
175

16. PRICE CODE

17. SECURITY CLASSIFICATION OF REPORT	18. SECURITY CLASSIFICATION OF THIS PAGE	19. SECURITY CLASSIFICATION OF ABSTRACT	20. LIMITATION OF ABSTRACT
Unclassified	Unclassified	Unclassified	Unlimited

Table of Contents

STATISTICAL METHODS FOR ANALYSIS OF NF CLINICAL DATA

INTRODUCTION

This project describes research in statistical methods that has been useful for statistical modeling and analysis of clinical data from NF1 and NF2 subjects. The statistical methods are classified into the areas:
(a) estimation of familial correlation for different types of data,
(b) assessment of multi-hit mutation models for incidence of tumours.

Accomplishing the project required development of some new statistical theory, as well as non-trivial computer programming to implement the new and existing theory.

One new statistical inference method for familial data is composite likelihood. This method is intended in general for situations in which a multivariate probability is too time consuming to compute because of numerical integrations; for the NF data, this situation occurred when the family size exceeded 4 to 6 (the lower bound on family size depends on the actual multivariate probability).

Clinical data exist in many formats including binary, categorical, count, and continuous information. Also common are censored data (e.g., only a lower bound is known for some measurements). One goal of the project was the creation of a software package for familial data analysis for different types of data, such as binary, count, and right-censored survival data. The modules based on composite likelihood were the most recent additions to the package.

BODY

Purpose of the project:

(A) To develop statistical methods that can be used to characterize the phenotype of individuals with NF1 and NF2.

(B) To develop methods to elaborate on the standard two-hit model of tumour formation taking into account additional pathogenic factors and allelic differences for tumours in NF1 and NF2.

Research Accomplishments:

The research accomplishments associated with each objective from the statement of work are summarized below.

Objective 1. Develop statistical methods for interval-censored data, and obtain estimates of age of onset distributions for NF1 and NF2 features, using longitudinal information in the databases.

This objective is being postponed as we currently do not have enough longitudinal information in the databases.

Objective 2. Develop statistical methods for familial correlations for non-continuous and censored data, and obtain estimates of intraclass and interclass correlations for quantitative and binary traits in NF1 and NF2.

The aims, as outlined in the initial grant proposal, have now been mostly completed with the completion of Yinshan Zhao's thesis (*ftp.stat.ubc.ca:pub/hjoe/zhao/zhao04_phd.pdf*) plus two submitted papers to statistics journals. A third, more applied paper, will be completed soon.

Estimation of familial correlations in clinical traits is related to the assessment of familial aggregation in genetic diseases. It is important to our understanding of the causes of variable expressivity in Mendelian diseases.

We give a short overview of Zhao's thesis. This work involves the theory for various estimating equation approaches that should lead to more reasonable computing time for estimating familial associations for traits in the form of right-censored survival, binary or count data. An example of a count variable is the number of tumors of a particular type; an example of a right-censored survival variable is the age of onset of a particular disease feature - those who do not have the feature are right-censored at the age of last clinical observation.

For most of the multivariate models for familial data, such as those with a latent multivariate normal distribution, the maximum likelihood approach is not computationally tractable when high-dimensional numerical integration is involved. It was necessary to develop other estimating approaches which are computationally less demanding, and relatively efficient (in the sense of variance of the sampling distribution of the estimator). Estimation using two types of composite likelihood equations were considered; these are based on the likelihoods of the univariate and bivariate margins of the multivariate model. These methods were shown to perform well for a number of multivariate models useful for familial data.

Other work done by Lisa Kuramoto, a research assistant, is summarized next.

Genotype-phenotype analyses, accounting for the familial associations, were done for some count variables in the NF2 database; count variables included the number of spinal tumors, number of meningiomas, and number of cutaneous schwannomas for NF2 patients (please see Baser ME, Kuramoto L, Joe H, *et al*, 2004). Further analysis of several NF2 phenotypes involved making subgroups for the genotype of a splice-site mutation; the splice site was split into one of exon 1-5, exon 6-10 and exon 11-15. The analyses suggest severity of disease depended on splice site location. Some conclusions are:

(a) subjects in the exon 1 to 5 category seem to have a higher prevalence and number of meningiomas than subjects in the other splice site mutation categories.
(b) subjects in the exon 11 to 15 category seem to have a higher age at onset than the other splice site mutation categories.

Currently, a manuscript is being written with the analyses.

Research by graduate student, Tracy Tucker, concludes work related to objective 2 with a clinical application to an NF1 problem: Some NF1 patients appear to have a greater risk than others for developing malignant peripheral nerve sheath tumors (MPNST). Tucker tested the hypothesis that MPNSTs are associated with the presence of both subcutaneous neurofibromas and internal neurofibromas in NF1 patients, but are not associated with cutaneous neurofibromas. Logistic regressive modeling and survival analysis curves of censored longitudinal quantitative and semi-quantitative data appeared to support the hypothesis and indicated the need for a longitudinal study of MPNST. (Manuscript in preparation).

Objective 3. Fit multi-hit mutation models for the incidence of NF2 and NF1 tumours by age, distinguish whether a two-hit or three-hit model provides a better fit to the data, and adapt the models to account for mutation type and other factors.

Two- and three-hit models of vestibular schwannomas were fit to data for NF2 subjects; this was published in Genetic Epidemiology [Woods et al 2003]. With the latest NF2 database with more data on mutation type, we considered the strength of the genotype-phenotype correlations when fitting the two-hit and three-hit models for vestibular schwanomas separately for several mutation types.

The analysis suggests that the age of onset of the first vestibular schwannoma is smaller for truncating mutations (nonsense and frameshift) than the other classes such as splice site, missense, large deletions.

For the fitted 2-hit model, the comparison of truncating mutations versus others suggested a common mutation rate but higher cell growth and death rates for the truncating mutation class. This interpretation depends on having the right order of magnitude for the number of Schwann cell precursors. The initial check has been done and final verification is ongoing now. A manuscript has been prepared for submission pending these final results.

Objective 4. Write C code to implement all of these statistical methods and provide a user-friendly interface for the code.

Software written in C and perl, is being developed in Unix/Linux; it runs also in Windows with Cygnus/Gnuwin [see www.cygwin.com], the public domain version of Unix for Windows. The implementation of the interface currently is through control files which specifies parameters and data files.

The modules included in the package are:
a) for binary response data, maximum likelihood estimation for the multivariate probit and logit models, and composite likelihood estimation methods for the multivariate probit model
b) for count data, maximum likelihood estimation for exchangeable correlation form and composite likelihood estimation for the general dependence form of the multivariate Poisson-lognormal model, and maximum likelihood estimation for the gamma mixture of negative binomial model
c) for continuous data, maximum likelihood estimation for the multivariate normal model
d) for right-censored continuous data, maximum likelihood estimation and composite likelihood estimation for the multivariate normal model

The latest modules are based the estimation methods from Zhao's PhD thesis research. In addition, there is code that can be used to generate codes for different relation classes (e.g, sib-sib, mother-offspring, father-offspring, parent-offsprint, degree 2, degree 3 etc). The estimation modules essentially then estimate a different correlation

parameter for different relation classes. By comparing the correlation estimates for the different relation classes, one can get some ideas of the genetic factors influencing the strength of familial association. The package has been designed in such a way that modules can be easily added for different models. For example, we are considering the multivariate normal copula model with negative binomial margins for familial count data, and the multivariate normal copula model with Weibull margins for familial onset-time censored data.

The final details were completed by programmer Hongbin Zhang who integrated and modularized the code for different multivariate models that were written by Lisa Kuramoto, Yinshan Zhao and me. Specific modules of the package were used in the several of the previous publications that came out of this grant.

The latest version of the software package will be put in the directory ftp://ftp.stat.ubc.ca/pub/hjoe/famil/

The software package will be referred to in updates of the recently submitted papers for this project.

The summary according to the proposed timeline of work is given below.

0-12 months :
- development of statistical theory for the simpler cases,
- coding into C programs and use on current NF1/NF2 databases

12-24 months :
- extension of theory to cover more general situations
- continuation of coding and data analysis
- presentation of preliminary results in technical papers and conferences

24-36 months :
- writing more general publications,
- conversion of C code to a form with friendlier input instructions, so that a non-computer programmer can use the computer programs.

The theory has been developed for objectives 2 and 3. The coding into C programs and use on current NF1/NF2 databases has been completed for the statistical methods, and implemented in an organized way into the software package. Ten manuscripts have been published or accepted for publication, three others have been submitted, and four more are in draft. A total of fourteen presentations were made, or will be made, at the 2000-2004 meetings of the American Society of Human Genetics, the 2003 and 2004

NNFF International Consortium for the Molecular Biology of NFI and NF2, in Aspen, Colorado, and the 2003 European Neurofibromatosis meeting, in Turku, Finland.

We fell one year behind the original schedule because of the theory in the PhD research; in advance it is hard to predict how quickly PhD students can accomplish things, thus the 2003-2004 year was a no-cost extension.

KEY RESEARCH ACCOMPLISHMENTS

- Comparison of two- and three-hit models for onset time of vestibular schwannomas for NF2 subjects.

- Development of new statistical theory and new multivariate models for analysis of NF1 and NF2 phenotype data that are discrete or censored.

- Completion of a software package for analysis of familial data of various types (binary, count, continuous, censored). The software written in the C programming languages, developed in Unix/Linux, runs also in Windows with Cygnus/Gnuwin (public domain version of Unix for Windows).

REPORTABLE OUTCOMES

Published Papers

Baser ME, Friedman JM, Aeschliman D, Joe H, Wallace AJ, Ramsden RT, Evans DG
Predictors of the risk of mortality in neurofibromatosis 2.
Am J Hum Genet. 71(4):715-23, 2002

Baser ME, Friedman JM, Wallace AJ, Ramsden RT, Joe H, Evans DG
Evaluation of clinical diagnostic criteria for neurofibromatosis 2.
Neurology 59: 1759-1765, 2002

Baser ME, Joe H, Kuramoto L, Friedman JM, Wallace AJ, Ramsden RT, Evans DGR
Genotype-phenotype correlations for cataracts in neurofibromatosis 2.
J Med Genet, 40, 758-760, 2003.

Baser ME, Kuramoto L, Joe H, Friedman JM, Wallace AJ, Gillespie JE, Ramsden RT, Evans DGR.
Genotype-phenotype correlations for nervous system tumors in neurofibromatosis 2: a population-based study,
Am J Hum Genet, 75, 231-240, 2004.

Castle B, Baser ME, Huson SM, Cooper DN, Upadhyaya M.
Evaluation of genotype-phenotype correlations in neurofibromatosis type 1
J Med Genet 40(10): 109e.

Mautner VF, Baser ME, Thakkar SD, Feigen UM, Friedman JM, Kluwe L.
Vestibular Schwannoma growth in patients with neurofibromatosis type 2: a longitudinal study.
J Neurosurg. 96(2):223-8, 2002

Palmer V, Szudek J, Joe H, Riccardi VM, and Friedman JM (2004).
Analysis of neurofibromatosis 1 (nf1) lesions by body segment
Am J Med Genet, 125A, 157-161, 2004

Szudek J, Joe H, Friedman JM.
Analysis of intrafamilial phenotypic variation in neurofibromatosis 1 (NF1).
Genet Epidemiol. 23(2):150-64, 2002.

Woods R, Friedman JM, Evans DG, Baser ME, Joe H
Exploring the "two-hit hypothesis" in NF2: tests of two-hit and three-hit models of vestibular schwannoma development.
Genet Epidemiol. 24(4):265-72, 2003.

Zhao Y, Kumar RA, Baser ME, Evans DG, Wallace A, Kluwe L, Mautner VF, Parry DM, Rouleau GA, Joe H, Friedman JM.
Intrafamilial correlation of clinical manifestations in neurofibromatosis 2 (NF2).
Genet Epidemiol. 23(3):245-59, 2002.

Papers submitted

Joe H and Latif AHMM (2004).
Computations for the familial analysis of binary traits
Submitted to *Computational Statistics.*

Zhao Y and Joe H (2004). Composite likelihood estimation in familial data analysis.
Submitted to *Canadian Journal of Statistics.*

Zhao Y and Joe H (2004). Inferences for odds ratio with dependent pairs.
Submitted to *Biometrika.*

Abstracts and Presentations: Aug 1, 2003 and later

Baser ME, Patankar T, Kluwe L, Mautner V-F, Makariou E, Parry DM,. Wallace AJ, Ramsden RT, Evans DGR, Jackson A.
Longitudinal vestibular schwannoma growth rates in people with neurofibromatosis 2 (NF2): a combined analysis of NF2 patients from three countries.
(Accepted for presentation: American Society of Human Genetics, 54th Annual Meeting, Toronto, October, 2004)

Baser ME, Friedman JM, Joe H, Evans DGR
The epidemiology of neurofibromatosis 2 (NF2).
(Presentation at the NNFF International Consortium For The Molecular Biology of NF1, NF2 and Schwannomanotsis, Aspen, Colorado, May 2004)

Lee, Bernard TK, Friedman JM
Phylogenetic Footprinting of the NF1 5 Upstream Region (5UR).
Am J Hum Genet 73 (Suppl):997, 2003.
(Presented, 53rd Annual Meeting, American Society of Human Genetics, November 2003, Los Angeles).

Ramsden RT, Evans DGR, Wallace AJ, Joe H, Baser ME.
Revised diagnostic criteria for neurofibromatosis 2.
Am J Hum Genet 73 (Suppl):593, 2003.
(Presented, 53rd Annual Meeting, American Society of Human Genetics, November 2003, Los Angeles).

Tucker T, Wolkenstein P, Friedman JM.
Association Between the Occurrence of Malignant Peripheral Nerve Sheath Tumours and Subcutaneous and Internal Neurofibromas in NF1
(Presentation to 10th European Neurofibromatosis Meeting, Turku, Finland, August 2003)

Zhao Y.
Composite Likelihood Estimation in Familial Data Analysis
(Presentation to Biometrics (WNAR) meeting in Albuquerque, New Mexico: June 26-June 30, 2004).

Abstracts and Presentations Prior to Aug 1, 2003
(Full details in the August 2001, 2002 and 2003 Annual Reports)

Baser ME, Woods R, Joe H, Kuramoto L, Friedman JM, Wallace AJ, Bijlsma E, Olschwang S, Papi L, Parry DM, Ramsden RT, Rouleau GA, Evans DGR. The location of constitutional neurofibromatosis 2 (*NF2*) splice-site mutations is associated with the number of intracranial meningiomas: results from an international NF2 database. (Presented at the NNFF International Consortium for the Molecular Biology of NF1 and NF2, 1-4 June 2003, Aspen CO).

Baser ME, Joe H, Kuramoto L, Friedman JM, Wallace AJ, Ramsden RT, Evans DGR. Genotype-phenotype correlations for cataracts in neurofibromatosis 2. (Presented at the NNFF International Consortium for the Molecular Biology of NF1 and NF2, 1-4 June 2003, Aspen CO).

Baser ME, Parry DM, Joe H, Kuramoto L, Friedman JM, Gillespie JE, Wallace AJ, Ramsden RT, Evans DGR. Genotype-phenotype correlations for spinal tumors in neurofibromatosis 2.
(Presented at the NNFF International Consortium for the Molecular Biology of NF1 and NF2, 1-4 June 2003, Aspen CO).

Baser ME, Joe H, Kuramoto L, Friedman JM, Gillespie JE, Wallace AJ, Ramsden RT, Evans DGR.
Genotype-phenotype correlations for peripheral nerve tumors in neurofibromatosis 2.
(Presented at the NNFF International Consortium for the Molecular Biology of NF1 and NF2, 1-4 June 2003, Aspen CO).

Baser ME, Friedman JM, Joe H, Wallace AJ, Ramsden RT, Evans DGR.
Genotype-phenotype correlations for presenile cataracts in neurofibromatosis 2.
Am J Hum Genet 71 (Suppl):428, 2002.
(Presented at the American Society of Human Genetics 52nd Annual Meeting, 2002 October 15-19, Baltimore).

Palmer C, Szudek C, Joe H, Riccardi VM, Friedman JM.
The development of cutaneous neurofibromas is influenced by familial and local factors in patients with Neurofibromatosis 1 (NF1).
Am J Hum Genet 67 (Suppl):677, 2000.
(Presented at the American Society of Human Genetics 50th Meeting, Philadelphia, October, 2000)

Szudek J,Joe H, J.M. Friedman JM.
Familial aggregation of neurofibromatosis 1 (NF1) clinical features.
Am J Hum Genet 67 (Suppl):1137, 2000.
(Presented at the American Society of Human Genetics 50th Meeting, Philadelphia, October, 2000)

Tzenova J, Joe H, Riccardi VM, Friedman JM. The effect of parental age on the occurrence of neurofibromatosis 1.
Am J Hum Genet 69 (Suppl):393, 2001.
(Presented at the American Society of Human Genetics 51st Annual Meeting, San Diego, October 2001).

Zhao Y, Kumar RA, Baser ME, Evans DGR, Wallace A, Rouleau GA, Mautner VF, Kluwe L, Joe H, Friedman JM. Allele class-independent intrafamilial correlation of age at onset, age at hearing loss and number of intracranial meningiomas in neurofibromatosis 2 (NF2).
Am J Hum Genet 69(Suppl):420, 2001.
(Presented at the American Society of Human Genetics 51st Annual Meeting, San Diego, October 2001).

Degrees Supported in Whole or Part by this Award.

Zhao, Yinshan (2004). Statistical modelling and inference for discrete and censored familial data. PhD thesis, Department of Statistics, University of British Columbia. [Defense in February 2004, submitted to University in March 2004, available at ftp.stat.ubc.ca:pub/hjoe/zhao/zhao04_phd.pdf]

Lee, Bernard (2003). Phylogenetic Footprinting of the NF1 5 Upstream Region (5UR). MSc thesis, Department of Medical Genetics, University of British Columbia,
(Please see details in 2003 annual report)

Aeschliman, Dana (2001). Survival Times of NF2 Patients. MSc thesis, Department of Statistics, University of British Columbia
(Please see details in 2002 annual report.)

Szudek, Jacek. (2001). Analysis of variable expressivity in neurofibromatosis 1. Ph.D. thesis, Department of Medical Genetics, University of British Columbia,
(Please see details in 2001 annual report)

Latif, A. H. Md. M. (2001). A comparison of methods for multivariate binary response with simulation studies. MSc thesis, Department of Statistics, University of British Columbia,
(Please see details in 2001 annual report)

Woods, Ryan. (2000). Models for the development of tumours in neurofibromatosis 2. MSc thesis, Department of Statistics, University of British Columbia, August 2000.
(Please see details in 2001 annual report)

Thesis in Progress:
Tucker, Tracy (PhD candidate). Neurofibroma formation mechanisms in NF1. Department of Medical Genetics, University of British Columbia.
(Please see this report for details of some of her work).

CONCLUSIONS

The goals of this project were to develop statistical methods that can be used to characterize the complex phenotypes of NF1 and NF2 and to model the mechanisms of tumor formation.

We have successfully developed new methods to handle various data types, including phenotypic data (of various formats such as binary or censored), genetic data, and data for individuals and families. The methods have been rigorously tested mathematically and software has been developed to make the methods generally available to other researchers.

Beyond the development of new statistical techniques, is their clinical application. Working in conjunction with genetic epidemiologists and clinicians in British Columbia, California, and the UK, we have had access to clinical data for both modeling and testing. For example, by incorporating techniques for handling survival data into a random effects model and using a mixture model for count data, we have been able to estimate intra-familial correlations in continuous variables such as age at onset of hearing loss (right censored), and number of intra-cranial meningiomas in NF2 (Zhao et al, 2002). Refining these calculations by taking into account the nature of the mutation, these statistical methods allow clinicians to make individual and familial predictions which are useful in genetic counselling. Further, the findings of such clinical studies may ultimately lead to an understanding of the mechanism whereby genetic mutations cause the various symptoms of NF1 or NF2

Genotype-phenotype correlations are also useful in genetic counselling or in identifying particularly high or low risk individuals for screening decisions. We have demonstrated such techniques in NF1 and NF2. For example, in Baser, Kuramato, Joe et al, 2003, we use a multivariate probit model to examine the relative risk of cataract formation. Similar methods have demonstrated that intracranial meningiomas, spinal tumors, and peripheral nerve sheath tumours are also influenced by the type of NF2 mutation.

We have also contributed to the understanding of the pathogenetics of tumour formation by modeling tumor development in vestibular schwannomas (Woods et al 2003): A traditional model for tumor formation, the two-hit model, suggest that two mutations are necessary before a tumor forms. In genetic conditions such as NF1 or NF2, where affected people are born with one mutation in a tumor suppressor gene, the two-hit model suggests that one additional mutation may be sufficient for tumor formation. We developed various models to test this hypothesis in vestibular schwannoma development in people with NF2. By fitting models to NF2 patient data, we were able to show that a three-hit model may well provide a better solution. These techniques can in future be applied to other tumours such as meningiomas.

Our work with NF1 (for example, Szudek et al, 2002) has enabled us to make predictions regarding the genetic cause of many of the features of this complex disorder. While controlling for gender and age we were able to look for patterns of associations. We examined familial aggregation for a number of symptoms in different classes of relatives (e.g., parent-child, siblings, second degree relatives). Our analyses indicate that some of the symptoms appear to be influenced by functional polymorphisms of the normal *NF1* allele whereas others are influenced by modifying genes, and others by the abnormal *NF1* gene itself. More than one genetic mechanism may well be influencing the phenotype simultaneously, and studies with larger families, with more uniformly collected data and in more diverse populations would help to clarify these mechanisms. Molecular genetic techniques, using SNPs or other methods, could be used in combination with these statistical methods to facilitate the identification of such putative modifying loci.

The methods we have developed and refined are useful for other genetic conditions, particularly where there is a complex phenotype or no obvious genotype-phenotype correlation. We have contributed openly available, well-documented code which will be useful to other statisticians and genetic epidemiologists who are interested in learning about the pathogenesis of inherited genetic disorders. Further, we have contributed a body of new publications characterizing the phenotypes of both NF1 and NF2.

APPENDIX 1

Abstracts accepted or presented after August 1, 2003 (Please refer to the annual reports for full text of the previous abstracts)

Longitudinal vestibular schwannoma growth rates in people with neurofibromatosis 2 (NF2): a combined analysis of NF2 patients from three countries. M.E. Baser,[1] T. Patankar,[2] L. Kluwe,[3] V.-F. Mautner,[4] E. Makariou,[5] D.M. Parry,[6] A.J. Wallace,[7] R.T. Ramsden,[8] D.G.R. Evans,[7] A. Jackson[2]

[1]Los Angeles, CA, U.S.A., [2]Division of Imaging Science and Biomedical Engineering, University of Manchester, Manchester, U.K., [3]Department of Neurosurgery, University Hospital Eppendorf, Hamburg, Germany, [4]Department of Neurology, Klinikum Nord Ochsenzoll, Hamburg, Germany, [5]Department of Radiology, Georgetown University Medical Center, Washington, D.C., U.S.A., [6]Genetic Epidemiology Branch, National Cancer Institute, Bethesda, MD, U.S.A., [7]University Department of Medical Genetics, St. Mary s Hospital, Manchester, U.K., [8]Department of Otolaryngology, Manchester Royal Infirmary, Manchester, U.K.

(Accepted for presentation: American Society of Human Genetics, 54th Annual Meeting, Toronto, October, 2004)

In two previous longitudinal studies of vestibular schwannoma (VS) growth rates in people with neurofibromatosis 2 (NF2), we found that growth rates tended to decrease with increasing age and that genotype-phenotype correlations were not apparent. To more definitively address these questions, we assessed VS growth rates in 84 NF2 patients from the United States, Germany, and the United Kingdom. The median follow-up was 3.9 years (range, 0.2 to 14.8 years). Box models were used to estimate VS volumes and linear regression was used to evaluate the association between tumor doubling time (TDT, in years) and covariates. VS growth rates decreased with increasing age at baseline ($\log_{10}$ TDT = .834 + .008 x age at baseline, SE_b = .004); people aged $\leq$ 15 years at baseline had the highest growth rates. VS growth rates were not significantly different between people with constitutional *NF2* splice-site mutations (N = 19) and those with nonsense or frameshift mutations (N = 26); there were too few other types of mutations to analyze separately. To estimate the effect of volumetric accuracy on growth rates, we used two methods (one- and two-component box models) to estimate volumes and TDT for 26 VSs that had intracanalicular and extracanalicular portions, which are measured separately in the two-component model. One-component baseline VS volumes were greater than two-component volumes by a median of 19%, and one-component TDTs were less than two-component TDTs by a median of 12%. These results suggest that different three-dimensional VS volumetric methods have a relatively small average effect on VS growth rates, possibly because the magnitude of long-term longitudinal VS volume change is often far greater than the magnitude of VS volume measurement error.

The epidemiology of neurofibromatosis 2 (NF2). M.E. Baser,[1] J.M. Friedman,[2] H. Joe,[3] D.G.R. Evans[4]

[1]Los Angeles, CA, U.S.A., [2]Department of Medical Genetics and [3]Department of Statistics, University of British Columbia, Vancouver, B.C., Canada, [4]University Department of Medical Genetics, St. Mary s Hospital, Manchester, U.K.

(Presentation at the NNFF International Consortium For The Molecular Biology of NF1, NF2 and SchwannomanotsisNF, Aspen, Colorado, May 2004)

Research on the epidemiology of NF2 has been limited by the rarity of the disease. Recently, there have been longitudinal studies of vestibular schwannoma (VS) growth rates in NF2 and the risk of mortality in NF2. Additional longitudinal studies are in progress on the development of symptoms and their relationship to the risk of mortality, and modeling patterns of VS growth rates. Other studies are based on two large NF2 databases. The United Kingdom NF2 registry is being used for several studies: genotype-phenotype correlations for each common type of NF2-associated nervous system tumor, empirical evaluation and development of diagnostic criteria for NF2, and two- and three-hit mathematical models of VS formation that include genotype-phenotype correlations. The international NF2 database has all published constitutional *NF2* mutations, data from the United Kingdom NF2 registry, unpublished data that are contributed by investigators around the world, and summary clinical information (as well as all published somatic *NF2* mutations in non-heritable tumors). The international NF2 database is being used to study genotype-phenotype correlations for the location of constitutional *NF2* splice-site mutations. A description of the international NF2 database and its comprehensive list of constitutional *NF2* mutations is being distributed to on-line human gene mutation databases.

Lee Bernard TK, Friedman JM.
Phylogenetic Footprinting of the NF1 5 Upstream Region (5UR).
(Presented, 53rd Annual Meeting, American Society of Human Genetics, November 2003, Los Angeles).
Medical Genetics, University of British Columbia, Vancouver, BC, Canada.

The 5UR of the human neurofibromatosis 1 gene was defined as the 59756 bp region between the NF1 translation start site and the end of the first upstream GenScan prediction (NT_010799.114). The 5URs of mouse and rat were defined as 59756 bp upstream of the translation start site of the NF1 homologs in these species. The 5UR in Fugu was defined as the 1488 bp segment between the known 5 flanking gene (FN5) and the NF1 translation start site. Sequence alignments were established by mVista, and windows of identity greater than that of the coding regions and extending 50 bp or more in length among all 3 mammalian species were identified with Frameslider, a Perl program written for this research. These highly homologous regions (HHRs) were compared to the Fugu 5UR using Pairwise BLAST and analyzed for potential transcription factor binding sites and other promoter-associated sequences with MATCH, MatInspector, Eurkaryotic Promoter Database and TRRD.

Three HHRs were discovered in the NF1 5UR. HHR1, located 42626-42696 bp upstream of translation start site, contains an AP-1 site shared by all four species. HHR2, located 640-689 bp upstream of translation start site, has no promising predictions for recognized transcription factor binding sites. HHR3, located 233-519 bp upstream of the NF1 translation start site, contains a previously-described CREB site that is shared by all three mammalian species.

HHR3 also includes a 24 bp sequence 310-333 bp upstream of the translation start that is identical in human, mouse and rat and differs by only1 bp in Fugu. Bioinformatic analysis and correlation with previously-published in vitro transcription studies indicate that this sequence, which we call NF1 Highly Conserved Sequence (NF1HCS), is likely to be involved in transcriptional regulation. NF1HCS lies 151bp downstream from the NF1 major transcriptional start site but appears to be a strong candidate for the NF1 core promoter element despite its position further downstream than any previously-described eukaryotic downstream core promoter element.

Ramsden RT, Evans DGR, Wallace AJ, Joe H, Baser ME.
Revised diagnostic criteria for neurofibromatosis 2.

(Presented at the 53rd Annual Meeting, American Society of Human Genetics, 4-8 November 2003, Los Angeles, CA)

We reported that each of the four sets of clinical diagnostic criteria for neurofibromatosis 2 (NF2) had low sensitivity at the time of the initial assessment (Neurology 2002;59:1579-1565). The purpose of this study was to determine the extent to which modifications to the Manchester diagnostic criteria increased sensitivity. The study had 221 NF2 patients in the United Kingdom NF2 registry who presented without bilateral vestibular schwannomas (155 people who did not have a family history of NF2 at initial assessment and 66 inherited cases). The modifications were: (1) in people without a family history of NF2, permitting the diagnosis when there are multiple meningiomas and only one, instead of two, other tumors or cataract (as in the NNFF criteria); in people with a 1st degree relative with NF2, permitting the diagnosis when there is only one, instead of two, tumors or cataract (as in the 1991 NIH criteria), but restricting 1st degree relatives to parents, (2) adding juvenile mononeuropathy ($\leq$ 15 years) as a diagnostic criterion, (3) in addition to clinical criteria, permitting the diagnosis when constitutional *NF2* mutations are identified. We used Kaplan-Meier analysis to determine the time course, from initial assessment to the most recent clinical evaluation, of the increasing proportion of people who would be diagnosed with NF2 using the Manchester criteria and the three modifications; the jackknife method was used to compute pointwise standard errors for differences in proportions of pairwise Kaplan-Meier curves between different sets of criteria. In people without a family history of NF2 at initial assessment (the most difficult group to diagnose), sensitivity was increased by incorporating features of the 1991 NIH criteria and the NNFF criteria (modification 1 above). The modified Manchester criteria were significantly more sensitive than the original Manchester criteria from four years after initial assessment to 17 years after initial assessment. In inherited cases, sensitivity was further increased by adding mononeuropathy as a diagnostic criterion and incorporating the positive results of mutation analysis. These results indicate that, in NF2 patients who present without bilateral vestibular schwannomas, modifications to the Manchester criteria can increase diagnostic sensitivity, although not at the time of the initial assessment.

Tucker T, Wolkenstein P, Friedman JM.
Association Between the Occurrence of Malignant Peripheral Nerve Sheath Tumours and Subcutaneous and Internal Neurofibromas in NF1

Department of Medical Genetics, University of British Columbia, Vancouver, Canada; and Department of Dermatology, Hopital Henri-Mondor

(Presentation to 10th European Neurofibromatosis Meeting, Turku, Finland, Aug., 2003)

Individuals with NF1 have a lifetime risk of about 10% of developing a malignant peripheral nerve sheath tumour (MPNST). Such tumours are one of the most frequent causes of death among people with NF1. Clinical experience suggests that most MPNSTs develop from pre-existing plexiform neurofibromas. The number, size, and type of benign neurofibromas vary greatly among NF1 patients, but it is not known if an individual's risk for developing MPNST bears any relationship to the burden of benign neurofibromas.

The Henri-Mondor Database contains information on 516 probands with NF1 diagnosed by the NIH Criteria. The average age was 35.0, and 64% were between 10 and 39 years of age. 44% were males and 56% females. A semi-quantitative estimate of the number of cutaneous neurofibromas and information on the presence or absence of 1 or more subcutaneous neurofibromas, internal neurofibromas and MPNSTs were recorded for each patient. Internal tumours where identified by screening the abdomen by ultrasound, CT or MRI examination and by screening the thorax by X-ray, CT or MRI examination. MPNSTs were diagnosed by biopsy. We used logistic regression to determine the association between each of these features; age was treated as a covariante. 7.6% of these patients had a MPNST, 28% had one or more internal plexiform neurofibromas, and 48% had one or more subcutaneous neurofibromas. The distribution of cutaneous neurofibromas was 17% with 10 or fewer, 38% with 11-100, and 31% with more than 100. MPNSTs were 14.5 times (95% confidence interval [CI] 2.7-79.0) more likely to be present in individuals with internal plexiform neurofibromas than in patients without internal neurofibromas. Individuals with subcutaneous neurofibromas were 5.3 (CI 2.1-13.8) times as likely to have internal plexiform neurofibromas and 3.4 (CI 1.3-8.8) times as likely to have a MPNST as patients without subcutaneous neurofibromas.

No association was observed between the estimated number of cutaneous neurofibromas and the presence of subcutaneous neurofibromas, internal neurofibromas, or MPNSTs. The observation that MPNSTs are associated with subcutaneous neurofibromas and strongly associated with internal neurofibromas suggests that individuals with such benign tumours may warrant increased surveillance for MPNST.

We are grateful to the Henri-Mondor Database Participants who contributed the data analyzed in this study.

Zhao Y.
Composite Likelihood Estimation in Familial Data Analysis
(Presentation to Biometrics (WNAR) meeting in Albuquerque, New Mexico: June 26-June 30, 2004)

We propose two estimation procedures based on composite likelihoods for multivariate models for which likelihood calculations are too time-consuming. We especially focus on two classes of models for familial data: the multinormal random effects models and the multinormal copula models. The parameters in the models under consideration can be classified as univariate marginal parameters and dependence parameters. The first method is a two-stage method in which the univariate marginal parameters are estimated based on the sum of log likelihoods of univariate margins and the dependence parameters are estimated separately based on the sum of log likelihoods of bivariate margins with the univariate marginal parameters replaced by their estimates. In the second method, all the parameters are estimated from the weighted sum of log likelihoods of bivariate margins. The composite likelihood methods can greatly reduce computation in parameter estimation, but with a price of efficiency loss. For some special cases, we compared the asymptotic efficiency of these two methods with the maximum likelihood method. We found that the performance of the two methods is reasonable, except that when the dependence is strong, the first approach is inefficient for the regression parameters. We also find that the second approach is generally better for the regression parameters, but less efficient for the dependence parameters when the dependence is weak.

APPENDIX 2

Submitted papers

Computations for the familial analysis of binary traits

Harry Joe and A. H. M. Mahbub-ul Latif
Department of Statistics, University of British Columbia
and Abteilung Medizische Statistik, Georg-August-Universität Göttingen

Summary

For familial aggregation of a binary trait, one method that has been used is the GEE2 (generalized estimating equation) method corresponding to a multivariate logit model. We solve the complex estimating equations for the GEE2 method using an automatic differentiation software which computes the derivatives of a function numerically using the chain rule of the calculus repeatedly on the elementary operations of the function. Based on this, we are able to show in a simulation study that the GEE2 estimates are quite close to the maximum likelihood estimates assuming a multivariate logit model, and that GEE2 is computationally faster when the dimension or family size is larger than four.

Keywords: binary response, multivariate probit and logit models, generalized estimating equations, familial aggregation

1. Introduction

In quantitative genetics and epidemiology, researchers are often interested in identifying important variables or traits related to a genetic disease and also in familial aggregation. The response variables measured for the disease can be discrete or continuous. In this paper, we focus on binary traits, such as presence/absence of a disease, and presence/absence of a symptom/feature of a genetic disease. For familial aggregation, for genetic hypotheses one would like to know the strength of dependence for different relationships in a family such as parent-offspring, sib-sib, degree 2 relationship (Falconer 1989). Our research is motivated by binary traits in the genetic disease neurofibromatosis; see Szudek et al. (2002).

One method for multivariate binary data is the GEE2 odds ratio regression or multivariate logit model. Liang, Zeger and Qaqish (1992), Molenberghs and Lesaffre (1994), Glonek and McCullagh (1995) and Joe (1997) considered this method/model from different points of view. GEE2 odds ratio regression corresponds to the multivariate logit model with a multivariate Plackett distribution (Molenberghs and Lesaffre 1994; Joe 1997). The formulation of Liang and Beaty (1991), and Liang, Zeger and Qaqish (1992) estimates regression and dependence (log odds ratio) parameters from a set of estimating equations without considering whether there is a probability model behind their assumptions.

The multivariate probit model (Ashford and Sowden 1970, Mendell and Elston 1974) is motivated for a binary trait based on a (latent) polygenic effect, so for familial analysis of a binary trait, it is more in-

terpretable than a multivariate logit model. Although odds ratios have a convenient interpretation, there is no physical or stochastic model that leads to the odds ratio as a natural dependence parameter. Joe (1997) considers the multivariate probit and multivariate logit models as multivariate analogues of the univariate probit and logit latent variable family of models.

In this paper, we compare GEE2 and maximum likelihood (ML) estimates assuming a multivariate logit model. The computation of GEE2 estimates includes the novel use of automatic differentiation software to solve the set of estimating equations which are not simple in form. The previous code for the GEE2 method was not general enough for binary familial data, such as that used in Szudek et al. (2002), that are not in the simpler interclass/intraclass format.

The organization of the remainder of the paper is as follows. The models are specified as latent vector models in Section 2. Computational details are given in Section 3 and comparisons are made in Section 4. Section 5 concludes with a discussion.

2. Models and methods for a binary trait

For a binary response variable Y, with covariate vector $\mathbf{x}$, common statistical methods are logistic and probit regression. Both of these methods are latent variable methods with the probabilistic representation is:

$$Y = I(Z \leq \alpha + \beta'\mathbf{x}), \tag{2.1}$$

where Z is standard normal (logistic) for the probit (logit) regression model. The model (2.1) can be written as

$$Y = I(X \geq \tau), \quad X = -Z + \alpha + \beta'\mathbf{x} + \tau \quad \text{with location} \quad \alpha + \beta'\mathbf{x} + \tau$$

where X is the liability and τ is the threshold. One can apply the Central Limit Theorem to arrive at the probit model when the liability is influenced by the additive effects of many genes. The logistic density is also bell-shaped, so probabilistic properties of logistic and probit regression are similar.

For familial data, the binary response vector is $(Y_1, \ldots, Y_d)$, where d is the family size. For a model for familial aggregation of a binary trait, one needs to define a joint probability distribution for $(Y_1, \ldots, Y_d)$ for $d \geq 2$, where the dependence parameter of responses (Y_i, Y_j) for two different members of a family, depends on the relation type.

Probit regression model easily extends to the multivariate probit model, with a latent multivariate normal random vector. The extension of logistic regression to its multivariate counterpart requires a way to define a multivariate logistic distribution with suitable dependence parameters. The extensions are explained below.

The multivariate probit model has been known for a long time (e.g., Ashford and Sowden 1970, Mendell and Elston 1974). The stochastic representation of the model, with common regression parameters for each

margin, is

$$Y_j = I(Z_j \le \alpha + \boldsymbol{\beta}'\mathbf{x}_j),\ j = 1, \ldots, d, \quad (Z_1, \ldots, Z_d) \sim N(\mathbf{0}, R_d) \tag{2.2}$$

where R_d is a correlation matrix. For models for familial aggregation, R_d can have one or more correlation parameters. For example, for the exchangeable dependence model there is a single correlation parameter ρ; for a model for nuclear families, there are three parameters: correlations ρ_{PP}, ρ_{SS} and ρ_{PO} for parent-parent, sib-sib, and parent-offspring respectively; for a model with members in several generations, there may be further correlation parameters for second and higher degree relatives.

For logistic regression, the regression parameter β for a binary covariate x has an odds ratio interpretation. For a pair (Y_1, Y_2), one can use the bivariate Plackett distribution which has an odds ratio as a dependence parameter:

$$\gamma = \gamma_{12} = \frac{\Pr(Y_1 = 1, Y_2 = 1; \mathbf{x}_1, \mathbf{x}_2)\ \Pr(Y_1 = 0, Y_2 = 0; \mathbf{x}_1, \mathbf{x}_2)}{\Pr(Y_1 = 1, Y_2 = 0; \mathbf{x}_1, \mathbf{x}_2)\ \Pr(Y_1 = 0, Y_2 = 1; \mathbf{x}_1, \mathbf{x}_2)} \tag{2.3}$$

for all $\mathbf{x}_1, \mathbf{x}_2$. Let $F_{12}(z_1, z_2)$ be the joint distribution of the latent pair (Z_1, Z_2) and $F(z) = (1 + e^{-z})^{-1}$ be the logistic cumulative distribution function. Then (2.3) is the same as

$$\gamma = \frac{F_{12}(\alpha + \boldsymbol{\beta}'\mathbf{x}_1, \alpha + \boldsymbol{\beta}'\mathbf{x}_2)\,[1 - F(\alpha + \boldsymbol{\beta}'\mathbf{x}_1) - F(\alpha + \boldsymbol{\beta}'\mathbf{x}_2) + F_{12}(\alpha + \boldsymbol{\beta}'\mathbf{x}_1, \alpha + \boldsymbol{\beta}'\mathbf{x}_2)}{[F(\alpha + \boldsymbol{\beta}'\mathbf{x}_1) - F_{12}(\alpha + \boldsymbol{\beta}'\mathbf{x}_1, \alpha + \boldsymbol{\beta}'\mathbf{x}_2)]\,[F(\alpha + \boldsymbol{\beta}'\mathbf{x}_2) - F_{12}(\alpha + \boldsymbol{\beta}'\mathbf{x}_1, \alpha + \boldsymbol{\beta}'\mathbf{x}_2)]} \tag{2.4}$$

and this equation can be solved for $F_{12}(\alpha + \boldsymbol{\beta}'\mathbf{x}_1, \alpha + \boldsymbol{\beta}'\mathbf{x}_2)$.

The multivariate Plackett extension is given in Molenberghs and Lessafre (1994), where (2.3) and (2.4) are extended to higher orders; for example, for $d = 3$ dimensions, with $\pi(y_1, y_2, y_3) = \Pr(Y_1 = y_1, Y_2 = y_2, Y_3 = y_3; \mathbf{x}_1, \mathbf{x}_2, \mathbf{x}_3)$,

$$\gamma_{123} = \frac{\pi(1,1,1)\,\pi(1,0,0)\,\pi(0,1,0)\,\pi(0,0,1)}{\pi(1,1,0)\,\pi(1,0,1)\,\pi(0,1,1)\,\pi(0,0,0)}. \tag{2.5}$$

For the d-dimensional product ratio, there are 2^{d-1} probabilities each in the numerator and denominator. Joe (1997) shows that these ratios do not lead to a proper multivariate logistic distribution if γ_{123} and higher order γ's are close to 0 or large. To have the same number of dependence parameters as the multivariate probit model, the third and higher order γ parameters are taken to be 1 (see Joe 1997 for a maximum entropy interpretation in this case). (2.5) and its higher-order equivalents lead to roots of polynomials that must be computed to obtain $F_{1\ldots d}(\alpha + \boldsymbol{\beta}'\mathbf{x}_1, \ldots, \alpha + \boldsymbol{\beta}'\mathbf{x}_d)$, the joint distribution of the latent multivariate logistic random vector.

To obtain maximum likelihood estimates of the parameters of the model (2.2) and the multivariate logit counterpart, multivariate rectangle probabilities are required, since

$$\Pr(Y_1 = y_1, \ldots, Y_d = y_d \mid \mathbf{x}_1, \ldots, \mathbf{x}_d) = \Pr(Z_1 \prec\succ_1 \alpha + \boldsymbol{\beta}'\mathbf{x}_1, \ldots, Z_d \prec\succ_d \alpha + \boldsymbol{\beta}'\mathbf{x}_d)$$

where $\prec\succ_j$ is $\le$ if $y_j = 1$ and is $>$ if $y_j = 0$.

Liang et al. (1992) develop a method called odds ratio regression or GEE2 and Liang and Beaty (1991) apply it for familial aggregation of a binary trait. They do not assume any joint distribution for $(Y_1, \ldots, Y_d)$ but estimate interclass and intraclass odds ratios using estimating equations that generalize method of moments equations. These estimating equations use multivariate Plackett probabilities for dimension 2, 3, and 4. Although Liang and Beaty (1991) didn't mention any underlying model for their method, their method corresponds to an estimation method for the multivariate logit model that is different from maximum likelihood. We will express their estimating equations in the more general context of familial data.

Let $\boldsymbol{\theta} = (\beta, \psi)$, where ψ is a vector of log odds ratios, with different odds ratio parameters for different relation types (similar to the correlations for the probit model). Let $\mathbf{y}_i' = (y_{i1}, \ldots, y_{id_i})$ and let $\mathbf{w}_i' = (y_{i1}y_{i2}, \ldots, y_{i,d_i-1}y_{id_i})$, $i = 1, \ldots, n$, with n families and d_i members in the ith family. Let $\boldsymbol{\mu}_i' = \boldsymbol{\mu}_i'(\beta) = (\mu_{i1}, \ldots, \mu_{id_i})$, where $\mu_{ij} = \mathrm{E}(y_{ij})$, and $\boldsymbol{\eta}_i' = \boldsymbol{\eta}_i'(\boldsymbol{\theta}) = (\mathrm{E}[y_{i1}y_{i2}], \ldots, \mathrm{E}[y_{i,d_i-1}y_{id_i}])$. The estimating equations have the form:

$$U(\boldsymbol{\theta}) = \sum_{i=1}^{n} \frac{\partial(\boldsymbol{\mu}_i', \boldsymbol{\eta}_i')}{\partial \boldsymbol{\theta}} \Sigma_i^{-1}(\boldsymbol{\theta}) \begin{pmatrix} \mathbf{y}_i - \boldsymbol{\mu}_i \\ \mathbf{w}_i - \boldsymbol{\eta}_i \end{pmatrix} = \mathbf{0}, \tag{2.6}$$

where $\Sigma_i(\boldsymbol{\theta})$ is the covariance matrix of $(\mathbf{y}_i, \mathbf{w}_i)$ based on multivariate Plackett probabilities up to dimension 4.

3. Computational implementations

Conceptually, the models in the previous section are straightforward, but computations for the maximum likelihood and GEE2 estimation methods are not straightforward. Both of these methods require iterative procedure to estimate the parameters.

For the maximum likelihood estimator (MLE) of the multivariate logit model, we have coded the computation of multivariate Plackett probabilities by recursively finding the roots of many polynomial equations. The log-likelihood can then be coded and the MLE of β and the ψ parameters can be obtained using an iterative quasi-Newton method; for example, the method in Nash (1990) is convenient as it also computes the inverse Hessian (asymptotic covariance matrix) at the MLE. Because of the recursions, the computational effort for maximum likelihood estimation is exponentially increasing in the dimension or family size d.

The GEE2 estimates of β and ψ are a solution of the estimating equations (2.6) and the Godambe information matrix (Godambe, 1991) at the GEE2 estimates is used as a asymptotic covariance matrix of the estimates. To solve (2.6), the computer program of Liang and Beaty (1991) and Qaqish et al. (1992) can be used but it has limitations in handling familial data in general pedigree form; it can only handle familial data in which each pair is either an interclass or intraclass pair. This code was written in Pascal and not easy to modify even after conversion to C with *p2c*. Therefore, we wrote a new implementation of

GEE2, in which the equations were coded in C++, and the estimates of the parameters β and ψ are obtained using the Newton-Raphson method. This method requires the computation of the Hessian matrix at each iteration and the elements of Hessian matrix are obtained from the first derivatives of the equations (2.6). To avoid differentiating complex estimating equations analytically, we have used an automatic differentiation software to compute the derivatives of the estimating equations.

Automatic differentiation (www.autodiff.org) is a relatively new procedure to compute derivatives of a function mechanically. It exploits the fact that every function is executed on a computer as a sequence of elementary ($+$, $-$, $*$, $\cdots$) and transcendental (log, sine, cosine, ...) operations. Using the chain rule of differential calculus repeatedly on these operations, automatic differentiation computes the derivatives of any user provided function. The main advantages of automatic differentiation over the existing methods of numerical differentiation are: (i) it is truncation error free and accurate to the working precision, (ii) can be incorporated with common high level programming languages. A number of automatic differentiation software, written in different programming languages such as FORTRAN, C/C++, etc., are available (Bischof et al., 1997) and are widely used in many fields which require numerical optimization such as engineering, oceanography, etc. It can be very useful tool in Statistics for obtaining numerical derivatives of complex log–likelihood functions or solving nonlinear systems of equations which are not analytically easy to work with.

For our implementation of GEE2, we have used the automatic differentiation software FADBAD (Bendtsen and Stauning 1996) which is written in C++ and found that this is faster than maximum likelihood for family sizes of 5 or more, even with the C++ overhead in automatic differentiation. This is expected because GEE2 only requires multivariate Plackett probabilities in dimensions 4 or less. Even with compiled programs in C/C++, the computational time will be of the order of minutes on fast Pentium computers if there are many families of size 6 or more.

Our program is written in a form that allows the user to specify general relation classes (see examples in Section 2) and there is a dependence parameter (odds ratio) for each relation class. For the simpler use of the programs, the dependence parameters are not functions of covariates. This is mainly due to mathematical or probabilistic consistency of the models; there is no known way of making the odds ratio dependence parameters be functions of a covariate $\mathbf{x}$ so that the resulting set of odds ratios are compatible for all $\mathbf{x}$. For a categorical covariate x, one could split the data into groups for estimates of the parameters or form extra relation classes. For example, if the gender of the parent might be a factor, one could use father-offspring and mother-offspring relation classes in place of the parent-offspring relation class.

4. Comparisons of the models/methods

Latif (2001) has a simulation study to compare maximum likelihood and GEE2 estimates for the multivariate logistic models which considers different predigrees, different number of families, simulations. The simulation results are similar in different cases, so in this paper we discuss only one of the simulations. This specific simulation has 500 simulations with 200 families, each family has five members of three generations: one grandparent, one parent, one uncle/aunt, two grandchildren.

The binary familial data are simulated from multivariate probit model with one covariate *age*. [Note that simulation from the multivariate logit model is much more difficult, since one cannot simulate the latent logistic variables easily because of the implicit equations defining the multivariate distribution functions.] The standard deviation of the standard logistic distribution is $\pi/\sqrt{3} = 1.81$, so for the same data, the regression coefficients of logistic regression are usually roughly 1.8 times the corresponding regression coefficients of probit regression. For two binary variables based on a latent bivariate standard normal distribution with correlation ρ, the odds ratio depends on the cut-off points, but is bounded by

$$B(\rho) = \left\{ \frac{1 + (2/\pi) \arcsin \rho}{1 - (2/\pi) \arcsin \rho} \right\}^2 . \tag{4.1}$$

The column 2 of Table I shows the true parameters used in multivariate probit model to simulate multivariate binary data; two different sets of parameters are considered. The columns 3–4 show the ML and GEE2 estimates of the multivariate logistic model. As expected the estimates of the regression coefficient is about 1.81 times of the corresponding parameter used in multivariate probit model, e.g. $0.2 \times 1.81 = 0.362 \approx 0.37$. The estimates of the dependence parameters (log odds ratios) correspond roughly to the upper limit shown in (4.1), e.g. $\log B(0.4) = 1.1$, $\log B(0.6) = 1.7$, $\log B(0.8) = 2.7$. The ML and GEE2 estimates were often the same to 2 or 3 significant digits. The standard deviation of the parameter estimates and the average standard errors in each line are roughly the same. That means, our study show that the ML and GEE2 estimates of regression and dependence parameters of multivariate logistic distribution are similar.

5. Discussion

The multivariate logit model and GEE2 estimation method are an alternative to the multivariate probit model for binary trait data, and may be useful to apply for a sensitivity analysis. Liang and Beaty (1991) mention that their odds ratio regression model is a more general model and avoids the unobservable continuous trait of the multivariate probit model. However we have shown that the probabilistic assumptions behind their method are conceptually very close to that of the multivariate probit model with latent logistic random

variables in place of latent normal random variables. Our simulations also show that the GEE2 and ML estimates of multivariate logistic model are similar.

We have also demonstrated the usefulness of automatic differentiation for the GEE2 equations. In general, automatic differentiation can be a useful tool in Statistics when there are complicated nonlinear functions to be solved.

Acknowledgements

This research is supported from an NSERC Canada grant and US Army Medical Research grant NF990038.

References

[1] Ashford JR, Sowden RR. Multivariate probit analysis. *Biometrics* 1970; **26**:535–546.

[2] Bendtsen C, Stauning O. FADBAD, a flexible C++ package for automatic differentiation. Technical report 1996-17, Department of Mathematical Modelling, Technical University of Denmark. http://www.imm.dtu.dk/fadbad.html

[3] Bischof CH, Roh L and Mauer A. ADIC — An Extensible Automatic Differentiation Tool for ANSI-C. *Software–Practice and Experience* 1997; **27**:1427–1456.

[4] Falconer DS. *Introduction to Quantitative Genetics*, 3rd edition. Longman Group, HK, 1989.

[5] Glonek GFV, McCullagh P. Multivariate logistic models. *Journal of the Royal Statistical Society, Series B* 1995; **57**:533–546.

[6] Godambe VP. (ed.) *Estimating Functions*. Oxford University Press, Oxford, 1991.

[7] Joe H. Approximations to multivariate normal rectangle probabilities based on conditional expectations. *Journal of the American Statistical Association* 1995; **90**:957–964.

[8] Joe H. *Multivariate Models and Dependence Concepts*. Chapman & Hall, London, 1997.

[9] Latif AHMM. A comparison of methods for multivariate familial binary response. M.Sc. Thesis 2001, Department of Statistics, University of British Columbia.

[10] Liang KY, Beaty TH. Measuring familial aggregation by using odds-ratio regression models. *Genetic Epidemiology* 1991; **8**: 361–370.

[11] Liang KY, Zeger SL, Qaqish B. Multivariate regression analyses for categorical data. *Journal of the Royal Statistical Society, Series B* 1992; **54**:3–24.

[12] Mendell NR, Elston RC. Multifactorial qualitative traits: genetic analysis and prediction of recurrence risks", *Biometrics* 1974; **30**:41–57.

[13] Molenberghs G, Lesaffre E. Marginal modelling of correlated ordinal data using a multivariate Plackett distribution. *Journal of the American Statistical Association* 1994; **89**:633–644.

[14] Nash JC. *Compact Numerical Methods for Computers: Linear Algebra and Function Minimisation*, second edition. Hilger, New York, 1990.

[15] Szudek J, Joe H, Friedman JM. Analysis of intra-familial phenotypic variation in neurofibromatosis 1 (Nf1) *Genetic Epidemiology* 2002; **23**:150–164.

Table I: Simulation data from multivariate probit: average of estimates, average absolute differences (ML and GEE2) and average SEs assuming a multivariate logit model.

	True	Parameter Estimates			Standard Errors		
	values	ML	GEE2	Diff.	ML	GEE2	Diff.
Const.	0.5	0.787	0.787	0.003	0.165	0.160	0.007
Age	1.0	1.796	1.798	0.011	0.406	0.394	0.021
SS	0.8	2.885	2.888	0.011	0.294	0.294	0.014
PO	0.6	1.944	1.947	0.021	0.273	0.271	0.018
D2	0.4	1.223	1.212	0.019	0.281	0.279	0.022
Const.	0.8	1.310	1.310	0.004	0.181	0.178	0.008
Age	0.2	0.374	0.375	0.011	0.399	0.393	0.021
SS	0.9	3.815	3.821	0.015	0.343	0.342	0.020
PO	0.5	1.527	1.534	0.018	0.267	0.263	0.020
D2	0.3	0.914	0.909	0.020	0.287	0.279	0.025

Composite Likelihood Estimation in Multivariate Data Analysis

Yinshan Zhao and Harry Joe
Department of Statistics
University of British Columbia

ABSTRACT

We propose two estimation procedures based on composite likelihoods for multivariate models with regression/univariate and dependence parameters for which likelihood calculations are too time-consuming. Examples are models in familial data analysis with discrete or censored response. The first method is a two-stage method in which the univariate parameters are estimated based on the sum of log likelihoods of univariate margins and the dependence parameters are estimated separately based on the sum of log likelihoods of bivariate margins with the univariate parameters replaced by their estimates from the first stage. In the second method, all the parameters are estimated from the weighted sum of log likelihoods of bivariate margins. The composite likelihood methods can greatly reduce computation in parameter estimation, but with a price of efficiency loss. For some special cases, we compare the asymptotic efficiency of these two methods with the maximum likelihood method. Our investigation includes the multivariate normal (MVN) model for a continuous variable, the multivariate probit model for a binary variable and the MVN for a right-censored variable. We find that the performance of the two methods is reasonable, except that when the dependence is strong, the first approach is inefficient for the regression parameters. We also find that the second approach is generally better for the regression parameters, but less efficient for the dependence parameters when the dependence is weak.

1 Introduction

For models used to analyze multivariate data, we consider estimation methods based on log-likelihoods of low-dimensional margins when the multivariate probabilities are too time-consuming to compute but low-dimensional margins probabilities are computable. The class of models we are considering have parameters that are common to different margins, for example, common regression parameters for different univariate margins, and common dependence parameters for different bivariate margins. In this paper, we use familial data as our example to illustrate the estimation methods.

A specific context of familial data is as follows. The sample is formed by families with varying sizes. We denote the number of families by n and the number of members in the ith family by k_i. There is a single response measurement on each individual. This response may be a continuous variable, an indicator of some symptom, the right censored onset time of a disease feature, or some other type of variable. We denote the response measurements of the ith family by $\mathbf{Y}_i = (Y_{i1}, \ldots, Y_{ik_i})'$. Often, there are also a set of covariates at the individual level, which we denote by $\mathbf{X}_i = (\mathbf{x}_{i1}, \ldots, \mathbf{x}_{ik_i})'$, a $k_i \times m$ matrix.

For a continuous response, a common model is the multivariate normal model (Srivastava and Ng, 1990). The correlation matrix for a family depends on the family structure. For a binary response, a common model is the multivariate probit model (MVP) with latent multivariate normal variables (Mendell and Elston, 1974). Again, the correlation matrix depends on the family structure. In general, the multinormal random effects models and the multinormal copula models introduced in Section 2 can be used to analyze various types of familial data. In these models, there are regression parameters which are univariate parameters, and correlation (dependence) parameters such as the sib-sib or parent-offspring correlations.

In many cases, for instance, the case of binary or right-censored responses, the joint likelihood for a family involves multi-dimensional integrals which become more and more difficult to evaluate when the family size increases. However, the densities of the univariate and bivariate margins can be easily calculated. All the parameters of the models considered in this paper are either univariate or bivariate parameters. Hence to estimate the parameters, we consider adding together log likelihoods of univariate or bivariate margins to form a composite likelihood (CL), so named by Lindsay (1988). The ideas extend to other CLs when there are parameters that belong to higher-order margins. Besides the computational advantage, a CL also inherits some properties of the ordinary likelihood. In particular, under regularity conditions, the estimates based on CL are consistent and asymptotically unbiased.

The following are some recent applications of CL in multivariate analysis: Xu (1996) proposed using inference functions formed by univariate and bivariate marginal likelihoods for multivariate discrete data; Heagerty and Lele (1998) and Curriero and Lele (1999) considered pairwise CL estimation for binary spatial data; Parner (2001) used pairwise likelihood contributions to analyze familial survival data; Jöreskog and Moustaki (2001) compared a CL approach with two other approaches in factor analysis of ordinal variables; Lele and Taper (2002) considered a CL approach to estimate the variance components of a MVN model.

In this paper, we study two CL estimation methods. One is based on the CLs of both

the univariate margins and the bivariate margins, and estimates the univariate and dependence parameters in two steps. The other only uses the bivariate CL and estimates all the parameters simultaneously. To illustrate the main ideas, we use a simple case of the MVP model as an example. Suppose $Y_{ij} = I(Z_{ij} > 0)$, where I is an indicator function and the latent variable Z_{ij} has a normal distribution with common mean μ and variance 1. Moreover, suppose $\text{Cov}(Z_{ij}, Z_{ij'}) = \rho$ for all i and $j \neq j'$. Then, there is one univariate parameter μ, and one dependence parameter ρ. In the first approach, we estimate μ by maximizing the function:

$$\Psi_1(\mu) = \sum_i \sum_j l_1(y_{ij}; \mu),$$

where $l_1(y_{ij}; \mu)$ is the univariate log likelihood of Y_{ij}. Then, we estimate ρ by maximizing the function

$$\Psi_2(\hat{\mu}, \rho) = \sum_i \sum_{j>j'} l_2(y_{ij}, y_{ij'}; \hat{\mu}, \rho),$$

with respect to ρ, where $l_2(y_{ij}, y_{ij'}; \mu, \rho)$ is the bivariate log likelihood of $(Y_{ij}, Y_{ij'})$ and $\hat{\mu}$ is the estimate obtained in the first step.

In the second approach, we estimate μ and ρ in one step by maximizing the function

$$\Psi_2^*(\mu, \rho) = \sum_i w_i \sum_{j>j'} l_2(y_{ij}, y_{ij'}; \mu, \rho),$$

where w_i is a weight depending on the family size. The motivation and choice of the weights are given in Section 4.2.

The above ideas work for models with covariates, but the notation is more complicated. General classes of models for which our CL methods apply are given in Section 2. Notation for the structure of the parameters in these models is given in Section 3. In Section 4, we introduce the two CL estimation procedures. In Section 5, we outline the jackknife method to estimate the covariance matrix of the CL estimates. In Section 6, we examine the efficiency of these procedures by comparing them with the ML method in some special cases, for which the comparison is actually possible. In Section 7, we apply the proposed methods to a data example. Section 8 concludes with some discussion and topics of further research.

2 Classes of models

In this section, we list two classes of models for whilch the composite likelihood estimation method would be useful.

Multinormal Random Effects Model. A random effects model has a hierarchical structure. The first level specifies the distribution of the observed response vector $\mathbf{Y}$ conditional on an unobservable random vector $\mathbf{\Lambda} = (\Lambda_1, \ldots, \Lambda_k)'$. Given $\mathbf{\Lambda} = \boldsymbol{\lambda} = (\lambda_1, \ldots, \lambda_k)'$, we assume that $Y_1, \ldots, Y_k$ are conditionally independent with probability density function (pdf) $g(y_i; \lambda_i, \boldsymbol{\alpha}_i)$, where $\boldsymbol{\alpha}_i$ denote other parameters which are not random. The second level specifies the distribution of $\mathbf{\Lambda}$. We assume that $h(\mathbf{\Lambda}) = \mathbf{Z} \sim N(\boldsymbol{\mu}, \boldsymbol{\Sigma})$, for some one-to-one function h. Examples include the Poisson-lognormal mixture model (Aitchison and Ho, 1989), and the multivariate lognormal frailty model (Hougaard, 2000, Chapter 10).

Multinormal Copula Model. Suppose $Y_i \sim G_i$, $i = 1, \ldots, k$. We use a multinormal copula to construct the joint distribution of $\mathbf{Y}$:

$$G(\mathrm{y}) = \Phi_k\big(\Phi_1^{-1}[G_1(y_1)], \ldots, \Phi_1^{-1}[G_k(y_k)]; \mathbf{R}\big),$$

where Φ_k is the cumulative distribution function (cdf) of k-variate normal distribution and $\mathbf{R}$ is a k-dimensional correlation matrix. The cdf G_i can be any (parametric) family of univariate distributions. For example, for count data, G_i may be the Poisson or negative binomial distribution, and for survival data, G_i may be the Weibull distribution.

3 Notation

In this section, we indicate the notation that will be used for developing the CL methods.

Let F_{k_i}, f_{k_i} and l_{k_i} denote respectively the cdf, pdf and log likelihood function of $\mathbf{Y}_i$. We impose the following distributional assumptions on $\mathbf{Y}_i$. Suppose Y_{ij} has univariate cdf $F_1(\cdot\,; \nu_{ij}, \boldsymbol{\gamma})$. The parameter ν_{ij} depends on covariates through a function η, i.e., $\nu_{ij} = \eta(\mathbf{x}_{ij}, \boldsymbol{\beta})$; $\boldsymbol{\beta}$ is a vector of regression coefficients when η is a transform of a linear function of $\mathbf{x}$. The parameter $\boldsymbol{\gamma}$ does not depend on covariates. In general, both ν and $\boldsymbol{\gamma}$ could be vectors. Let $\boldsymbol{\theta}_1 = (\boldsymbol{\beta}', \boldsymbol{\gamma}')'$ denote the parameter vector common to Y_{ij}. Next, suppose for $j \neq j'$ that $(Y_{ij}, Y_{ij'})$ has bivariate cdf $F_2(\cdot, \cdot\,; \delta_{ijj'})$ where $\delta_{ijj'}$ is a function of a vector of dependence parameters denoted by $\boldsymbol{\theta}_2$. Typically $\delta_{ijj'}$ is a single element of $\boldsymbol{\theta}_2$ which depends on the relation of individuals j and j' in family i. We further assume that the joint cdf of $\mathbf{Y}_i$, F_{k_i} is fully specified by the univariate and bivariate parameters, $\boldsymbol{\theta} = (\boldsymbol{\theta}_1', \boldsymbol{\theta}_2')' = (\boldsymbol{\beta}', \boldsymbol{\gamma}', \boldsymbol{\theta}_2')'$.

The above notation covers the classes models from Section 2. To illustrate the notation, we give two examples below: multivariate normal and multivariate probit. Another example is the multivariate Poisson log-normal model for multivariate count data.

Example 1 MVN model. $F_1(\cdot;\nu,\gamma)$ is the $N(\mu,\sigma^2)$ distribution with $\nu=\mu=\mathbf{x}'\boldsymbol{\beta}$, $\gamma=\sigma^2$. For an exchangeable dependence model, $\text{Corr}(Y_{ij},Y_{ij'})=\delta_{ijj'}=\alpha$ for $j>j'$, and $\boldsymbol{\theta}_2=\alpha$. For an example of a non-exchangeable dependence model, suppose $k_i=3$, $\mathbf{Y}_i=(Y_{i1},Y_{i2},Y_{i3})'$, and $\delta_{i21}=\delta_{i31}=\alpha_1$ and $\delta_{i32}=\alpha_2$. Then, $\boldsymbol{\theta}_2=(\alpha_1,\alpha_2)'$.

Example 2 MVP model. $F_1(\cdot;\nu,\gamma)$ is the Bernoulli($\Phi(\nu)$) distribution with $\nu=\mathbf{x}'\boldsymbol{\beta}$ and γ null. For an exchangeable dependence model, suppose the correlation among the latent variables is a constant α. Then $\boldsymbol{\theta}_2=\alpha$. Similar to Example 1, one can have non-exchangeable dependence.

4 Estimation Procedures based on Composite Likelihood

The first and second subsections respectively contain the two-stage and one-stage CL methods based on univariate and bivariate margins. The third subsection contains some asymptotic results of the two methods.

4.1 Two-stage Estimation Procedure (CL1)

We estimate $\boldsymbol{\theta}_1=(\boldsymbol{\beta}',\boldsymbol{\gamma}')'$ by maximizing the CL function of univariate margins (UCL):

$$\Psi_{UCL}(\boldsymbol{\theta}_1)=\sum_{i=1}^{n}\sum_{j=1}^{k_i} l_1(Y_{ij};\nu_{ij},\gamma)),$$

where $\nu_{ij}=\eta(\mathbf{x}_{ij},\boldsymbol{\beta})$. Note that Ψ_{UCL} is a log likelihood if $Y_{i1},\cdots,Y_{ik_i}$ are independent for each i. Differentiating Ψ_{UCL} with respect to $\boldsymbol{\theta}_1$ leads to the following composite score function:

$$\boldsymbol{\psi}_{1,CL1}(\boldsymbol{\theta}_1)=\begin{pmatrix} \sum_i\sum_j \frac{\partial l_1(Y_{ij},\nu_{ij},\gamma)}{\partial\nu}\cdot\frac{\partial\nu_{ij}}{\partial\boldsymbol{\beta}} \\ \sum_i\sum_j \frac{\partial l_1(Y_{ij},\nu_{ij},\gamma)}{\partial\gamma}\end{pmatrix} \tag{1}$$

With $\boldsymbol{\theta}_1$ fixed as the estimate from Ψ_{UCL}, we estimate $\boldsymbol{\theta}_2$ by maximizing the CL function of bivariate margins (BCL), which is the summation of the log likelihoods of pairs $(Y_{ij},Y_{ij'})$, $j>j'$:

$$\Psi_{BCL}(\boldsymbol{\theta}_1,\boldsymbol{\theta}_2)=\sum_{i=1}^{n}\sum_{j>j'} l_2(Y_{ij},Y_{ij'};\delta_{ijj'},\nu_{ij},\nu_{ij'},\gamma). \tag{2}$$

The corresponding estimating function is

$$\boldsymbol{\psi}_{2,CL1}(\boldsymbol{\theta}_1,\boldsymbol{\theta}_2)=\frac{\partial\Psi_{BCL}(\boldsymbol{\theta}_1,\boldsymbol{\theta}_2)}{\partial\boldsymbol{\theta}_2}=\sum_i\sum_{j>j'}\frac{\partial l_2(Y_{ij},Y_{ij'};\delta_{ijj'},\nu_{ij},\nu_{ij'},\gamma)}{\partial\delta}\frac{\partial\delta_{ijj'}}{\partial\boldsymbol{\theta}_2}. \tag{3}$$

Let $\psi_{CL1} = (\psi'_{1,CL1}, \psi'_{2,CL1})'$. The estimate of $\boldsymbol{\theta}$, denoted by $\hat{\boldsymbol{\theta}}_{CL1}$, is the solution of $\psi_{CL1}(\boldsymbol{\theta}) = \mathbf{0}$. Computationally, this procedure can be implemented in two steps:

Step 1: estimate $\boldsymbol{\theta}_1$ by $\hat{\boldsymbol{\theta}}_{1,CL1}$, a solution of $\psi_{1,CL1}(\boldsymbol{\theta}_1) = \mathbf{0}$ (usually equivalent to maximizing $\Psi_{UCL}(\boldsymbol{\theta}_1)$).

Step 2: estimate $\boldsymbol{\theta}_2$ by $\hat{\boldsymbol{\theta}}_{2,CL1}$, a solution of $\psi_{2,CL1}(\hat{\boldsymbol{\theta}}_{1,CL1}, \boldsymbol{\theta}_2) = \mathbf{0}$ (usually equivalent to maximizing $\Psi_{BCL}(\hat{\boldsymbol{\theta}}_{1,CL1}, \boldsymbol{\theta}_2)$).

4.2 One-stage Bivariate Composite Likelihood Estimation Procedure (CL2)

An alternative to the two-stage method is to estimate the two sets of parameters simultaneously by maximizing the BCL function Ψ_{BCL} defined in (2). However, this method could overemphasize large families (for univariate parameters) since they contribute quadratically increasing number of pairs to the BCL. It is sensible to weight the contribution of each family according to its size. An individual from a family of size k appears in $k-1$ pairs. Therefore we weight this contribution of the family by $1/(k-1)$. When $Y_{i1}, \ldots, Y_{ik_i}$ are independent,

$$\sum_{j>j'} l_2(Y_{ij}, Y_{ij'}) = \sum_{j>j'} [l_1(Y_{ij}) + l_1(Y_{ij'})] = (k_i - 1) \sum_{j} l_1(Y_{ij}).$$

After weighted by $1/(k_i - 1)$, the CL function is the log likelihood function of $\mathbf{Y}_i$.

For those families with one member, we set the weight as 1 and use the univariate log-likelihood. Thus, the estimating function of the CL2 method is

$$\Psi_{CL2}(\boldsymbol{\theta}) = \sum_{i=1}^{n} w_i l_{(i)}(\boldsymbol{\theta}),$$

where $w_i = 1$, $l_{(i)}(\boldsymbol{\theta}) = l_1(Y_{i1}; \boldsymbol{\theta})$ when $k_i = 1$, and $w_i = 1/(k_i - 1)$, $l_{(i)}(\boldsymbol{\theta}) = \sum_{j>j'} l_2(Y_{ij}, Y_{ij'}; \boldsymbol{\theta})$ otherwise. It yields the following estimating function

$$\psi_{CL2}(\boldsymbol{\theta}) = \frac{\partial \Psi_{CL2}(\boldsymbol{\theta})}{\partial \boldsymbol{\theta}} = \sum_{i} w_i \mathbf{h}_i(\boldsymbol{\theta}),$$

where $\mathbf{h}_i(\boldsymbol{\theta}) = \partial l_{(i)}(\boldsymbol{\theta}) / \partial \boldsymbol{\theta}$.

4.3 Asymptotic Properties

Theorem 1 states the general asymptotic properties that cover the two CL methods.

Let $\psi_{(n)}(\boldsymbol{\theta}) = \sum_i^n \psi_i(\boldsymbol{\theta})$ be the inference function generated from the CL method, where $\psi_i(\boldsymbol{\theta})$ is the contribution of family i. Let $\hat{\boldsymbol{\theta}}_n$ be a solution of $\psi_{(n)}(\boldsymbol{\theta}) = \mathbf{0}$. Under similar

regularity conditions applied to the MLE (Serfling, 1980), $\mathrm{E}_{\boldsymbol{\theta}}\boldsymbol{\psi}_i(\boldsymbol{\theta}) = \mathbf{0}$ (Lindsay, 1988), therefore $\boldsymbol{\psi}_{(n)}$ is unbiased.

Theorem 1 *Assume that the size of the largest family is bounded and the sample can be considered as a finite mixture of family structures. Under the usual regularity conditions on the log-likelihood of univariate and bivariate margins, as* $n \to \infty$,

$$\sqrt{n}(\hat{\boldsymbol{\theta}}_n - \boldsymbol{\theta}) \xrightarrow{d} N\big(\mathbf{0}, \mathbf{G}_{\boldsymbol{\psi}}^{-1}(\boldsymbol{\theta})\big),$$

where $G_{\boldsymbol{\psi}}(\boldsymbol{\theta})$ *is the Godambe information matrix defined as:*

$$\mathbf{G}_{\boldsymbol{\psi}}(\boldsymbol{\theta}) = \left[\lim_{n\to\infty} \mathbf{D}_{\boldsymbol{\psi}}(\boldsymbol{\theta})\right]' \left[\lim_{n\to\infty} \mathbf{M}_{\boldsymbol{\psi}}(\boldsymbol{\theta})\right]^{-1} \left[\lim_{n\to\infty} \mathbf{D}_{\boldsymbol{\psi}}(\boldsymbol{\theta})\right], \tag{4}$$

with

$$\mathbf{D}_{\boldsymbol{\psi}}(\boldsymbol{\theta}) = -\frac{1}{n}\mathrm{E}_{\boldsymbol{\theta}}\left\{\frac{\partial \boldsymbol{\psi}_{(n)}(\boldsymbol{\theta})}{\partial \boldsymbol{\theta}'}\right\} \quad \textit{and} \quad \mathbf{M}_{\boldsymbol{\psi}}(\boldsymbol{\theta}) = \frac{1}{n}\mathrm{E}_{\boldsymbol{\theta}}\{\boldsymbol{\psi}_{(n)}(\boldsymbol{\theta})\boldsymbol{\psi}'_{(n)}(\boldsymbol{\theta})\}.$$

This follows from the usual Taylor expansion to second order; see Godambe (1991).

The covariance matrix of $\hat{\boldsymbol{\theta}}_n$ is approximated by $\mathbf{V} = n^{-1}\mathbf{D}_{\boldsymbol{\psi}}^{-1}\mathbf{M}_{\boldsymbol{\psi}}(\mathbf{D}_{\boldsymbol{\psi}}^{-1})'$, provided $\mathbf{D}_{\boldsymbol{\psi}}^{-1}$ exists.

For the CL1 method, let $\mathbf{D}_{1,ll'} = -\mathrm{E}(\partial\psi_{l,CL1}/\partial\boldsymbol{\theta}_{l'})$ and $\mathbf{M}_{1,ll'} = \mathrm{E}(\psi_{l,CL1}\psi'_{l',CL1})$, $l, l' = 1, 2$. Then,

$$\mathbf{D}_{\boldsymbol{\psi}} = \mathbf{D}_{CL1} = \frac{1}{n}\begin{pmatrix} \mathbf{D}_{1,11} & \mathbf{0} \\ \mathbf{D}_{1,21} & \mathbf{D}_{1,22} \end{pmatrix} \text{ and } \mathbf{M}_{\boldsymbol{\psi}} = \mathbf{M}_{CL1} = \frac{1}{n}\begin{pmatrix} \mathbf{M}_{1,11} & \mathbf{M}_{1,12} \\ \mathbf{M}_{1,21} & \mathbf{M}_{1,22} \end{pmatrix} \tag{5}$$

it follows that

$$\begin{aligned}
\mathrm{Var}(\hat{\boldsymbol{\theta}}_{1,CL1}) &\approx \mathbf{D}_{1,11}^{-1}\mathbf{M}_{1,11}(\mathbf{D}_{1,11}^{-1})', \\
\mathrm{Var}(\hat{\boldsymbol{\theta}}_{2,CL1}) &\approx \left(-\mathbf{D}_{1,22}^{-1}\mathbf{D}_{1,21}\mathbf{D}_{1,11}^{-1} \quad \mathbf{D}_{1,22}^{-1}\right)\mathbf{M}_{CL1}\begin{pmatrix} -\mathbf{D}_{1,22}^{-1}\mathbf{D}_{1,21}\mathbf{D}_{1,11}^{-1} \\ \mathbf{D}_{1,22}^{-1} \end{pmatrix}, \\
\mathrm{Cov}(\hat{\boldsymbol{\theta}}_{1,CL1}, \hat{\boldsymbol{\theta}}_{2,CL1}) &\approx \left(\mathbf{D}_{1,11}^{-1} \quad \mathbf{0}\right)\mathbf{M}_{CL1}\begin{pmatrix} -\mathbf{D}_{1,22}^{-1}\mathbf{D}_{1,21}\mathbf{D}_{1,11}^{-1} \\ \mathbf{D}_{1,22}^{-1} \end{pmatrix}.
\end{aligned}$$

For the CL2 method,

$$\mathbf{D}_{\boldsymbol{\psi}} = \mathbf{D}_{CL2} = -\frac{1}{n}\sum_i w_i \mathrm{E}\left\{\frac{\partial \mathrm{h}_i(\boldsymbol{\theta})}{\partial \boldsymbol{\theta}'}\right\} \text{ and } \mathbf{M}_{\boldsymbol{\psi}} = \mathbf{M}_{CL2} = \frac{1}{n}\sum_i w_i^2 \mathrm{E}\left\{\mathrm{h}_i(\boldsymbol{\theta})\mathrm{h}_i'(\boldsymbol{\theta})\right\}.$$

Theorems 2 and 3 show respectively the asymptotic properties of the CL1 and CL2 estimators when $Y_{i1}, \ldots, Y_{ik_i}$ are independent for each i. The theorems are proved by comparing the Godambe information matrix of $\boldsymbol{\psi}_{CL1}$ or $\boldsymbol{\psi}_{CL2}$ with average Fisher's information matrix:

$$\bar{\mathbf{F}}(\boldsymbol{\theta}) = \lim_{n\to\infty} \frac{1}{n} \sum_i \mathrm{E}\left[\frac{\partial l_{k_i}(\mathbf{Y}_i, \boldsymbol{\theta})}{\partial \boldsymbol{\theta}}\right]\left[\frac{\partial l_{k_i}(\mathbf{Y}_i, \boldsymbol{\theta})}{\partial \boldsymbol{\theta}}\right]'. \tag{6}$$

The proofs are straightforward but involves analyzing submatrices of the information matrices; they are given in Zhao (2004).

Theorem 2 *Assume the conditions in Theorem 1. Let* $\mathbf{G}_{CL1}(\boldsymbol{\theta})$ *be the Godambe information matrix defined in (4) with* $D_{\boldsymbol{\psi}}$ *and* $M_{\boldsymbol{\psi}}$ *as in (5) and* $\bar{\mathbf{F}}(\boldsymbol{\theta})$ *be Fisher's information matrix defined in (6). Suppose* $\boldsymbol{\theta}_0 = (\boldsymbol{\theta}'_{0,1}, \boldsymbol{\theta}'_{0,2})'$ *is the true value of* $\boldsymbol{\theta}$. *When* $Y_{i1}, \ldots Y_{ik_i}$ *are independent for each* i, *i.e.* $f_{k_i}(\mathbf{y}_i; \boldsymbol{\theta}_0) = \prod_j f_1(y_{ij}; \boldsymbol{\theta}_{0,1})$, *we have (a)*

$$\mathbf{G}_{CL1}(\boldsymbol{\theta}_0) = \bar{\mathbf{F}}(\boldsymbol{\theta}_0)$$

when $\boldsymbol{\theta}_{0,2}$ *is in the interior of the parameter space; and (b)*

$$\lim_{\boldsymbol{\theta}_2 \to \boldsymbol{\theta}_{0,2}} \mathbf{G}_{CL1}(\boldsymbol{\theta}_{0,1}, \boldsymbol{\theta}_2) = \lim_{\boldsymbol{\theta}_2 \to \boldsymbol{\theta}_{0,2}} \bar{\mathbf{F}}(\boldsymbol{\theta}_{0,1}, \boldsymbol{\theta}_2)$$

when $\boldsymbol{\theta}_{0,2}$ *is on the boundary of the parameter space and* $\bar{\mathbf{F}}(\boldsymbol{\theta})$ *and* $\mathbf{G}_{CL1}(\boldsymbol{\theta})$ *are continuous at* $\boldsymbol{\theta}_{0,2}$.

Theorem 3 *Assume the conditions in Theorem 1. Under independence, i.e.,* $f_k(\mathbf{y}; \boldsymbol{\theta}_0) = \prod_j f_1(y_j; \boldsymbol{\theta}_{0,1})$, *we have*

$$\begin{aligned} &\mathrm{AVar}(\hat{\boldsymbol{\theta}}_{1,CL2}) = \mathrm{AVar}(\hat{\boldsymbol{\theta}}_{1,MLE}), \\ &\mathrm{AVar}(\hat{\boldsymbol{\theta}}_{2,CL2}) - \mathrm{AVar}(\hat{\boldsymbol{\theta}}_{2,MLE}) \text{ is non-negative definite,} \end{aligned}$$

where AVar *denotes asymptotic covariance matrix. The relations hold for the limits of the covariance matrices if* $\boldsymbol{\theta}_{0,2}$ *is on the boundary of the parameter space.*

Theorem 2 suggests that under independence the CL1 approach is asymptotically equivalent to the ML method. Theorem 3 suggests that under independence the CL2 estimate of $\boldsymbol{\theta}_1$ is asymptotically as efficient as the MLE whereas that of $\boldsymbol{\theta}_2$ is less efficient than the MLE.

5 Jackknife Estimate of the Asymptotic Covariance Matrix of $\hat{\boldsymbol{\theta}}$

Here, $\hat{\boldsymbol{\theta}}$ denotes either the CL1 or the CL2 estimate of $\boldsymbol{\theta}$. Different methods can be considered to estimate the asymptotic covariance matrix of $\hat{\boldsymbol{\theta}}$. One approach is to evaluate the Godambe information matrix at $\hat{\boldsymbol{\theta}}$ analytically. This can be time-consuming or even sometimes impossible. Another approach is the jackknife with one family removed at a time. Let $\tilde{\boldsymbol{\theta}}_{-i}$ be the estimator of $\boldsymbol{\theta}$ with $\mathbf{Y}_i$ deleted. The jackknife estimator of the covariance matrix of $\hat{\boldsymbol{\theta}}$ is

$$\mathbf{V}_J = \sum_i^n (\tilde{\boldsymbol{\theta}}_{-i} - \hat{\boldsymbol{\theta}})(\tilde{\boldsymbol{\theta}}_{-i} - \hat{\boldsymbol{\theta}})'.$$

A proof of consistency of this estimator for the i.i.d. case and the case with covariates is given by Joe (1997) (Chapter 10). The theorem can be directly applied to familial data with fixed family structure. Normally, family structures are not identical, but we assume that the population under consideration is a finite mixture of family structures. Since Joe's results hold for each family structure. and the estimating function is a summation over all family structures, the consistency can be generalized from his proof.

For large samples, the jackknife estimator can be obtained by deleting a block of families at a time in order to reduce the computation time.

6 Efficiency Comparisons

The CL methods are considered for reasons of computational ease. Theoretically they are not fully efficient. We would like to know when the CL estimates tend to lose more efficiency and how much the efficiency loss is. In this section, we offer some answers to these questions.

We define the asymptotic relative efficiency (ARE) of the CL estimate as

$$\text{ARE}(\hat{\theta}_{CL}) = \text{AVar}(\hat{\theta}_{MLE})/\text{AVar}(\hat{\theta}_{CL}),$$

where $\text{AVar}(\hat{\theta}_{MLE})$ and $\text{AVar}(\hat{\theta}_{CL})$ are derived from the inverses of Fisher's and the Godambe information matrices respectively.

We make comparisons for three types of variables: continuous, binary and survival subject to right censoring. For each type of data we select one distribution as a representative: the MVN for continuous, the MVP for binary and the MVN with random right censoring for survival. For each model, we select some cases in which the comparisons can be made. With these comparisons, we gain some insight into how the efficiency is affected by factors, such as degree of dependence, family size and data type.

6.1 Models and Methods

Covariate

In all the cases, we consider one covariate. Let $\mathbf{x}_i = (x_{i1}, \ldots, x_{ik_i})$ be the vector of covariate values of family i. To simplify the comparisons, we assume that the values in $\mathbf{x}_i$ are independent realizations of a random variable with mean 0 and variance 1. The assumptions on the mean and the variance can be easily satisfied by centering and scaling.

Dependence Structures

One dependence structure we investigate is the exchangeable dependence structure. The other one is the dependence structure of family units containing one parent and multiple offspring (relevant for data on family members affected with an autosomal dominant genetic disorder). The second case has two levels of dependence: parent-offspring and sib-sib associations. We also consider families with either fixed or varying family sizes. Results of these two cases can give us some idea for more complicated dependence structures.

Models

We list the representative models used for the continuous, binary or right-censored familial data. Under each model, we summarize the special cases chosen to indicate some general patterns in the efficiencies of the CL1 and CL2 estimates.

(1) Continuous response: MVN model

In this model, $\mathbf{Y}_i \sim N(\mathbf{X}_i\boldsymbol{\beta}, \sigma^2\mathbf{R}_i(\boldsymbol{\alpha}))$, where $\boldsymbol{\beta} = (\beta_0, \beta_1)'$ and $\mathbf{R}_i(\boldsymbol{\alpha}) = [\rho_{ijj'}(\boldsymbol{\alpha})]$ with $\boldsymbol{\alpha} = (\alpha_1, \ldots, \alpha_q)'$.

The closed form of the likelihood of a MVN distribution enables us to derive the theoretical asymptotic variances of both the ML and the CL estimates, so that the efficiency can be compared analytically. We treat the covariate as a random variable and the variances are derived based on its asymptotic properties. The ARE of $\hat{\beta}_1$ have a relatively simple expression and allows us to study its general properties. For other parameters, we calculate the efficiencies for some special cases:

Case 1 Exchangeable non-negative dependence.

Case 2 One parent and multiple offspring. The number of offspring varies from 1 to 5 with equal proportion. The parent-offspring correlation (ρ_1) and the sib-sib correlation (ρ_2) need to satisfy: $k^*\rho_1^2 - (k^* - 1)\rho_2 < 1$ (Srivastava and Katapa, 1986), where k^* is the maximum number of offspring in a family. We fix the value of ρ_1 at four levels, (0, 0.3, 0.5 and 0.8), while vary the value of ρ_2 within its full range.

Case 3 One parent and multiple offspring with various combinations of family sizes. We focus on studying the impact of the distribution of family sizes on the efficiencies. We generated 500 sets of families and for each set, randomly generate families with numbers of offspring varying from 1 to 7. Therefore, each set has a different combination of family sizes. We calculated the efficiencies for each combination at $\rho_1 = 0.4$ and $\rho_2 = 0.8$. We chose ρ_2 far away from ρ_1 since the effect of the relative dispersion of family sizes is more obvious under strong conditional sib-sib dependence.

Our investigation of the MVN model is more thorough than the other two distributions. We hope the results can provide us with insight into the general behavior of the CL estimates, not just limited to the continuous response.

(2) Binary response: MVP model

In a MVP model, it is assumed that the observed binary response vector $\mathbf{Y}_i$ depends on a latent random vector $\mathbf{Z}_i \sim N(\boldsymbol{\mu}_i, \mathbf{R}_i(\boldsymbol{\alpha}))$, where $\boldsymbol{\mu}_i = \mathbf{X}_i\boldsymbol{\beta}$. When the value of Z_{ij} exceeds the fixed threshold 0, $Y_{ij} = I(Z_{ij} > 0)$.

β_0	β_1	$\Pr(Y=1)$	β_0	β_1	$\Pr(Y=1)$	β_0	β_1	$\Pr(Y=1)$
0	0	0.50	0.67	0	0.749	1.65	0	0.951
0	1	$0.159 \sim 0.841$	0.67	1	$0.371 \sim 0.953$	1.65	1	$0.742 \sim 0.996$
0	2	$0.023 \sim 0.977$	0.67	2	$0.092 \sim 0.996$	1.65	2	$0.363 \sim 1.000$

Table 1: Range of $\Pr(Y = 1)$ for each combination of β_0 and β_1 (MVP model).

In our comparisons, we simulate the values of the covariate from a uniform distribution on $(-1, 1)$. These values are independent both within a family and among families. The efficiency is compared at different levels of β_0 and β_1 (listed in Table 1). Only positive values of $\boldsymbol{\beta}$ were investigated. By symmetry, the results can be extended to negative values. The efficiencies are calculated for the following cases:

Case 1 Bivariate case ($k_i = 2$ for all families). We focus on the impact of the familial dependence on the efficiency of $\hat{\beta}_{1,CL1}$. We generate $\mathbf{x}_i$ values for 1000 families. The $\text{ARE}_{\hat{\beta}_{1,CL1}}$ is evaluated at the nine combinations of β_0 and β_1 in Table 1 with ρ varying in the range $(-1, 1]$.

Case 2 Exchangeable dependence with varying family sizes. We generate the covariate values of 500 families with their sizes being randomly generated from 1 to 4. We compute

the efficiencies of the CL1 and CL2 estimates of all the parameters for the first four combinations of β_0 and β_1 in Table 1. The other combinations are not included since in those cases the numerical results are not reliable when ρ exceeds a certain level. For each combination, ρ varies from 0 to 0.9.

Case 3 One parent and multiple offspring. We generate the size and covariate values for 500 families. In each family, the number of offspring was randomly generated from 1 to 3. The same four combinations for β_0 and β_1 in Case 2 are considered. We first fix the parent-offspring correlation ρ_1 at 0.3 vary the sib-sib correlation ρ_2 from 0 to 0.9. We, then, set ρ_1 at 0.6 and vary ρ_2 from 0.3 to 0.9.

(3) Survival Data Subject to Right Censoring: MVN Model

Comparisons of this case will help us to gain some knowledge on how the CL1 or CL2 estimates are affected by the presence of censoring. We consider the MVN model for the log survival as in (1) with $\nu_{ij} = \beta_0 + \beta_1 x_{ij}$, but with the response subject to random right censoring. The comparisons are done by simulations in which the likelihood is evaluated by numerical integration.

In the simulation study, we consider an exchangeable dependence structure. Four levels of dependence were considered: $\rho = 0.1$, 0.4, 0.7 and 0.9. We fix $\beta_0 = 1$, $\beta_1 = 1$ and $\sigma^2 = 4$ since they have little impact on the efficiency. In each simulation we generate 5,000 samples each containing 2,000 families. The family size are randomly generated from 1 to 4. The values of the covariate is generated from uniform $(-1, 1)$. The data are generated with three different censoring rates: 0, 0.2, 0.4 and 0.8. The log censoring random variable is assumed to be $N(\mu_C, \sigma^2)$ with μ_C chosen to achieve the censoring rates.

6.2 Results

In our investigations, we find that the efficiencies are mainly affected by two factors, degree of dependence and distribution of family sizes. Therefore, we summarize our results by these two factors. Under each factor, we present our results by type of parameter: the regression parameter (β_1), the other univariate parameters (β_0 and σ^2) and the dependence parameters.

Impact of Dependence

(a) β_1

(1) MVN. We first give the expression of $\text{ARE}_{\hat{\beta}_{1,CL1}}$ and show the results of the special cases. We, then, give the expression of $\text{ARE}_{\hat{\beta}_{1,CL2}}$ and compare it with $\text{ARE}_{\hat{\beta}_{1,CL1}}$.

The MLE of $\boldsymbol{\beta}$ is $\hat{\boldsymbol{\beta}}_{MLE} = \left(\sum_i \mathbf{X}_i'\mathbf{R}_i^{-1}\mathbf{X}_i\right)^{-1}\sum_i \mathbf{X}_i'\mathbf{R}_i^{-1}\mathbf{Y}_i$. The variance of $\hat{\boldsymbol{\beta}}_{MLE}$ is

$$\mathrm{Var}(\hat{\boldsymbol{\beta}}_{MLE}) = \sigma^2\left(\sum_i \mathbf{X}_i^T\mathbf{R}_i^{-1}\mathbf{X}_i\right)^{-1}.$$

The CL1 estimate of $\boldsymbol{\beta}$ is the ordinary least squares estimate, i.e., $\hat{\boldsymbol{\beta}}_{CL1} = \left(\sum_i \mathbf{X}_i'\mathbf{X}_i\right)^{-1}\sum_i \mathbf{X}_i'\mathbf{Y}_i$. Consequently,

$$\mathrm{Var}(\hat{\boldsymbol{\beta}}_{CL1}) = \sigma^2\Big(\sum_i \mathbf{X}_i'\mathbf{X}_i\Big)^{-1}\Big(\sum_i \mathbf{X}_i'\mathbf{R}_i\mathbf{X}_i\Big)\Big(\sum_i \mathbf{X}_i'\mathbf{X}_i\Big)^{-1}.$$

By treating the covariate as a random variable with mean 0 and variance 1, we obtain

$$\mathrm{AVar}(\hat{\boldsymbol{\beta}}_{1,MLE}) \simeq \sigma^2/\sum_i \mathrm{tr}\,\mathbf{R}_i^{-1} \tag{7}$$

$$\mathrm{AVar}(\hat{\boldsymbol{\beta}}_{1,CL1}) \simeq \sigma^2/K, \tag{8}$$

where $K = \sum_i k_i$, the total number of individuals. The relative efficiency of $\hat{\beta}_{1,CL1}$ is approximately

$$\mathrm{ARE}_{\hat{\beta}_{1,CL1}} = \frac{\mathrm{AVar}(\hat{\beta}_{1,MLE})}{\mathrm{AVar}(\hat{\beta}_{1,CL1})} = \frac{K}{\sum_i \mathrm{tr}\,\mathbf{R}_i^{-1}}.$$

When the dependence is strong, $\mathbf{R}_i$ is close to be singular and, as a result, $\mathrm{ARE}_{\hat{\beta}_{1,CL1}}$ can be close to 0.

For Case 1, common correlation ρ and family size k, the expression can be simplified as

$$\mathrm{ARE}_{\hat{\beta}_{1,CL1}} = 1 - \frac{(k-1)\rho^2}{1+(k-1)\rho}.$$

Clearly, the estimate $\hat{\beta}_{1,CL1}$ loses efficiency when ρ increases. As ρ approaches 1, $\mathrm{ARE}_{\hat{\beta}_{1,CL1}}$ approaches to 0. This is because when $\rho = 1$, $\hat{\beta}_{1,MLE}$ has no estimation error, whereas $\hat{\beta}_{1,CL1}$ has estimation error.

Figure 1 shows $\mathrm{ARE}_{\hat{\beta}_{1,CL1}}$ of Case 2 (one parent and multiple offspring). The efficiency decreases with ρ_1 and approaches zero when the conditional sib-sib correlation, $\tilde{\rho}_2 = (\rho_2 - \rho_1^2)/(1-\rho_1^2)$, approaches to its lower and upper bounds.

The CL2 estimate is $\hat{\boldsymbol{\beta}}_{CL2} = \left(\sum_i \mathbf{X}_i'\mathbf{A}_i^*\mathbf{X}_i\right)^{-1}\sum_i \mathbf{X}_i'\mathbf{A}_i^*\mathbf{Y}_i$, where $\mathbf{A}_i^* = 1$ if $k_i = 1$, otherwise, $\mathbf{A}_i^* = \left(a_{ijj'}/(1-k_i)\right)$ with

$$a_{ijj'} = \begin{cases} \sum_{l\neq j}(1-\rho_{ijl}^2)^{-1} & \text{for } j = j', \\ -\rho_{ijj'}(1-\rho_{ijj'}^2)^{-1} & \text{for } j \neq j'. \end{cases}$$

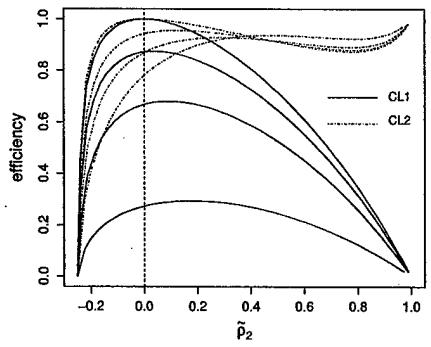

Figure 1: $\text{ARE}_{\hat{\beta}_{1,CL2}}$ and $\text{ARE}_{\hat{\beta}_{1,CL1}}$ for Case 2 (MVN model). $\tilde{\rho}_2$ is the sib-sib correlation conditional on the parent. The solid lines are the efficiencies of the CL1 method at different levels of the ρ_1 and the dashed lines are those of the CL2 method.

The variance of $\hat{\boldsymbol{\beta}}_{CL2}$ is

$$\text{Var}(\hat{\boldsymbol{\beta}}_{CL2}) = \sigma^2\Big(\sum_i \mathbf{X}_i'\mathbf{A}_i^*\mathbf{X}_i\Big)^{-1}\Big(\sum_i \mathbf{X}_i'\mathbf{A}_i^*\mathbf{R}_i\mathbf{A}_i^*\mathbf{X}_i\Big)\Big(\sum_i \mathbf{X}_i'\mathbf{A}_i^*\mathbf{X}_i\Big)^{-1}.$$

By treating the covariate as a random variable with mean 0 and variance 1, we have

$$\text{AVar}(\hat{\beta}_{1,CL2}) \simeq \frac{\sum \text{tr}\,\mathbf{B}_i^*}{(\sum \text{tr}\,\mathbf{A}_i^*)^2}\sigma^2, \tag{9}$$

where $\mathbf{B}_i^* = \mathbf{A}_i^*\mathbf{R}_i\mathbf{A}_i^*$.

The following theorem, with proof in the Appendix, shows that the CL2 estimate of β_1 is asymptotically more efficient than the CL1 estimate.

Theorem 4 *For the case of one covariate, under the assumption that the values of* $x_{i1}, \ldots, x_{ik_i}$ *are independent realizations of a random variable with mean 0 and variance 1,*

$$AVar(\hat{\beta}_{1,CL2}) \leq AVar(\hat{\beta}_{1,CL1}),$$

where $AVar(\hat{\beta}_{1,CL1})$ *and* $AVar(\hat{\beta}_{2,CL1})$ *are given in (8) and (9), respectively.*

For the exchangeable case with $k_i \geq 2$, $\text{ARE}_{\hat{\beta}_{1,CL2}} = \{[1+\rho-\rho^2(1-a)](1-b\rho)\}^{-1}$, where $a = K^{-1}\sum k_i/(k_i-1)$ and $b = K^{-1}\sum k_i/[1+(k_i-1)\rho]$. When $\rho > 0$, since $0 \leq a \leq 1$ and $b \geq 1/\bar{k}$, where $\bar{k} = K/n$, $\text{ARE}_{\hat{\beta}_{1,CL2}} \geq (1+\rho-\rho^2)^{-1}(1-\rho/\bar{k})^{-1} \geq (1+\rho-\rho^2)^{-1} \geq 0.8$.

The $\text{ARE}_{\hat{\beta}_{1,CL2}}$ for Case 2 is plotted in Figure 1. The plots show that, unlike the CL1 estimator, the CL2 estimator performs very well when ρ_1 or $\tilde{\rho}_2$ is large.

(2) MVP. The results for the bivariate case (Case 1) are plotted in Figure 2. Similar to the MVN model, the stronger the dependence among $\mathbf{Z}_i$, the less efficient is $\hat{\beta}_{1,CL1}$. When $\beta_1 = 0$ and $\rho = 1$, $\text{ARE}_{\hat{\beta}_{1,CL1}} = 0$. When $\beta_1 \neq 0$, there is a less efficiency loss.

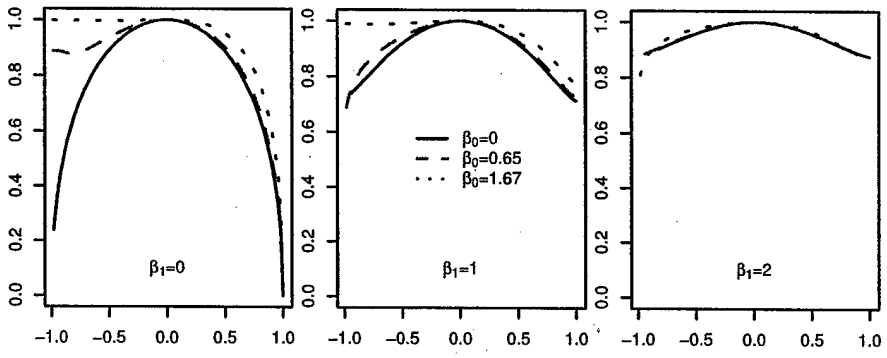

Figure 2: ARE of $\hat{\beta}_{1,CL1}$ when family size $k = 2$ (Case 1, MVP model).

The results for the exchangeable case (Case 2) are show in Figure 3. The CL2 estimator of β_1 is better than the CL1 estimator, especially when ρ is close to 1 and β_1 is close to 0. For the case of one parent and multiple offspring (Case 3), given ρ_1, the impact of ρ_2 on the efficiency is similar to the exchangeable case; also, the CL1 estimate loses more efficiency when $\rho_1 = 0.6$ than when $\rho_1 = 0.3$.

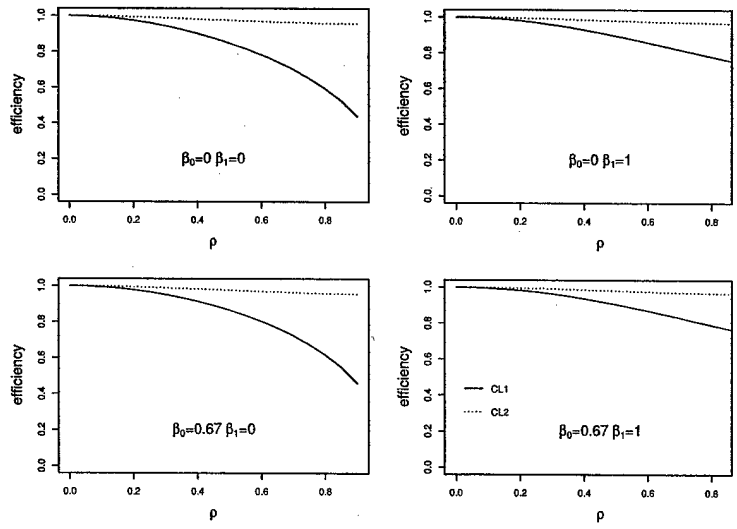

Figure 3: ARE of $\hat{\beta}_{1,CL1}$ and $\hat{\beta}_{1,CL2}$ for the exchangeable case with family size varying from 1 to 4 (Case 2, MVP model).

(3) MVN with Right Censoring. The efficiencies from the simulations are shown in Table 2. Regardless of the degree of censoring, $\hat{\beta}_{1,CL1}$ loses efficiency as ρ increases. However, the loss of efficiency becomes less when the censoring rate r increases. Whereas, the performance of $\hat{\beta}_{1,CL2}$ is satisfactory, even though it loses some efficiency as ρ increases.

		CL1				CL2			
ρ	r	β_0	β_1	σ^2	ρ	β_0	β_1	σ^2	ρ
0.1	0	0.996	0.985	1.000	0.991	0.998	0.997	1.000	0.913
	0.2	0.995	0.984	0.999	0.997	0.996	0.995	1.000	0.889
	0.5	0.994	0.988	0.996	0.992	0.995	0.996	0.999	0.876
	0.8	0.998	0.994	0.999	0.996	1.000	0.999	1.000	0.884
0.4	0	0.937	0.788	0.979	0.957	0.960	0.968	0.987	0.967
	0.2	0.945	0.807	0.980	0.946	0.974	0.970	0.993	0.964
	0.5	0.945	0.842	0.973	0.936	0.978	0.969	0.992	0.928
	0.8	0.962	0.906	0.976	0.943	0.986	0.977	0.993	0.903
0.7	0	0.885	0.447	0.924	0.916	0.942	0.958	0.961	0.957
	0.2	0.882	0.480	0.909	0.908	0.944	0.949	0.961	0.952
	0.5	0.874	0.547	0.902	0.891	0.949	0.945	0.966	0.922
	0.8	0.894	0.677	0.905	0.887	0.964	0.939	0.966	0.898
0.9	0	0.846	0.160	0.863	0.885	0.924	0.966	0.934	0.943
	0.2	0.841	0.183	0.845	0.876	0.926	0.947	0.937	0.940
	0.5	0.840	0.239	0.839	0.869	0.943	0.932	0.949	0.925
	0.8	0.871	0.353	0.867	0.889	0.982	0.913	0.976	0.919

Table 2: ARE of the CL1 and CL2 for the exchangeable case with family size varying from 1 to 4 (MVN model with right censoring).

(b) β_0 and σ^2

From all the cases we investigated, the performance the CL1 and CL2 estimates is satisfactory. In general, the efficiencies decrease with the degree of dependence, but the impact of the dependence on these estimates is fairly small. Since the parameters β_0 and σ^2 are often considered as less important in familial analysis, we do not give the details of the comparisons. As an example, see Table 2 for the case of MVN model with right censoring.

(c) Dependence parameters

(1) MVN. In Figure 4, we plot the efficiency of $\hat{\rho}_{CL1}$ and $\hat{\rho}_{CL2}$ for the exchangeable case with two family sizes 2 and 6 of proportion 3:1. In Figure 5, we plot the results of the case of one parent and multiple offspring (Case 2).

(2) MVP. Figure 6 shows the results of the exchangeable case (Case 2). The results are

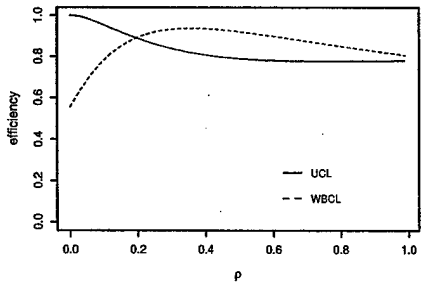

Figure 4: Efficiency of $\hat{\rho}_{CL1}$ and $\hat{\rho}_{CL2}$ for the exchangeable case (Case 1, MVN model); family sizes are 2 or 6 with proportion 3:1.

similar for Case 3 (one parent and multiple offspring). The efficiencies of CL1 and CL2 are quite high in all cases.

(3) MVN with right censoring The results are shown in Table 2. The efficiencies of both the CL estimates slightly decrease when the dependence become stronger. The impact of the dependence is similar to the case when there is no censoring. It appears that the CL2 method is slightly less efficient at a high censoring rate than at a low censoring rate.

(d) Conclusion

In summary, $\hat{\beta}_{1,CL1}$ is most affected by the degree of dependence. The ARE can be close to 0 when the dependence is strong. For the binary and censoring cases, the impact of dependence on $\hat{\beta}_{1,CL1}$ is less than that for the continuous case. On the other hand, $\hat{\beta}_{1,CL2}$ is much less affected by the dependence. The efficiency is considerably improved when the dependence is strong.

In most cases we investigated, both CL methods yield reasonable estimates of the dependence parameters. The CL2 method is generally better for stronger dependence, even though exceptions can occur; the CL1 method is better for weaker dependence.

The Impact of Family Sizes

The impact of the distribution of family sizes is investigated for the CL1 method and only based on the MVN model.

(a) Exchangeable dependence

In this case, we have $\text{ARE}_{\hat{\beta}_{1,CL1}} = [1 + b\rho^2/(1-\rho)]^{-1}$, where

$$b = \frac{1}{K}\sum \frac{k_i(k_i-1)}{1+(k_i-1)\rho}.$$

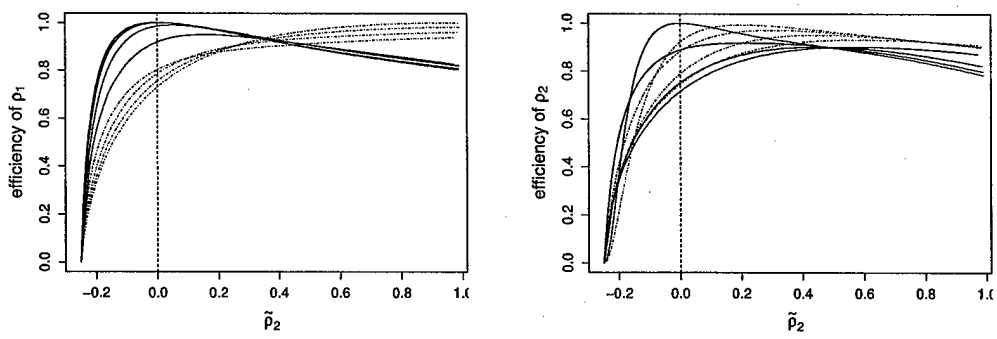

(a) ρ_1 (b) ρ_2

Figure 5: The efficiencies of the CL dependence parameter estimators for Case 2 (one parent and multiple offspring; MVN model). $\tilde{\rho}_2$ is the sib-sib correlation conditional on the parent. The solid lines are the efficiencies of the CL1 method at different levels of the ρ_1 and the dashed lines are those of the CL2 method.

The term $\dfrac{k(k-1)}{1+(k-1)\rho}$ is a strictly convex function of k since

$$\frac{d^2}{dk^2}\left[\frac{k(k-1)}{1+(k-1)\rho}\right] = \frac{2(1-\rho)}{[1+(k-1)\rho]^3} \geq 0.$$

By Jensen's inequality,

$$b \geq \frac{\bar{k}-1}{1+(\bar{k}-1)\rho}.$$

It follows that

$$\mathrm{ARE}_{\hat{\beta}_{1,CL1}} \leq 1 - \frac{(\bar{k}-1)\rho^2}{1+(\bar{k}-1)\rho}.$$

Equality holds if and only if $k_i = \bar{k}$ for all i. This implies that: one, for given K and n, the efficiency of $\mathrm{ARE}_{\hat{\beta}_{1,CL1}}$ is always lower when family sizes vary; two, roughly speaking, $\mathrm{ARE}_{\beta_{1,CL1}}$ decreases when $\bar{k}$ increases.

For other parameters, the expressions are more complicated. But, there is one thing in common for all of our studied cases: the estimates are most efficient when the family sizes are equal.

(b) One parent and multiple offspring

In Figure 7 and 8, we plot the efficiency against the mean of k_i^* (number of offspring), $\bar{k}^*$, and the variance-mean ratio of k_i^*, V/M. The following patterns were observed:

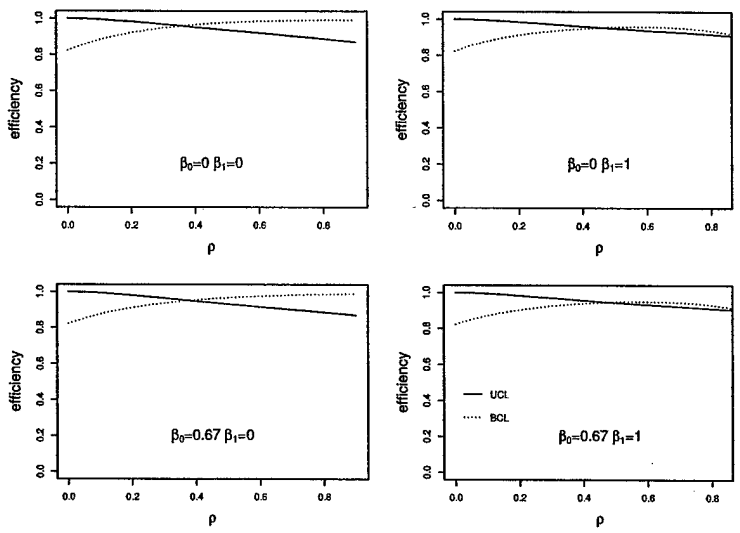

Figure 6: ARE of $\hat{\rho}_{CL1}$, and $\hat{\rho}_{CL2}$ for exchangeable dependence with varying family sizes (Case 2, MVP model).

1. $\text{ARE}_{\hat{\beta}_{1,CL1}}$ mainly depends on $\bar{k}^*$. Figure 7 shows that the efficiency is monotonely decreasing in $\bar{k}^*$.

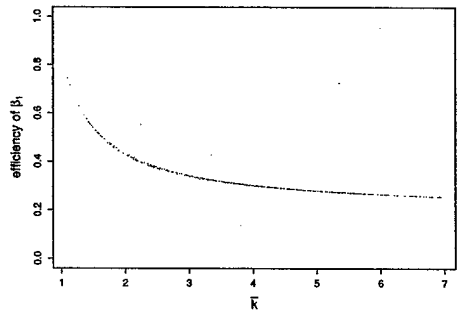

Figure 7: ARE of $\hat{\beta}_{1,CL1}$ against average number of offspring, $\bar{k}^*$ for one parent and multiple offspring with various combinations of family sizes (Case3, MVN model).

2. Figure 8 shows the efficiencies of the other four parameters. The x-axis is $\bar{k}^*$ and the y-axis is the variance-mean ratio of the k_i^*s. For $\hat{\beta}_{0,CL1}$, $\hat{\sigma}^2_{CL1}$ and $\hat{\rho}_{2,CL1}$, the efficiency is almost linearly decreasing (at a slow rate) with both $\bar{k}^*$ and V/M. On the other hand, $\text{ARE}_{\hat{\rho}_{1,CL1}}$ is mainly affected by V/M.

(c) Conclusion:

In general, the efficiencies of the CL1 estimates tend to decrease as the average family size increases and the relative dispersion of family size increases. When the relative dispersion of

family sizes is large, the data are mainly formed by either small or large families. Individuals or pairs contributed by different families are equally weighted in the CL1 method. That is why large relative dispersion of family size combined with high dependence has a strong effect on the efficiency.

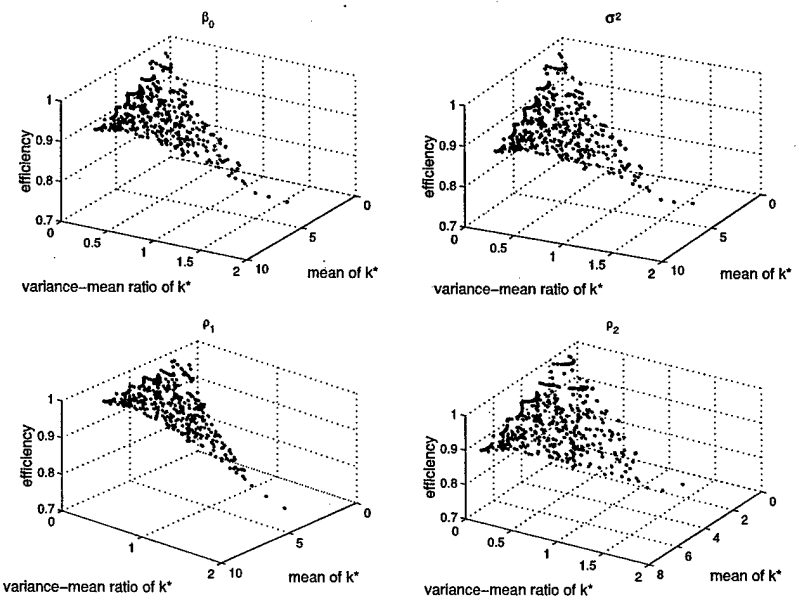

Figure 8: ARE of $\hat{\beta}_{0,CL1}$, $\hat{\sigma}^2_{CL1}$, $\hat{\rho}_{1,CL1}$ and $\hat{\rho}_{2,CL1}$ for one parent and multiple offspring with various combinations of family sizes (Case3, MVN model).

7 Example

This research is motivated by analysis of data from patients affected by an autosomal dominant genetic disorder neurofibromatosis 1 (NF1) (Friedman and Birch, 1997). In this section, we use a multivariate probit model to analyze the presence of subcutaneous neurofibromas on NF1 patients and use the CL methods to estimate the parameters.

The data are from two large NF1 databases: the National Neurofibromatosis Foundation International Database and the Neurofibromatosis Institute Database. We assume that the families are representative and behave like a random sample. There are 867 patients included in our analysis. These patients are from 371 different families. Among all the families there are 12 of size one, 264 of size two, 68 with three, 18 with four, 5 with five, 2 with six and 2 with seven. The numbers of affected pairs included are summarized in Table 3.

Since subcutaneous neurofibromas are known to be increasing in frequency with age, age is included as a covariate (on the log-log scale). We consider three dependence parameters:

Type of relative pair	Number of Pairs
siblings	353
parent-offspring	264
second degree	57
third degree	23
fourth degree	1

Table 3: Number of affected pairs included in the analysis of presence of subcutaneous neurofibromas in NF1 patients.

ρ_{ss} (sib-sib correlation), ρ_{po} (parent-offspring correlation) and ρ_{2+} (correlation between any relative pair higher than second degree). The correlation between a third or fourth degree relative pair is set to be equal to the correlation between a second degree relative pair because there are only 24 pairs of third or fourth degree. The parameters are estimated using the CL1, CL2 and MLE methods. The maximum family size is seven in this dataset, so we are able to compute the MLE using the second order approximation of Joe (1995) for MVN rectangle probabilities. The standard errors of the CL1 and CL2 estimates are obtained by the jackknife method. The results are reported in Table 4.

	CL1		CL2		MLE	
	estimate	s.e.	estimate	s.e.	estimate	s.e.
Covariate coefficients:						
intercept	-3.109	0.291	-3.121	0.288	-3.199	0.240
age*	2.517	0.254	2.536	0.250	2.606	0.207
Correlations:						
sib-sib (ρ_{ss})	0.660	0.099	0.594	0.121	0.652	0.093
parent-offspring (ρ_{po})	0.493	0.116	0.443	0.109	0.463	0.096
other (ρ_{2+})	0.710	0.311	0.698	0.322	0.670	0.275

age*=log(log(age+2))

Table 4: Parameter estimates of the Probit model for the presence of subcutaneous neurofibromas in NF1 patients.

The point estimates from all the three methods basically agree with each other. The standard errors of the CL1 and CL2 estimates are close to each other, but around 20% larger than those of the MLEs. It is no surprise that the estimates of ρ_{2+} have large standard errors because there are only a small number of 2+ relative pairs and half of them are from four families. The estimated correlations suggest that the dependence structure is not far from exchangeable.

8 Discussion and further research

The two proposed CL methods can greatly reduce computation in parameter estimation when the ML method is computationally too difficult to implement. The example and others in Zhao (2004). demonstrate that the CL1 and CL2 methods work well in practice. Our investigations in the asymptotic efficiency comparisons showed that the relative asymptotic efficiencies of these two methods are satisfactory except for some extreme cases. Moreover, those investigations help us better understand under what situations these methods work well and provide hints on how to improve them. Based on our investigations, we recommend the CL2 method when the initial data analysis suggests a strong dependence. It generally provides better estimation for all the parameters, especially the regression parameters. However, it may be numerically more difficult to implement since computation increases when the total number of parameters increases. We recommend the CL1 method when the initial data analysis suggests a weak dependence. Moreover, when the CL2 method is utilized, we can use the CL1 estimate as the starting value.

As noted in Section 4, the estimation with the CL methods can be done with numerical optimization rather than solving systems of non-linear equations. If the sample size is not large, the numerical optimalization should be done with a constraint that the estimated dependence parameters lie inside the parameter space of the multivariate joint distribution. Without this constraint, the solution of the estimating equations may be outside of the parameter space. For models based on the MVN distribution, the constraint on the dependence parameters is that the correlation matrix of each family is positive definite.

To improve the efficiency of estimating $\boldsymbol{\beta}$ in the CL1 method, we consider adding weights in the estimating function in (1). When F_1 is parametrized so that $\nu_{ij} = \eta(\mathbf{x}_{ij}; \boldsymbol{\beta})$, then in (1), one could change the estimating equation for $\boldsymbol{\beta}$ from $\sum_i \sum_j \frac{\partial l(Y_{ij};\nu_{ij},\boldsymbol{\gamma})}{\partial \nu} \frac{\partial \nu_{ij}}{\partial \boldsymbol{\beta}}$ to

$$\sum_i X_i^* W_i \mathbf{g}(Y_{i1}, \ldots, Y_{ik_i}; \boldsymbol{\beta}, \boldsymbol{\gamma}),$$

where $\mathbf{g}(Y_{i1}, \ldots, Y_{ik_i}; \boldsymbol{\beta}, \boldsymbol{\gamma})$ is the vector of $\partial l(Y_{ij}; \nu_{ij}, \boldsymbol{\gamma})/\partial \nu$ for $j = 1, \ldots, k_i$, W_i is a $k_i \times k_i$ weight matrix, $\mathbf{X}_i^* = (\partial \eta(\mathbf{x}_{i1})/\partial \boldsymbol{\beta}, ..., \partial \eta(\mathbf{x}_{ik})/\partial \boldsymbol{\beta})$ $[\mathbf{X}_i^* = (\mathbf{x}_{i1}, \ldots, \mathbf{x}_{ik_i})$ when $\eta(\mathbf{x}, \boldsymbol{\beta}) = \mathbf{x}'\boldsymbol{\beta}]$. Based on the matrix version of the Cauchy-Schwarz inequality (Chaganty, 1997), we can determine the optimal $\mathbf{W}_i$'s; the asymptotic efficiency of the estimates of $\boldsymbol{\beta}$ with these $\mathbf{W}_i$'s has been shown to be close to the asymptotic efficiency of the ML estimator of $\boldsymbol{\beta}$ for special cases of the MVN and MVP models. Future research could be done on weighted versions of the estimating equations in (1) and (3); this includes an iterative approach to determine

good weight matrices.

Finally, we provide some remarks on the CL and related estimating equation methods.

The CL1 and CL2 methods are not restricted to the models in this paper or to familial data. In particular, the CL2 method works for multivariate models, whether or not the parameters are common to the different margins. It works even when the univariate margins do not belong to the same distribution family. The parameters can be estimated as long as the bivariate marginal likelihoods can be evaluated. Therefore, we can consider a more general form of the BCL function:

$$\Psi^*_{BCL}(\boldsymbol{\theta}) = \sum_{i=1}^{n} w_i \sum_{j>j'} l_{i,jj'}(Y_{ij}, Y_{ij'}; \boldsymbol{\theta}),$$

where $l_{i,jj'}$ is the log likelihood of bivariate margin of $(Y_{ij}, Y_{ij'})$. This estimation approach can be considered if the high-dimensional likelihood is too difficult or impossible to compute.

The idea can be extended to trivariate CL. However, as the dimension becomes higher, the computational demands increase, so the implementation of such an approach may be more difficult. When all the parameters are either univariate or bivariate parameters, it is not known if the efficiency will be improved by using the likelihoods of marginal distribution of higher order.

Appendix: Proof of Theorem 4

(1) We first show that $\sum \operatorname{tr} \mathbf{A}_i^* \geq K$. For $k_i = 1$, $\operatorname{tr} \mathbf{A}_i^* = 1$. For $k_i > 1$,

$$\operatorname{tr} \mathbf{A}_i^* = (k_i - 1)^{-1} \sum_{j=1}^{k_i} \sum_{l \neq j} (1 - \rho_{ijl}^2)^{-1} \geq (k_i - 1)^{-1} \sum_{j=1}^{k_i} (k_i - 1) = k_i.$$

(2) Next we show that $\operatorname{tr} \mathbf{B}_i^* \leq \operatorname{tr} \mathbf{A}_i^*$. It is true when $k_i = 1$. For $k_i > 1$, we have

$$\operatorname{tr} \mathbf{A}_i^* = (k_i - 1)^{-1} \sum_{j=1}^{k_i} a_{ijj} \quad \text{and} \quad \operatorname{tr} \mathbf{B}_i^* = (k_i - 1)^{-2} \sum_{j=1}^{k_i} \mathbf{a}_{ij}' \mathbf{R}_i \mathbf{a}_{ij},$$

where $\mathbf{a}_{ij}$ is the jth column of $\mathbf{A}_i$. It suffices to show $\mathbf{a}_{ij}' \mathbf{R}_i \mathbf{a}_{ij} \leq a_{ijj}(k_i - 1)$. For $j = 1$,

$$\mathbf{a}_{i1}' \mathbf{R}_i \mathbf{a}_{i1} = a_{i11}^2 + 2a_{i11} \sum_{j=2}^{k_i} a_{i1j} \rho_{i1j} + \sum_{j=2}^{k_i} a_{i1j}^2 + \sum_{j \neq j' \geq 2} a_{i1j} a_{i1j'} \rho_{ijj'} \leq (k_i - 1) a_{i11}.$$

Since

$$a_{i11} + \sum_{j=2}^{k_i} a_{i1j} \rho_{i1j} = \sum_{j=2}^{k_i} \frac{1}{1 - \rho_{i1j}^2} - \sum_{j=2}^{k_i} \frac{\rho_{i1j}^2}{1 - \rho_{i1j}^2} = k_i - 1,$$

$$
\begin{aligned}
\mathbf{a}_{i1}'\mathbf{R}_i\mathbf{a}_{i1} &= (k_i-1)a_{i11} + a_{i11}\sum_{j=2}^{k_i} a_{i1j}\rho_{i1j} + \sum_{j=2}^{k_i} a_{i1j}^2 + \sum_{j\neq j'\geq 2} a_{i1j}a_{i1j'}\rho_{ijj'} \\
&= (k_i-1)a_{i11} - \Big(\sum_{j=2}^{k_i}\frac{1}{1-\rho_{i1j}^2}\Big)\Big(\sum_{j=2}^{k_i}\frac{\rho_{i1j}^2}{1-\rho_{i1j}^2}\Big) + \sum_{j=2}^{k_i}\frac{\rho_{i1j}^2}{(1-\rho_{i1j}^2)^2} \\
&\quad + \sum_{j\neq j'\geq 2}\frac{\rho_{i1j}\rho_{i1j'}\rho_{ijj'}}{(1-\rho_{i1j}^2)(1-\rho_{i1j'}^2)} \\
&= (k_i-1)a_{i11} - \sum_{j\neq j'\geq 2}\frac{\rho_{i1j}^2}{(1-\rho_{i1j}^2)(1-\rho_{i1j'}^2)} + \sum_{j\neq j'\geq 2}\frac{\rho_{i1j}\rho_{i1j'}\rho_{ijj'}}{(1-\rho_{i1j}^2)(1-\rho_{i1j'}^2)} \\
&= (k_i-1)a_{i11} - \sum_{j\geq j'\geq 2}\frac{\rho_{i1j}^2+\rho_{i1j'}^2-2\rho_{i1j}\rho_{i1j'}\rho_{ijj'}}{(1-\rho_{i1j}^2)(1-\rho_{i1j'}^2)}.
\end{aligned}
$$

Since $\rho_{i1j}^2+\rho_{i1j'}^2 \geq 2|\rho_{i1j}\rho_{i1j'}| \geq 2|\rho_{i1j}\rho_{i1j'}\rho_{ijj'}|$, we have $\rho_{i1j}^2+\rho_{i1j'}^2-2\rho_{i1j}\rho_{i1j'}\rho_{ijj'} \geq 0$. Thus, we proved that $\mathbf{a}_{i1}'\mathbf{R}_i\mathbf{a}_{i1} \leq (k_i-1)a_{i11}$. By symmetry, the inequality holds for all j.

From (1) and (2) we can easily obtain that $\mathrm{AVar}(\hat{\beta}_{1,CL2}) \leq \mathrm{AVar}(\hat{\beta}_{1,CL1})$. The equality holds when $\mathbf{R}_i = \mathbf{I}$ for all i. □

Acknowledgements

This research is part of the Ph.D. thesis of the first author. Support from US Army grant NF990038 is gratefully acknowledged.

References

Aitchison, J. and Ho, C. H. (1989). The multivariate Poisson-log normal distribution. *Biometrika*, 76:643–653.

Chaganty, N. R. (1997). Loss in efficiency due to misspecification of the correlation structure in gee. In *Proceedings of the 51st session of the International Statistical Institute, Istanbul, Turkey*, volume 2, pages 127–128.

Curriero, F. and Lele, S. (1999). A composite likelihood approach to semivariogram estimation. *Journal of Agricultural, Biological and Environmental Statistics*, 4:9–28.

Friedman, J. M. and Birch P. H. (1997). Type 1 Neurofibromatosis: a descriptive analysis of the disorder in 1728 patients. *American Journal of Medical Genetics*, 70:138-143.

Godambe, V. P. (1991). *Estimating Functions.* Oxford University Press, New York.

Heagerty, P. and Lele, S. (1998). A composite likelihood approach to binary data in space. *Journal of the American Statistical Association*, 93:1099–1111.

Hougaard, P. (2000). *Analysis of Multivariate Survival Data.* Springer, New York.

Joe, H. (1995). Approximation to multivariate normal rectangle probabilities based on conditional expectations. *Journal of the American Statistical Association*, 90:957–964.

Joe, H. (1997). *Multivariate Models and Dependence Concepts.* Chapman & Hall, London.

Jöreskog, K. G. and Moustaki, I. (2001). Factor analysis of ordinal variables: a comparison of three approaches. *Multivariate Behavioral Research*, 36:347–386.

Lele, S. and Taper, M. L. (2002). A composite likelihood approach to (co)variance components estimation. *Journal of Statistical Planning and Inference*, 103:117–135.

Lindsay, B. G. (1988). Composite likelihood methods. *Contemporary Mathematics*, 80:221–39.

Mendell N. and Elston R. (1974). Multifactorial qualitative traits: genetic analysis and prediction of recurrence risks. *Biometrics*, 30:41–57.

Parner, E. T. (2001). A composite likelihood approach to multivariate survival data. *Scandinavian Journal of Statistics*, 28:295–302.

Serfling, R. J. (1980). *Approximation Theorems of Mathematical Statistics.* John Wiley & Sons, New York.

Srivastava, M. S. and Katapa, R. (1986). Comparison of estimators of interclass and intraclass correlations from familial data. *The Canadian Journal of Statistics*, 14:29–46.

Srivastava, M. S. and Ng, F. (1990). Estimation of intraclass correlation in regression models. *Gujarat Statistics Review, Professor Khatri Memorial Volume*, 229–236.

Xu, J. J. (1996). *Statistical Modelling and Inference for Multivariate and Longitudinal Discrete Response Data.* PhD thesis, Department of Statistics, University of British Columbia.

Zhao, Y. (2004). *Statistical Modelling and Inference For Discrete and Censored Familial Data.* PhD thesis, Department of Statistics, University of British Columbia.

Inferences for Odds Ratio with Dependent Pairs

Y. Zhao and H. Joe

Department of Statistics, University of British Columbia,

British Columbia, Canada, V6T 1Z4

July 9, 2004

SUMMARY. In familial data analyses, quantifying familial association is scientifically important. As analogies of the intraclass and interclass correlations of a normally distributed trait, we study intraclass and interclass (log) odds ratios for a binary trait. We propose non-parametric estimators of the odds ratios under the assumptions of exchangeability and closure of multivariate binary distributions under margins. These estimators are straightforward, except for the consideration of how to weight by family size. The main results are the derivations of the asymptotic variances of the estimators. The relative efficiencies of the non-parametric estimators are studied for some parametric models. It shows that our estimators are highly efficient, and that weighting by family size is recommended for the intraclass odds ratio. The computations of the estimators and their standard errors are illustrated with two examples.

KEY WORDS: interclass and intraclass odds ratio, familial data, binary trait.

---

email: yinshan@stat.ubc.ca, harry@stat.ubc.ca

1. Introduction

For continuous familial data for which a multivariate normal distribution can be assumed for each family, the interclass and intraclass correlations are used to describe the familial associations. The intraclass correlation is of interest when a common correlation is assumed for each pair of observations in the same family. The interclass correlation is of interest when there are two classes in each family and exchangeability is assumed for each class within a family. The interclass correlation is the correlation between a pair with one member from each class. See for example Donner and Koval (1988) and Srivastava and Katapa (1986).

This paper is concerned with binary familial data. We study the intraclass and interclass (log) odds ratios as the analogies of the intraclass and interclass correlations. This research is motivated by an study of clinical features on patients affected by neurofibromatosis 1 (NF1), an autosomal dominant genetic disorder (Szudek et al., 2000) with highly variable expressivity. The objective is to quantify the association between the occurrence of the same clinical feature in relatives affected with NF1. Comparison of the degree of association between different types of relatives will help us to identify the (genetic and non-genetic) sources of the variation.

We are specially interested in two types of associations: interclass association, such as association between parent and offspring; and intraclass association, such as association between siblings. The following is an example of interclass odds ratio. Let X and Y be the indicators of the occurrence of a feature for a parent and his/her offspring, respectively. If the feature is present, we say that the individual is affected. In this case the indicator

equals 1. Then there are four possible outcomes of (X, Y): (1, 1), (1, 0), (0, 1), and (0, 0). Suppose the probability vector associated with the four outcomes are $\mathbf{P} = (P_1, P_2, P_3, P_4)'$. The parent-offspring odds ratio, denoted by r_{12} is $[P_1P_4]/[P_2P_3]$. The intraclass odds ratio, denoted by r, is defined in a similar way.

When we have n independent and identically distributed (i.i.d.) pairs of indicators (X_i, Y_i), $i = 1, \ldots, n$, we can form a 2×2 contingency table as illustrated in Table 1. The vector of counts (O_1, O_2, O_3, O_4) is a random sample from Multinomial $(n; \mathbf{P})$. The odds ratio is estimated by

$$\hat{r}_{12} = \frac{O_1O_4}{O_2O_3}. \tag{1}$$

The log odds ratio γ_{12} is estimated by $\hat{\gamma}_{12} = \log(\hat{r}_{12})$ with asymptotic standard error (s.e.) $n^{-1}\sum_l 1/P_l$ (based on the i.i.d. assumption).

[Table 1 about here.]

For familial data with a varying number of members per family, a simple way to estimate the odds ratio is to from a contingency table with all possible relative pairs. For example, form a contingency table with all the parent-offspring pairs to estimate the parent-offspring odds ratio. In this case, the pairs from a family containing more than two members are not independent. Under the assumptions of exchangeability and closure under margins, the cross-product ratio of the table is still a consistent estimate of the odds ratio. However, the dependence among pairs will affect the variance of the estimator. Therefore, we need to adjust the asymptotic variance of the estimator accordingly.

The idea of forming a 2×2 contingency table by all possible relative pairs has been used by Hunt et al. (1988) to test familial aggregation for families of a fixed size. The test is based on the standard χ^2 statistic generated from the contingency table. They showed that the standard χ^2 statistic is appropriate for intraclass aggregation despite the dependence among the pairs. For interclass aggregation, an adjustment based on the affected rate and the intraclass aggregation is needed. Some of moment calculations in this paper are borrowed from Hunt et al. (1988).

The rest of this paper is organized as follows. In Section 2, we derive the asymptotic variance of the estimator of the interclass log odds ratio. We propose estimation of the asymptotic variance and do an efficiency comparison of the proposed non-parametric estimator with the MLE generated from parametric models. In Section 3, we study estimation of the intraclass log odds ratio. Since the simple estimator tends to emphasize large families disproportionately, weights are considered to improve the efficiency. We compare the efficiencies of the unweighted and weighted estimators with the MLE based on parametric models. Two applications of these methods are given in Sections 2.5 and 3.6.

2. Interclass Odds Ratio

We are interested in estimating an interclass odds ratio when we have multivariate binary data of the following form. For family i ($1 \leq i \leq n$), there are k_{i1} members in class 1 and k_{i2} members in class 2; for our applications we will think of class 1 as parents (with $k_{i1} = 1$ or 2) and class 2 as offspring. The binary values for family i are $\mathbf{X}_i = (X_{i1}, \ldots, X_{ik_{i1}})$ for class 1 and $\mathbf{Y}_i = (Y_{i1}, \ldots, Y_{ik_{i2}})$ for class 2.

Within a family, exchangeability is assumed in each class and closure under margins is assumed for the joint probability distribution. That is, there is a probability distribution $p(\mathbf{x}, \mathbf{y}; k_1, k_2)$ such that

$$\Pr(\mathbf{X}_i = \mathbf{x}, \mathbf{Y}_i = \mathbf{y}) = \Pr(\mathbf{X}_i = \mathbf{x}^*, \mathbf{Y}_i = \mathbf{y}^*) = p(\mathbf{x}, \mathbf{y}; k_{i1}, k_{i2})$$

where $\mathbf{x}^*$ and $\mathbf{y}^*$ are arbitrary permutations of $\mathbf{x}$ and $\mathbf{y}$, respectively. Under this assumption, there is a common interclass odds ratio across families:

$$r_{12} = \frac{p(1,1;1,1)p(0,0;1,1)}{p(1,0;1,1)p(0,1;1,1)} = \frac{P_1 P_4}{P_2 P_3}.$$

2.1 *Estimator of log odds ratio* γ_{12}

For each family, we pair each member of class 1 with each member of class 2, and, then, use pairs from all the families to form a contingency table as in Table 1. Since the probability that a pair falls in cell l, $l = 1, \ldots, 4$, is P_l for all the pairs, $\mathrm{E}(O_l) = NP_l$, where N is the total number of cross-class pairs. Therefore, $\hat{P}_l = O_l/N$ is an unbiased estimate of P_l. As a result, $\hat{r}_{12} = [O_1 O_4]/[O_2 O_3]$ is an asymptotically consistent estimator of the interclass odds ratio. We estimate the log odds ratio is by $\hat{\gamma}_{12} = \log \hat{r}_{12}$.

2.2 *Asymptotic variance of* $\hat{\gamma}_{12}$

We first derive some general results, and then state them for the special case of $k_{i1} = 1$ for all i.

General

Since $\hat{\gamma}_{12}$ is a function of $\mathbf{O} = (O_1, O_2, O_3, O_4)'$, we first obtain $\mathrm{Var}(\mathbf{O})$, and then use the Delta method to obtain the asymptotic variance of $\hat{\gamma}_{12}$. Clearly the distribution of $\mathbf{O}$ is no longer multinomial since the pairs contributed by the same family are not independent due to the intraclass dependence and repeated use of the same individual in multiple pairs.

Let $\mathbf{O}_i = (O_{il}, l = 1, ..., 4)$, be the counts in the contingency table contributed by family i. Let $I_{ij}^{(l)}$ be the indicator that the jth pair contributed by family i falls in cell l. Then $O_{il} = \sum_{j=1}^{N_i} I_{ij}^{(l)}$. The variance of O_{il} is

$$\text{Var}\,(O_{il}) = \sum_{j=1}^{N_i} \text{Var}\,(I_{ij}^{(l)}) + \sum_{j' \neq j} \text{Cov}\,(I_{ij}^{(l)}, I_{ij'}^{(l)}) = N_i P_l (1 - P_l) + b_i (P_{ll}^{(i)} - P_l^2),$$

where $N_i = k_{i1} k_{i2}$, the number of cross-class pairs formed by family i, $b_i = N_i(N_i - 1)$ and $P_{ll}^{(i)}$ is the probability that pairs j and j' both fall in cell l. The covariance between O_{il} and O_{im}, $l \neq m$, is

$$\begin{aligned}
\text{Cov}(O_{il}, O_{im}) &= \text{Cov}\left(\sum_{j=1}^{N_i} I_{ij}^{(l)}, \sum_{j'=1}^{N_i} I_{ij'}^{(m)}\right) = \sum_{j=1}^{N_i} \sum_{j'=1}^{N_i} \text{Cov}\,(I_{ij}^{(l)}, I_{ij'}^{(m)}) \\
&= \sum_{j=1}^{N_i} \text{Cov}\,(I_{ij}^{(l)}, I_{ij}^{(m)}) + \sum_{j' \neq j} \text{Cov}\,(I_{ij}^{(l)}, I_{ij'}^{(m)}) \\
&= -N_i P_l P_m + b_i (P_{lm}^{(i)} - P_l P_m),
\end{aligned}$$

where $P_{lm}^{(i)}$ is the probability that pairs j and j' fall in cells l, m respectively. Since the two pairs are symmetric, $P_{lm}^{(i)} = P_{ml}^{(i)}$.

Next we derive the $P_{lm}^{(i)}$s. If we randomly choose two distinct pairs from all the pairs within family i, there are three different types of combinations:

type I: two pairs containing the same member from class 1 and different members from class 2. This occurs with probability

$$a_I^{(i)} = \frac{k_{i1} k_{i2} (k_{i2} - 1)}{N_i (N_i - 1)} = \frac{k_{i2} - 1}{N_i - 1};$$

type II: two pairs containing the same member from class 2 and different members from class 1. This occurs with probability $a_{II}^{(i)} = \dfrac{k_{i1} - 1}{N_i - 1}$.

type III: two pairs containing no common members. This occurs with probability $a_{III}^{(i)} = 1 - a_I^{(i)} - a_{II}^{(i)}$.

When $k_{i1} = 1$ (and $N_i = k_{i2}$), $a_I^{(i)} = 1$, $a_{II}^{(i)} = a_{III}^{(i)} = 0$; when $k_{i2} = 2$, $a_I^{(i)} = a_{III}^{(i)} = (k_{i2} - 1)/(2k_{i2} - 1)$, $a_{II}^{(i)} = 1/(2k_{i2} - 1)$.

Let $P_{lm|d}$ be the probability that two distinct pairs fall in cells l and m given that the pair set is of type d, $d =$ I, II or III. Then $P_{lm}^{(i)} = \sum_d a_d^{(i)} P_{lm|d}$.

The variance and covariance of $\mathbf{O}$ can be easily obtained based on the previous results. Since $O_l = \sum_i O_{il}$, we have

$$\text{Var}\,(O_l) = NP_l(1 - P_l) + \sum_{i=1}^{n} b_i(P_{ll}^{(i)} - P_l^2) \tag{2}$$

$$\text{Cov}\,(O_l, O_m) = -NP_lP_m + \sum_{i=1}^{n} b_i(P_{lm}^{(i)} - P_lP_m), \quad \text{for } l \neq m. \tag{3}$$

The asymptotic variance of $\hat{\gamma}$, σ^2 given by the Delta method is

$$\sigma^2 = \frac{\partial \gamma_{12}}{\partial \mathbf{P}'} \text{Cov}\,(\hat{\mathbf{P}}) \frac{\partial \gamma_{12}}{\partial \mathbf{P}} = \frac{1}{N^2} \frac{\partial \gamma_{12}}{\partial \mathbf{P}'} \text{Cov}\,(\mathbf{O}) \frac{\partial \gamma_{12}}{\partial \mathbf{P}},$$

where $\dfrac{\partial \gamma_{12}}{\partial \mathbf{P}'} = \left(\dfrac{1}{P_1}, -\dfrac{1}{P_2}, -\dfrac{1}{P_3}, \dfrac{1}{P_4}\right)'$. Algebraic simplification leads to the following result.

RESULT 1. *The asymptotic variance of* $\hat{\gamma}_{12}$ *is*

$$\sigma^2 = \frac{1}{N}\sigma_0^2 + \frac{1}{N}\sum_d B_d v_d, \tag{4}$$

where $\sigma_0^2 = \sum_{l=1}^{4} P_l^{-1}$, $B_d = \sum_i b_i a_d^{(i)}/N$ *and*

$$v_d = \left[\sum_{l=1}^{4} \frac{P_{ll|d}}{P_l^2}\right] + \frac{2P_{14|d}}{P_1P_4} + \frac{2P_{23|d}}{P_2P_3} - \frac{2P_{12|d}}{P_1P_2} - \frac{2P_{13|d}}{P_1P_3} - \frac{2P_{24|d}}{P_2P_4} - \frac{2P_{34|d}}{P_3P_4}, \tag{5}$$

$d = I, II$ *and* III.

The term σ_0^2/N in (4) is the asymptotic variance of $\hat{\gamma}_{12}$ based on N independent pairs.

The magnitude of v_I depends on the degree of conditional association between the class 2 members given the status of one of the class 1 member. Let X be the indicator of the class 1 member and Y_1, Y_2 be those of the two class 2 members. As shown in Appendix A, v_I can be written as

$$v_I = c_1\left(\frac{1}{P_1}+\frac{1}{P_2}\right)+c_4\left(\frac{1}{P_3}+\frac{1}{P_4}\right), \tag{6}$$

where c_1 is the conditional correlation of Y_1 and Y_2 given $X=1$, and c_4 is the conditional correlation given $X=0$. As a result,

$$v_I \begin{cases} <0 & \text{if the class 2 individuals are conditionally negatively dependent,} \\ =0 & \text{if the class 2 individuals are conditionally independent,} \\ >0 & \text{if the class 2 individuals are conditionally positively dependent.} \end{cases}$$

Likewise,

$$v_{II} = c_1'\left(\frac{1}{P_1}+\frac{1}{P_3}\right)+c_4'\left(\frac{1}{P_2}+\frac{1}{P_4}\right),$$

where c_1' and c_4' are the conditional correlations of two class 1 members given the value of one class 2 member. However, there is no such an intuitive interpretation for v_{III}.

Special case: $k_{i1}=1$ for all i

When $k_{i1}=1$ for all i, $a_{II}^{(i)}=a_{III}^{(i)}=0$. Then we have the following result:

RESULT 2. *When $k_{i1}=1$ for all i, the asymptotic variance of $\hat{\gamma}_{12}$ is*

$$\sigma^2=(\sigma_0^2+B_I v_I)/N,$$

with $N=\sum_{i=1}^n k_{i2}$ and $B_I=\sum_{i=1}^n k_{i2}(k_{i2}-1)/N$.

The term B_I is a function of the sample mean (M) and variance ($V=\sum(k_{i2}-M)^2/n$) of the k_{i2}s. In fact, $B_I=V/M+(M-1)$. When the family size is a constant k, $B_I=k-1$ and $\sigma^2=(\sigma_0^2+(k-1)v_I)/N$.

In general, the variance of $\hat{\gamma}_{12}$ increases when either c_1 or c_4 becomes larger. For the case when the class 2 members are independent conditional on the status of the class 1 member, $c_1 = c_4 = 0$, and $v_I = 0$. Hence $\sigma^2 = \sigma_0^2/N$, the same variance as having N independent pairs. For the case when the class 2 members are perfectly dependent conditional on the status of the class 1 member, $c_1 = c_4 = 1$, $v_I = \sigma_0^2$ and $\sigma^2 = (B_I + 1)\sigma_2^2/N$. So when perfect dependence occurs, if the family size is a constant, $\sigma^2 = k\sigma_0^2/N = \sigma_0^2/n$. As would be expected, this is the variance achieved considering only one class 2 member from each family. If the family size is not a constant, then $(B_I+1)/N > 1/n$, that is, the estimate is less efficient than considering only one class 2 member in each family.

2.3 *Methods to estimate the asymptotic variance of $\hat{\gamma}_{12}$ in (4)*

To estimate the asymptotic variances of $\hat{\gamma}_{12}$, we need to estimate $P_{lm|d}$ for $d = I, II, III$. The empirical frequencies of different pair types can be used. However, if there is limited number of families containing three or more members, such estimates of the probabilities are not reliable. In this case, we can use the jackknife method to estimate the variance of $\hat{\gamma}_{12}$.

An alternative approach with $k_{i1} = 1$ for all i is the following. In this case, we only need to estimate v_I, which involve the conditional correlations c_1 and c_4 in (A.2). To estimate c_1, we use all the families whose corresponding class 1 member has value 1. We denote the set of such families by I_1. Suppose I_1 contains n_1 families, and, in total, N_1 class 2 members. We form an ANOVA table with the Y values of these class 2 members. Let $\bar{Y}_i = \sum_j Y_{ij}/k_i$ for $i \in I_1$ and $\bar{\bar{Y}}_1 = \sum_{i \in I_1} \sum_j Y_{ij}/N$. The sum of squares within and between

families are:

$$SSE = \sum_{i \in I_1} \sum_j (Y_{ij} - \bar{Y}_i)^2 \text{ and } SSB = \sum_{i \in I_1} k_i (\bar{Y}_i - \bar{\bar{Y}}_1).$$

The corresponding mean squares are $MSE = SSE/(N_1 - n_1)$ and $MSB = SSB/(n_1 - 1)$. From the expected sum of squares (Searle et al., 1992),

$$\hat{\sigma}_B^2 = \frac{(n_1 - 1)(MSB - MSE)}{\sum_{i \in I_1} k_{i2}(1 - k_{i2}/N_1)}$$

is an unbiased estimate of $\text{Cov}(Y_{ij}, Y_{ij'})$, for $i \in I_1$, and $\hat{\sigma}_B^2 + MSE$ is an unbiased estimate of $\text{Var}(Y_{ij})$ for $i \in I_1$. Then an estimate of c_1 is given by $\hat{c}_1 = \hat{\sigma}_B^2/(\hat{\sigma}_B^2 + MSE)$, with $\hat{\sigma}_B^2$ set to be 0 if it is negative. In a similar way, c_4 can be estimated based the ANOVA table of the Y values of all class 2 members from families with $x_{i1} = 0$.

2.4 *Asymptotic relative efficiency of* $\hat{\gamma}_{12}$

Suppose that the joint distribution of the binary variables can be described by a parametric model $p(\mathbf{x}, \mathbf{y}; k_1, k_2; \boldsymbol{\theta})$, which is exchangeable in $\mathbf{x}$ and in $\mathbf{y}$, and is closed under margins. Then

$$\gamma_{12}(\boldsymbol{\theta}) = \log p(1,1;1,1;\boldsymbol{\theta}) + \log p(0,0;1,1;\boldsymbol{\theta}) - \log p(1,0;1,1;\boldsymbol{\theta}) - \log p(0,1;1,1;\boldsymbol{\theta}).$$

An estimate of γ_{12} can be obtained based on the MLE of $\boldsymbol{\theta}$, $\hat{\boldsymbol{\theta}}$. This estimate, denoted by $\gamma_{12}(\hat{\boldsymbol{\theta}})$, is more efficient than the proposed non-parametric estimate. In this subsection, we investigate the asymptotic efficiency loss.

In order to compare the efficiency, we need to derive the asymptotic variance of $\gamma_{12}(\hat{\boldsymbol{\theta}})$. Let $V_{\hat{\boldsymbol{\theta}}}$ be the asymptotic covariance matrix of $n^{1/2}(\hat{\boldsymbol{\theta}} - \boldsymbol{\theta})$, which is the inverse of Fisher information $\mathcal{I}$. If the proportion of families with

sizes k_1, k_2 is (asymptotically) q_{k_1,k_2} for $k_1 = 1, \ldots, m_1$, $k_2 = 1, \ldots, m_2$, then

$$\mathcal{I} = \sum_{k_1=1}^{m_1} \sum_{k_2=1}^{m_2} q_{k_1,k_2} \sum_{\mathbf{x}\in\{0,1\}^{k_1}} \sum_{\mathbf{y}\in\{0,1\}^{k_2}} \frac{\frac{\partial p(\mathbf{x},\mathbf{y};k_1,k_2;\boldsymbol{\theta})}{\partial \boldsymbol{\theta}} \frac{\partial p(\mathbf{x},\mathbf{y};k_1,k_2;\boldsymbol{\theta})}{\partial \boldsymbol{\theta}'}}{p(\mathbf{x},\mathbf{y};k_1,k_2;\boldsymbol{\theta})}.$$

The asymptotic variance of $n^{1/2}[\gamma_{12}(\hat{\boldsymbol{\theta}}) - \gamma_{12}]$ is $\frac{\partial \gamma_{12}}{\partial \boldsymbol{\theta}'} V_{\hat{\boldsymbol{\theta}}} \frac{\partial \gamma_{12}}{\partial \boldsymbol{\theta}}$.

We calculate the relative efficiency, i.e., the the asymptotic variance ratio between $\gamma_{12}(\hat{\boldsymbol{\theta}})$ and $\hat{\gamma}_{12}$, for specific parametric models. Our conclusions are:

(a) The relative efficiency is typically above 0.9.

(b) The relative efficiency decreases as the dependence becomes strong.

(c) The relative efficiency tends to decrease as the variance-mean ratio of family size increases.

In this paper, we illustrate these patterns using the multivariate binary beta-binomial model (Section 7.1 of Joe, 1997). we set $k_{i1} = 1$ and k_{i2} varying from 1 to 4 with equal frequency. (If we change the distribution of family sizes, the efficiency exhibits the same general patterns but with different magnitudes.)

The multivariate binary beta-binomial model is specified as the following: The probability of the presence of the binary trait among class 1 members is denoted by π; given the state of the class 1 member, $X_i = I$, I=0 or 1, (the subscript j_1 is omitted since $k_{i1} = 1$), the joint conditional distribution of $\mathbf{Y}_i$ follows a multivariate binary beta-binomial model with parameters (α_I, β_I). Thus, the joint conditional probability of $\mathbf{Y}_i$ is

$$\Pr(\mathbf{Y}_i = \mathbf{y} | X_i = I) = \frac{B(\alpha_I + y_+, \beta_I + k - y_+)}{B(\alpha_I, \beta_I)}, \tag{7}$$

where $\mathbf{y} \in \{0,1\}^{k_{i2}}$, y_+ is the sum of the elements in $\mathbf{y}$ and $B(\,\cdot\,,\,\cdot\,)$ is the Beta function.

To illustrate (a) and (b), we use a simple case with $\alpha_1 = \beta_0 = \alpha, \alpha_0 = \beta_1 = \beta$, that is, $c_1 = c_4 = 1/(\alpha + \beta + 1)$. In this case, the efficiency is not affected by the value of π by the symmetry of the conditional distribution, and, so, we set $\pi = 0.5$. The efficiency of $\hat{\gamma}_{12}$ is plotted in Figure 1. When both α and β are small, e.g. the class 2 members are strongly correlated, the efficiency is relatively low. But even when the correlation is almost 1, it is still above 0.85.

[Figure 1 about here.]

Similar results can be seen with our calculations based on the multivariate probit model (Zhao, 2004).

Pattern (c) is shown in Figure 2, in which each point corresponds to the efficiency associated with a particular distribution of family size. In all cases, the number of class 2 members in a family is set to be 1 to 4 but with a randomly generated frequency. So, the variance-mean ratio varies from case to case. The efficiencies are calculated with all the parameters of the beta-binomial model kept constant ($\alpha_1 = 2, \beta_1 = 1, \alpha_0 = 1, \beta_0 = 2, \pi = 0.5$).

[Figure 2 about here.]

2.5 *An example*

In this subsection, we estimate the parent-offspring odds ratio for the presence of intertriginous freckling in NF1 patients. There are 261 families containing one affected parent and his/her affected offspring. Among these families there are 187 with one child, 52 with two children, 22 with three to

five. In total, there are 364 parent-offspring pairs. The prevalence of intertriginous freckling is 0.88 among the parents and 0.80 among the offspring. The estimates of P_1 to P_4 from these pairs are

$\hat{P}_1 = 0.714$ (both affected), $\hat{P}_2 = 0.165$ (only the parent affected),
$\hat{P}_4 = 0.030$ (both unaffected), $\hat{P}_3 = 0.091$ (only the offspring affected).

To obtain the standard error of the log odds ratio given in (4), we use the ANOVA approach presented in Section 2.3 to estimate the conditional correlations c_1 and c_4 (defined in (A.2)). The results are: $\hat{c}_1 = 0.004$ and $\hat{c}_4 = 0.200$.

The jackknife method, in which one family was removed at a time, is also used to obtain the standard error. Both estimates are given in Table 2.

[Table 2 about here.]

The naive standard error in the table is calculated ignoring the dependence among the pairs, which is not very different from the other two standard errors, since the conditional associations among siblings are weak. The standard error based on (4) is slightly larger than the jackknife standard error.

3. Intraclass Odds Ratio

Consider a random sample of n families, each containing a varying number of members; in applications, typically the members are siblings. Let k_i be the number of members in family i and $\mathbf{Y}_i = (Y_{i1}, \ldots, Y_{ik_i})$ be the vector for a binary trait. We assume exchangeability and closure under margins, that is, there is a distribution $p(\mathbf{y}; k)$ such that for $\mathbf{y}$ of length k_i,

$$\Pr(\mathbf{Y}_i = \mathbf{y}) = \Pr(\mathbf{Y}_i = \mathbf{y}^*) = p(\mathbf{y}; k_i)$$

for $\mathbf{y}^*$ being any arbitrary permutation of $\mathbf{y}$. From the assumption of closure under margins, the intraclass odds ratio is

$$r = \frac{p(1,1;2)p(0,0;2)}{p(1,0;2)p(0,1;2)} = \frac{P_1 P_4}{P_2 P_3} = \frac{4P_1 P_4}{(1-P_1-P_4)^2}. \tag{8}$$

where $P_1 = p(1,1;2)$, $P_4 = p(0,0;2)$, $P_2 = P_3 = 1 - P_1 - P_4 = p(1,0;2)$.

3.1 *Estimator of log odds ratio* γ

For family i, there are $\binom{k_i}{2}$ possible pairs. The total number of pairs is $N = \sum_{i=1}^{n} \binom{k_i}{2}$. Each pair may fall into three categories: both equal to 1, one equal to 1 and the other equal to 0, and both equal to 0. Let O_1 be the count of pairs both equal to 1 and O_4 be the count of those both equal to 0. Then $\hat{P}_l = O_l/N$ is an unbiased estimate of P_l, for $l = 1, 4$. We estimate r in (8) by

$$\hat{r} = \frac{4O_1 O_4}{(N - O_1 - O_4)^2}. \tag{9}$$

The corresponding log odds ratio estimate is

$$\hat{\gamma} = \log O_1 - 2\log(N - O_1 - O_4) + \log O_4 + \log 4. \tag{10}$$

3.2 *Asymptotic variance of* $\hat{\gamma}$

With similar derivations to Section 2, we have

$$\text{Var}\,(O_l) = NP_l(1-P_l) + \sum_{i=1}^{n} b_i (P_{ll}^{(i)} - P_l^2), \quad \text{for } l = 1, 4, \tag{11}$$

$$\text{Cov}\,(O_1, O_4) = -NP_1P_4 + \sum_{i=1}^{n} b_i (P_{14}^{(i)} - P_1P_4), \tag{12}$$

with $b_i = \binom{k_i}{2}\left(\binom{k_i}{2} - 1\right)$ and $P_{lm}^{(i)} = (1-a_i)P_{lm|4} + a_i P_{lm|3}$, $l, m = 1, 4$, where a_i is the probability that two random pairs from the $\binom{k_i}{2}$ possible pairs contain only three distinct members and $P_{ij|3}$ is the probability that two such pairs fall in the cell l and m respectively, while $P_{ij|4}$ is the same probability for two

random pairs containing four members. Since $P_{14|3} = 0$, $P_{14}^{(i)} = (1 - a_i)P_{14|4}$. It was shown by Hunt et al. (1988)

$$a_i = \frac{k_i(k_i-1)(k_i-2)/2}{\binom{k_i}{2}\left(\binom{k_i}{2}-1\right)/2} = \frac{4}{k_i+1}, \quad k_i > 2.$$

With substitution for $P_{lm}^{(i)}$, (11) and (12) become

$$\begin{aligned} \mathrm{Var}\,(O_l) &= NP_l(1-P_l) + \sum_{i=1}^{n}\left(b_i a_i P_{ll|3} + b_i(1-a_i)P_{ll|4} - b_i P_l^2\right), \\ \mathrm{Cov}\,(O_1, O_4) &= -NP_1P_4 + \sum_{i=1}^{n}\left(b_i(1-a_i)P_{14|4} - b_i P_1 P_4\right). \end{aligned}$$

Let

$$B_1 = \sum_i b_i a_i/N,\ B_2 = \sum_i b_i(1-a_i)/N \text{ and } B_3 = \sum_i b_i/N = B_1 + B_2; \quad (13)$$

$$\mathbf{V}_0 = \begin{pmatrix} P_1 & 0 \\ 0 & P_4 \end{pmatrix} - \begin{pmatrix} P_1^2 & P_1P_4 \\ P_1P_4 & P_4^2 \end{pmatrix}, \qquad \mathbf{V}_1 = \begin{pmatrix} P_{11|3} & 0 \\ 0 & P_{44|3} \end{pmatrix},$$

$$\mathbf{V}_2 = \begin{pmatrix} P_{11|4} & P_{14|4} \\ P_{14|4} & P_{44|4} \end{pmatrix}, \qquad \mathbf{V}_3 = -\begin{pmatrix} P_1^2 & P_1P_4 \\ P_1P_4 & P_4^2 \end{pmatrix}.$$

The covariance matrix of (O_1, O_4), denoted by $\mathbf{V}$, can be written as:

$$\mathbf{V} = N\mathbf{V}_0 + N\sum_{d=1}^{3} B_d \mathbf{V}_d.$$

Let $\boldsymbol{\phi} = \frac{1}{N}\left(\frac{\partial\gamma}{\partial P_1}, \frac{\partial\gamma}{\partial P_4}\right)'$, where $\frac{\partial\gamma}{\partial P_1} = \frac{1}{P_1} + \frac{1}{P_2}$ and $\frac{\partial\gamma}{\partial P_4} = \frac{1}{P_4} + \frac{1}{P_2}$.

The asymptotic variance of $\hat{\gamma}$ given by the Delta method is:

$$\sigma^2 = N\boldsymbol{\phi}'\mathbf{V}_0\boldsymbol{\phi} + N\sum_{d=1}^{3} B_d \boldsymbol{\phi}'\mathbf{V}_d\boldsymbol{\phi}.$$

If we write

$$\begin{aligned}
\sigma_0^2 &= N^2\boldsymbol{\phi}'\mathbf{V}_0\boldsymbol{\phi} = \frac{1}{P_1} + \frac{1}{P_4} + \frac{2}{P_2}, \\
v_1 &= N^2\boldsymbol{\phi}'\mathbf{V}_1\boldsymbol{\phi} = P_{11|3}\left(\frac{1}{P_1} + \frac{1}{P_2}\right)^2 + P_{44|3}\left(\frac{1}{P_2} + \frac{1}{P_4}\right)^2, \\
v_2 &= N^2\boldsymbol{\phi}'\mathbf{V}_2\boldsymbol{\phi} = \sum_{l,m\in\{1,4\}} P_{lm|4}\left(\frac{1}{P_l} + \frac{1}{P_2}\right)\left(\frac{1}{P_m} + \frac{1}{P_2}\right), \\
v_3 &= N^2\boldsymbol{\phi}'\mathbf{V}_3\boldsymbol{\phi} = -\frac{1}{P_2^2},
\end{aligned} \tag{14}$$

then we have the following result.

RESULT 3. *The asymptotic variance of the intraclass log odds ratio estimator given in (10) is*

$$\sigma^2 = \frac{1}{N}\sigma_0^2 + \frac{1}{N}\sum_{d=1}^{3} B_d v_d, \tag{15}$$

with B_d defined in (13) and v_d defined in (14).

When each family contains the same number of members, say k, then

$$\sigma^2 = \frac{2}{nk(k-1)}\left\{\sigma_0^2 + \frac{k-2}{2}\left[4v_1 + (k-3)v_2 + (k+1)v_3\right]\right\}.$$

For the special case where the Y_{ij}'s are mutually independent for each i (with k_i varying), let $p = \Pr(Y_{ij} = 1)$ and $q = 1-p$, we have $P_1 = p^2$, $P_4 = q^2$, $P_2 = pq$, $P_{14|4} = p^2q^2$ and $P_{11|L} = p^L$, $P_{44|L} = q^L$, for $L = 3, 4$. Consequently, $v_1 = v_2 = -v_3 = p^{-2}q^{-2}$ and $\sum_{d=1}^{3} B_d v_d = p^{-2}q^{-2}[B_1 + B_2 - B_3] = 0$. Hence $\sigma^2 = \sigma_0^2/N$, which is the same variance when the sample contains N independent pairs. Surprisingly, although the pairs are not independent due to the inclusion of the same individuals in multiple pairs, the asymptotic variance of $\hat{\gamma}$ is not inflated.

Generally, when family members are positively dependent, $\sigma^2 > \sigma_0^2$.

3.3 *Weighted estimator of* γ

In the contingency table, a large family contributes many more pairs than a small family. Since the number of pairs is disproportional to the family size, the large families might be over-emphasized. With this concern, we consider assigning weights to the families.

Let n_k be the number of families of size k and $\mathbf{O}^{(k)} = (O_1^{(k)}, O_4^{(k)})$ be the counts from these families. Consider a weight w_k for $\mathbf{O}^{(k)}$. Then the weighted total counts are $\mathbf{O}_w = \sum_k w_k \mathbf{O}^{(k)}$. We estimate the log odds ratio by

$$\hat{\gamma}_w = \log \frac{4O_{w1}O_{w4}}{(N' - O_{w1} - O_{w4})^2}, \tag{16}$$

where $N' = \sum_k w_k n_k \binom{k}{2}$. Next we derive its asymptotic variance.

Let $\mathbf{V}^{(k)} = \mathrm{Var}\,(\mathbf{O}^{(k)})/[n_k\binom{k}{2}]$. Then the covariance matrix of $\mathbf{O}_w$ is

$$\mathbf{V}_w = \sum_k w_k^2 n_k \binom{k}{2} \mathbf{V}^{(k)}.$$

Let $\boldsymbol{\phi}_w = \left(1/P_1 + 1/P_2, 1/P_4 + 1/P_2\right)'$. If we write $\tau_k = (N')^2 \boldsymbol{\phi}_w' \mathbf{V}^{(k)} \boldsymbol{\phi}_w$, the asymptotic variance of $\hat{\gamma}_w$ is

$$\sigma_w^2 = \boldsymbol{\phi}_w' \mathbf{V}_w \boldsymbol{\phi}_w = \frac{1}{(N')^2} \sum_k w_k^2 n_k \binom{k}{2} \tau_k.$$

Similar to Result 3, it can be shown that $\tau_k = \sigma_0^2 + \sum_{d=1}^3 B_d^{(k)} v_d$, where the $B_d^{(k)}$s are given by (13). In particular, $\tau_2 = \sigma_0^2$ since $B_d^{(2)} = 0$, for all d. Without loss of generality, we set $w_2 = 1$. Let $N' = n_2 + \sum_{k\geq 3} w_k n_k \binom{k}{2}$. Then,

$$\sigma_w^2 = \frac{1}{(N')^2} \left(n_2\tau_2 + \sum_{k\geq 3} w_k^2 n_k \binom{k}{2} \tau_k \right).$$

To find the optimal weights, we differentiate σ_w^2 with respect to the w_ks and set the derivatives equal to 0 and, then, solve the resulting equations:

$$w_k\tau_k - N'\sigma_w^2 = 0, \quad \text{for } k \geq 3,$$

RESULT 4. *The optimal weights which minimize the asymptotic variance of* $\hat{\gamma}_w$ *in (16) are* $w_k = \tau_2/\tau_k$. *The resulting asymptotic variance is* $\sigma^2_{w_{opt}} = \sigma_0^2/N'$.

The derivation of $\sigma^2_{w_{opt}}$ is as follows:

$$\sigma^2_{w_{opt}} = \frac{1}{(N')^2}\Big[n_2\tau_2 + \sum_{k\geq 3}\frac{\tau_2^2}{\tau_k}n_k\binom{k}{2}\Big] = \frac{\tau_2}{N'}\Big[\frac{n_2}{N'} + \frac{1}{N'}\sum_{k\geq 3}w_k n_k\binom{k}{2}\Big] = \frac{\tau_2}{N'} = \frac{\sigma_0^2}{N'}$$

by the definition of N'. The weight w_k depend on P_1, P_4 and $P_{lm|L}$, for $l,\ m = 1,\ 4$ and $L = 3,\ 4$. In practice, these probabilities are unknown and need to be estimated. Therefore $\hat{\gamma}_w$ has to be obtained iteratively.

Instead of estimating the optimal weights, a simple approach to down-weight the large families is to set $w_k = 2/(k-1)$ so that $w_k n_k\binom{k}{2}$ is proportional to k.

RESULT 5. *When set* $w_k = 2/(k-1)$, *the asymptotic variance of* $\hat{\gamma}_w$ *is*

$$\sigma^2_{w_{simple}} = \frac{1}{(N')^2}\sum_k \frac{n_k k}{k-1}\Big\{2\sigma_0^2 + (k-2)\left[4v_1 + (k-3)v_2 + (k+1)v_3\right]\Big\}. \quad (17)$$

with $N' = \sum_k n_k k$.

3.4 *Methods to estimate the asymptotic variance of* $\hat{\gamma}$

To estimate the asymptotic variance of $\hat{\gamma}$, we need to estimate $P_{ij|3}$ and $P_{ij|4}$. A simple way to obtain the estimates is to use the sample proportions based on all possible sets of four members to estimate the $P_{ij|4}$ and use all

the possible sets of three members to estimate the $P_{ij|3}$. However, if there are limited number of families containing three or more members, such estimates of the probabilities are not reliable. In this case, the jackknife method can be used to estimate the variance of $\hat{\gamma}$.

3.5 *Efficiency comparison*

We investigate the efficiency of the weighted and unweighted estimators by comparing them with the MLE based on a parametric model. Consider a parametric exchangeable model $p(\mathbf{y}; k, \boldsymbol{\theta})$ which is closed under margins and defined for all $k \geq 2$. Then, the bivariate margin of Y_i, Y_j is $p(y_i, y_j; 2, \boldsymbol{\theta})$ for all $i \neq j$. The log odds ratio based on the parametric model is

$$\gamma(\boldsymbol{\theta}) = \log p(1,1;2,\boldsymbol{\theta}) + \log p(0,0;2,\boldsymbol{\theta}) - \log p(1,0;2,\boldsymbol{\theta}) - \log p(0,1;2,\boldsymbol{\theta}).$$

Let $\hat{\boldsymbol{\theta}}$ be the MLE and $V_{\hat{\boldsymbol{\theta}}}$ be the asymptotic covariance matrix of $n^{1/2}(\hat{\boldsymbol{\theta}} - \boldsymbol{\theta})$, i.e., the inverse of Fisher's information $\mathcal{I}$. If the proportion of families with size k is (asymptotically) q_k for $k = 2, \ldots, k_{max}$, then

$$\mathcal{I} = \sum_{k=2}^{k_{max}} q_k \sum_{\mathbf{y} \in \{0,1\}^k} \frac{\partial p(\mathbf{y}; k, \boldsymbol{\theta})}{\partial \boldsymbol{\theta}} \frac{\partial p(\mathbf{y}; k, \boldsymbol{\theta})}{\partial \boldsymbol{\theta}'} \Big/ p(\mathbf{y}; k, \boldsymbol{\theta}).$$

The asymptotic variance of $n^{1/2}[\gamma(\hat{\boldsymbol{\theta}}) - \gamma]$ is $\frac{\partial \gamma}{\partial \boldsymbol{\theta}'} V_{\hat{\boldsymbol{\theta}}} \frac{\partial \gamma}{\partial \boldsymbol{\theta}}$.

Based on calculations for specific parametric models, our conclusions are the following.

(a) The relative efficiency with the optimal weights is close to 1 (> 0.9).

(b) The relative efficiency of the unweighted estimator decreases when the dependence increases and is not much affected by p; the relative efficiency can get below 0.6.

(c) The relative efficiency for the estimator with simple weights is lower when the dependence is weak, but it is typically above 0.8.

We illustrate these patterns using a multivariate binary beta-binomial model with parameters $(\alpha,\ \beta)$. The probability of $\mathbf{Y}_k = \mathbf{y}_k$ is given in (7). The intraclass odds ratio r is $(\alpha+1)(\beta+1)/(\alpha\beta)$ and $p = \Pr(Y_{ij} = 1) = \alpha/(\alpha+\beta)$.

We set the distribution of family sizes as uniform for $k = 2, 3, 4, 5$ and vary the intraclass dependence at four different values of p: 0.05, 0.20, 0.35 and 0.50. When p is above 0.5, it generates the same results as $1-p$. In Figures 3, we plot the efficiency under three situations: unweighted, weighted by optimal weights and weighted by family size (referred to as simple weights), The plots show that the unweighted estimator (solid line) loses efficiency when the dependence increases; whereas its efficiency does not seem affected much by the affected rate. The optimal weights (dotted line) greatly enhance the efficiency, particularly when the dependence is high. Except for the case of $p = 0.05$, its efficiency is always above 0.95. Using the simple weights is worse than no weights when the dependence is weak, however, the performance of this estimator improves when the dependence increases and is almost as good as the optimally weighted estimator for strong dependence. The plots also show that its efficiency climbs faster when p is closer to 0.5.

[Figure 3 about here.]

We provide another example based on the multivariate probit model in Zhao (2004).

We also investigate how the distribution of family sizes affects the efficiencies of the three estimators based on the multivariate binary beta-binomial model. We fix p at 0.5 and the intraclass odds ratio at a low level (1.44) and a high level (9). We consider only two different family sizes: 2 and 6 and take the distribution of family sizes with $f_2 + f_6 = 1$, where f_2 and f_6 are the proportions of families of size 2 and 6, respectively. In Figure 4 the efficiency is plotted against f_2. In both case, the unweighted estimator is least efficient when $f_2 = 15/16$, that is, when each type of family contributes equal number of pairs to the contingency table. The efficiency of the estimator with optimal weights increases monotonically with the proportion f_2. When the odds ratio is small, the estimator with simple weights is least efficient when $f_2 = 6/7$, that is, each type of family contributes an equal number of individuals to the sample, whereas the efficiency of this estimator is almost coincident with that of the optimal weights when the odds ratio is high.

Moreover, the efficiency of both the estimators, unweighted or weighted by family size, decreases almost linearly with the variance-mean ratio of the number of pairs contributed by each family.

[Figure 4 about here.]

Lastly we give some considerations on using weights. When the dependence among family members is weak, the loss of efficiency is modest if the unweighted estimator is used, therefore, there is no compelling reason to use any weights. On the contrary, when the dependence is very strong and there is a great deal of variation in family size, the simple weights are recommended since they work almost as well as the optimal weights and are easy to use.

3.6 *An example*

In this subsection, we estimate the sib-sib odds ratio for the presence of intertriginous freckling in NF1 patients. There are 193 families with at least two siblings. Among them there are 151 families with two siblings, 30 with three and 11 with four. There is one large family with eight siblings, all affected. In total, there are 335 sibling pairs.

We compute both the unweighted and simply weighted estimates of the sib-sib log odds ratio. Theoretically, the standard errors of these two estimates can be compute based on (15) and (17) if we can estimate $P_{ij|3}$ and $P_{ij|4}$, the probabilities of two pairs falling in respective categories. However, to obtain reliable estimates of these probabilities, usually a large number of families with size over two is needed. In this dataset, there are not enough families to produce the estimates. Therefore, we use the jackknife method to obtain the standard errors. The results are reported in Table 3.

[Table 3 about here.]

After weighting, there is a slight decrease in the estimate of P_1 and a slight increase in the estimate of P_4; the estimate of the log odds ratio has a smaller standard error. We also calculate the naive standard error (0.314) for the unweighted estimate, which is more than 10% smaller than the jackknife standard error.

4. Conclusion

We have proposed simple methods to estimate the intraclass and interclass odds ratio across families with varying sizes. They are based on the standard 2×2 contingency table and are easy to carry out. We derived the asymptotic

variance of the odds ratio estimators taking into account the dependence between pairs within a family. The usual standard error, i.e., that based on the asymptotic variance for independent pairs, will be too small when there is positive association within families; hence, it will lead to a confidence interval that is too short.

Acknowledgements

This research is part of the Ph.D. thesis of the first author. Support from US Army grant NF990038 is gratefully acknowledged.

References

Donner, A. and Koval, J.J. (1988). The estimation of intraclass correlation in the analysis of family data. *Biometrics* **36**, 19–25.

Hunt, S., Hasstedt, S., and Williams, R. (1988). Testing for familial aggregation of a dichotomous trait. *Genetic Epidemiology* **3**, 299–312.

Joe, H. (1997). *Multivariate Models and Dependence Concepts.* Chapman & Hall, London.

Searle, S.R., Casella, G., and McCulloch, C.E. (1992). *Variance Components.* John Wiley & Sons, Inc., New York.

Srivastava, M.S. and Katapa, R. (1986). Comparison of estimators of interclass and intraclass correlations from familial data. *Canadian Journal of Statistics* **14**, 29-46.

Szudek, J., Birch, P., Riccardi, V.M., Evans, D., and Friedman, J. (2000). Association of clinical features in neurofibromatosis 1 (nf1). *Genetic Epidemiology* **19**, 429–439.

Zhao, Y. (2004). *Statistical Modelling and Inference For Discrete and Censored Familial Data.* PhD thesis, Department of Statistics, University of British Columbia.

Appendix A

Proof of equation (6)

The term v_I depends on type I pair sets in which the two pairs share the same member from class 1. Since $P_{lm|I} = 0$ when $l = 1, 2$ and $m = 3, 4$ or when $l = 3, 4$ and $m = 1, 2$,

$$v_I = \sum_{l=1}^{4} \frac{P_{ll|I}}{P_l^2} - 2\frac{P_{12|I}}{P_1 P_2} - 2\frac{P_{34|I}}{P_3 P_4} = \sum_{l=1}^{4} \frac{c_l}{P_l}, \tag{A.1}$$

where

$$c_l = \frac{P_{ll|I}}{P_l} - \frac{P_{ll'|I}}{P_{l'}}, \quad l' = \begin{cases} 1 & \text{if } l = 2, \\ 2 & \text{if } l = 1, \\ 3 & \text{if } l = 4, \\ 4 & \text{if } l = 3. \end{cases} \tag{A.2}$$

Let X be the indicator of the class 1 member and Y_1, Y_2 be those of the two class 2 members. We write $p_{y_i|x} = \Pr(Y_i = y_i | X = x)$ and $p_{y_1 y_2|x} = \Pr(Y_1 = y_1, Y_2 = y_2 | X = x)$, for x, y_1 and y_2 in $\{0, 1\}$. Then

$$\frac{P_{11|I}}{P_1} = \frac{\Pr(X = 1, Y_1 = 1, Y_2 = 1)}{\Pr(X = 1, Y_2 = 1)} = \frac{p_{11|1}}{p_{1|1}},$$

$$\frac{P_{12|I}}{P_2} = \frac{\Pr(X = 1, Y_1 = 1, Y_2 = 0)}{\Pr(X = 1, Y_2 = 0)} = \frac{p_{10|1}}{p_{0|1}} = \frac{p_{1|1} - p_{11|1}}{1 - p_{1|1}}.$$

It follows that

$$c_1 = \frac{p_{11|1} - p_{1|1}^2}{p_{1|1}(1 - p_{1|1})},$$

which is the conditional correlation of Y_1 and Y_2 given $X = 1$. It can be shown that $c_1 = c_2$. By symmetry, $c_3 = c_4$ is the conditional correlation of Y_1 and Y_2 given $X = 0$. Therefore, v_I can be simplified as in (6).

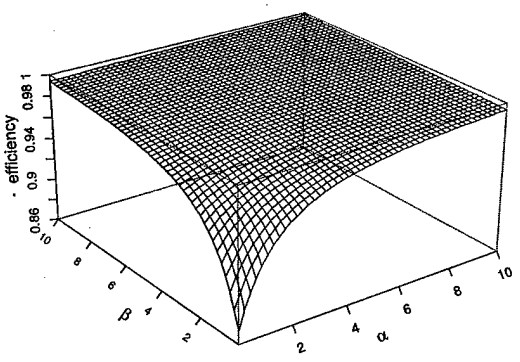

Figure 1. Efficiency of $\hat{\gamma}_{12}$ based on a beta-binomial model when $\alpha_1 = \beta_0 = \alpha, \alpha_0 = \beta_1 = \beta$

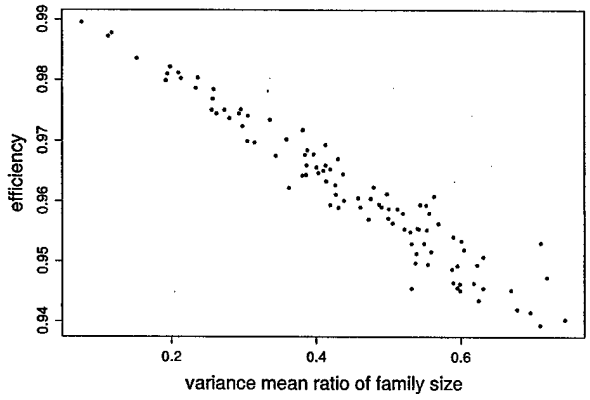

Figure 2. Efficiency of $\hat{\gamma}_{12}$ against the variance-mean ratio of family size (beta-binomial model).

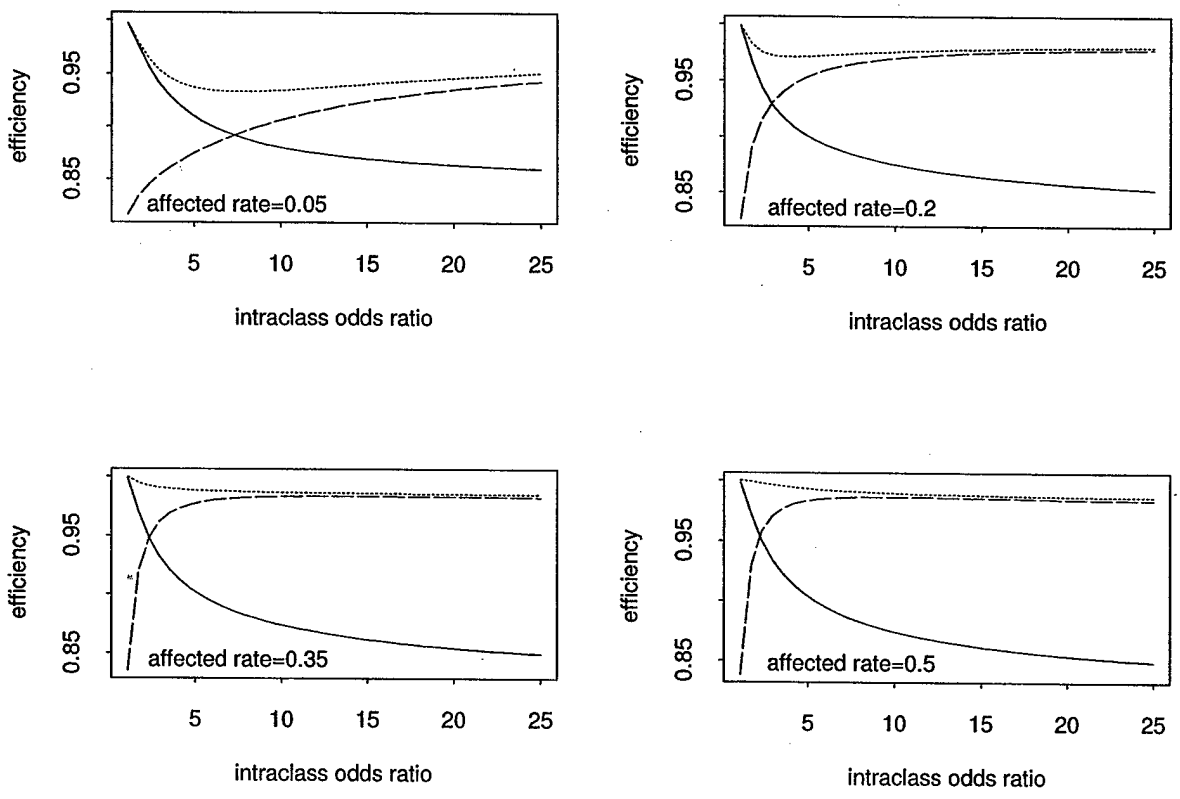

Figure 3. Efficiency comparison of γ estimators. Solid line: no weights, dotted line: optimal weights, dashed line: simple weights (Multivariate binary beta-binomial).

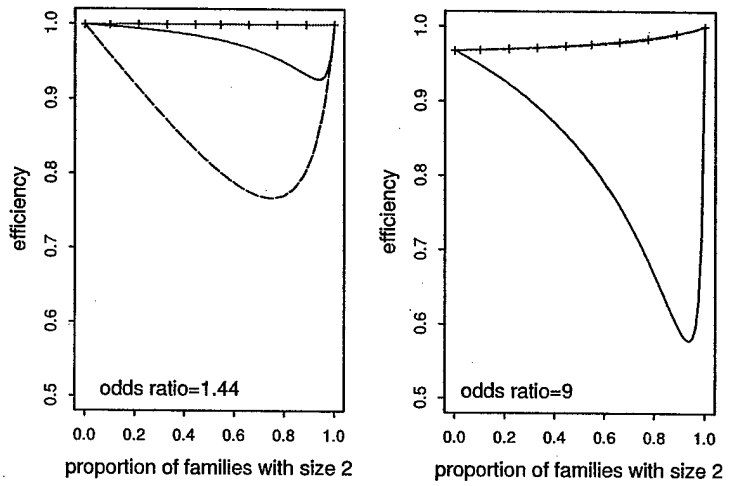

Figure 4. Efficiency comparison of γ estimators with varying proportions of families with size 2 and 6. Solid line: no weights, dotted line with "+": optimal weights, dashed line: simple weights. In the figure on the right hand side, the dotted line with "+" and the dashed line are on top of each other.

		Y	
		1	0
X	1	O_1	O_2
	0	O_3	O_4

Table 1

Contingency table formed by independent pairs

log odds ratio	s.e.	naive s.e.	jackknife s.e.
0.368	0.402	0.377	0.387

Table 2

Estimate of parent-offspring log odds ratio for the presence of intertriginous freckling in NF1 patients.

	with no weights	with simple weights
$\hat{P}_1$ (both affected)	0.704	0.668
$\hat{P}_4$ (both unaffected)	0.075	0.096
$\hat{\gamma}$ (log odds ratio)	1.461	1.531
Jackknife standard error of $\hat{\gamma}$	0.357	0.348

Table 3

Estimates of sib-sib log odds ratio for the presence of intertriginous freckling in NF1 patients.

APPENDIX 3

Published papers

Am. J. Hum. Genet. 71:715–723, 2002

Predictors of the Risk of Mortality in Neurofibromatosis 2

Michael E. Baser, J. M. Friedman,[1] Dana Aeschliman,[2] Harry Joe,[2] Andrew J. Wallace,[3] Richard T. Ramsden,[4] and D. Gareth R. Evans[3]

Departments of [1]Medical Genetics and [2]Biostatistics, University of British Columbia, Vancouver; [3]Department of Medical Genetics, St. Mary's Hospital, and [4]Department of Otolaryngology, Manchester Royal Infirmary, Manchester, United Kingdom

To evaluate clinical and molecular predictors of the risk of mortality in people with neurofibromatosis 2 (NF2), we analyzed the mortality experience of 368 patients from 261 families in the United Kingdom NF2 registry, using the Cox proportional-hazards model and the jackknife method. Age at diagnosis, intracranial meningiomas, and type of treatment center were informative predictors of the risk of mortality. In Cox models, the relative risk of mortality increased 1.13-fold per year decrease in age at diagnosis (95% confidence interval [CI] 1.08–1.18) and was 2.51-fold greater in people with meningiomas compared with those without meningiomas (95% CI 1.38–4.57). The relative risk of mortality in patients treated at specialty centers was 0.34 compared with those treated at nonspecialty centers (95% CI 0.12–0.98). In a separate model, the relative risk of mortality in people with constitutional *NF2* missense mutations was very low compared with those with other types of mutations (nonsense or frameshift mutations, splice-site mutations, and large deletions), but the CI could not be well quantified because there was only one death among people with missense mutations. We conclude that age at diagnosis, the strongest single predictor of the risk of mortality, is a useful index for patient counseling and clinical management (as are intracranial meningiomas). To ensure optimal care, we recommend that people with NF2 be referred to specialty treatment centers.

Introduction

Neurofibromatosis 2 (NF2 [MIM 101000]) is an autosomal dominant disorder that is caused by inactivating mutations or loss of both alleles of the *NF2* tumor-suppressor gene (Rouleau et al. 1993; Trofatter et al. 1993). Vestibular schwannomas (VSs), intracranial meningiomas, spinal tumors, peripheral nerve tumors, and presenile lens opacities are common in NF2 (Evans et al. 1992*a*; Parry et al. 1994; Mautner et al. 1996). VSs occur in ~95% of adults with NF2 (bilateral VSs are pathognomonic for NF2), meningiomas in ~50%, and presenile lens opacities in ~60%–80%. Spinal tumors occur in ~90% of people with NF2, although only 30% of these people have symptomatic spinal tumors (Mautner et al. 1995).

Cross-sectional studies of genotype-phenotype correlations in NF2 have found that, in general, constitutional nonsense and frameshift *NF2* mutations are associated with severe disease; missense mutations, in-frame deletions, and large deletions with mild disease; and splice-site mutations are associated with variable disease severity (Mérel et al. 1995; Kluwe et al. 1996, 1998; Parry et al. 1996; Ruttledge et al. 1996; Evans et al. 1998*a*). There have been few longitudinal studies of NF2, because of the rarity of the disease (Evans et al. 1992*b*; Antinheimo et al. 2000). In two recent short-term longitudinal studies of the predictors of VS growth rates in NF2, VS growth rates tended to be higher in people with a younger age at onset or diagnosis of NF2, but they were highly variable, even among affected relatives of similar ages in a single family (Baser et al. 2002; Mautner et al. 2002). As yet, there have not been any longitudinal studies of other common tumors in NF2, such as intracranial meningiomas or spinal tumors, which also cause considerable morbidity (Evans et al. 2000).

NF2 is a chronic disease in which life expectancy, although often shortened, is lengthy. Short-term studies of the growth rates of NF2-associated tumors, especially studies of a single tumor type, do not reflect the total disease burden of NF2 or the efficacy of treatment as well as do long-term studies that utilize a more inclusive measure of health, such as mortality. Evans et al. (1992*a*) found that mean actuarial survival in people with NF2 was 62 years, and Parry et al. (1994) reported that broad categories of NF2 disease severity (mild, intermediate, and severe) were correlated with age at death. Neither of these studies evaluated specific clinical or molecular characteristics as potential predictors of the risk of mor-

Received March 5, 2002; accepted for publication June 24, 2002; electronically published August 22, 2002.

Address for correspondence and reprints: Dr. Michael E. Baser, 2257 Fox Hills Drive, Los Angeles, CA 90064. E-mail: baser@earthlink.net

Presented in part at the 49th Annual Meeting of the American Society of Human Genetics, in San Francisco, on October 19–23, 1999.

0002-9297/2002/7104-0003$15.00

tality. In the present study, we evaluated clinical and molecular predictors of the risk of mortality in a large series of people with NF2.

Subjects and Methods

Patient Population

The United Kingdom NF2 registry is based in the Department of Medical Genetics, St. Mary's Hospital, Manchester. People are ascertained by contacting neurosurgeons, otolaryngologists, neurologists, pediatricians, dermatologists, and geneticists throughout the United Kingdom, and the collection is augmented in the North West Region by the Regional Cancer Registry. The present study was subject to continuing ethics committee evaluation, and participants gave informed consent.

As of February 15, 2002, the registry had 425 people from 282 families. For the present study, we excluded three groups of people: (1) We excluded known somatic mosaics ($N = 17$; shown to be mosaic at the molecular level). Almost all reported *NF2* somatic mosaics have mild disease, despite having nonsense or frameshift mutations that typically cause severe disease in classical NF2 (Evans et al. 1998*b*; Kluwe and Mautner 1998). (2) We excluded people who were born before 1930 ($N = 34$). All such individuals in the United Kingdom NF2 registry were identified through younger affected relatives. The pre-1930 group was excluded because it did not meet the proportional-hazards assumption for the Cox analysis. Specifically, type of treatment center and meningiomas did not predict the risk of mortality in people who were born before 1930, in contrast to those born after 1930. (3) We excluded people with missing information on either age at diagnosis ($N = 2$) or presence of intracranial meningiomas ($N = 4$), two covariates that are necessary for analysis of the risk of mortality.

The resultant study group had 368 people from 261 families, all of whom met the Manchester clinical diagnostic criteria for NF2 (Evans et al. 1992*a*) or had identified constitutional *NF2* mutations. The distribution of the number of affected family members was 206 families with one affected member, 27 families with two affected members, 15 families with three affected members, 7 families with four affected members, 3 families with five affected members, 1 family with six affected members, and 2 families with seven affected members. There were 43 two-generation families and 9 three-generation families. There were 223 people with new mutations (individuals with sporadic disease and founders) and 145 people with inherited mutations.

NF2 *Mutation Analysis*

Genomic DNA samples prepared from peripheral leukocytes were amplified with primers for all 17 exons of the *NF2* gene, and screening was performed for constitutional *NF2* mutations, using SSCP analysis, as described elsewhere (Evans et al. 1998*a*).

Statistical Analysis

Potential predictors of the risk of mortality were first assessed using univariate Kaplan-Meier survival curves. The covariates examined were age at onset of symptoms, age at diagnosis, sex, type of constitutional *NF2* mutation, inheritance (new mutation or inherited case), generation (in the 52 multigeneration families), presence and number of each type of NF2 nervous system tumor (VSs, intracranial meningiomas, spinal tumors, and peripheral nerve tumors), lens opacities, number of surgical operations, calendar year of diagnosis, and type of treatment center (specialty or nonspecialty). The specialty treatment centers were hospitals with NF2 specialist management teams (Manchester Royal Infirmary, Addenbrooke's Hospital [Cambridge], and Royal London Hospital).

The number of tumors at diagnosis was used because data from serial examinations were not routinely available. A potential concern about this choice is that imaging done prior to the late 1980s (i.e., with computerized tomography) may be of poorer quality and may tend to underestimate the number of tumors, in comparison with imaging done more recently (i.e., with magnetic resonance imaging). Several lines of evidence indicate that this potential bias is negligible in people with meningiomas or spinal tumors. The number of meningiomas did not vary significantly by calendar year of diagnosis ($P = .95$), after adjustment, using linear regression, for age at diagnosis of the first intracranial meningioma. Some people present with VSs but later develop intracranial meningiomas or have meningiomas that may not have been detected at presentation because of suboptimal imaging. Of the 136 people with both VSs and meningiomas, 25% were diagnosed with meningiomas after their VSs were diagnosed, and the median time between detection of VSs and meningiomas in these people was only four years. Some people may not have spinal imaging early in the course of their disease, but the median time between initial assessment and diagnosis of spinal tumors was only one year.

The presentation of NF2 is different in adults than in children, whose initial sign or symptom is often unrelated to VSs (Mautner et al. 1993; MacCollin and Mautner 1998). For this reason, interactions between age at diagnosis and number of each type of nervous system tumor were evaluated in the Cox models; none of these interactions were statistically significant. Age at onset of symptoms and age at diagnosis were highly correlated

Table 1

Characteristics of 368 People with NF2 in the Study Population

Characteristic	No.	%
Vital status:[a]		
Alive	295	80.2
Dead	73	19.8
Sex:		
Female	191	51.9
Male	177	48.1
Inheritance:		
New mutation	223	60.6
Inherited mutation	145	39.4
Age at onset of symptoms (years):		
1–19	153	41.8
20–39	155	42.3
≥40	34	9.3
Asymptomatic	24	6.6
Age at diagnosis (years):		
1–19	116	31.5
20–39	186	50.6
≥40	66	17.9
VS:		
None	23	6.3
Unilateral	33	9.0
Bilateral	310	84.7
Intracranial meningiomas:		
Absent	203	55.2
Present	165	44.8
Type of constitutional *NF2* mutation:[b]		
Nonsense	43	13.5
Frameshift deletion	27	8.5
Frameshift insertion	10	3.1
Splice donor site	19	6.0
Splice acceptor site	36	11.3
Missense	22	6.9
Large deletion	47	14.8
Not identified	114	35.8
Type of treatment center:		
Nonspecialty	259	70.4
Specialty	109	29.6

[a] As of February 15, 2002.

[b] Frequency of mutations in 318 people from 216 families that were screened for constitutional *NF2* mutations (molecular model).

($r^2 = .63$, $P < .001$); age at diagnosis was used in the analysis because tumor burden was usually first evaluated at this time. Age at diagnosis and calendar year of diagnosis were not highly correlated ($r^2 = .01$, $P = .15$). Initial data analyses included some separate analyses for people with new mutations and those with inherited disease, but the two groups were similar in survival rates (as shown by Kaplan-Meier curves), so people with new mutations and those with inherited disease were combined in further analyses. Proband/nonproband status and new mutation/inherited mutation status were highly correlated, so proband status was not considered further as a covariate.

The covariates that were most highly associated with the risk of mortality in single-predictor Cox proportional hazards models were added sequentially to a multiple-predictor Cox model until there was only a minor decrease in the log partial likelihood. The log partial likelihood, an output-summary value of Cox regression analysis, using S-Plus (Venables and Ripley 1997, is considered to be an indicator of how well a set of potential predictors explain the variation in survival times; because of the dependence within families, it is not the actual partial likelihood. We constructed two Cox models, one without and one with information on the type of constitutional *NF2* mutation. The resulting two models are called the "clinical model" and the "molecular model." The mutation type covariate is categorical and is coded as several binary variables. These variables were indicators of splice-site mutations, missense mutations, large deletions, and unidentified mutations, each compared with nonsense or frameshift mutations. The category of unidentified mutations can include different types of mutations but was treated as a single category for the purpose of this analysis. The molecular model excluded 46 people who had not been screened for constitutional *NF2* mutations, 2 people with in-frame deletions, and 2 people with chromosomal translocations.

The Cox model assumes independence of families and independence of members within families. The latter part of this assumption is violated when there is correlation between family members. When the data are positively correlated, the SEs of parameters estimated under the assumption of independence will tend to be too small, which could lead to an erroneous conclusion that an

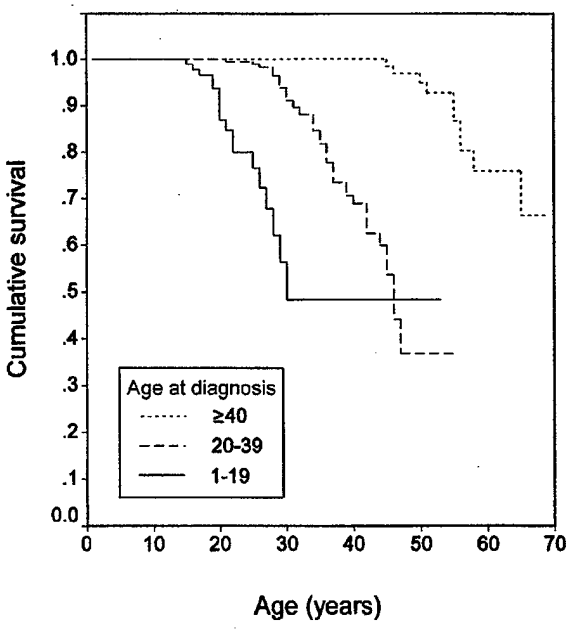

Figure 1 Kaplan-Meier survival curve (log-rank test): age at diagnosis ($P < .0001$).

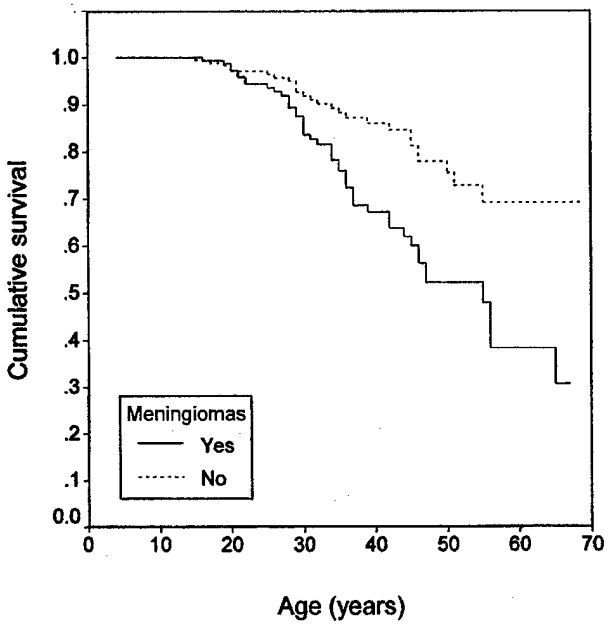

Figure 2 Kaplan-Meier survival curve (log-rank test): intracranial meningiomas ($P = .0003$).

effect is important. To surmount this problem for the Cox models, the delete-one jackknife method, with family as the unit, was used to determine the adjusted parameter estimates and their SEs in the Cox model. The jackknife is a standard statistical method that is commonly used to correct for bias in parameter estimates and to provide SEs in nonstandard sampling situations (Mosteller and Tukey 1977).

In addition to fitting Cox models, we fitted log-normal regression models (regressing log survival on sets of predictor variables), using the S-Plus function called "survreg." The results are qualitatively the same as those of the Cox model. To assess the amount of intrafamilial correlation, ρ, the simplest approach is to add familial dependence to the log-normal regression model and use a multivariate log-normal distribution for the vector of log survival for each family. The simplest dependence structure is exchangeable dependence; this assumes a common correlation for each pair of family members. This dependence obtains from a random-effects model with a common family effect plus individual effects. In notation, the model is $\log Y_{ij} = \beta_0 + \beta' x_{ij} + F_i + E_{ij}$, where i is the index for families, j is the index for members within a family, Y is the survival time, x_{ij} is a vector of covariates, F_is are independent family effects that have a normal distribution with mean 0 and variance σ_F^2, E_{ij}s are independent individual effects that have a normal distribution with mean 0 and variance σ_E^2. The ratio of variances between and within families is $\theta = \sigma_F^2/\sigma_E^2$, and the intrafamilial correlation is $\rho = \theta/(1 + \theta)$. For a family with left-censored Y_{ij}, the likelihood contribution involves a multivariate normal-rectangle probability; for the random-effects model given above, the rectangle probability can be computed as a one-dimensional numerical integral. The log-likelihood can be numerically maximized with a quasi-Newton routine, to obtain maximum-likelihood estimates of the parameters.

Results

The characteristics of the study population are presented in table 1. The mean ± SE age at onset of symptoms was 22 ± 1 years, and the mean age at diagnosis was 27 ± 1 years. The median length of follow-up from initial clinical evaluation was 7 years (range 0–37 years). Ninety-eight percent of people were diagnosed after 1970. Ninety-four percent of people had VSs, and 45% had intracranial meningiomas. Age at diagnosis did not vary significantly by meningioma status (presence or absence of intracranial meningiomas) (mean ± SE 28 ± 1 years with meningiomas absent, 27 ± 1 years with meningiomas present). Constitutional *NF2* mutations were identified in 120 (56%) of the 216 families that were screened for mutations. Seventy-four (20%) of the 368 people died during follow-up: 51 of tumor burden, 14 of complications in the immediate postoperative period, 3 of malignancies arising from an NF2-associated tumor, 2 each of traffic accidents and suicide, and 1 each of a fall due to NF2-associated imbalance and a myocardial infarction.

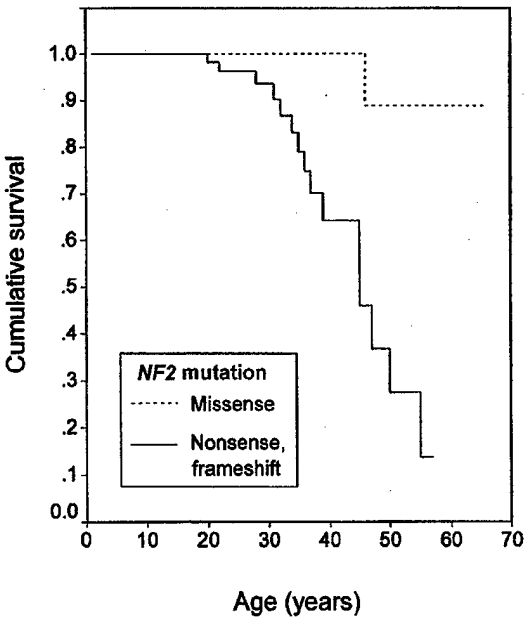

Figure 3 Kaplan-Meier survival curve (log-rank test): type of constitutional *NF2* mutation ($P = .0020$).

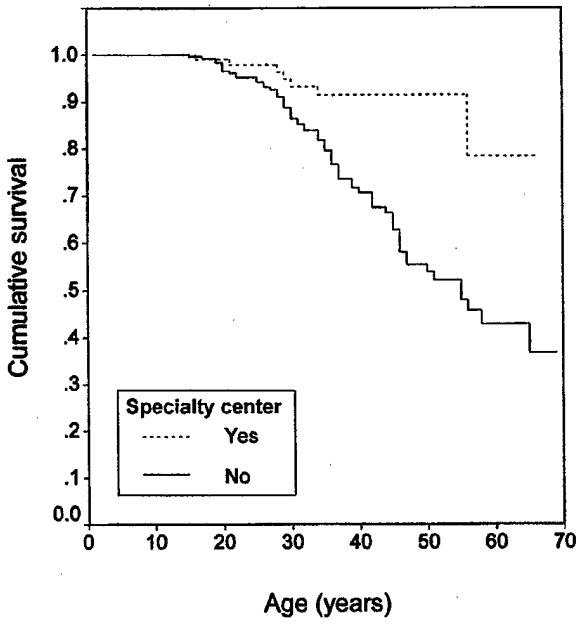

Figure 4 Kaplan-Meier survival curve (log-rank test): type of treatment center ($P = .0001$).

In single-predictor Cox models, five covariates were at least moderately associated with the risk of mortality: age at diagnosis, intracranial meningioma status, type of constitutional *NF2* mutation, type of treatment center, and calendar year of diagnosis. Kaplan-Meier survival curves are presented in figures 1–4. These covariates were included sequentially in multiple-predictor Cox models.

In the clinical model, the best multiple-predictor Cox model had three covariates, which were, in order of importance, age at diagnosis, type of treatment center, and meningioma status. The relative risk (RR) of mortality increased 1.13-fold per year decrease in age at diagnosis (95% CI 1.08–1.18) and was 2.51-fold greater in people with meningiomas compared with those without meningiomas (95% CI 1.38–4.57). The RR of mortality in people treated at specialty centers was 0.34 compared with those treated at nonspecialty centers (95% CI 0.12–0.98). The coefficients for these covariates were stable across Cox models with different sets of predictors. See table 2 for the summary of this Cox model; SEs were based on the jackknife method with the family as the sampling unit. Calendar year of diagnosis had little additional predictive value after age at diagnosis was included. In a separate model that included the covariates of age at diagnosis and type of treatment center but substituted number of meningiomas for presence of meningiomas, the RR of mortality did not significantly increase with increasing number of meningiomas; however, each group had relatively few people (61 people with one meningioma, 63 with two or three meningiomas, and 35 with more than three meningiomas).

In the molecular model, the best multiple-predictor Cox model had three covariates, which were, in order of importance, age at diagnosis, type of treatment center, and mutation type. Meningioma status had little additional predictive value after these three variables were in the model. See table 3 for a summary of this Cox model; the βs for the four mutation types are relative to nonsense or frameshift mutations. The main conclusion is that people with missense mutations have a much lower risk of mortality than do people with any of the other types of mutations. This can be seen from the number of deaths among people with the five types of mutations: 15 of 80 for nonsense or frameshift mutations, 15 of 55 for splice-site mutations, 9 of 47 for large deletions, 19 of 114 for unidentified mutations, and 1 of 22 for missense mutations. Because there is only one death in the missense mutation group, the jackknife does not provide a reliable SE estimate for β for the missense mutation group; the data in table 3 for this variable are based on the omission of two jackknife outliers.

For the random-effects model for log survival time, the covariates of age at diagnosis, type of treatment center, and presence of meningiomas were fitted. The summary of the parameter estimates is given in table 4. The estimated intrafamilial correlation is $0.56 = 1.25/(1 + 1.25)$, with a wide 95% CI of 0.0–0.73. The data set is small and has a high censoring rate, so the intrafamilial correlation cannot be estimated precisely. However, the random-effects model appears to adapt well to censored data.

Discussion

In the present study, we found that four covariates were informative predictors of the risk of mortality in people

Table 2

Parameter Estimates and SEs for the Clinical Model (261 Families with NF2)

Variable	β	SE_β	RR	95% CI_{RR}
Age at diagnosis (per year decrease)	.12	.02	1.13	1.08–1.18
Intracranial meningiomas (present vs. absent)	.92	.31	2.51	1.38–4.57
Type of treatment center (specialty vs. nonspecialty)	−1.07	.54	.34	.12–.98

Table 3

Parameter Estimates and SEs for the Molecular Model (216 Families with NF2)

Variable	β	SE_β	RR	95% CI_{RR}
Age at diagnosis (per year decrease)	.14	.03	1.15	1.09–1.21
Type of treatment center (specialty vs. nonspecialty)	−1.21	.63	.30	.08–1.05
Type of constitutional *NF2* mutation (vs. nonsense or frameshift):				
Splice-site	.22	.67	1.24	.33–4.70
Missense	−2.49	.51	.08	.03–.23
Large deletion	−.29	.49	.75	.28–2.00
Unidentified	−.31	.51	.73	.26–2.00

with NF2. The risk of mortality increased with decreasing age at diagnosis and was greater in people with intracranial meningiomas compared with those without meningiomas. The risk of mortality was lower in people with constitutional *NF2* missense mutations than in those with other types of mutations and in people who were treated at specialty centers compared with those who were treated at nonspecialty centers. The simplicity of age at diagnosis, by far the strongest single predictor of risk of mortality in NF2, makes it a useful index for patient counseling and clinical management; intracranial meningiomas are also useful in this regard. A possible reason for the higher risk of mortality in people with NF2 who are diagnosed at younger ages is that tumor growth is generally more rapid in these patients (Baser et al. 2002; Mautner et al. 2002), perhaps because of a higher rate of somatic cell growth or a larger proportion of growing cells in young people. Age at onset (which is highly correlated with age at diagnosis) and number of non-VS intracranial tumors are key indices of NF2 disease severity (Parry et al. 1994). Other covariates, such as sex, inheritance, and year of diagnosis, were not as useful predictors of the risk of mortality. However, as more information is collected on people with NF2 in the future, the assessment of the risk of mortality should be repeated with these covariates, since it is possible that the present data are insufficient to detect some associations.

In the clinical model, the empirical importance of the type of treatment center is comparable to that of meningioma status. The effect of treatment in specialty centers is not due to marked differences in the characteristics of people who were seen at specialty and nonspecialty treatment centers. New mutations in these two groups were similar with respect to age at onset of symptoms, age at diagnosis, and prevalence of meningiomas. Similar proportions of people with inherited mutations were treated at specialty and nonspecialty centers.

In all likelihood, a major cause of the lower risk of mortality in people with NF2 who are treated in specialty centers is the increasing rate of favorable operative outcomes and the decreasing rate of postoperative complications with increasing surgical experience. When new surgical teams are being trained for VS surgery, there are clear trends, as the number of surgeries increases, toward improved postoperative preservation of facial nerve function, complete resection rate, and hearing preservation, as well as a lowered incidence of serious complications, such as cerebrospinal fluid leaks (Buchman et al. 1996; Welling et al. 1999). In Denmark, decentralized VS neurosurgery was associated with very high rates of perioperative mortality (8.5%) and serious surgical complications (35.6%) (Charabi et al. 1992). People with benign meningioma who are treated in academic hospitals have significantly lower mortality, after adjustment for other risk factors, than do those who are treated in community hospitals (McCarthy et al. 1998). In addition to more extensive surgical experience, specialty centers have coordinated expertise in the multiple clinical specialties that are needed to properly diagnose NF2 and to treat affected individuals and their at-risk family members (Evans et al. 1993; Jackler 1998). To ensure optimal care, we recommend that people with NF2 be referred to specialty centers.

Almost all of the people in this study were diagnosed after 1970. During the last three decades, there have been considerable improvements in neuroimaging techniques that have permitted earlier detection of small tumors. In combination with improvements in neurosurgical treatments, this has led to better clinical management and a much greater incentive to diagnose VSs and NF2. The noninclusion of the more recent years of diagnosis in the multiple-predictor Cox models does not suggest that improvements in clinical care lack benefit.

Table 4

Parameter Estimates and SEs for the Random-Effects Model for Log Survival (261 Families with NF2)

Variable	Estimate	SE
σ_E	.18	.03
θ	1.25	.73
β_0	3.15	.06
Age at diagnosis (per year increase)	−.23	.02
Intracranial meningiomas (present vs. absent)	−.07	.04
Type of treatment center (specialty vs. nonspecialty)	.21	.06

In all likelihood, insufficient time has elapsed for such benefit to be reflected in decreased mortality. In addition, the benefits from incremental improvements in clinical care throughout the post-1970 era may be more subtle, with respect to risk of mortality, than those that occurred with the advent of computerized tomography scanning in the early 1970s.

Of the people with NF2 who have access to treatment, relatively few die of their VSs. In the modern era of improved microsurgical techniques, operative mortality in specialized neuro-otology treatment centers is ≤1%, and recurrence rates are nil when the entire VS and vestibular nerves are excised. Intracranial meningiomas and spinal tumors are common in NF2, and these recurrent tumors often require repeated surgeries. There is considerable pre- and postoperative morbidity due to seizures, paralysis, wasting, pneumonia, and accidents associated with meningiomas and spinal tumors (Evans et al. 2000).

In the molecular model, the risk of mortality appeared to be much lower in people with missense mutations than in those with other types of mutations. Experimental studies have suggested possible mechanisms through which constitutional *NF2* missense mutations cause milder disease than do nonsense or frameshift *NF2* mutations. Missense mutations produce an *NF2* protein (termed "merlin" or "schwannomin") that is stable but defective in negative growth regulation, whereas nonsense mutations do not produce stable protein (Gutmann et al. 1998). Naturally occurring missense mutations have reduced, but not absent, activity of the merlin-binding protein βII-spectrin (Scoles et al. 1998).

Since *NF2* mutation type is strongly associated with age at diagnosis in cross-sectional studies, a logical question is why age at diagnosis is more strongly associated than the type of *NF2* mutation with the risk of mortality. Age at diagnosis may be more strongly associated because both age at diagnosis and age at death reflect a composite of disease-influencing factors, whereas mutation type is only one of these factors. Other factors are the stochastic loss of the second *NF2* allele (Baser et al. 1996) and putative modifying genes (Bruder et al. 1999*a*, 1999*b*).

Constitutional *NF2* mutations that are not found by SSCP could be mutations in the 3′ or 5′ UTRs, the promoter region, or untranscribed transcriptional control elements; intronic mutations that are not covered by SSCP primers; large deletions, insertions, or other rearrangements; or mutations in patients who are somatic mosaics (Zucman-Rossi et al. 1998). Other epigenetic events (i.e., methylation) could result in loss of *NF2* expression (Kino et al. 2001). There is no evidence for locus heterogeneity in NF2 (Narod et al. 1992). In 60 United Kingdom families that have people with NF2 in two or more generations, all families have linkage to *NF2*, and *NF2* mutations have been identified in all but six families (D.G.R.E., unpublished data).

Approximately 20% of NF2 new mutations are thought to be somatic mosaics, and almost all have mild disease, despite having constitutional nonsense or frameshift *NF2* mutations (Evans et al. 1998*b*; Kluwe and Mautner 1998). We excluded known somatic mosaics from the analysis, and, although some somatic mosaics probably were not detected, the resultant bias is likely to be minor. Among the 187 people with new mutations who underwent molecular screening, pathogenic *NF2* mutations were not identified in 88. Sixty-eight of these people with new mutations were ≤20 years of age at the onset of symptoms, or they had two or more meningiomas or four or more spinal tumors. These people are unlikely to be mosaic, because they have severe disease. The remaining 20 people with new mutations had mild disease. If 20% of them were mosaic, then we failed to identify only four mosaic individuals in the screened group.

In summary, the strongest single predictor of the risk of mortality in NF2 is age at diagnosis, which is a useful index for patient counseling and clinical management, as is meningioma status. People with constitutional *NF2* missense mutations appear to have a much lower risk of mortality than do those with other types of mutations. Our finding that people with NF2 who are treated at specialty centers have a lower risk of mortality is consistent with studies of unilateral sporadic VS, in which surgical outcomes were improved and operative complications were reduced in proportion to increasing surgical experience. To ensure optimal care, we recommend that people with NF2 be referred to specialty treatment centers.

Acknowledgments

This work was supported in part by the FBT Foundation and U.S. Army grant U.S.A.R.M.C. NF990038.

Electronic-Database Information

Accession number and URL for data in this article are as follows:

Online Mendelian Inheritance in Man (OMIM), http://www.ncbi.nlm.nih.gov/Omim/ (for NF2 [MIM 101000])

References

Antinheimo J, Sankila R, Carpén O, Pukkala E, Sainio M, Jääkeläinen J (2000) Population-based analysis of sporadic and type 2 neurofibromatosis-associated meningiomas and schwannomas. Neurology 54:71–76

Baser ME, Friedman JM, Evans DGR (1999) Predictors of

survival in neurofibromatosis. Am J Hum Genet Suppl 65: A61

Baser ME, Makariou EV, Parry DM (2002) Predictors of vestibular Schwannoma growth in patients with neurofibromatosis type 2. J Neurosurg 96:217–222

Baser ME, Ragge NK, Riccardi VM, Janus T, Gantz B, Pulst S (1996) Phenotypic variability in monozygotic twins with neurofibromatosis 2. Am J Med Genet 64:563–567

Bruder CEG, Ichimura K, Blenow E, Ikeuchi T, Yamaguchi T, Yuasa Y, Collins VP, Dumanski JP (1999*a*) Severe phenotype of the neurofibromatosis type 2 gene in patients with a 7.4 Mbp constitutional deletion on chromosome 22: possible localization of a neurofibromatosis type 2 modifier gene? Genes Chromosomes Cancer 25:184–190

Bruder CEG, Ichimura K, Tingby O, Hirakawa K, Komatsuzaki A, Tamura A, Yuasa Y, Collins VP, Dumanski JP (1999*b*) A group of schwannomas with interstitial deletions on 22q located outside the *NF2* locus shows no detectable mutations in the *NF2* gene. Hum Genet 104:418–424

Buchman CA, Chen DA, Flannagan P, Wilberger JE, Maroon JC (1996) The learning curve for acoustic tumor surgery. Laryngoscope 106:1406–1411

Charabi S, Tos M, Thomsen J, Borgesen SE (1992) Suboccipital acoustic neuroma surgery: results of decentralized neurosurgical tumor removal in Denmark. Acta Otolaryngol 112: 810–815

Evans DG, Sainio M, Baser ME (2000). Neurofibromatosis type 2. J Med Genet 37:897–904

Evans DGR, Huson SM, Donnai D, Neary W, Blair V, Newton V, Harris R (1992*a*) A clinical study of type 2 neurofibromatosis. Q J Med 84:603–618

Evans DGR, Huson SM, Donnai D, Neary W, Blair V, Teare D, Newton V, Strachan T, Ramsden R, Harris R (1992*b*) A genetic study of type 2 neurofibromatosis in the United Kingdom. I. Prevalence, mutation rate, fitness, and confirmation of maternal transmission effect on severity. J Med Genet 29: 841–846

Evans DGR, Ramsden R, Huson SM, Harris R, Lye R, King TT (1993) Type 2 neurofibromatosis: the need for supraregional care? J Laryngol Otol 107:401–406

Evans DGR, Trueman L, Wallace A, Collins S, Strachan T (1998*a*) Genotype/phenotype correlations in type 2 neurofibromatosis (NF2): evidence for more severe disease associated with truncating mutations. J Med Genet 35:450–455

Evans DGR, Wallace AJ, Wu CL, Trueman L, Ramsden RT, Strachan T (1998*b*) Somatic mosaicism: a common cause of classic disease in tumor-prone syndromes? lessons from type 2 neurofibromatosis. Am J Hum Genet 63:727–736

Gutmann DH, Geist RT, Xu H-m, Kim JS, Saporito-Irwin S (1998) Defects in neurofibromatosis 2 protein function can arise at multiple levels. Hum Mol Genet 7:335–345

Jackler RK (1998) The perils of decentralized care in otology/neuro-otology. Am J Otol 19:691–692

Kino T, Takeshima H, Nakao M, Nishi T, Yamamoto K, Kimura T, Saito Y, Kochi M, Kuratsu J, Saya H, Ushio Y (2001) Identification of the cis-acting region in the *NF2* gene promoter as a potential target for mutation and methylation-dependent silencing in schwannoma. Genes Cells 6:441–454

Kluwe L, Beyer S, Baser ME, Hazim W, Haase W, Fünsterer C, Mautner VF (1996) Identification of *NF2* germ-line mutations and comparison with NF2 phenotypes. Hum Genet 98:534–538

Kluwe L, MacCollin M, Tatagiba M, Thomas S, Hazim W, Haase W, Mautner VF (1998) Phenotypic variability associated with 14 splice-site mutations in the *NF2* gene. Am J Med Genet 77:228–233

Kluwe L, Mautner VF (1998) Mosaicism in sporadic neurofibromatosis 2 patients. Hum Mol Genet 7:2051–2055

MacCollin M, Mautner VF (1998) The diagnosis and management of neurofibromatosis 2 in childhood. Semin Pediatr Neurol 5:243–252

Mautner VF, Baser ME, Thakkar SD, Feigen UM, Friedman JM, Kluwe L (2002) Vestibular schwannoma growth in patients with neurofibromatosis type 2: a longitudinal study. J Neurosurg 96:223–228

Mautner VF, Lindenau M, Baser ME, Hazim W, Tatagiba M, Haase W, Samii M, Wais R, Pulst SM (1996) The neuroimaging and clinical spectrum of neurofibromatosis 2. Neurosurgery 38:880–885

Mautner VF, Tatagiba M, Guthoff R, Samii M, Pulst SM (1993) Neurofibromatosis 2 in the pediatric age group. Neurosurgery 33:92–96

Mautner VF, Tatagiba M, Lindenau M, Fünsterer C, Pulst SM, Baser ME, Kluwe L, Zanella FE (1995) Spinal tumors in patients with neurofibromatosis type 2: MR imaging study of frequency, multiplicity, and variety. AJR Am J Roentgenol 165:951–955

McCarthy BJ, Davis FG, Freels S, Surawicz TS, Damek DM, Grutsch J, Mench HR, Laws ER Jr (1998) Factors associated with survival in patients with meningioma. J Neurosurg 88: 831–839

Mérel P, Hoang-Xuan K, Sanson M, Bijlsma E, Rouleau G, Laurent-Puig P, Pulst S, Baser M, Lenoir G, Sterkers JM, Philippon J, Resche F, Mautner VF, Fisher G, Hulsebos T, Aurias A, Delattre O, Thomas G (1995) Screening for germline mutations in the *NF2* gene. Genes Chromosomes Cancer 12:117–127

Mosteller F, Tukey JW (1977) Data analysis and regression: a second course in statistics. Addison-Wesley, Reading, MA

Narod SA, Parry DM, Parboosingh J, Lenoir GM, Ruttledge M, Fischer G, Eldridge R, Martuza RL, Frontali M, Haines J, Gusella JF, Rouleau GA (1992) Neurofibromatosis type 2 appears to be a genetically homogeneous disease. Am J Hum Genet 51:486–496

Parry DM, Eldridge R, Kaiser-Kupfer MI, Bouzas EA, Pikus A, Patronas N (1994) Neurofibromatosis 2 (NF2): clinical characteristics of 63 affected individuals and clinical evidence for heterogeneity. Am J Med Genet 52:450–461

Parry DM, MacCollin MM, Kaiser-Kupfer MI, Pulaski K, Nicholson HS, Bolesta M, Eldridge R, Gusella JF (1996) Germ-line mutations in the neurofibromatosis 2 gene: correlations with disease severity and retinal abnormalities. Am J Hum Genet 59:529–539

Rouleau GA, Merel P, Lutchman M, Sanson M, Zucman J, Marineau C, Hoang-Xuan K, Demczuk S, Desmaze C, Plougstel B, Pulst SM, Lenoir G, Bijlsma E, Fashold R, Dumanski J, de Jong P, Parry D, Eldridge R, Aurias A, Delattre O, Thomas G (1993) Alteration in a new gene encoding a putative membrane-organizing protein causes neuro-fibromatosis type 2. Nature 363:515–521

Ruttledge MH, Andermann AA, Phelan CM, Claudio JO, Han

F-y, Chretien N, Rangaratnam S, MacCollin M, Short P, Parry D, Michels V, Riccardi VM, Weksberg R, Kitamura K, Bradburn JM, Hall BD, Propping P, Rouleau GA (1996) Type of mutation in the neurofibromatosis type 2 gene (*NF2*) frequently determines severity of disease. Am J Hum Genet 59:331–342

Scoles DR, Huynh DP, Morcos PA, Coulsell ER, Robinson NGG, Tamanoi F, Pulst SM (1998) Neurofibromatosis 2 tumour suppressor schwannomin interacts with βII-spectrin. Nat Genet 18:354–359

Trofatter JA, MacCollin MM, Rutter JL, Murrell JR, Duyao MP, Parry DM, Eldridge R, Kley N, Menon AG, Pulaski K, Haase VH, Ambrose CM, Munroe D, Bove C, Haines JL, Martuza RL, MacDonald ME, Seizinger BR, Short MP, Buckler AJ, Gusella JF (1993) A novel moesin-, ezrin-, radixin-like gene is a candidate for the neurofibromatosis 2 tumor suppressor. Cell 72:791–800

Venables WN, Ripley BD (1997) Modern applied statistics with S-Plus. 2nd ed. Springer, New York

Welling DB, Slater PW, Thomas RD, McGregor JM, Goodman JE (1999) The learning curve in vestibular schwannoma surgery. Am J Otol 20:644–648

Zucman-Rossi J, Legoix P, Sarkissian HD, Cheret G, Sor F, Bernardi A, Cazes L, Giraud S, Ollagnon E, Lenoir G, Thomas G (1998) NF2 gene in neurofibromatosis type 2 patients. Hum Mol Genet 7:2095–2101

Evaluation of clinical diagnostic criteria for neurofibromatosis 2

M.E. Baser, PhD; J.M. Friedman, MD, PhD; A.J. Wallace, PhD; R.T. Ramsden, MD; H. Joe, PhD; and D.G.R. Evans, MD

Abstract—*Background:* Four sets of clinical diagnostic criteria for neurofibromatosis 2 (NF2) have been developed by groups of expert clinicians, but sensitivity has never been formally assessed. The sets of criteria differ for people without bilateral vestibular schwannomas, which are pathognomonic for NF2. *Objective:* To empirically evaluate the four existing sets of clinical diagnostic criteria for NF2. *Methods:* The study was based on 163 of 403 people in the United Kingdom NF2 registry (41%) who presented without bilateral vestibular schwannomas. The authors applied the sets of criteria to each person at initial assessment and at the most recent clinical evaluation (mean ± SE length of follow-up, 13 ± 1 years). *Results:* In people with "definite NF2" and a negative family history of NF2, the 1987 US NIH and 1991 NIH criteria each identify 78% of people at the most recent clinical evaluation but 0% at initial assessment. The National Neurofibromatosis Foundation (NNFF) criteria and the Manchester criteria each identify higher proportions at both time points (NNFF criteria, 91% and 10%; Manchester criteria, 93% and 14%), but the proportions at initial assessment are still low. *Conclusions:* None of the existing sets of criteria are adequate at initial assessment for diagnosing people who present without bilateral vestibular schwannomas as having NF2, particularly people with a negative family history of NF2. The authors recommend that a single, revised set of diagnostic criteria be devised to replace all of the existing sets of criteria.

NEUROLOGY 2002;59:1759–1765

Neurofibromatosis 2 (NF2) is an autosomal dominant disease, caused by inactivating mutations of the *NF2* tumor suppressor gene,[1,2] with an incidence of 1 in 33,000 to 40,000 live births.[3] Clinical features of NF2 typically include nervous system tumors (vestibular schwannomas, intracranial meningiomas, spinal tumors, and peripheral nervous system tumors), and ocular abnormalities.[4-6] In 1987, a US NIH Consensus Conference established clinical diagnostic guidelines to differentiate NF2 from NF1.[7] Although the two diseases were then known to be genetically distinct,[8] their frequent confusion in the medical literature and the need to avoid misdiagnosis in linkage studies prompted the development of these criteria.

As the full clinical spectrum of NF2 became better defined by molecular analysis and neuroimaging, the 1987 NIH criteria proved to be too restrictive for use in routine diagnosis. Revisions to the criteria were recommended by a second NIH Consensus Conference in 1991,[9] the Manchester group in 1992,[4] and a group organized by the National Neurofibromatosis Foundation (NNFF) in 1997.[10] Each set of criteria was developed by a group of expert clinicians, but the sensitivity, specificity, and clinical utility of these diagnostic guidelines have never been formally assessed.

All four sets of criteria diagnose NF2 in people with bilateral vestibular schwannomas and in people with a first-degree relative with NF2 and either a unilateral vestibular schwannoma at less than 30 years of age or at least two other characteristic disease features of NF2 (meningioma, schwannoma, glioma, presenile cataract). The diagnostic systems differ in other respects (table 1). Half of all people with NF2 have a family history of the disease.[4]

The purpose of this study was to examine the diagnostic efficiency of the four sets of criteria in people who do not have bilateral vestibular schwannomas but who do have other signs of NF2. We found that none of the existing sets of criteria is satisfactory for diagnosing such people at initial assessment. Overall and at the time of the most recent clinical evaluation, the Manchester criteria are the most sensitive.

Methods. The study population was selected from the United Kingdom NF2 registry. NF2 patients are ascertained by contacting neurosurgeons, otolaryngologists, neurologists, pediatricians, dermatologists, and geneticists throughout the UK. Patients are also identified through the Regional Cancer Registry in the North West Region. As of 1 April 2002, the registry had clinical and molecular information on 427 people with proven or suspected NF2 from 282 families. We excluded asymptomatic at-risk members of NF2 families who were diagnosed through genetic screening and did not have clinical information (n = 13) and 11 other people with insufficient clinical informa-

From Los Angeles, CA (Dr. Baser); Departments of Medical Genetics (Dr. Friedman) and Biostatistics (Dr. Joe), University of British Columbia, Vancouver, Canada; and Department of Medical Genetics (Drs. Wallace and Evans), St. Mary's Hospital, and Department of Otolaryngology (Dr. Ramsden), Manchester Royal Infirmary, Manchester, UK.

Supported in part by the FBT Foundation.

Presented in part at the 50th Annual Meeting, American Society of Human Genetics, Philadelphia, PA, October 3 to 7, 2000.

Received April 2, 2002. Accepted in final form August 15, 2002.

Address correspondence and reprint requests to Dr. Michael E. Baser, 2257 Fox Hills Dr., Los Angeles, CA 90064; e-mail: baser@earthlink.net

***Table 1** Clinical diagnostic criteria for NF2*

1987 NIH criteria

A. Bilateral vestibular schwannomas

B. First-degree family relative with NF2 *and* unilateral vestibular schwannoma *or* any two of: meningioma, schwannoma, glioma, neurofibroma, juvenile posterior subcapsular lenticular opacity

1991 NIH criteria

A. Bilateral vestibular schwannomas

B. First-degree family relative with NF2 *and* unilateral vestibular schwannoma *or* any one of: meningioma, schwannoma, glioma, neurofibroma, juvenile posterior subcapsular lens opacity

Manchester criteria*

A. Bilateral vestibular schwannomas

B. First-degree family relative with NF2 *and* unilateral vestibular schwannoma *or* any two of: meningioma, schwannoma, glioma, neurofibroma, posterior subcapsular lenticular opacities

C. Unilateral vestibular schwannoma *and* any two of: meningioma, schwannoma, glioma, neurofibroma, posterior subcapsular lenticular opacities

D. Multiple meningiomas (two or more) *and* unilateral vestibular schwannoma *or* any two of: schwannoma, glioma, neurofibroma, cataract

NNFF criteria†

A. Confirmed or definite NF2

1. Bilateral vestibular schwannomas

2. First-degree family relative with NF2 *and* unilateral vestibular schwannoma at less than 30 y of age *or* any two of: meningioma, schwannoma, glioma, juvenile lens opacity (posterior subcapsular cataract or cortical cataract)

B. Presumptive or probable NF2

1. Unilateral vestibular schwannoma at less than 30 y of age *and* at least one of: meningioma, schwannoma, glioma, juvenile lens opacity (posterior subcapsular cataract or cortical cataract)

2. Multiple meningiomas (two or more) *and* unilateral vestibular schwannoma at less than 30 y of age *or* at least one of: schwannoma, glioma, juvenile lens opacity (posterior subcapsular cataract or cortical cataract)

* In the Manchester criteria, "any two of" refers to two individual tumors or cataract, whereas in the other sets of criteria, it refers to two tumor types or cataract.

† For the purposes of this study, the NNFF criteria for confirmed or definite NF2 and for presumptive or probable criteria were considered to be equivalent.

NF2 = neurofibromatosis 2; NNFF = National Neurofibromatosis Foundation.

tion for this study. Of the remaining 403 people, 240 (59%) had bilateral vestibular schwannomas at initial assessment.

This study was based on the 163 people (41%) who did not have bilateral vestibular schwannomas at initial assessment (108 new mutations and 55 inherited cases; 138 NF2 families). Of these 163 people, 64 had left and right vestibular schwannomas diagnosed at the same time but previously presented with other NF2-related abnormalities (meningioma, schwannoma, glioma, neurofibroma, presenile cataract), 42 had only a unilateral vestibular schwannoma during follow-up, 40 presented with a unilateral vestibular schwannoma but developed a contralateral vestibular schwannoma during follow-up, and 17 did not have any vestibular schwannomas during follow-up. Of the 104 people who had bilateral vestibular schwannomas by the end of follow-up, left and right vestibular schwannomas were diagnosed at the same time in 64 people, but there was a delay of 1 to 5 years in 22 people, 6 to 10 years in 12 people, 11 to 15 years in 4 people, and more than 15 years in 2 people.

The NNFF criteria have separate categories for confirmed or definite NF2 and presumptive or probable NF2 (see table 1). For the purposes of this study, these two categories were considered to be equivalent. In new mutations from the United Kingdom NF2 registry that were screened for constitutional *NF2* mutations, mutations were found in 57% of 21 people who met the NNFF criteria for presumptive or probable NF2, a fraction similar to the 55% of 168 people with bilateral vestibular schwannomas.

At the end of follow-up, 59 people had a first-degree relative with NF2. Seventeen of these people did not have an affected first-degree relative at initial assessment. The affected first-degree relative was a parent in 53 patients and an offspring in 6 patients. In only one instance was the parent initially assessed after the offspring was diagnosed with NF2. An additional six people died before their first-degree relative was diagnosed with NF2. For the purposes of this study, these people were classified as not having an affected relative during follow-up, but this information was considered in determining inheritance.

The 163 people who did not have bilateral vestibular schwannomas at initial assessment were divided into two groups. People with "definite NF2" were those who met the specific criteria, by the end of follow-up, that all four sets of clinical diagnostic criteria have in common. In each set of criteria, persons are diagnosed with NF2 if they have bilateral vestibular schwannomas or a first-degree relative with NF2 and either a unilateral vestibular schwannoma at less than 30 years of age or two other characteristic NF2 disease feature types (meningioma, schwannoma, glioma, presenile cataract). Identified constitutional *NF2* mutations were also used to define "definite NF2." One hundred forty-one people were classified as having "definite NF2": 104 had bilateral vestibular schwannomas by the end of follow-up, 98 had identified constitutional *NF2* mutations, 8 had a first-degree relative with NF2 and a unilateral vestibular schwannoma at less than 30 years of age, and 6 had an affected first-degree relative, no vestibular schwannomas, but at least two other characteristic types of NF2 disease features. People with "possible NF2" (n = 22) had some characteristic features of NF2 but did not meet the criteria for "definite NF2." The length of follow-up was not significantly different between people with "definite NF2" and those with "possible NF2" (mean ± SE, 13 ± 1 and 11 ± 2 years).

The four sets of diagnostic criteria were applied to these two groups to determine the proportion of people who met each set of criteria. We evaluated the diagnostic criteria at two time points: initial assessment and most recent clinical evaluation. The United Kingdom NF2 registry has the age at diagnosis of each tumor type and the age at which

Table 2 *Four sets of NF2 clinical diagnostic criteria applied to 163 people in the United Kingdom NF2 registry who presented without bilateral vestibular schwannomas, by time of evaluation, disease group, and family history*

	No. (%) of patients identified by time of evaluation, disease group,† and family history‡					
	Initial assessment			Most recent clinical evaluation§		
	"Definite NF2"			"Definite NF2"		
	family history			family history		
Diagnostic criteria*	Negative, n = 99	Positive, n = 42	"Possible NF2," n = 22	Negative, n = 85	Positive, n = 56	"Possible NF2," n = 22
1987 NIH	0 (0)	19 (45)	0 (0)	66 (78)	55 (98)	0 (0)
1991 NIH	0 (0)	42 (100)	0 (0)	66 (78)	56 (100)	3 (14)
NNFF	10 (10)	17 (40)	5 (23)	77 (91)	54 (96)	10 (46)
Manchester	14 (14)	29 (69)	7 (32)	79 (93)	55 (98)	22 (100)

* See table 1 for definition of the different sets of diagnostic criteria.

† Seventeen first-degree relatives of people with "definite NF2" were diagnosed after initial assessment (14 "definite NF2" patients and 3 "possible NF2" patients).

‡ "Definite NF2": people who had bilateral vestibular schwannomas by the end of follow-up or who had a first-degree relative with NF2 and either a unilateral vestibular schwannoma at less than 30 y of age or at least two other characteristic disease feature types of NF2 or who had an identified constitutional *NF2* mutation. "Possible NF2": people who had some characteristic disease features of NF2 but who did not meet the criteria for "definite NF2."

§ The mean ± SE period of follow-up was 13 ± 1 years.

NF2 = neurofibromatosis 2; NNFF = National Neurofibromatosis Foundation.

first-degree relatives were diagnosed, and for the analysis based on initial assessment, we considered only those abnormalities and affected relatives that existed at that time point.

Using Kaplan–Meier analysis, we determined the time course, from initial assessment to the most recent clinical evaluation, of the increasing proportion of people who would be diagnosed with NF2 using the different sets of criteria as a result of new disease features developing or a first-degree relative being newly diagnosed. Only those manifestations and affected first-degree relatives that were present in each year of follow-up were considered. Because the Kaplan–Meier curves for the different sets of diagnostic criteria are based on the same people, we used the jackknife method,[11] with family as the unit, to compute pointwise standard errors for differences in proportions of pairwise Kaplan–Meier curves.

Results. Table 2 presents the proportion of the 163 people who presented without bilateral vestibular schwannomas at initial assessment that were identified using each set of diagnostic criteria. At initial assessment, the 1987 NIH criteria and the 1991 NIH criteria each identified 0% of people with "definite NF2" and a negative family history of NF2, whereas the NNFF criteria and the Manchester criteria identified greater but still low proportions (10% and 14%). The 1991 NIH criteria identified 100% of people with "definite NF2" and a positive family history of NF2, whereas the other sets of criteria identified 45% to 69%. The 1987 NIH criteria and the 1991 NIH criteria did not identify any people with "possible NF2" as having NF2, whereas the NNFF criteria and the Manchester criteria identified greater but still low proportions (23% and 32%).

As expected, greater proportions of people were diagnosed with NF2 using each set of criteria at the most recent clinical evaluation than at initial assessment (i.e., after an average of 13 years from initial assessment). At the most recent clinical evaluation, the 1987 NIH criteria and the 1991 NIH criteria each identified 78% of people with "definite NF2" and a negative family history of NF2. The NNFF and Manchester criteria identified NF2 in higher proportions of these people (91% and 93%). All four sets of criteria identified high proportions of people with "definite NF2" and a positive family history of NF2 (96% to 100%). The Manchester criteria identified NF2 in 100% of people with "possible NF2," but the other sets of criteria identified NF2 in much lower proportions (0% to 46%).

Figure 1 illustrates the proportion of the 121 people in this study with a negative family history of NF2 at initial assessment that met each of the four sets of diagnostic criteria with increasing length of time from initial assessment, using Kaplan–Meier analysis. At 1 year from initial assessment, the proportion of people that met the diagnostic criteria for NF2 was 27% using the Manchester criteria, 23% using the NNFF criteria, 5% using the 1991 NIH criteria, and 4% using the 1987 NIH criteria. At 5 years from initial assessment, these proportions were 49% using the Manchester criteria, 44% using the NNFF criteria, 27% using the 1991 NIH criteria, and 24% using the 1987 NIH criteria.

Table 3 presents the differences in proportions of people identified as having NF2 in comparisons between the different sets of diagnostic criteria (pointwise comparisons, corresponding to jump points in the Kaplan–Meier curves). For the Manchester criteria and the 1991 NIH criteria, the difference in proportions was significantly greater than zero from initial assessment to 25 years after initial assessment. For the NNFF criteria and the 1991 NIH criteria, the difference in proportions was significantly greater than zero from initial assessment to 15 years after initial

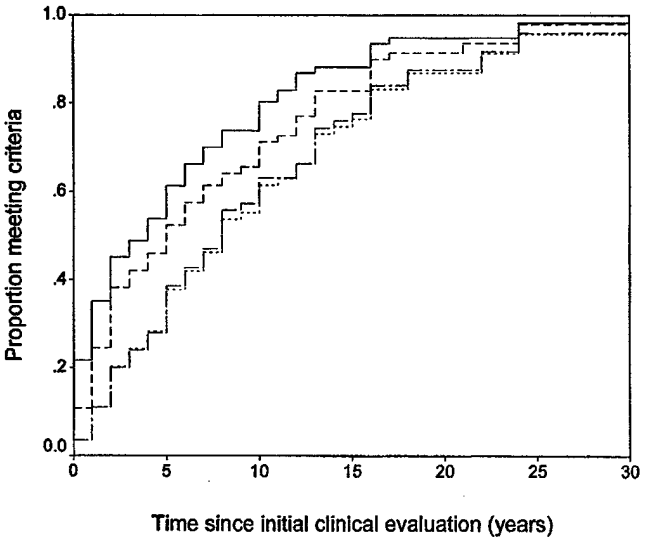

Figure 1. Proportion of 121 people with a negative family history of neurofibromatosis 2 (NF2) at initial assessment that meet the four sets of clinical diagnostic criteria with increasing length of time from initial assessment (Kaplan–Meier analysis). Solid line = Manchester criteria; dashed line = National Neurofibromatosis Foundation criteria; dash–dot line = 1991 NIH criteria; dotted line = 1987 NIH criteria.

assessment. For the Manchester criteria and the NNFF criteria, the difference in proportions was significantly greater than zero at initial assessment and from 5 to 20 years after initial assessment.

There were 8 known somatic mosaics (determined through molecular analysis) among the 98 new mutations that were screened for constitutional *NF2* mutations. At initial assessment, only the Manchester criteria identified any of the mosaics (one) as having NF2. At the most recent clinical evaluation, the 1987 NIH criteria and 1991 NIH criteria each identified four mosaics as having NF2, the NNFF criteria identified five mosaics, and the Manchester criteria identified all eight mosaics. The median age at onset of symptoms in the eight mosaics was 28 years (range 23 to 46 years) and the median age at diagnosis was 43 years (range 27 to 62 years). At initial assessment, four of the mosaics had unilateral vestibular schwannomas, two had peripheral nervous system schwannomas, one had spinal tumors, and one had cataracts. At the most recent clinical evaluation, four of the mosaics had unilateral vestibular schwannomas, four had bilateral vestibular schwannomas, four had spinal tumors, two had peripheral nervous system schwannomas, two had intracranial meningiomas, two had cataracts, and one had a non-VIII nerve cranial nerve tumor.

Discussion. Bilateral vestibular schwannomas are pathognomic for NF2, but 163 of the 403 people with clinical information in the United Kingdom NF2 registry (41%) did not have bilateral vestibular schwannomas at initial assessment. The four sets of clinical diagnostic criteria identify different proportions of these 163 people as having NF2, in both "definite NF2" and "possible NF2" patients. People with a negative family history of NF2 at initial assessment present the greatest diagnostic difficulties. By Kaplan–Meier analysis, the Manchester criteria and the NNFF criteria each identify significantly higher proportions of these people than the 1991 NIH criteria, but the Manchester criteria usually identify a significantly higher proportion than the NNFF criteria.

The 1991 NIH criteria identify the highest proportion of people with "definite NF2" and a positive family history of NF2 because this set of criteria requires only one instead of two characteristic disease features to establish the diagnosis in people with a family history of the disease. However, the 1987 NIH criteria and the 1991 NIH criteria each require a positive family history to diagnose NF2 in people who do not have bilateral vestibular schwannomas. As a result, the NIH criteria identify the lowest proportion of people with "definite NF2" and a negative family history of NF2 and few people with "possible NF2." The three people with "possible NF2" who were identified at the most recent clinical evaluation using the 1991 NIH criteria each had a family member who had been diagnosed with NF2 after initial assessment, no vestibular schwannomas, or a unilateral vestibular schwannoma at age 30 or older and one other characteristic disease feature of NF2.

Unlike the NIH criteria, a diagnosis of NF2 can be made using the Manchester criteria and the NNFF criteria in people who do not have bilateral vestibular schwannomas or a family history of NF2 but who do have other characteristic disease features. The Manchester criteria and the NNFF criteria have similar wording, but the Manchester criteria identify a higher proportion of people than the NNFF criteria because the Manchester criteria are based on the number of disease features of any type (i.e., the number of individual tumors), whereas the NNFF criteria and the NIH criteria are based on the number of different feature types. For example, in a person with two intracranial meningiomas, the Manchester criteria count the two meningiomas as two disease features, whereas the NNFF criteria and the NIH criteria count the two meningiomas as a single disease feature because they are the same histologic type of tumor.

The Manchester criteria also differ from the NNFF criteria because the Manchester criteria do not require an age at diagnosis of unilateral vestibular schwannoma of less than 30 years. This age requirement decreases sensitivity and is not needed to increase specificity because people with unilateral vestibular schwannoma who do not have a family history of NF2 or any other characteristic disease features of NF2 have a very low probability of developing NF2. The probability decreases from 1% in people who are diagnosed with a unilateral vestibular schwannoma at ages 10 to 19 years to 0.45% in those aged 20 to 29 years to 0.15% in those aged 30 to 39 years.[12] Figure 2 presents data from the UK showing that 54% of NF2 patients with new muta-

Table 3 *Pointwise comparisons of Kaplan–Meier curves in figure 1, difference in proportions of people identified as having NF2 using different sets of diagnostic criteria, by time since initial assessment*

	Comparisons between sets of diagnostic criteria					
	Manchester v 1991 NIH		NNFF v 1991 NIH		Manchester v NNFF	
Time since initial assessment, y	Difference in proportions	95% CI	Difference in proportions	95% CI	Difference in proportions	95% CI
0	0.174	0.107–0.241	0.124	0.065–0.183	0.050	0.005–0.095
1	0.215	0.141–0.289	0.174	0.101–0.247	0.040	0.000–0.089
2	0.230	0.154–0.306	0.190	0.114–0.266	0.039	0.000–0.086
3	0.236	0.160–0.312	0.197	0.121–0.273	0.039	0.000–0.086
4	0.240	0.158–0.322	0.193	0.113–0.273	0.046	0.000–0.093
5	0.233	0.139–0.307	0.170	0.088–0.252	0.053	0.010–0.096
6	0.234	0.148–0.320	0.175	0.093–0.257	0.060	0.015–0.105
7	0.228	0.144–0.312	0.170	0.088–0.252	0.058	0.015–0.101
8	0.191	0.113–0.269	0.126	0.048–0.204	0.065	0.020–0.110
9	0.196	0.125–0.270	0.133	0.059–0.207	0.063	0.020–0.106
10	0.195	0.119–0.271	0.118	0.045–0.191	0.078	0.031–0.125
11	0.221	0.141–0.301	0.148	0.070–0.226	0.074	0.029–0.119
12	0.199	0.123–0.275	0.124	0.050–0.198	0.075	0.030–0.120
13	0.177	0.103–0.251	0.116	0.043–0.189	0.061	0.014–0.118
14	0.158	0.087–0.229	0.100	0.031–0.169	0.059	0.012–0.116
15	0.151	0.080–0.222	0.085	0.020–0.150	0.066	0.023–0.107
16	0.140	0.064–0.216	0.069	0.000–0.107	0.071	0.020–0.122
17	0.144	0.066–0.222	0.077	0.001–0.153	0.067	0.016–0.118
18	0.135	0.064–0.206	0.073	0.004–0.142	0.061	0.012–0.110
19	0.123	0.056–0.192	0.069	0.000–0.138	0.054	0.070–0.101
20	0.118	0.049–0.187	0.067	0.000–0.136	0.050	0.003–0.097
21	0.111	0.042–0.180	0.067	0.000–0.136	0.044	0.000–0.089
22	0.095	0.030–0.160	0.051	0.000–0.116	0.044	0.000–0.089
23	0.062	0.009–0.115	0.018	0.000–0.073	0.044	0.000–0.089
24	0.058	0.003–0.113	0.034	0.000–0.097	0.024	0.000–0.061
25	0.060	0.009–0.111	0.049	0.000–0.104	0.011	0.000–0.042
30	0.052	0.000–0.148	0.017	0.000–0.117	0.035	0.000–0.074

Differences in proportions and 95% CI are constant in the interval between 25 and 30 y after initial assessment.

NNFF = National Neurofibromatosis Foundation.

tions are diagnosed with their first vestibular schwannoma at less than 30 years old compared with only 5% of people with unilateral vestibular schwannomas, but conversely 46% of NF2 patients with new mutations are diagnosed with their first vestibular schwannoma at 30 years and older. Screening for constitutional *NF2* mutations in the small fraction of people with unilateral vestibular schwannoma who present at younger than 30 years can identify people with NF2.[12-14]

In the current study, the NNFF age requirement reduced sensitivity. Solely because of the age requirement, 14 people who were diagnosed with unilateral vestibular schwannomas at 30 years or older were not identified by the NNFF criteria but were identified by the Manchester criteria. There were 4 people with "definite NF2," including 3 somatic mosaics, and 10 people with "possible NF2." In most NF2 somatic mosaics, disease manifestations are milder and vestibular schwannomas are of later onset than in people with classic NF2.[15-17] The odds of somatic mosaicism in NF2 increase 11-fold per decade increase in age at diagnosis of NF2 and are 7-fold greater in NF2 patients with no vestibular schwannomas or a unilateral vestibular schwannoma than in those with bilateral vestibular schwannomas.[17]

A "gold standard" does not exist for distinguishing normal individuals from those who actually have NF2 in every case. The current study focuses on sensitivity, but there is considerable evidence that

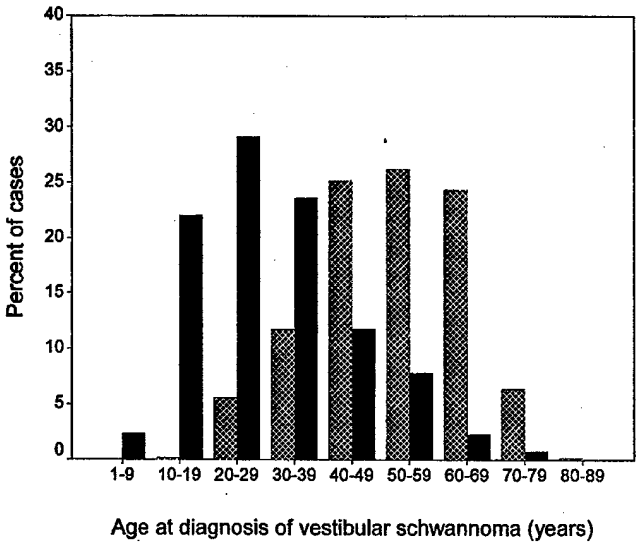

Figure 2. Distribution of age at diagnosis of 481 people with unilateral vestibular schwannoma in the St. Mary's Hospital geographic catchment area (Manchester, UK) and age at first vestibular schwannoma of 127 NF2 patients with new mutations in the United Kingdom NF2 registry (time period for both groups, 1987 to 1997). People with known NF2 are excluded from the group with unilateral vestibular schwannoma, and known NF2 somatic mosaics (defined through molecular testing) are excluded from the NF2 group with new mutations. The median age at diagnosis for people with unilateral vestibular schwannoma is 53 years, and the median age at diagnosis of first vestibular schwannoma for NF2 patients with new mutations is 29 years. Solid columns = first NF2 vestibular schwannoma; cross-hatched columns = unilateral vestibular schwannoma.

specificity is high (about 99%) and similar for each set of diagnostic criteria.[12-14] As noted above, people with unilateral vestibular schwannoma who do not have a family history of NF2 or characteristic disease features of NF2 have a very low probability of developing NF2, and this probability decreases with increasing age at diagnosis of vestibular schwannoma.[13,14] Sporadic unilateral vestibular schwannoma can occur in two first-degree relatives by chance, giving the appearance of heritable vestibular schwannomas. Sporadic unilateral vestibular schwannoma has a lifetime prevalence of about 1 in 1,000, and assuming that people have an average of five first-degree relatives, the lifetime probability of sporadic unilateral vestibular schwannoma occurring by chance in two first-degree relatives is 0.5%.[12]

Two people in this study are of particular interest because of their late age at diagnosis of their first vestibular schwannoma. They were diagnosed with their first vestibular schwannoma at ages 60 and 72, and each developed a contralateral vestibular schwannoma 2 years later. Neither had a family history of NF2 or any other clinical feature of the disease. One person had molecular testing and was found to be mosaic for a constitutional *NF2* frameshift mutation. The other person also might be a somatic mosaic or a rare person with two sporadic unilateral vestibular schwannomas who does not have NF2 (this is most likely in older people, in whom the incidence of unilateral sporadic vestibular schwannoma is highest).[18] A third possibility is that the person might have nonmosaic NF2 with unusually mild expression, perhaps as a result of a "weak" mutant allele. The two adult children of this person do not have clinical features of NF2; in such instances, family molecular genetic studies may be useful.

A more sensitive set of diagnostic criteria for NF2 can be developed by adding mononeuropathy as a clinical diagnostic criterion and incorporating the results of genetic testing.[19] In the United Kingdom NF2 registry, mononeuropathy (foot drop, wrist drop, facial palsy, or III nerve palsy) occurs in 31% of people with an age at onset of symptoms of less than 15 years but in only 3% of those with an age at onset of 15 years or older. NF2-associated mononeuropathy has been reported in previous studies,[20-24] as has a more generalized peripheral neuropathy.[4,5,25] The differential diagnosis should exclude polio.[4] In general, the presenting symptom in young people with NF2 is less likely to be vestibular than in adults with NF2.[22,26,27]

NF2 is 99% penetrant by age 60,[28] and genetic testing to identify pathogenic constitutional *NF2* mutations or *NF2* mutation carriers can increase sensitivity with minimal decrease in specificity.[19] Negative results from single-strand conformational polymorphism (SSCP) analysis on blood samples, a commonly used method,[29] cannot rule out NF2 because such testing would not identify mutations in the 3' or 5' untranslated regions, the promoter region, untranscribed transcriptional control elements, or introns that are not covered by conventional SSCP primers; large deletions, insertions, or other rearrangements; or mutations in patients who are somatic mosaics if the mutant line is not sufficiently abundant in the tissue tested.[30] Other epigenetic events (i.e., methylation) also could result in loss of *NF2* expression.[31] Segregation analysis using tightly linked genetic markers can identify *NF2* mutation carriers in at-risk members of NF2 families. Segregation analysis is more rapid and less expensive than mutation analysis and, in conjunction with clinical information, often can discriminate between *NF2* mutation carriers and noncarriers with a high degree of certainty.[32,33]

We recommend that a single revised set of diagnostic criteria be devised to replace all of the existing diagnostic systems for NF2. In future work, we will empirically validate our suggestions for revised criteria.

References

1. Trofatter JA, MacCollin MM, Rutter JL, et al. A novel moesin-, ezrin-, radixin-like gene is a candidate for the neuro-

fibromatosis 2 tumor suppressor. Cell 1993;72:791–800. Published erratum in Cell 1993;75:826.
2. Rouleau GA, Merel P, Lutchman M, et al. Alteration in a new gene encoding a putative membrane-organizing protein causes neuro-fibromatosis type 2. Nature 1993;363:515–521.
3. Evans DGR, Huson SM, Donnai D, et al. A genetic study of type 2 neurofibromatosis in the United Kingdom. I. Prevalence, fitness, and confirmation of maternal transmission effect on severity. J Med Genet 1992;29:841–846.
4. Evans DGR, Huson SM, Donnai D, et al. A clinical study of type 2 neurofibromatosis. Q J Med 1992;84:603–618.
5. Parry DM, Eldridge R, Kaiser–Kupfer MI, Bouzas EA, Pikus A, Patronas N. Neurofibromatosis 2 (NF2): clinical characteristics of 63 affected individuals and clinical evidence for heterogeneity. Am J Med Genet 1996;52:450–461.
6. Mautner VF, Lindenau M, Baser ME, et al. The neuroimaging and clinical spectrum of neurofibromatosis 2. Neurosurgery 1996;38:880–885.
7. Rouleau GA, Wertelecki W, Haines JL, et al. Genetic linkage analysis of bilateral acoustic neurofibromatosis to a DNA marker on chromosome 22. Nature 1987;329:246–248.
8. National Institutes of Health Consensus Development Conference. Neurofibromatosis Conference Statement. Arch Neurol 1988;45:575–578.
9. Consensus Development Panel. National Institutes of Health Consensus Development Conference Statement on Acoustic Neuroma, December 11–13, 1991. Arch Neurol 1994;51:201–207.
10. Gutmann DH, Aylsworth A, Carey JC, et al. The diagnostic evaluation and multidisciplinary management of neurofibromatosis 1 and neurofibromatosis 2. JAMA 1997;278:51–57.
11. Mosteller F, Tukey JW. Data analysis and regression, a second course in statistics. Reading: Addison-Wesley, 1977.
12. Wu CL, Thakker N, Neary W, et al. Differential diagnosis of type 2 neurofibromatosis: molecular discrimination of NF2 and sporadic vestibular schwannomas. J Med Genet 1998;35: 973–977.
13. Evans DG, Lye R, Neary W, et al. Probability of bilateral disease in people presenting with a unilateral vestibular schwannoma. J Neurol Neurosurg Psychiatry 1999;66:764–767.
14. Mohyuddin A, Neary WJ, Wallace A, et al. Molecular genetic analysis of the *NF2* gene in young patients with unilateral vestibular schwannomas. J Med Genet 2002;39:315–322.
15. Kluwe L, Mautner VF. Mosaicism in sporadic neurofibromatosis 2 patients. Hum Mol Genet 1998;7:2051–2055.
16. Evans DG, Wallace AJ, Wu CL, Trueman L, Ramsden RT, Strachan T. Somatic mosaicism: a common cause of classic disease in tumor-prone syndromes? Lessons from type 2 neurofibromatosis. Am J Hum Genet 1998;63:727–736.
17. Baser ME, Wallace AJ, Strachan T, Evans DGR. Clinical and molecular correlates of somatic mosaicism in neurofibromatosis 2. J Med Genet 2000;37:542–543.
18. Howitz MF, Johansen C, Tos M, Charabi S, Olsen JH. Incidence of vestibular schwannoma in Denmark, 1977–1995. Am J Otol 2000;21:690–694.
19. Baser ME, Friedman JM, Wallace A, Ramsden RT, Evans DGR. Evaluation of neurofibromatosis 2 diagnostic criteria in NF2 patients without bilateral vestibular schwannomas. Am J Hum Genet 2000;67(suppl 2):A359.
20. Iwata A, Kunimoto M, Inoue K. Schwann cell proliferation as the cause of peripheral neuropathy in neurofibromatosis-2. J Neurol Sci 1998;156:201–204.
21. Kilpatrick TJ, Hjorth RJ, Gonzales MF. A case of neurofibromatosis 2 presenting with a mononeuritis complex. J Neurol Neurosurg Psychiatry 1992;55:391–393.
22. Evans DGR, Birch JM, Ramsden RT. Paediatric presentation of type 2 neurofibromatosis. Arch Dis Child 1999;81:496–499.
23. Trivedi R, Byrne J, Huson SM, Donaghy M. Focal amyotrophy in neurofibromatosis 2. J Neurol Neurosurg Psychiatry 2000; 69:257–261.
24. Gijtenbeek JMM, Gabreëls-Festen AAWM, Lammens M, Zwarts MJ, van Engelen BGM. Mononeuropathy multiplex as the initial manifestation of neurofibromatosis type 2. Neurology 2001;56:1766–1768.
25. Sperfeld AD, Hein C, Schröder JM, Ludolph AC, Hanemann CO. Occurrence and characterization of peripheral nerve involvement in neurofibromatosis type 2. Brain 2002;125:996–1004.
26. Mautner V-F, Tatagiba M, Guthoff R, Samii M, Pulst S-M. Neurofibromatosis 2 in the pediatric age group. Neurosurgery 1993;33:92–96.
27. MacCollin M, Mautner V-F. The diagnosis and management of neurofibromatosis 2 in childhood. Semin Pediatr Neurol 1998;5:243–252.
28. Evans DGR, Huson SM, Donnai D, et al. A genetic study of type 2 neurofibromatosis in the United Kingdom. II. Guidelines for genetic counseling. J Med Genet 1992;29:847–852.
29. Jacoby LB, MacCollin M, Louis DN, et al. Exon scanning for mutation of the *NF2* gene in schwannomas. Hum Mol Genet 1994;3:413–416.
30. Zucman-Rossi J, Legoix P, Der Sarkissian H, et al. *NF2* gene in neurofibromatosis type 2 patients. Hum Mol Genet 1998;7: 2095–2101.
31. Kino T, Takeshima H, Nakao M, et al. Identification of the cis-acting region in the *NF2* gene promoter as a potential target for mutation and methylation-dependent silencing in schwannoma. Genes Cells 2001;6:441–454.
32. Ruttledge MH, Narod SA, Dumanski JP, et al. Presymptomatic diagnosis for neurofibromatosis 2 with chromosome 22 markers. Neurology 1993;43:1753–1760.
33. Baser ME, Mautner V-F, Ragge NK, et al. Presymptomatic diagnosis of neurofibromatosis 2 using linked genetic markers, neuroimaging, and ocular examinations. Neurology 1996; 47:1269–1277.

LETTER TO JMG

Genotype-phenotype correlations for cataracts in neurofibromatosis 2

M E Baser, L Kuramoto, H Joe, J M Friedman, A J Wallace, R T Ramsden, D G R Evans

J Med Genet 2003;**40**:758–760

Neurofibromatosis 2 (NF2) is an autosomal dominant disease that is caused by inactivating mutations of the *NF2* tumour suppressor gene.[1 2] Multiple central and peripheral nervous system tumours and ocular abnormalities are common in NF2; bilateral vestibular schwannomas are pathognomonic for the disease. Genotype-phenotype correlations are well established for NF2 associated tumours. In general, constitutional nonsense or frameshift *NF2* mutations are associated with severe NF2 (that is, earlier onset of symptoms and more tumours), splice site mutations with variable disease severity, and missense mutations with mild disease.

Genotype-phenotype correlations have not been reported for the non-tumour manifestations of NF2. The most common of these manifestations is presenile cataracts, which occur in about 60–80% of people with NF2.[3–5] In animal models, lens fibre cells that are more differentiated express less *Nf2* protein than the epithelial regions of the lens, suggesting that the *Nf2* protein may play a role in lens epithelial cell migration or elongation.[6] The purpose of this study was to determine if there were genotype-phenotype correlations for cataracts in NF2.

Key points

- Genotype-phenotype correlations have not been established for the non-tumour manifestations of neurofibromatosis 2 (NF2), such as cataracts.
- When compared to people with classical NF2 and nonsense or frameshift mutations, the relative risk of cataracts was significantly less than 1 in somatic mosaics, in people with large deletions, and in people with new unfound mutations and onset of symptoms at ages ≥20 years, who probably have somatic mosaicism or large deletions.
- These results extend the genotype-phenotype correlations that have been reported for the tumour manifestations of NF2.

PATIENTS AND METHODS

The study was based on the United Kingdom NF2 registry in the Department of Medical Genetics, St Mary's Hospital, Manchester. NF2 patients are ascertained by contacting neurosurgeons, otolaryngologists, neurologists, paediatricians, dermatologists, and geneticists throughout the United Kingdom, augmented in the North West Region by the Regional Cancer Registry. The study was subject to continuing ethics committee evaluation and patients consented to participation. Patients were screened for constitutional *NF2* mutations using single strand conformational polymorphism analysis (SSCP) as previously described,[7] and examined for cataracts using slitlamp biomicroscopy at the time of diagnosis of NF2. For this study, cataracts were defined as present or absent (that is, posterior subcapsular cataracts and cortical cataracts were aggregated). There were 255 people from 190 families (159 people with new mutations and 96 inherited cases; 132 females and 123 males) (table 1).

For univariate analyses, Fisher's exact test was used for binary variables and the two-tailed *t* test was used for continuous variables. A multivariate probit model with an exchangeable correlation structure within families was used with various sets of covariates to account for possible familial dependence.[8] From a regression coefficient β, an approximate relative risk ($RR = \exp\{2^* \beta\}$) and confidence interval (CI) for presence of cataracts can be calculated. In the probit model, the reference group in comparisons between people with different types of *NF2* mutations was people who had constitutional nonsense or frameshift *NF2* mutations.

There is a potential bias towards a lower age at onset of symptoms or age at diagnosis in inherited cases owing to the family history of the disease. In the study group as a whole, there were no significant differences in these ages between people with new mutations and inherited cases for any type of *NF2* mutation. Also, using a probit model, the RR of cataracts was not significantly associated with age at diagnosis (see below). Therefore, for all mutation categories except unfound mutations, we combined people with new mutations and inherited cases. In the large group of people with unfound mutations, we retained the division between those with new mutations and inherited disease because people with new unfound mutations may be somatic mosaics. We used age at onset of symptoms to categorise people with new unfound mutations by disease severity (severe disease, onset of symptoms at ages <20 years; mild disease, onset of symptoms at ages ≥20 years).[3]

RESULTS

As expected, the mean age at onset of symptoms and age at diagnosis were higher in people with non-truncating mutations and in somatic mosaics than in people with classical NF2 and nonsense or frameshift mutations (table 1). The overall prevalence of cataracts was 33%, but the prevalence of cataracts was significantly lower in somatic mosaics and in people with new unfound mutations and onset of symptoms at ages ≥20 years than in people with classical NF2 and nonsense or frameshift mutations. In people with cataracts, 29% were diagnosed with cataracts at ages <10 years, and 47% at ages <20 years (mean 23 (SE 2) years). Seventy percent were diagnosed with cataracts before their first non-ocular sign or symptom.

In the multivariate probit model summarised in table 2, the RR of cataracts did not significantly increase with increasing age at diagnosis, after accounting for the type of constitutional *NF2* mutation. This was also the case in the other probit models (data not shown). This is probably due to the

Table 1 Characteristics of study population by type of *NF2* mutation

	Nonsense or frameshift					Unfound (mutations)			
							People with new mutations (age of onset (y))		
	Classical	Somatic mosaic	Splice site	Missense	Large deletion	Inherited cases	<20 years	>20 years	Total
No. of people/families	73/56	17/17	47/25	15/6	25/14	14/11	23/23	41/41	255/190
Age (y), mean (SD)									
Onset of symptoms†	16 (9)	32 (12)	23 (12)	30 (14)	21 (9)	25 (16)	12 (6)	34 (9)	22 (12)
Diagnosis	21 (12)	38 (12)	27 (15)	38 (21)	23 (9)	29 (17)	22 (12)	40 (11)	28 (15)
Current	27 (12)	44 (12)	32 (16)	45 (21)	30(11)	35 (20)	29 (12)	46 (13)	34 (16)
Intracranial meningiomas (%)	56	59	34	27	52	14	70	51	48
Cataracts (%)	45	18	38	27	28	36	39	10	33

†Excludes 15 inherited cases who were asymptomatic at the time of diagnosis of NF2.
Comparisons to people with classical NF2 and nonsense or frameshift mutations (p values are computed based on an assumption of independence, which is violated to a slight degree owing to families with multiple affected relatives):
Somatic mosaics: age at onset, age at diagnosis, current age, $p<0.001$; cataracts, $p=0.053$.
Splice site mutations: age at onset, $p=0.001$; age at diagnosis, $p=0.023$; current age, $p=0.043$; intracranial meningiomas, $p=0.024$.
Missense mutations: age at onset, $p=0.003$; age at diagnosis, $p=0.006$; current age, $p<0.001$; intracranial meningiomas, $p=0.049$.
Large deletions: age at onset, $p=0.032$.
Unfound mutations:
Inherited cases: intracranial meningiomas, $p=0.007$.
People with new mutations and age at onset 20 years: cataracts, $p<0.001$.
SD, standard deviation.

relatively young study population (mean age at diagnosis 28 years (SE 1); only 5% diagnosed at ages >55 years and 2% at ages >60 years), since the prevalence of posterior subcapsular and cortical cataracts in people aged <55 years in the general population is very low.[10]

The RR of cataracts was less than 1 in all mutation groups as compared to people with classical NF2 and nonsense or frameshift mutations. The RR was significantly lower than 1 in somatic mosaics (RR = 0.20, 95% CI = 0.10 to 0.40), in people with large deletions (RR = 0.39, 95% CI = 0.16 to 0.98), and in people with new unfound mutations and onset of symptoms at ages ≥20 years (RR = 0.09, 95% CI = 0.03 to 0.28). The RR of cataracts in people with missense mutations was lower than 1 but not statistically significantly so (RR = 0.38, 95% CI = 0.14 to 1.08).

DISCUSSION

The low RR of cataracts in somatic mosaics, in people with large deletions, and in people with new unfound mutations and older onset of symptoms is consistent with the generally mild disease in NF2 patients with each of these types of mutations or conditions. The low RR of cataracts in people with new unfound mutations and older onset of symptoms could be due to several types of mutations or conditions that are unlikely to be identified by SSCP, and that are known to be associated or likely to be associated with mild NF2. These mutations or conditions are somatic mosaicism; large deletions, insertions, or other rearrangements; mutations in the 3 or 5 untranslated regions, the promoter region, or untranscribed transcriptional control elements; intronic mutations that are not covered by conventional SSCP primers; or other epigenetic events causing loss of *NF2* expression, such as methylation.

Somatic mosaicism and large deletions are the most likely of these possibilities. In the present study, 17 (18%) of the 92 patients with new mutations and identified constitutional *NF2* mutations were somatic mosaics. The estimated prevalence of somatic mosaicism in NF2 patients with new mutations is 25–30%.[11 12] Some of the NF2 patients with new unfound mutations and mild disease may be somatic mosaics in whom conventional DNA sequencing of lymphocyte DNA PCR product has failed to identify a difference from the normal sequence because the mutant allele is present at too low a level to be detected. Constitutional *NF2* large deletions

Table 2 Multivariate probit model for cataracts

Covariate	Estimated prevalence of cataracts from model (%)	Parameter estimate (SE)	RR	95% CI
Age at diagnosis (per year)		0.15 (0.58)	1.00	0.98 to 1.02
Exchangeable dependence (familial correlation)		0.11 (0.16)		
Type of *NF2* mutation				
Nonsense or frameshift				
Classical NF2	45	Reference group	Reference group	
Somatic mosaic	17	−0.82 (0.18)	0.20	0.10 to 0.40
Splice site	39	−0.17 (0.19)	0.71	0.34 to 1.50
Missense	28	−0.48 (0.26)	0.38	0.14 to 1.08
Large deletion	28	−0.47 (0.23)	0.39	0.16 to 0.98
Unfound				
People with new mutations				
Age at onset <20 years	39	−0.15 (0.15)	0.74	0.40 to 1.36
Age at onset ≥20 years	9	−1.20 (0.28)	0.09	0.03 to 0.28
Inherited cases	36	−0.23 (0.34)	0.63	0.16 to 2.45

RR = relative risk, CI = confidence interval, SE = standard error.

have been found in 21% of NF2 families using microarray comparative genomic hybridisation,[13] and in 32% of NF2 families using multiple mutation screening methods.[14]

The intrafamilial correlation for cataracts was weak (and statistically insignificant) in all multivariate probit models that were tried, although there were relatively few families with multiple affected relatives. Several other clinical features of NF2 (age at onset of symptoms, age at diagnosis, and number of intracranial meningiomas) have strong familial correlations.[15] The prevalence of cataracts in the present study was lower than in other studies,[3–5] probably because the population-based United Kingdom NF2 registry is less heavily weighted towards NF2 patients with severe disease than studies of patients from tertiary referral clinics,[4 5] and because some cataract examinations were done by medical specialists other than ophthalmologists. Non-ophthalmologists may miss faint cataracts, but in such cases it is unlikely that faint cataracts are missed more frequently in people with mild NF2 than in those with severe NF2 (that is, it will not bias genotype-phenotype correlations). In a previous study based on the UK NF2 registry, all patients were examined using slitlamp biomicroscopy by a non-ophthalmologist, and the prevalence of cataracts was similar in mild cases (35%) and in severe cases (40%).[9]

The genotype-phenotype correlations for cataracts in the present study extend the correlations that have been reported for the tumour manifestations of NF2. The high prevalence of cataracts in young NF2 patients, and their frequent occurrence before the tumour manifestations of NF2, underline the importance of non-8th nerve signs and symptoms of NF2 in children and adolescents as a useful aid to diagnosis in this age group.[16]

ACKNOWLEDGEMENTS

Supported in part by the FBT Foundation and US Army grant USARMC NF990038.

Authors' affiliations
M E Baser, Los Angeles, CA, USA
L Kuramoto, H Joe, Department of Biostatistics, University of British Columbia, Vancouver, BC, Canada
J M Friedman, Department of Medical Genetics, University of British Columbia, Vancouver, BC, Canada
A J Wallace, D G R Evans, Department of Medical Genetics, St Mary's Hospital, Manchester, UK
R T Ramsden, Department of Otolaryngology, Manchester Royal Infirmary, Manchester, UK

Correspondence to: Dr M E Baser, 2257 Fox Hills Drive, Los Angeles, CA 90064, USA; michael.baser@sbcglobal.net

REFERENCES

1 **Trofatter JA**, MacCollin MM, Rutter JL, Murrell JR, Duyao MP, Parry DM, Eldridge R, Kley N, Menon AG, Pulaski K, Haase VH, Ambrose CM, Munroe D, Bove C, Haines JL, Martuza RL, MacDonald ME, Seizinger BR, Short MP, Buckler AJ, Gusella JF. A novel moesin-, ezrin-, radixin-like gene is a candidate for the neurofibromatosis 2 tumor suppressor (published erratum appears in Cell 1993;75:826). *Cell* 1993;**72**:791–800.
2 **Rouleau GA**, Merel P, Lutchman M, Sanson M, Zucman J, Marineau C, Hoang-Xuan K, Demczuk S, Desmaze C, Plougastel B, Pulst SM, Lenoir G, Bijlsma E, Fashold R, Dumanski J, de Jong P, Parry D, Eldridge R, Aurias A, Delattre O, Thomas G. Alteration in a new gene encoding a putative membrane-organizing protein causes neurofibromatosis type 2. *Nature* 1993;**363**:515–21.
3 **Parry DM**, Eldridge R, Kaiser-Kupfer MI, Bouzas EA, Pikus A, Patronas N. Neurofibromatosis 2 (NF2): clinical characteristics of 63 affected individuals and clinical evidence for heterogeneity. *Am J Med Genet* 1994;**52**:450–61.
4 **Mautner VF**, Lindenau M, Baser ME, Hazim W, Tatagiba M, Haase W, Samii M, Wais R, Pulst SM. The neuroimaging and clinical spectrum of neurofibromatosis 2. *Neurosurgery* 1996;**38**:880–5.
5 **Ragge NK**, Baser ME, Klein J, Nechiporuk A, Sainz J, Pulst SM, Riccardi VM. Ocular abnormalities in neurofibromatosis 2. *Am J Ophthalmol* 1995;**120**:634–41.
6 **Claudio JO**, Veneziale RW, Menko AS, Rouleau GA. Expression of schwannomin in lens and Schwann cells. *Neuroreport* 1997;**8**:2025–30.
7 **Evans DGR**, Trueman L, Wallace A, Collins S, Strachan T. Genotype/phenotype correlations in type 2 neurofibromatosis (NF2): evidence for more severe disease associated with truncating mutations. *J Med Genet* 1998;**35**:450–5.
8 **Ashford J**, Sowden R. Multivariate probit analysis. *Biometrics* 1970;**26**:535–46.
9 **Evans DGR**, Huson SM, Donnai D, Neary W, Blair V, Newton V, Harris R. A clinical study of type 2 neurofibromatosis. *Q J Med* 1992;**84**:603–18.
10 **Klein BE**, Klein R, Linton KL. Prevalence of age-related lens opacities in a population. The Beaver Dam Eye Study. *Ophthalmology* 1992;**99**:546–52.
11 **Kluwe L**, Mautner VF, Heinrich B, Dezube R, Jacoby LB, Friedrich RE, MacCollin M. Molecular study of frequency of mosaicism in neurofibromatosis 2 patients with bilateral vestibular schwannomas. *J Med Genet* 2003;**40**:109–14.
12 **Moyhuddin A**, Baser ME, Watson C, Purcell S, Ramsden RT, Heiberg A, Wallace A, Evans DGR. Somatic mosaicism in neurofibromatosis 2: prevalence and risk of disease transmission to offspring. *J Med Genet* 2003;**40**:459–63.
13 **Bruder CEG**, Hirvelä C, Tapia-Paez I, Fransson I, Segraves R, Hamilton G, Zhang XX, Evans DG, Wallace AJ, Baser ME, Zucman-Rossi J, Hergersberg M, Boltshauser E, Papi L, Rouleau GA, Poptodorov G, Jordanova A, Rask-Andersen H, Kluwe L, Mautner V, Sainio M, Hung G, Mathiesen T, Möller C, Pulst SM, Harder H, Heiberg A, Honda M, Niimura M, Sahlén S, Blennow E, Alberton DG, Pinkel D, Dumanski JP. High-resolution deletion analysis of constitutional DNA from neurofibromatosis type 2 (NF2) patients using microarray-CGH. *Hum Mol Genet* 2001;**10**:271–82.
14 **Zucman-Rossi J**, Legoix P, Sarkissian HD, Cheret G, Sor F, Bernardi A, Cazes L, Giraud S, Ollagnon E, Lenoir G, Thomas G. NF2 gene in neurofibromatosis type 2 patients. *Hum Mol Genet* 1998;**7**:2095–101.
15 **Zhao Y**, Kuman RA, Baser ME, Evans DGR, Wallace A, Kluwe L, Mautner VF, Parry DM, Rouleau GA, Joe H, Friedman JM. Intrafamilial correlation of clinical manifestations of in neurofibromatosis 2 (NF2). *Genet Epidemiol* 2002;**23**:245–59.
16 **MacCollin M**, Mautner VF. The diagnosis and management of neurofibromatosis 2 in childhood. *Semin Pediatr Neurol* 1998;**5**:243–52.

Am. J. Hum. Genet. 75:000–000, 2004

Genotype-Phenotype Correlations for Nervous System Tumors in Neurofibromatosis 2: A Population-Based Study

Michael E. Baser,[1] Lisa Kuramoto,[2] Harry Joe,[2] J. M. Friedman,[3] Andrew J. Wallace,[4] James E. Gillespie,[5] Richard T. Ramsden,[6] and D. Gareth R. Evans[4]

[1]Los Angeles; Departments of [2]Statistics and [3]Medical Genetics, University of British Columbia, Vancouver; [4]University Department of Medical Genetics, St. Mary's Hospital, and Departments of [5]Radiology and [6]Otolaryngology, Manchester Royal Infirmary, Manchester, United Kingdom

Neurofibromatosis 2 (NF2) is an autosomal dominant disease that is characterized by tumors on the vestibular branch of the VIII cranial nerve, but other types of nervous system tumors usually occur as well. Genotype-phenotype correlations are well documented for overall NF2 disease severity but have not been definitively evaluated for specific types of non–VIII nerve tumors. We evaluated genotype-phenotype correlations for various types of non–VIII nerve tumors in 406 patients from the population-based United Kingdom NF2 registry, using regression models with the additional covariates of current age and type of treatment center (specialty or nonspecialty). The models also permitted consideration of intrafamilial correlation. We found statistically significant genotype-phenotype correlations for intracranial meningiomas, spinal tumors, and peripheral nerve tumors. People with constitutional *NF2* missense mutations, splice-site mutations, large deletions, or somatic mosaicism had significantly fewer tumors than did people with constitutional nonsense or frameshift *NF2* mutations. In addition, there were significant intrafamilial correlations for intracranial meningiomas and spinal tumors, after adjustment for the type of constitutional *NF2* mutation. The type of constitutional *NF2* mutation is an important determinant of the number of NF2-associated intracranial meningiomas, spinal tumors, and peripheral nerve tumors.

Introduction

Neurofibromatosis 2 (NF2 [MIM 101000]) is an autosomal dominant disease that is caused by inactivating mutations of the *NF2* tumor-suppressor gene (Rouleau et al. 1993; Trofatter et al. 1993). The clinical abnormalities of NF2 may include vestibular schwannomas (typically bilateral), intracranial meningiomas, spinal tumors, peripheral nerve tumors, and ocular abnormalities, such as presenile cataracts (Evans et al. 1992*a*; Parry et al. 1994; Mautner et al. 1996*b*). Genotype-phenotype correlations for overall NF2 disease severity were first reported in 1995, soon after the identification of the *NF2* gene; by 1998, these correlations were well established. In general, constitutional *NF2* nonsense or frameshift mutations are associated with severe NF2, and missense mutations, in-frame deletions, and somatic mosaicism are associated with mild NF2 (Mérel et al. 1995; Kluwe et al. 1996, 1998; Parry et al. 1996; Ruttledge et al. 1996; Evans et al. 1998*a*, 1998*b*; Kluwe and Mautner 1998).

Initial genotype-phenotype correlation studies of NF2 were limited by the generality of the definition of disease severity, which was often reported only as "mild," "moderate," or "severe." The mild and severe disease categories correspond to the historical nomenclature of "Gardner" (mild) and "Wishart" (severe) subtypes, which were based on the clinical observation that the severity of NF2 tends to "run true" within a family (Wishart 1822; Gardner and Frazier 1930). Another category, "Lee-Abbott," which corresponds to very severe NF2, was not consistently adopted by subsequent studies (Lee and Abbott 1969).

More recent genotype-phenotype correlation studies tend to use indices, such as age at onset of symptoms of NF2, that portray the continuum of overall disease severity. Age at onset of symptoms reflects the burden of the many different types of clinical abnormalities in NF2. In patients with NF2 who present symptomatically, the initial symptom is related to vestibular schwannomas in 1/3 to 2/3 of patients (Evans et al. 1992*a*; Parry et al. 1994; Mautner et al. 1996*b*). Patients with NF2 whose initial symptom occurs in adulthood tend to present with VIII nerve symptoms, whereas the initial symptom of children with NF2 is often related to clinical abnormalities other than vestibular schwannomas (Mautner et al. 1993; MacCollin and Mautner 1998; Evans et al. 1999; Nunes and MacCollin 2003).

Parry et al. (1994) used age at onset of NF2 symptoms as a criterion to define overall disease severity (aged <20

Received March 24, 2004; accepted for publication May 12, 2004; electronically published June 9, 2004.

Address for correspondence and reprints: Dr. Michael E. Baser, 10622 Kinnard Avenue, #203, Los Angeles, CA 90024. E-mail: michael.baser@verizon.net

0002-9297/2004/7502-00XX$15.00

years, severe disease; aged ≥20 years, mild disease). The importance of age at onset of NF2 symptoms as a predictor of subsequent disease course has been validated in longitudinal studies. Age at onset of symptoms or age at diagnosis are the most important predictors of vestibular schwannoma growth rates in NF2 (Baser et al. 2002*b*; Mautner et al. 2002) and of the risk of death in patients with NF2 (Baser et al. 2002*a*; Otsuka et al. 2003).

In the past decade, *NF2* mutation analysis techniques have been refined, and the definition of the clinical spectrum of NF2 has been broadened. However, genotype-phenotype correlation studies have been based on relatively few patients because of the rarity of the disease (Evans et al. 1992*b*), and genotype-phenotype correlations have been established only for overall NF2 disease severity, not for the various types of non–VIII nerve tumors that often occur in NF2. In the present study, we found genotype-phenotype correlations for the number of NF2-associated intracranial meningiomas, spinal tumors, and peripheral nerve tumors. We also found significant correlations within families for intracranial meningiomas and spinal tumors.

Methods

Patients

Data for this study were obtained from the population-based United Kingdom NF2 registry (Department of Medical Genetics, St. Mary's Hospital, Manchester). Patients with NF2 are ascertained by contacting neurosurgeons, otolaryngologists, neurologists, pediatricians, dermatologists, and geneticists throughout the United Kingdom, augmented in the North West Region by the Regional Cancer Registry. The study was subject to continuing ethics committee evaluation, and patients consented to participation.

People were eligible for inclusion if they met the Manchester clinical diagnostic criteria for NF2 (Evans et al. 1992*a*) ($n = 394$) or did not meet these criteria but had an identified constitutional *NF2* mutation ($n = 12$). We included only those patients who had been screened for constitutional *NF2* mutations and had available clinical information from imaging studies of intracranial meningiomas, had spinal tumors or tumors of cranial nerves other than the VIII nerve, or had available clinical information from physical examination on peripheral nerve tumors. The analysis excluded several groups with too few people to analyze separately: somatic mosaics who had identified *NF2* mutations other than nonsense or frameshift mutations ($n = 8$) and people with constitutional *NF2* in-frame deletions ($n = 3$) or chromosomal translocations involving the *NF2* locus ($n = 3$). The 406 people included in the study were from 267 families (247 people with new mutations and 159 inherited cases; 200 females and 206 males). There were data for 389 people with intracranial meningiomas, 351 people with spinal tumors, 332 people with peripheral nerve tumors, and 319 people with tumors of cranial nerves other than the VIII nerve (278 people had all four types of tumors). The analyses for each type of tumor were based on the people who had data for that specific type of tumor.

Detection of NF2 Mutations

Samples were tested for the presence of point mutations by direct sequencing of Meta-PCR products (Wallace et al. 1999). The entire cDNA of the *NF2* gene was covered in four Meta-PCR reactions. Gel-purified Meta-PCR products were then sequenced in both orientations by use of BigDye v2 chemistry, according to the manufacturer's instructions. Sequencing electropherograms were scanned for mutations by use of the trace subtraction algorithm "TraceDiff," which is available as a component of the Staden package. In samples in which mutations were identified, the presence of mutations was confirmed by use of the genomic DNA sample for repetition of the Meta-PCR amplification and both sequencing reactions. Large deletions, nonsense mutations, frameshift mutations, and mutations affecting invariate splice-site sequences were assumed to be pathogenic. Missense changes were defined as pathogenic if they had been published and shown to affect *NF2* expression or function. For other missense changes, parental samples were analyzed; if the mutation arose de novo in the patient, this was taken as strong evidence of pathogenicity.

Dosage analysis was performed using a quantitative PCR-based assay in 10-mL volumes with 100 ng genomic DNA. Exons 1, 4, 8, and 15 from the *NF2* gene and three amplicons derived from the cystic fibrosis gene were amplified within a multiplex PCR. The *NF2* primers and control primers all had identical "universal" forward and reverse sequences at their 5′ termini and were present at low concentration in the PCR reaction (50 nM). Universal forward and reverse primers were also included but at a higher concentration (0.5 mM) than the genomic-specific primers. The universal forward primer was 5′-labeled with the fluorescent dye FAM, thereby allowing fluorescent quantification of the PCR products from each amplicon. The PCR reactions were arrested at 23 cycles to maintain the amplification reaction within the logarithmic phase. Electrophoresis and quantitative measurement of yield of each product was performed on an ABI3100 Genetic Analyzer with Genescan and Genotyper software. Relative peak heights of all amplicons of each test sample were compared with a normalized average of five negative controls by use of the dosage quotient (DQ) method (Yau et al. 1996). Calculations

Table 1

Characteristics of 406 People with NF2, by Type of *NF2* Mutation

Characteristic	Type of *NF2* Mutation							
						Unfound Mutations		
	Nonsense or Frameshift		Splice Site	Missense	Large Deletion	Inherited Cases	People with New Mutations, with Age at Onset of Symptoms	
	Classical	Somatic Mosaic					<20 years	≥20 years
No. of people/families	111/75	23	78/39	26/8	48/20	25/7	29	66
Age in years (mean ± SD):								
At onset of symptoms[a]	19 ± 12	30 ± 11	23 ± 12	32 ± 17	24 ± 13	22 ± 13	13 ± 8	36 ± 12
At diagnosis	23 ± 13	37 ± 11	28 ± 15	41 ± 21	28 ± 14	26 ± 13	22 ± 10	43 ± 13
Vestibular schwannoma (%):								
None	7	0	13	0	2	13	3	3
Unilateral	6	26	3	19	4	0	3	20
Bilateral	87	74	84	81	94	87	94	77
Intracranial meningioma (%)	53	65	38	22	42	30	62	48
Peripheral nerve tumors (%)	66	39	52	25	54	79	75	39
Spinal tumors (%)	69	57	47	57	33	62	73	45
Tumors of non–VIII nerve cranial nerves (%)	45	27	33	24	39	28	54	28

[a] Excludes 20 inherited cases who were asymptomatic at the time of diagnosis of NF2.

were performed on Microsoft Excel spreadsheets written specifically for this purpose. A sample from a patient with an *NF2* deletion was included as a control within each run of samples. If only a single *NF2* measurement showed a DQ measurement within the deleted range (0.35–0.65), the test was repeated. If results of the repeated test agreed with the first result, the deleted exon was amplified and sequenced with primers that lay external to the dosage primer binding sites, to exclude the possibility that a polymorphism of the primer binding site had affected amplification efficiency.

Magnetic Resonance Imaging (MRI) of the Brain and Spine

Each patient had an MRI examination of the brain and full spinal cord at the time of NF2 diagnosis. Subsequent MRI examinations were performed as indicated clinically or for purposes of routine follow-up, as determined by the patient's physician. The brain precontrast MRI protocol included sagittal T1-weighted spin echo imaging (5-mm slices) and axial T2-weighted turbo spin echo imaging (5-mm slices). The brain postcontrast protocol included axial T1-weighted spin echo imaging (3-mm slices through the posterior fossa; 5-mm slices through the rest of the brain) and coronal T1-weighted spin echo imaging (5-mm slices through the whole brain). If the patient had a previous translabyrinthine removal of a vestibular schwannoma, then the postcontrast axial 3-mm slices were done with fat suppression. The spinal canal postcontrast MRI protocol included sagittal and coronal T1-weighted spin echo imaging (4-mm slices). Axial T1-weighted spin echo images and sagittal T2-weighted turbo spin echo images also were included, if indicated. The number of spinal tumors, as counted by the radiologist (J.E.G.), was confirmed by another physician (D.G.R.E.), who reread the spinal MRIs.

Statistical Analysis

The cross-sectional associations of the type of constitutional *NF2* mutation with the various kinds of nervous system tumors were assessed by regression models. Numerical maximum likelihood was estimated using the quasi-Newton method. Computations were performed using C programs developed at the Department of Statistics, University of British Columbia.

The models were chosen on the basis of the nature of the dependent variable. A gamma mixture of negative binomials model was used to model the association of the type of constitutional *NF2* mutation with the number of intracranial meningiomas, spinal tumors, and peripheral nerve tumors, because the count distribution of these types of tumors was heavily right skewed. A probit model was used to evaluate the association of the type of constitutional *NF2* mutation with the presence or absence of tumors of cranial nerves other than the VIII nerve. In addition, all of the models had an exchangeable correlation structure within families that permitted assessment of intrafamilial effects beyond those produced by the type of constitutional *NF2* mutation. The other covariates were the potential confounders of current age (when tumor burden was most recently assessed by MRI) and type of treatment center (specialty or nonspecialty). The genotype-phenotype correlation tables present, for each type of *NF2* mutation, the av-

Table 2

Genotype-Phenotype Correlations for Intracranial Meningiomas

Type of *NF2* Mutation[a]	Sample Average of No. of Intracranial Meningiomas	Model-Based Estimated Average of No. of Intracranial Meningiomas	95% CI for Count Ratios[b]
Nonsense or frameshift:			
Classical NF2	1.2	1.4	1.00[c]
Somatic mosaic	2.8	2.5	.74–3.85
Splice-site	1.0	.9	.34–1.12
Missense	***.3***	***.3***	***.06–.64***
Large deletion	***.9***	1.0	.30–1.43
Unfound mutations:			
Inherited cases	.7	.8	.22–1.30
People with new mutations:			
Age at onset <20 years	1.9	2.2	.77–2.92
Age at onset ≥20 years	1.6	1.2	.41–1.63

NOTE.—Statistically significant results are shown in bold italics.

[a] Other covariates: Intrafamilial correlation coefficient = .24 (95% CI .10–.39). Current age (per year): 1.01 (95% CI 1.00–1.02). Type of treatment center (specialty vs. nonspecialty): .92 (95% CI .61–1.40).

[b] Compared with people with classical NF2 and nonsense or frameshift mutations.

[c] Reference group.

erage number or prevalence of tumors in the sample and the model-based number or prevalence of tumors that were estimated using maximum likelihood, as described above.

The type of mutation variable was categorical and coded as eight binary variables. The variables were indicators of somatic mosaicism (defined at the molecular level and including only mosaics with nonsense or frameshift mutations), splice-site mutations, missense mutations, large deletions, and unfound mutations, each compared with nonsense or frameshift mutations. Since a large proportion of patients with NF2 (especially those with new mutations) have unfound mutations, people with unfound mutations were divided into three subgroups: inherited cases, people with new mutations and onset of symptoms of NF2 at age <20 years (i.e., severe disease), and people with new mutations and onset of symptoms of NF2 at age ≥20 years (i.e., mild disease).

People who met the Manchester clinical diagnostic criteria for NF2 (Evans et al. 1992*a*) and who had full constitutional *NF2* nonsense or frameshift mutations were the reference group in comparisons between different types of *NF2* mutations. Genotype-phenotype correlations were evaluated using tumor count ratios or relative risks (RR) and their 95% CIs from the models. Count ratios or RR with 95% CIs that excluded zero were considered to be statistically significant.

Results

The characteristics of the study population are presented in table 1. People with somatic mosaicism or constitutional *NF2* splice-site mutations, missense mutations, or large deletions were significantly older at onset of NF2 symptoms and at NF2 diagnosis than were people with classical NF2 and constitutional *NF2* nonsense or frameshift mutations. The results of the genotype-phenotype–correlation analyses for the various types of nervous system tumors are presented in tables 2–5. Relative to people with classical NF2 and constitutional nonsense or frameshift *NF2* mutations, there tended to be fewer tumors in somatic mosaics and in people with constitutional *NF2* splice-site mutations, missense mutations, or large deletions (see appendix [online only] for list of unique *NF2* mutations).

People with classical NF2 and nonsense or frameshift mutations had a model-based estimated average of 1.4 meningiomas (table 2). There were significantly fewer (an average of 0.3) meningiomas in people with missense mutations.

There were extensive genotype-phenotype correlations for peripheral nerve tumors (table 3). People with classical NF2 and nonsense or frameshift mutations had a model-based estimated average of 4.0 peripheral nerve tumors. There were significantly fewer peripheral nerve tumors in somatic mosaics (an average of 1.4) and in people with splice-site mutations (an average of 1.3), missense mutations (an average of 1.6), or large deletions (an average of 1.6).

People with classical NF2 and nonsense or frameshift mutations had a model-based estimated average of 4.1 spinal tumors (table 4). There were significantly fewer spinal tumors in people with splice-site mutations (an average of 2.1) or large deletions (an average of 0.8). There were fewer spinal tumors in somatic mosaics, but not significantly so.

Table 3

Genotype-Phenotype Correlations for Peripheral Nerve Tumors

Type of *NF2* Mutation[a]	Sample Average of No. of Peripheral Nerve Tumors	Model-Based Estimated Average of No. of Peripheral Nerve Tumors	95% CI for Count Ratios[b]
Nonsense or frameshift:			
Classical NF2	3.6	4.0	1.00[c]
Somatic mosaic	***1.4***	***1.4***	***.16–.73***
Splice-site	***1.3***	***1.3***	***.19–.58***
Missense	***1.5***	***1.6***	***.18–.93***
Large deletion	***1.6***	***1.6***	***.21–.79***
Unfound mutations:			
Inherited cases	2.6	2.8	.33–1.44
People with new mutations:			
Age at onset <20 years	4.1	4.3	.58–2.02
Age at onset ≥20 years	***1.4***	***1.4***	***.20–.60***

NOTE.—Statistically significant results are shown in bold italics.

[a] Other covariates: Intrafamilial correlation coefficient = .13 (95% CI −.03 to .29). Current age (per year): .99 (95% CI .98–1.01). Type of treatment center (specialty vs. nonspecialty): 1.19 (95% CI .75–1.87).

[b] Compared with people with classical NF2 and nonsense or frameshift mutations.

[c] Reference group.

Tumors occurred on all cranial nerves other than the VIII nerve but were most common on the V nerve (13% of subjects), the XII nerve (7%), and the II, VII, and X nerves (3%–4% each). Tumors of cranial nerves other than the VIII nerve were analyzed in the aggregate, because the prevalence of tumors on individual cranial nerves was low. In people with classical NF2 and nonsense or frameshift mutations, the model-based estimated prevalence of tumors of cranial nerves other than the VIII nerve was 45% (table 5). There were not significant genotype-phenotype correlations.

In addition to genotype-phenotype correlations for specific types of mutations, people with new unfound mutations and older age at onset of symptoms tended to have milder disease than people with classical NF2 and nonsense or frameshift mutations. Compared with the reference group, people with new mutations and older age at onset of symptoms had a significantly lower model-based estimated number of peripheral nerve tumors and spinal tumors (tables 3 and 4). The model-based estimated prevalence of tumors of cranial nerves other than the VIII nerve was lower, but not significantly so.

Other covariates contributed significantly to the models for meningiomas and spinal tumors, after adjustment for the type of constitutional *NF2* mutation. There were significant intrafamilial correlations for meningiomas (an average of 0.24) and spinal tumors (an average of 0.21). The number of meningiomas increased significantly with increasing age (1.01 per year of age), and there were significantly more spinal tumors on average (2.4) in people who were seen in specialty centers than in those who were seen in nonspecialty centers.

Discussion

There are genotype-phenotype correlations for the number of NF2-associated intracranial meningiomas, spinal tumors, and peripheral nerve tumors. These results extend the genotype-phenotype correlations that have been reported for overall NF2 disease severity (Mérel et al. 1995; Kluwe et al. 1996, 1998; Parry et al. 1996; Ruttledge et al. 1996; Evans et al. 1998*a*, 1998*b*; Kluwe and Mautner 1998). The present study and other genotype-phenotype correlation studies that used data from the United Kingdom NF2 registry (Evans et al. 1998*a*; Baser et al. 2003) are based on patient information from a variety of types of clinics throughout the United Kingdom, whereas other such studies often have been based on patients from neurofibromatosis clinics (Mérel et al. 1995; Kluwe et al. 1996, 1998; Parry et al. 1996; Ruttledge et al. 1996). Studies that are based on patients from specialty clinics may be biased toward people with more severe disease, and there may be other biases from specialized referral patterns.

Intracranial meningiomas occur in about half of patients with NF2 (Evans et al. 1992*a*; Parry et al. 1994; Mautner et al. 1996*b*). The present study demonstrates that the penetrance of meningiomas increases with increasing age, after adjustment for the type of *NF2* mutation in a regression model. The genotype-phenotype correlation of missense mutations with meningiomas is of interest because missense mutations produce NF2 protein (termed "merlin" or "schwannomin") that is defective in negative growth regulation, whereas nonsense mutations do not produce stable merlin (Gutmann et al. 1998). Missense mutations also produce merlin

Table 4

Genotype-Phenotype Correlations for Spinal Tumors

Type of *NF2* Mutation[a]	Sample Average of No. of Spinal Tumors	Model-Based Estimated Average of No. of Spinal Tumors	95% CI for Count Ratios[b]
Nonsense or frameshift:			
Classical NF2	4.1	4.1	1.00[c]
Somatic mosaic	2.1	1.7	.21–1.16
Splice site	***2.1***	***2.1***	***.26–.94***
Missense	2.0	2.2	.23–1.99
Large deletion	***.8***	***.8***	***.10–.52***
Unfound mutations:			
Inherited cases	1.9	1.6	.15–1.06
People with new mutations:			
Age at onset <20 years	6.1	4.5	.72–3.32
Age at onset ≥20 years	1.1	1.1	.13–.50

NOTE.—Statistically significant results are shown in bold italics.

[a] Other covariates: Intrafamilial correlation coefficient = .21 (95% CI .10–.32). Current age (per year): 1.00 (95% CI .97–1.03). Type of treatment center (specialty vs. nonspecialty): 2.42 (95% CI 1.62–8.70).

[b] Compared with people with classical NF2 and nonsense or frameshift mutations.

[c] Reference group.

with reduced but not absent binding with βII-spectrin (Scoles et al. 1998), which may be caused by complex conformational changes that alter merlin folding and affect access to a binding site (Scoles et al. 2002).

Spinal tumors are found in up to 90% of patients with NF2 when the full spine is scanned by MRI (Mautner et al. 1995). In the present study, patients with NF2 who had been seen at specialty treatment centers had a significantly higher number of spinal tumors, after adjustment for the type of *NF2* mutation and other covariates in a regression model. Patients with NF2 who are seen at specialty treatment centers may be more likely to have full spine MRI, which would lead to the association of specialty treatment centers with a higher number of spinal tumors. Intradural and extradural extramedullary spinal tumors in patients with NF2 are usually schwannomas or meningiomas, whereas intramedullary tumors are usually ependymomas or astrocytomas. A previous study noted that intramedullary spinal tumors were less common in NF2-affected patients with several types of *NF2* mutations in the aggregate (splice-site mutations, missense mutations, or in-frame deletions) than in those with nonsense or frameshift mutations (Patronas et al. 2001). However, specific genotype-phenotype correlations were not found in that study.

Peripheral nerve tumors occur in about half of people with NF2 (Mautner et al. 1997). The prevalence of peripheral nerve tumors is significantly less in people with mild NF2 than in those with severe NF2 (Mautner et al. 1997). This is suggestive of genotype-phenotype correlations, but, prior to this study, such correlations had not been evaluated.

Spinal tumors and peripheral nerve tumors were less common in people with somatic mosaicism than in people with classical NF2 and constitutional *NF2* nonsense or frameshift mutations. Each of these types of tumors was also less common in people with new unfound mutations and older age at onset of symptoms than in people in the reference group. The latter association is not a specific genotype-phenotype correlation, because patients with unfound *NF2* mutations may have different types of mutations. However, it is likely that most of these patients have somatic mosaicism. A similar pattern occurs in NF2-associated cataracts, which are less common in people with somatic mosaicism or new unfound mutations and older age at onset of symptoms than in people with classical NF2 and constitutional *NF2* nonsense or frameshift mutations (Baser et al. 2003).

Somatic mosaicism occurs in an estimated 25%–30% of patients with NF2 who have new mutations (Evans et al. 1998*b*; Kluwe and Mautner 1998; Kluwe et al. 2003; Moyhuddin et al. 2003). The relatively low efficiency (~60%) of conventional mutation screening techniques in detecting constitutional *NF2* mutations in patients with NF2 who have new mutations has been attributed to somatic mosaicism. In somatic mosaics, conventional DNA sequencing of lymphocyte DNA PCR product often fails to identify a difference from the normal sequence because the mutant allele is present at too low a level to be detected. In this study, somatic mosaics with nonsense or frameshift mutations had significantly fewer peripheral nerve tumors than did people with full constitutional *NF2* nonsense or frameshift mutations.

In this study, spinal tumors and peripheral nerve tu-

Table 5

Genotype-Phenotype Correlations for Non–VIII Nerve Cranial Nerve Tumors

Type of *NF2* Mutation[a]	Sample Average of Prevalence of Non–VIII Nerve Cranial Nerve Tumors (%)	Model-Based Estimated Prevalence of Non–VIII Nerve Cranial Nerve Tumors (%)	RR[b]	95% CI
Nonsense or frameshift:				
Classical NF2	44	45	1.00[c]	
Somatic mosaic	27	27	.37	.10–1.37
Splice-site	33	35	.60	.23–1.57
Missense	24	24	.31	.06–1.62
Large deletion	41	42	.85	.28–2.58
Unfound mutations:				
Inherited cases	28	24	.31	.07–1.44
People with new mutations				
Age at onset <20 years	54	54	1.54	.51–4.62
Age at onset ≥20 years	28	28	.39	.15–1.01

[a] Other covariates: Intrafamilial correlation coefficient = .36 (95% CI −.13 to .64). Current age (per year): 1.00 (95% CI .85–1.17). Type of treatment center (specialty vs. nonspecialty): 1.00 (95% CI .28–3.52).

[b] Compared with people with classical NF2 and nonsense or frameshift mutations.

[c] Reference group.

mors were less common in people with constitutional *NF2* large deletions than in people with constitutional *NF2* nonsense or frameshift mutations. There have been other reports of mild NF2 in people with constitutional *NF2* large deletions (Lopez-Correa et al. 2000; Bruder et al. 2001). Constitutional *NF2* large deletions are found in 21%–32% of families with NF2, when multiple screening methods or microarray-comparative genomic hybridization are used (Zucman-Rossi et al. 1998; Bruder et al. 2001). Conventional mutation screening techniques such as SSCP analysis are unable to detect large deletions in autosomal genes because those methods are not designed to measure gene dosage. When a large deletion is present, the normal allele alone is amplified and analyzed; consequently, the deletion is cryptic to the analytical method. A gene dosage method was used to detect large deletions in this study.

Historically, NF2 disease severity was said to "run true" in families, but some studies noted marked intrafamilial clinical variability (Kluwe and Mautner 1996; Mautner et al. 1996*a;* Scoles et al. 1996). In a previous study based on an international NF2 clinicomolecular database, we found that there were strong intrafamilial correlations for age at onset of hearing loss (all mutation types, 0.51; families with missense mutations, 0.67), and there were significant but weaker intrafamilial correlations for intracranial meningiomas (all mutation types, 0.29; families with splice-site mutations, 0.39) (Zhao et al. 2002). The present study confirms this conclusion with respect to intracranial meningiomas in a partially overlapping data set and additionally demonstrates that there is a significant (although weak) intrafamilial correlation for spinal tumors. These intrafamilial correlations were observed in regression models after adjustment for the type of mutation, and it is possible that the correlations reflect differences in the phenotypic effects produced by individual *NF2* alleles that comprise a mutation type. It is also possible that the intrafamilial correlations are evidence of other genetic loci that affect the NF2 phenotype. Other evidence suggests that modifying genes may affect the clinical manifestations of NF2 (Bruder et al. 1999).

The type of constitutional *NF2* mutation is an important determinant of the number of NF2-associated intracranial meningiomas, spinal tumors, and peripheral nerve tumors. Constitutional *NF2* splice-site mutations may have different effects, depending on the location within the gene; that is, 3′ mutations may cause less severe NF2 than do 5′ mutations (Kluwe et al. 1998). Recent longitudinal studies have found that the age at onset of symptoms of NF2 and age at diagnosis of NF2 are the strongest predictors of vestibular schwannoma growth rates (Baser et al. 2002*b;* Mautner et al. 2002) and the risk of mortality (Baser et al. 2002*a;* Otsuka et al. 2003). People with constitutional *NF2* missense mutations have a lower risk of mortality than do those with constitutional *NF2* nonsense or frameshift mutations (Baser et al. 2002*a*). Additional longitudinal genotype-phenotype correlation studies of associations between the type of constitutional *NF2* mutation and the development of specific types of NF2-associated tumors may provide information that is useful for the clinical management of people with NF2.

Acknowledgments

This work was supported, in part, by the FBT Foundation. We thank the patients with NF2 and their families for participating in this study.

Electronic-Database Information

The URLs for data presented herein are as follows:

Online Mendelian Inheritance in Man (OMIM), http://www.ncbi.nlm.nih.gov/Omim/ (for NF2)
Staden, http://staden.sourceforge.net/ (for the trace subtraction algorithm "TraceDiff")

References

Baser ME, Friedman JM, Aeschliman D, Joe H, Wallace AJ, Ramsden RT, Evans DGR (2002*a*) Predictors of the risk of mortality in neurofibromatosis 2. Am J Hum Genet 71:715–723

Baser ME, Kuramoto L, Joe H, Friedman JM, Wallace AJ, Ramsden RT, Evans DGR (2003) Genotype-phenotype correlations for cataracts in neurofibromatosis 2. J Med Genet 40:758–760

Baser ME, Makariou EV, Parry DM (2002*b*) Predictors of vestibular schwannoma growth in patients with neurofibromatosis type 2. J Neurosurg 96:217–222

Bruder CEG, Hirvela C, Tapia-Paez I, Fransson I, Segraves R, Hamilton G, Zhang XX, et al (2001) High resolution deletion analysis of constitutional DNA from neurofibromatosis type 2 (NF2) patients using microarray-CGH. Hum Mol Genet 10:271–282

Bruder CEG, Ichimura K, Blennow E, Ikeuchi T, Yamaguchi T, Yuasa Y, Collins VP, Dumanski JP (1999) Severe phenotype of neurofibromatosis type 2 in a patient with a 7.4-MB constitutional deletion on chromosome 22: possible location of a neurofibromatosis type 2 modifier gene? Genes Chromosomes Cancer 25:184–190

Evans DGR, Birch JM, Ramsden RT (1999) Paediatric presentation of type 2 neurofibromatosis. Arch Dis Child 81:496–499

Evans DGR, Huson SM, Donnai D, Neary W, Blair V, Newton V, Harris R (1992*a*) A clinical study of type 2 neurofibromatosis. Q J Med 84:603–618

Evans DGR, Huson SM, Donnai D, Neary W, Blair V, Teare D, Newton V, Strachan T, Ramsden R, Harris R (1992*b*) A genetic study of type 2 neurofibromatosis in the United Kingdom. I. Prevalence, mutation rate, fitness, and confirmation of maternal transmission effect on severity. J Med Genet 29: 841–846

Evans DGR, Trueman L, Wallace A, Collins S, Strachan T (1998*a*) Genotype/phenotype correlations in type 2 neurofibromatosis (NF2): evidence for more severe disease associated with truncating mutations. J Med Genet 35:450–455

Evans DGR, Wallace AJ, Wu CL, Trueman L, Ramsden RT, Strachan T (1998*b*) Somatic mosaicism: a common cause of classic disease in tumor-prone syndromes? Lessons from type 2 neurofibromatosis. Am J Hum Genet 63:727–736

Gardner WJ, Frazier CH (1930) Bilateral acoustic neuromas: a clinical study and field survey of a family of five generations with bilateral deafness in thirty-eight members. Arch Neurol Psychiatr 23:266–302

Gutmann DH, Geist RT, Xu H-m, Kim JS, Saporito-Irwin S (1998) Defects in neurofibromatosis 2 protein function can arise at multiple levels. Hum Mol Genet 7:335–345

Kluwe L, Beyer S, Baser ME, Hazim W, Haase W, Fünsterer C, Mautner V-F (1996) Identification of *NF2* germ-line mutations and comparison with NF2 phenotypes. Hum Genet 98:534–538

Kluwe L, MacCollin M, Tatagiba M, Thomas S, Hazim W, Haase W, Mautner V-F (1998) Phenotypic variability associated with 14 splice-site mutations in the *NF2* gene. Am J Med Genet 77:228–233

Kluwe L, Mautner V-F (1996) A missense mutation in the NF2 gene results in moderate and mild clinical phenotypes of neurofibromatosis type 2. Hum Genet 97:224–227

——— (1998) Mosaicism in sporadic neurofibromatosis 2 patients. Hum Mol Genet 7:2051–2055

Kluwe L, Mautner V-F, Heinrich B, Dezube R, Jacoby LB, Friedrich RE, MacCollin M (2003) Molecular study of frequency of mosaicism in neurofibromatosis 2 patients with bilateral vestibular schwannomas. J Med Genet 40:109–114

Lee DK, Abbott ML (1969) Familial central nervous system neoplasia: case report of a family with von Recklinghausen's neurofibromatosis. Arch Neurol 20:154–160

Lopez-Correa C, Zucman-Rossi J, Brems H, Thomas G, Legius E (2000) *NF2* gene deletion in a family with a mild phenotype. J Med Genet 37:75–77

MacCollin M, Mautner V-F (1998) The diagnosis and management of neurofibromatosis 2 in childhood. Semin Pediatr Neurol 5:243–252

Mautner V-F, Baser ME, Kluwe L (1996*a*) Phenotypic variability in two families with novel splice-site and frameshift *NF2* mutations. Hum Genet 98:203–206

Mautner V-F, Baser ME, Thakkar SD, Feigen UM, Friedman JM, Kluwe L (2002) Vestibular schwannoma growth in patients with neurofibromatosis type 2: a longitudinal study. J Neurosurg 96:223–228

Mautner V-F, Lindenau M, Baser ME, Hazim W, Tatagiba M, Haase W, Samii M, Wais R, Pulst S-M (1996*b*) The neuroimaging and clinical spectrum of neurofibromatosis 2. Neurosurgery 38:880–886

Mautner V-F, Lindenau M, Baser ME, Kluwe L, Gottschalk J (1997) Skin abnormalities in neurofibromatosis 2. Arch Dermatol 133:1539–1543

Mautner V-F, Tatagiba M, Guthoff R, Samii M, Pulst S-M (1993) Neurofibromatosis in the pediatric age group. Neurosurgery 33:92–96

Mautner V-F, Tatagiba M, Lindenau M, Funsterer C, Pulst S-M, Baser ME, Kluwe L, Zanella FE (1995) Spinal tumors in patients with neurofibromatosis type 2: MR imaging study of frequency, multiplicity, and variety. AJR Am J Roentgenol 165:951–955 (erratum 166:1231)

Mérel P, Hoang-Xuan K, Sanson M, Bijlsma E, Rouleau G, Laurent-Puig P, Pulst S, Baser M, Lenoir G, Sterkers JM, Philippon J, Resche F, Mautner V-F, Fischer G, Hulsebos T, Aurias A, Delattre O, Thomas G (1995) Screening for germ-

line mutations in the *NF2* gene. Genes Chromosomes Cancer 12:117–127

Moyhuddin A, Baser ME, Watson C, Purcell S, Ramsden RT, Heiberg A, Wallace AJ, Evans DGR (2003) Somatic mosaicism in neurofibromatosis 2: prevalence and risk of disease transmission to offspring. J Med Genet 40:459–463

Nunes F, MacCollin M (2003) Neurofibromatosis 2 in the pediatric population. J Child Neurol 18:718–724

Otsuka G, Saito K, Nagatani T, Yoshida J (2003) Age at symptom onset and long-term survival in patients with neurofibromatosis type 2. J Neurosurg 99:480–483

Parry DM, Eldridge R, Kaiser-Kupfer MI, Bouzas E, Pikus A, Patronas N (1994) Neurofibromatosis 2 (NF2): clinical characteristics of 63 affected individuals and clinical evidence for heterogeneity. Am J Med Genet 52:450–461

Parry DM, MacCollin MM, Kaiser-Kupfer MI, Pulaski K, Nicholson HS, Bolesta M, Eldridge R, Gusella JF (1996) Germline mutations in the neurofibromatosis 2 gene: correlations with disease severity and retinal abnormalities. Am J Hum Genet 59:529–539

Patronas NJ, Courcoutsakis N, Bromley CM, Katzman GL, MacCollin M, Parry DM (2001) Intramedullary and spinal canal tumors in patients with neurofibromatosis 2: MR imaging findings and correlation with genotype. Radiology 218:434–442

Rouleau GA, Mérel P, Lutchman M, Sanson M, Zucman J, Marineau C, Hoang-Xuan K, Demczuk S, Desmaze C, Plougastel B, Pulst SM, Lenoir G, Bijlsma E, Fashold R, Dumanski J, de Jong P, Parry D, Eldridge R, Aurias A, Delattre O, Thomas G (1993) Alteration in a new gene encoding a putative membrane-organizing protein causes neurofibromatosis type 2. Nature 363:515–521

Ruttledge MH, Andermann AA, Phelan CM, Claudio JO, Han F-y, Chretien N, Rangaratnam S, MacCollin M, Short P, Parry D, Michels V, Riccardi VM, Weksberg R, Kitamura K, Bradburn JM, Hall BD, Propping P, Rouleau GA (1996) Type of mutation in the neurofibromatosis type 2 gene (*NF2*) frequently determines severity of disease. Am J Hum Genet 59:331–342

Scoles D, Chen M, Pulst S-M (2002) Effects of NF2 missense mutations on schwannomin interactions. Biochem Biophys Res Commun 290:366–374

Scoles DR, Baser ME, Pulst S-M (1996) A missense mutation in the neurofibromatosis 2 gene occurs in patients with mild and severe phenotypes. Neurology 47:544–546

Scoles DR, Huynh DP, Morcos PA, Coulsell ER, Robinson NGG, Tamanoi F, Pulst S-M (1998) Neurofibromatosis 2 tumour suppressor schwannomin interacts with βII-spectrin. Nat Genet 18:354–359

Trofatter JA, MacCollin MM, Rutter JL, Murrell JR, Duyao MP, Parry DM, Eldridge R, Kley N, Menon AG, Pulaski K, Haase VH, Ambrose CM, Munroe D, Bove C, Haines JL, Martuza RL, MacDonald ME, Seizinger BR, Short MP, Buckler AJ, Gusella JF (1993) A novel moesin-, ezrin-, radixin-like gene is a candidate for the neurofibromatosis 2 tumor suppressor. Cell 72:791–800 (erratum 75:826)

Wallace AJ, Wu C-L, Elles RG (1999) Meta-PCR: a novel method for creating chimaeric DNA molecules and increasing the productivity of mutation screening techniques. Genetic Testing 3:173–183

Wishart JH (1822) Case of tumours in the skull, dura mater, and brain. Edinburgh Med Surg J 18:393–397

Yau SC, Bobrow M, Mathew CG, Abbs SJ (1996) Accurate diagnosis of carriers of deletions and duplications in Duchenne/Becker muscular dystrophy by fluorescent dosage analysis. J Med Genet 33:550–558

Zhao Y, Kumar RA, Baser ME, Evans DG, Wallace A, Kluwe L, Mautner V-F, Parry DM, Rouleau GA, Joe H, Friedman JM (2002) Intrafamilial correlation of clinical manifestations in neurofibromatosis 2 (NF2). Genet Epidemiol 23:245–259

Zucman-Rossi J, Legoix P, Sarkissian HD, Cheret G, Sor F, Bernardi A, Cazes L, Giraud S, Ollagnon E, Lenoir G, Thomas G (1998) *NF2* gene in neurofibromatosis type 2 patients. Hum Mol Genet 7:2095–2101

ELECTRONIC LETTER

Evaluation of genotype-phenotype correlations in neurofibromatosis type 1

B Castle, M E Baser, S M Huson, D N Cooper, M Upadhyaya

J Med Genet 2003;**40**:e109 (http://www.jmedgenet.com/cgi/content/full/40/10/e109)

Neurofibromatosis type 1 (NF1) is an autosomal dominant disease with complete penetrance and extremely variable expression, and an incidence of approximately 1 in 4000 live births. Despite the high incidence of NF1, neither the natural history nor the genetic epidemiology of the disorder are well understood. People with NF1 have reduced reproductive fitness and life expectancy,[1] but the cause of the high mutation rate at the *NF1* locus is unknown.

The most prominent clinical hallmarks of NF1 are café-au-lait (CAL) macules, neurofibromas, Lisch nodules of the iris, and axillary freckling.[2] Other clinical manifestations are abnormalities of the cardiovascular, gastrointestinal, renal, and endocrine systems, facial and body disfigurement, cognitive deficit, and malignancies of the peripheral nerve sheath and central nervous system. About 25% of people with NF1 develop one or more of these clinical complications, which together cause significant morbidity and mortality.[3] The tumours that occur in NF1 are dermal and plexiform neurofibromas, optic gliomas, malignant peripheral nerve sheath tumours (MPNSTs), pheochromocytomas, and rhabdomyosarcomas.[1] Children with NF1 have an increased risk of developing myeloid disease, particularly juvenile chronic myeloid leukaemia. Some 30–40% of NF1 patients develop plexiform neurofibromas[2–4] that become MPNSTs in 5–10% of cases,[5–7] often in pre-existing plexiform neurofibromas.

The *NF1* gene on chromosome 17q11.2 spans more than 350 kb of genomic DNA and contains 60 exons.[8] The 8457 bp open reading frame predicts a protein of 2818 amino acids with an estimated mass of 327 kDa.[9 10] The *NF1* gene product, neurofibromin, contains a 360 amino acid region with homology to the catalytic domain of the mammalian guanosine triphosphatase activating protein. Neurofibromin is a GTPase activating protein for members of the p21ras (Ras) protein family. Loss of neurofibromin function leads to downstream cell growth activation because neurofibromin negatively regulates Ras output by accelerating the conversion of active Ras-GTP to inactive Ras-GDP. Three genes (*EVI2A*,*EVI2B* and *OMGP*) are embedded within intron 27 but are transcribed in the opposite direction to the *NF1* gene.[11 12] However, in a comparative study of various *NF1* gross gene deletions, Viskochil[8] concluded that haploinsufficiency of the three embedded genes did not contribute to the clinical features of NF1.

Genetic counselling is problematic in NF1 owing to the marked inter- and intra-familial variation in NF1 expression. The exploration of genotype–phenotype correlations in NF1 is still in its infancy because of the extensive mutational heterogeneity of the gene, and because large scale mutation screening is laborious owing to the size and complexity of the gene. In this study, we characterised constitutional *NF1* gene mutations in 113 NF1 patients, and statistically evaluated genotype–phenotype correlations in 110 of these patients. We also considered atypical cases in detail because allelic heterogeneity is a possible cause of some NF1 phenotypes, particularly Watson syndrome and NF Noonan syndrome (NFNS).[13–15]

Key points

- Neurofibromatosis type 1 (NF1) is an autosomal dominant disease with complete penetrance and extremely variable expression, with an incidence of approximately 1 in 4000 live births.
- Despite the high incidence of NF1, neither the natural history nor the genetic epidemiology of the disorder is well understood. In this study, we characterised constitutional *NF1* gene mutations in 113 NF1 patients and statistically evaluated genotype–phenotype correlations in 110 of these patients.
- The clinical abnormalities were café-au-lait macules, axillary freckling, number of dermal and nodular neurofibromas, macrocephaly, short stature, ratio of head circumference to height, pectus excavatus, learning disabilities, and plexiform and spinal neurofibromas.
- Logistic regression analysis was used to calculate relative risks (RR) and 95% confidence intervals (CI) for binary outcomes, while linear regression analysis was used for continuous outcomes.
- When compared with people with nonsense or frameshift mutations and adjusted for age at examination, individuals with missense mutations had an RR of Lisch nodules that was lower than unity, although of borderline statistical significance (RR=0.26, 95% CI=0.07 to 1.04, p=0.06).
- This exploratory finding nevertheless merits investigation in other NF1 patient populations.

METHODS

The constitutional *NF1* gene mutations were identified in one laboratory using a battery of different mutation detection techniques: single strand conformational polymorphism analysis, heteroduplex analysis, the protein truncation test, dideoxy fingerprinting, denaturing high performance liquid chromatography, and direct DNA sequencing.[16–20] Clinical data were obtained from medical records of examinations within the previous 2 years, or if recent medical data were

Abbreviations: CAL, café-au-lait; MPNSTs, malignant peripheral nerve sheath tumours; NF, neurofibromatosis; NFNS, neurofibromatosis Noonan syndrome; NIH, (US) National Institutes of Health

unavailable, the patients were re-examined. The examining physician was blinded to the patient's mutation.

There were 113 NF1 patients with identified *NF1* gene mutations. Three of these patients were excluded from the statistical analysis of genotype–phenotype correlations: two patients who did not meet the US National Institutes of Health (NIH) diagnostic criteria for NF1[21] and a single patient with an identified *NF1* large gene deletion. The common clinical abnormalities were coded as: Lisch nodules (present/absent), number of CAL macules (0, 1–6, >6), axillary freckling (present/absent), number of dermal and nodular neurofibromas (0, 1–10, 11–100, 101–500, >500), macrocephaly (present/absent), short stature (present/absent), the ratio of head circumference (cm) to height (m) (OFC/height ratio), pectus excavatum (present/absent), learning difficulties (present/absent), plexiform neurofibromas (present/absent), scoliosis (present/absent), and spinal neurofibromas (present/absent). Percentiles for the OFC/height ratio were calculated using charts.[22 23] The prevalence of other clinical abnormalities (glioma, sarcoma, phaeochromocytoma, gastrointestinal neurofibromas, pulmonary stenosis, renal artery stenosis, delayed puberty, aqueduct stenosis, Watson syndrome, Noonan syndrome, epilepsy, bone dysplasia) was too low (5% or less) for meaningful statistical analysis.

Logistic regression analysis was used to calculate relative risks (RR) and 95% confidence intervals (CI) for binary outcomes. Linear regression analysis was used for continuous outcomes. Each regression model had the covariates of the type of constitutional *NF1* mutation and age at examination (as a continuous variable). The mutation covariate was coded as several binary variables (indicators of missense and splice site mutations, each compared to nonsense or frameshift mutations). Age at examination was included as a covariate because the penetrance of many NF1 disease features increases with age.[24 25] A logarithmic transformation was used for age at examination, which ranged from 2 to 70 years. There is a potential bias toward lower age at examination in non-probands relative to probands, but proband status did not contribute significantly to any of the models after including age at examination as a covariate, so probands and non-probands were combined in subsequent analyses. There were eight families with two affected relatives and two families with three affected relatives.

We evaluated genotype–phenotype correlations for each common clinical abnormality individually and for three groups of disease features:[26] (*a*) CAL macules, axillary freckling, and Lisch nodules, (*b*) dermal, nodular, and plexiform neurofibromas, and (*c*) macrocephaly, optic glioma, and other neoplasms. A patient was categorised as belonging to a group if at least two disease features in the group were present.

RESULTS

The identified constitutional *NF1* gene lesions ranged from single base pair substitutions to gross deletions, but the microlesions appeared to be uniformly distributed across the gene (http://www.uwcm.ac.uk/study/medicine/medical_genetics/research/nf1/supplementary_data.html). The prevalence of common clinical abnormalities in this study was generally similar to those of other published studies (table 1). Delayed and precocious puberty occur in NF1,[27 28] but the exact prevalence is unknown. In this study, 6% of males and 5% of females had delayed puberty at16 years of age. One patient had an empty sella turcica without abnormal pituitary function and a second patient with very short stature had isolated growth hormone deficiency with otherwise normal pituitary function. There were no patients with precocious puberty.

Genotype–phenotype correlations

Eighty four patients had ocular examinations. As expected, the relative risk (RR) of Lisch nodules increased with increasing age at examination (table 2). When compared with people with nonsense or frameshift mutations, people with missense mutations had an RR of Lisch nodules that was lower than unity but of borderline statistical significance (RR = 0.26, 95% CI 0.07 to 1.04, p = 0.06, Cox and Snell $R^2 = 0.10$). There were no significant genotype–phenotype correlations for any other individual abnormalities or for any of the three groups of disease features (data not shown).

Atypical cases

There were two patients who did not fulfil the NIH diagnostic criteria for NF1 and who were not included in the statistical analysis of genotype–phenotype correlations. One was a 10 year old child who, in common with his mother, had CAL macules but no other stigmata suggestive of NF1. The *NF1* mutation in the family was a missense substitution (R1809L). The second patient was a 27 year old woman with no family history of NF1 and no CAL spots, freckling, or Lisch nodules. She had a small number (<10) of cutaneous and nodular neurofibromas, confirmed on biopsy. In addition, she had a vestibular schwannoma and a schwannoma of the posterior fossa involving the vagus nerve. A cervical cord ependymoma was resected, leaving the patient paraplegic. Although initially considered as a possible case of NF type 2, a single base pair insertion in exon 37 (6792 ins A) of the *NF1* gene was subsequently identified in this patient.

There were three patients with NFNS. The first NFNS patient was a 6 year old boy from a large Ashkenazi kindred with NF1. He had only four CAL macules on examination but had been developing cutaneous neurofibromas since the age of 2 years, and had intracranial tumours and hydrocephalus secondary to aqueduct stenosis, which had required shunting. There were no Lisch nodules and he was not macrocephalic. He had facial dysmorphism suggestive of Noonan syndrome but had an inactivating splice site mutation in the *NF1* gene (IVS 29+1 G→C).

The second NFNS patient was a 20 year old man who fulfilled the NIH diagnostic criteria for NF1, and had a pectus excavatum, learning difficulties, and mild hydrocephalus. He was also thought to have aqueduct stenosis causing hydrocephalus, which did not require shunting at the time of examination. The *NF1* mutation was a microdeletion (2133 del CC). There was no evident cardiac abnormality in these two patients.

The third NFNS patient was a 10 year old boy who was born prematurely and had facial dysmorphism, widely spaced nipples, and an atrial–septal defect. His *NF1* mutation was a microinsertion (4093 ins TG).

There were three patients with Watson syndrome. Two had mild to moderate pulmonary stenosis that was documented on echocardiography. Neither had a history of significant learning difficulties, but they did not complete their schooling. One patient had a novel 3 bp deletion (AAT) within exon 17 of the *NF1* gene leading to a loss of ATG (methionine) in exon 17,[29] and the other had a paternally inherited nonsense mutation in exon 29 (S1745X). This patient's father also had mild pulmonary stenosis with stigmata of NF1. The third patient was a 49 year old man with significant learning difficulties, behavioural problems associated with epilepsy, and pulmonary stenosis. He had an intragenic *NF1* gene deletion of >20 bp.

Another atypical patient was a 31 year old woman who had stigmata of NF1 almost exclusively in the cranial region. There were four CAL macules on the head and neck only, and multiple large histologically confirmed neurofibromas on the scalp and behind the ears. There was also macrocephaly but

Table 1 Prevalence of common clinical features of NF1 in this study and in previously published studies

Clinical feature	Prevalence in this study (%)	Prevalence in previous studies (%)	References
CAL macules	98	100 (at 15 years of age)	2 23 27
Axillary freckling	41	85	71 72
Neurofibromas	81	98–100	27 72
Lisch nodules	82	92–95	27 73
Macrocephaly	40	45	27 74
Short stature	50	30–40	27 72
OFC/height ratio>95%	97	Unknown	None
Pectus excavatus	12	Up to 30	71 72
Learning difficulty	35	30–60	75 76
Plexiform neurofibromas	37	27	27

no other manifestations of NF1 in the rest of the body. In addition, the proband was diagnosed with Van der Woude syndrome at the age of 6 months, with a cleft palate and lip pits, which were surgically treated. The *NF1* mutation was a microdeletion in exon 22 (3731 del T).

DISCUSSION

NF1 patients with missense mutations had an RR of Lisch nodules that was less than 1, and of borderline statistical significance when compared to NF1 patients with nonsense or frameshift mutations and adjusted for age at examination. This exploratory finding merits investigation in other NF1 patient populations, although it is difficult to evaluate the pathogenicity of missense mutations without functional studies. In this study, multiple statistical comparisons were made for the different clinical abnormalities and different mutation types, but as these analyses were exploratory, not confirmatory, we chose to test associations at the $\alpha = 0.05$ level.

From the clinical viewpoint, our findings are notable for two reasons. The OFC/height ratio was at or above the 95th percentile in 97% of cases, but the prevalence of macrocephaly was 40% and the prevalence of short stature was 50%. This suggests that an increase in the OFC/height ratio is a useful clinical indicator of NF1, even in the absence of absolute macrocephaly or short stature. The finding of delayed puberty in 6% of males and 5% of females at 16 years of age confirms that this is an NF1 related phenomenon.

We did not find genotype–phenotype correlations for other common clinical features of NF1, similar to the findings of most other studies of genotype–phenotype correlations in NF1.[4 30–33]

The only exception is the correlation of large *NF1* gene deletions (up to 1.5 Mb genomic DNA) with an earlier age of onset of cutaneous neurofibromas, learning disability, dysmorphic features, and developmental delay.[18 34–38] However, not all patients with a gross *NF1* gene deletion have this NF1 phenotype,[18 36] and flanking DNA sequence (or the lack of it) may affect the phenotype. Easton *et al.*[30] modelled the genetic contributions to eight traits in 175 people with NF1 (CAL macules, neurofibromas, head circumference, plexiform neurofibromas, optic gliomas, scoliosis, epilepsy, and remedial education). There were no significant correlations between the traits, indicating that the phenotypic expression of NF1 was largely determined by trait specific loci unlinked to the *NF1* gene.

We were not able to evaluate genotype–phenotype correlations for some of the most clinically significant disease features of NF1, such as the various types of cancer. The RR of these complications is very high compared with the general population, but the prevalence in NF1 is relatively low, and there were too few patients with these complications in this study to support statistical analysis.

Identical *NF1* gene mutations can occur in unrelated patients with very different phenotypes.[11 19 38–41] Owing to the absence of strong genotype–phenotype correlations,[30] *NF1* mutation analysis has very limited predictive utility for specific sequelae. *NF1* mutation analysis has greater diagnostic utility because mutation detection can confirm the aetiology of the disease in the relatively few families and individuals in whom the clinical phenotype does not fulfil the NIH diagnostic criteria. A provisional diagnosis of NF1 improves clinical management by triggering the initiation of routine blood pressure monitoring in patients from an early age and alerting medical care providers to the possibility of clinical complications. A firm diagnosis allows counselling regarding mode of inheritance, recurrence risk, and potentially, prenatal diagnosis.

Allelic heterogeneity is a possible cause of some of the multiple phenotypes in NF1, particularly Watson syndrome (multiple CAL macules, pulmonic stenosis, and dull intelligence),[13] NFNS,[15] and familial spinal neurofibromatosis.[42] To date, however there is no evidence to support allelic heterogeneity as a cause for any of these three atypical phenotypes, nor did we find such evidence in the present study, as detailed below.

Allelic heterogeneity is not likely to be responsible for Watson syndrome because the three patients in the present study with Watson syndrome had *NF1* mutations of differing types and locations. Divergent *NF1* gene mutations have been

Table 2 Results of logistic regression with presence of Lisch nodules as the outcome

Covariate	RR	95% CI	P
Age at examination (per unit increase in logarithm of age)	8.53	1.43 to 50.83	0.02
Type of constitutional *NF1* mutation (compared with nonsense or frameshift mutations)			
Missense mutation	0.26	0.07 to 1.04	0.06
Splice site mutation	0.55	0.09 to 3.27	0.51

CI, confidence interval; RR, relative risk.

identified: an 80 kb deletion in a Watson syndrome patient,[16] and a 42 bp duplication that segregated in a family with a phenotype suggestive of NFNS.[43]

About 12–13% of NF1 patients who are specifically examined for Noonan syndrome have a clinical phenotype that is similar to Noonan syndrome,[14 15] but Carey,[44] and Carey and Viskochil[32] reviewed these patients, and concluded that they did not have typical Noonan syndrome, as features of Noonan syndrome without cardiovascular malformation have been observed in many NF1 patients. The three patients in the present study with features of Noonan syndrome had *NF1* mutations of differing types and locations. As two of these patients had hydrocephalus associated with features of aqueduct stenosis, the dysmorphic features of Noonan syndrome could be a secondary effect, and NFNS may not be a distinct clinical entity. There is clinical overlap between Noonan syndrome and NF1, but the Noonan syndrome gene (*PTPN11*) has been mapped to 12q24.1 and there is no suggestion of locus heterogeneity for NF1.

Spinal neurofibromas have been reported in up to 38% of NF1 patients, but only 5% of these patients have spinal neurofibromatosis.[42] All patients in our study who had familial spinal neurofibromatosis also fulfilled the NIH diagnostic criteria for NF1, and had Lisch nodules and dermal neurofibromas, as has been previously reported.[42 45] Ars *et al*[42] described a frameshift mutation in exon 46 (8042 ins A) that cosegregated with spinal neurofibromatosis. In another study, two unrelated NF1 patients with spinal neurofibromatosis had an *NF1* missense mutation in exon 33 (L2067P) and an *NF1* splice site mutation (IVS31-5 A→G).[46] A recurrent *NF1* splice site mutation (IVS19b-3 C→G) was identified in a patient with spinal neurofibromatosis.[47] In the present study, patients with spinal neurofibromatosis also had different types of mutations. These findings indicate that specific *NF1* gene mutations are not associated with spinal neurofibromatosis.

One NF1 patient in this study also had Van der Woude syndrome, a dominantly inherited disorder with locus heterogeneity. The majority of Van der Woude patients have linkage to the 1q32–41 locus,[48] but there is a second locus on 1p34.[49] A modifier locus exists on 17p11.2,[50] but there is no evidence to suggest an association with the *NF1* locus at 17q11.2. This patient may be segregating two distinct and unrelated autosomal dominant conditions.

The marked clinical variability between multiple affected relatives in NF1 families also could be due to the nature, timing, or location of the "second hit" mutations at the *NF1* locus in dermal and plexiform neurofibromas,[51–55] MPSNTs,[56–58] pheochromocytomas,[59] pilocytic astrocytomas,[60] and juvenile chronic myelogenous leukaemia cells.[61] Variable expressivity has also been observed in other tumour prone genetic conditions such as neurofibromatosis 2, tuberous sclerosis 1 and 2, and familial adenomatous polyposis.[62 63]

Somatic mosaicism, which has been documented in over 60 monogenic disorders,[64] is another potential cause of inter-individual phenotypic variation. Somatic mosaicism can occur sufficiently early in embryonic life to involve both somatic and germline cells, and such individuals may also be at risk of having affected children.[65] Somatic mosaicism in NF1 is thought to be the cause of segmental neurofibromatosis.[66] There is inter-individual variation in mitotic recombination,[67] and the genes that control this process may be an important cause of clinical variability within NF1 families. Serra *et al*[68] reported that mitotic recombination was the causal mechanism for the loss of heterozygosity of an *NF1* constitutional mutation.

Our study gives further support to the probable importance of modifying loci, as suggested by Easton *et al*[30] This hypothesis is supported by the observation of many investigators that identical *NF1* gene mutations often give rise to very different phenotypes in unrelated patients. *GDNF* is a candidate modifier gene in NF1,[69] and preliminary work in a mouse model of NF1 has also suggested the existence of modifying genes.[70] The identification of modifying genes in humans will be difficult and will require large cohorts of patients identified through multicentre collaborations, but the study of modifying genes may eventually allow more accurate prediction of specific clinical features and complications of NF1 that could possibly lead to new therapeutic approaches.

ACKNOWLEDGEMENTS

We are grateful to the UK Neurofibromatosis Association and the National Lottery Board for their financial support. We thank all the clinicians, patients and their families for their help.

Authors' affiliations

B Castle, D N Cooper, M Upadhyaya, Institute of Medical Genetics, University of Wales College of Medicine, Heath Park, Cardiff CF14 4XN, UK
M E Baser, 2257 Fox Hills Drive, Los Angeles, CA 90064, USA
S M Huson, Department of Clinical Genetics, Oxford Radcliffe Hospitals NHS Trust, Oxford OX3 7LJ, UK

Correspondence to: Dr M Upadhyaya, Institute of Medical Genetics, University of Wales College of Medicine, Heath Park, Cardiff CF14 4XN, UK; upadhyaya@cardiff.ac.uk

REFERENCES

1 **Friedman J.** Epidemiology of neurofibromatosis type 1. *Am J Med Genet* 1999;**89**:1–6.
2 **Friedman JM,** Gutmann DH, MacCollin M, Riccardi Y. Neurofibromatosis: phenotype, natural history, and pathogenesis. Baltimore: Johns Hopkins University Press, 1999.
3 **Huson SM,** Compston DAS, Harper PS. A genetic study of von Recklinghausen neurofibromatosis in Southeast Wales.1: Guidelines for genetic counselling. *J Med Genet* 1989;**26**:712–21.
4 **Upadhyaya M,** Cooper DN. The mutation spectrum in neurofibromatosis type 1 and its underlying mechanism. Chapter 5. In: Upadhyaya M, Cooper D, eds. *Neurofibromatosis type 1: from genotype to phenotype.* Oxford: BIOS Scientific, 1998:65–87.
5 **Rasmussen SA,** Overman J, Thomson SA, Colman SD, Abernathy CR, Trimpert RE, Moose R, Virdi G, Roux K, Bauer M, Rojiani AM, Maria BL, Muir D, Wallace MR. *Genes Chromosomes Cancer* 2000;**28**:425–31.
6 **Evans DG,** Baser ME, McGaughran J, Sharif S, Howard E, Moran A. Malignant peripheral nerve sheath tumours in neurofibromatosis 1. *J Med Genet* 2002;**39**:311–14.
7 **Ferner R,** Gutmann DH. International consensus statement on malignant peripheral nerve sheath tumours in neurofibromatosis 1. *Cancer Res* 2002;**62**:1573–7.
8 **Viskochil D.** Gene structure and expression. Chapter 3. In: Upadhyaya M, Cooper D, eds. *Neurofibromatosis type 1: from genotype to phenotype.* Oxford: BIOS Scientific, 1998:39–56.
9 **Xu GF,** O'Connell P, Viskochil D, Cawthon R, Robertson M, Culver M, Dunn D, Stevens J, Gesteland R, White R, Weiss R. The neurofibromatosis type 1 gene encodes a protein related to GAP. *Cell* 1990;**62**:599–608.
10 **Marchuk DA,** Saulino AM, Tavakkol R, Swaroop M, Wallace MR, Andersen LB, Mitchell AL, Gutmann DH, Boguski M, Collins FS. cDNA cloning of the type 1 neurofibromatosis gene: complete sequence of NF1 gene product. *Genomics* 1991;**11**:931–40.
11 **Cawthon RM,** Weiss R, Xu GF, Viskochil D, Culver M, Stevens J, Robertson M, Dunn D, Gesteland R, O'Connell P, White R. A major segment of the neurofibromatosis type 1 gene: DNA sequence, genomic structure and point mutations. *Cell* 1990;**62**:193–201.
12 **Viskochil D,** Cawthon R, O'Connell P, Xu GF, Stevens J, Culver M, Carey J, White R. The gene encoding the oligodendrocyte- myelin glycoprotein is embedded within the neurofibromatosis type 1 gene. *Mol Cell Biol* 1991;**11**:906–12.
13 **Allanson JE,** Upadhyaya M, Watson GH, Partington M, MacKenzie A, Lahey D, MacLeod H, Sarfarazi M, Broadhead W, Harper PS, Huson SM. Watson syndrome: is it a subtype of type 1 neurofibromatosis? *J Med Genet* 1991;**28**:752–6.
14 **Buehning L,** Curry CJ. Neurofibromatosis-Noonan syndrome. *Pediatr Dermatol* 1995;**12**:267–71.
15 **Colley A,** Donnai D, Evans D. Neurofibromatosis/Noonan phenotype: a variable feature of type 1 neurofibromatosis. *Clin Genet* 1996;**49**:59–64.
16 **Upadhyaya M,** Shen M, Cherryson A, Farnham J, Maynard J, Huson SM, Harper PS. Analysis of mutations at the neurofibromatosis 1 (NF1) locus. *Hum Mol Genet* 1992;**1**:735–40.

17 **Osborn M**, Upadhyaya M. Evaluation of the protein truncation test and mutation detection in the NF1 gene: mutation analysis of 15 known and 40 unknown mutations. *Hum Genet* 1999;**105**:327–32.
18 **Upadhyaya M**, Ruggieri M, Maynard J, Osborn M, Hartog C, Mudd S, Penttinen M, Cordeiro I, Ponder M, Ponder BA, Krawczak M, Cooper DN. Gross deletions of the neurofibromatosis type 1 (NF1) gene are predominantly of maternal origin and commonly associated with learning disability, dysmorphic features and developmental delay. *Hum Genet* 1998;**102**:591–97.
19 **Upadhyaya M**, Osborn MJ, Maynard J, Kim MR, Tamanoi F, Cooper DN. Mutational and functional analysis of the neurofibromatosis type 1(NF1) gene. *Hum Genet* 1997;**99**:88–92.
20 **Han S**, Cooper DN, Upadhyaya M. Evaluation of denaturing high performance liquid chromatography (DHPLC) for the mutational analysis of the neurofibromatosis type 1 (NF1) gene. *Hum Genet* 2001;**109**:487–97.
21 **National Institutes of Health**. Consensus development conference statement: neurofibromatosis. *Arch Neurol* Chicago, 1988;**45**:575–8.
22 **Szudek J**, Birch P, Friedman J. Growth in North American white children with neurofibromatosis 1 (NF1). *J Med Genet* 2000;**37**:933–8.
23 **Najjar M**, Rowland M. *Anthropometric reference data and prevalence of overweight, United States, 1976–80. Vital and health statistics 1981*, Series 11, No.238. DHHS Publications (PHS) 87-1688, Public Health Service. Washington: US Government Printing Office, 1987.
24 **Huson S**. Neurofibromatosis type 1: historical perspective and introductory overview, Chapter 1. In: Upadhyaya M, Cooper DN, eds. *Neurofibromatosis type 1: from genotype to phenotype*. Oxford: BIOS Scientific, 1998:1–20.
25 **DeBella K**, Szudek J, Friedman J. Use of the National Institutes of Health criteria for diagnosis of neurofibromatosis 1 in children. *Pediatrics* 2000;**105**:608–614.
26 **Szudek J**, Evans DGR, Friedman JF. Patterns of association of clinical features in neurofibromatosis 1 (NF1). *Hum Genet* 2003;**112**:289–97.
27 **Listernick R**, Louis DN, Packer RJ, Gutmann DH. Optic pathway gliomas in children with neurofibromatosis type 1: consensus statement from the NF1 optic pathway glioma task force. *Ann Neurol* 1997;**41**:143–9.
28 **Huson S**, Harper P, Compston D. Von Recklinghausen neurofibromatosis: a clinical and population study in south-east Wales. *Brain* 1988;**111**:1355–81.
29 **Shen M**, Harper P, Upadhyaya M. Neurofibromatosis type 1 (NF1): the search for mutations by PCR-heteroduplex analysis on Hydrolink gels. *Hum Mol Genet* 1993;**2**:1861–4.
30 **Easton DF**, Ponder MA, Huson SM, Ponder BA. An analysis of variation in expression of neurofibromatosis type 1 (NF1): evidence for modifying genes. *Am J Hum Genet* 1993;**53**:305–13.
31 **Easton D**. Genotype-phenotype relationships in neurofibromatosis type 1. Chapter 10. n: Upadhyaya M, Cooper DN, eds. *Neurofibromatosis type 1: from genotype to phenotype*. Oxford: BIOS Scientific, 1998:167–74.
32 **Carey J**, Viskochil D. Neurofibromatosis type 1: A model condition for the study of the molecular basis of variable expressivity in human disorder. *Am J Med Genet* 1999;**89**:7–13.
33 **Szudek J**, Joe H, Friedman JM. Analysis of intrafamilial phenotypic variation in neurofibromatosis type 1 (NF1). *Genet Epidemiol* 2002;**23**:150–64.
34 **Kayes LM**, Burke W, Riccardi VM, Bennett R, Ehrlich P, Rubenstein A, Stephens K. Deletions spanning the neurofibromatosis 1 gene: identification and phenotype of five patients. *Am J Hum Genet* 1994;**54**:424–36.
35 **Wu BL**, Austin MA, Schneider GH, Boles RG, Korf BR. Deletion of the entire *NF1* gene detected by the FISH: four deletion patients associated with severe manifestations. *Am J Med Genet* 1995;**59**:528–35.
36 **Tonsgard JH**, Yelavarthi KK, Cushner S, Short MP, Lindgren V. Do NF1 gene deletions result in a characteristic phenotype? *Am J Med Genet* 1997;**73**:80–6.
37 **Riva P**, Corrado L, Natacci F, Castorina P, Wu BL, Schneider GH, Clementi M, Tenconi R, Korf BR, Larizza L. NF1 microdeletion syndrome: refined FISH characterisation of sporadic and familial deletions with locus-specific probes. *Am J Hum Genet* 2000;**66**:100–9.
38 **Lopez-Correa C**, Dorschner M, Brems H, Lazaro C, Clementi M, Upadhyaya M, Dooijes D, Moog U, Kehrer-Sawatzki H, Rutkowski JL, Fryns JP, Marynen P, Stephens K, Legius E. Recombination hotspot in NF1 microdeletion patients. *Hum Mol Genet* 2001;**10**:1387–92.
39 **Ainsworth P**, Rodenhiser D, Costa M. Identification and characterization of sporadic and inherited mutations in exon 31 of the neurofibromatosis (NF1) gene. *Hum Genet* 1993;**91**:151–6.
40 **Horiuchi T**, Hatta N, Matsumoto M, Ohtsuka H, Collins FS, Kobayashi Y, Fujita S. Nonsense mutations at Arg-1947 in two cases of familial neurofibromatosis type 1 in Japanese. *Hum Genet* 1994;**93**:81–3.
41 **Shen M**, Harper P, Upadhyaya M. Molecular genetics of neurofibromatosis type 1. *J Med Genet* 1996;**33**:2–17.
42 **Ars E**, Kruyer H, Gaona A, Casquero P, Rosell J, Volpini V, Serra E, Lazaro C, Estivill X. A clinical variant of neurofibromatosis type 1: familial spinal neurofibromatosis with a frameshift mutation in the gene. *Am J Hum Genet* 1998;**62**:834–41.
43 **Tassabehji M**, Strachan T, Sharland M, Colley A, Donnai D, Harris R, Thakker N. Tandem duplication within a neurofibromatosis type 1 (NF1) gene exon in a family with features of Watson syndrome and Noonan syndrome. *Am J Hum Genet* 1993;**53**:90–5.
44 **Carey JC**. Neurofibromatosis-Noonan syndrome. *Am J Med Genet* 1998;**75**:263–264.
45 **Pulst SM**, Riccardi VM, Fain P. Korenberg JR Familial spinal neurofibromatosis: clinical and DNA linkage analysis *Neurology* 1991;**41**:1923–5.
46 **Kaufmann D**, Muller R, Bartelt B, Wolf M, Kunzi-Rapp K, Hanemann CO, Fahsold R, Hein C, Vogel W, Assum G. Spinal neurofibromatosis without café-au-lait macules in two families with null mutations of the gene. *Am J Hum Genet* 2001;**69**:1395–400.
47 **Wimmer K**, Muhlbauer M, Eckart M, Callens T, Rehder H, Birkner T, Leroy JG, Fonatsch C, Messiaen L. A patient severely affected by spinal neurofibromas carries a recurrent splice site mutation in the NF1 gene. *Eur J Hum Genet* 2000;**10**:334–8.
48 **Sander A**, Schmelzle R, Murray J. Evidence for a microdeletion in 1q32—41 involving the gene responsible for van der Woude sydrome. *Hum Mol Genet* 1994;**3**:575–8.
49 **Koillinen H**, Wong FK, Rautio J, Ollikainen V, Karsten A, Larson O, Teh BT, Huggare J, Lahermo P, Larsson C, Kere J. Mapping of the second locus for the van der Woude syndrome to chromosome 1p34. *Eur J Hum Genet* 2001;**9**:747–52.
50 **Sertie AL**, Sousa AV, Steman S, Pavanello RC, Passos-Bueno MR. Linkage analysis in a large Brazilian family with van der Woude sydrome suggests the existence of a susceptibility locus for cleft palate at 17p11.2–p11.1. *Am J Hum Genet* 1999;**65**:433–40.
51 **Sawada S**, Florell S, Purandare SM, Ota M, Stephens K, Viskochil D. Identification of *NF1* mutations in both alleles of a dermal neurofibroma. *Nat Genet* 1996;**14**:110–12.
52 **Serra E**, Puig S, Otero D, Gaona A, Kruyer H, Ars E, Estivill X, Lazaro C. Confirmation of a double-hit model for the NF1 gene in benign neurofibromas. *Am J Hum Genet* 1997;**61**:512–19.
53 **Eisenbarth I**, Beyer K, Krone W, Assum G. Toward a survey of somatic mutation of the NF1 gene in benign neurofibromas of patients with neurofibromatosis type 1. *Am J Hum Genet* 2000;**66**:393–401.
54 **John AM**, Ruggieri M, Ferner R, Upadhyaya M. A search for evidence of somatic mutations in the NF1 gene. *J Med Genet* 2000;**37**:44–9.
55 **Rutkowski JL**, Wu K, Gutmann DH, Boyer PJ, Legius E. Genetic and cellular defects contributing to benign tumor formation in neurofibromatosis type 1. *Hum Mol Genet* 2000;**9**:1059–66.
56 **Legius E**, Marchuk DA, Collins FS, Glover TW. Somatic deletion of the neurofibromatosis type 1 gene in a neurofibrosarcoma supports a tumour suppressor gene hypothesis. *Nat Genet* 1993;**3**:122–6.
57 **Lothe RA**, Slettan A, Saeter G, Brogger A, Borresen AL, Nesland JM. Alterations at chromosome 17 loci in peripheral nerve sheath tumours. *J Neuropathol Exp Neurol* 1995;**54**:65–73.
58 **Rasmussen SA**, Overman J, Thomson SA, Colman SD, Abernathy CR, Trimpert RE, Moose R, Virdi G, Roux K, Bauer M, Rojiani AM, Maria BL, Muir D, Wallace MR. Chromosome 17 loss-of-heterozygosity studies in benign and malignant tumours in neurofibromatosis type 1. *Genes Chromosome Cancer* 2000;**28**:425–31.
59 **Xu W**, Mulligan LM, Ponder MA, Liu L, Smith BA, Mathew CG, Ponder BA. Loss of NF1 alleles in phaeochromocytomas from patients with type 1 neurofibromatosis. *Genes Chromosomes Cancer* 1992;**4**:337–42.
60 **Gutmann DH**, Donahoe J, Brown T, James CD, Perry A. Loss of neurofibromatosis 1 (NF1) gene expression in NF1-associated pilocytic astrocytomas. *Neuropathol Appl Neurobiol* 2000;**26**:361–7.
61 **Shannon KM**, O'Connell P, Martin GA, Paderanga D, Olson K, Dinndorf P, McCormick F. Loss of the normal NF1 allele from the bone marrow of children with type 1 neurofibromatosis and malignant myeloid disorders. *New Engl J Med* 1994;**330**:597–601.
62 **Evans DG**, Wallace AJ, Wu CL, Trueman L, Ramsden RT, Strachan T. Somatic mosaicism: a common cause of classic disease in tumor-prone syndromes? Lessons from type 2 neurofibromatosis. *Am J Hum Genet* 1998;**63**:727–36.
63 **Verhoef S**, Bakker L, Tempelaars AM, Hesseling-Janssen AL, Mazurczak T, Jozwiak S, Fois A, Bartalini G, Zonnenberg BA, van Essen AJ, Lindhout D, Halley DJ, van den Ouweland AM. High rate of mosaicism in tuberous sclerosis complex. *Am J Hum Genet* 1999;**64**:1632–7.
64 **Gottlieb B**, Beitel LK, Trifiro MA. Somatic mosaicism and variable expressivity. *Trends Genet* 2001;**17**:79–82.
65 **Ruggieri M**, Huson S. The clinical and diagnostic implications of mosaicism in the neurofibromatoses. *Neurology* 2000;**56**:1433–43.
66 **Ruggieri M**. The different forms of neurofibromatosis. *Childs Nerv Syst* 1999;**15**:295–308.
67 **Holt D**, Dreimanis M, Pfeiffer M, Firgaira F, Morley A, Turner D. Interindividual variation in mitotic recombination. *Am J Hum Genet* 1999;**65**:1423–7.
68 **Serra E**, Rosenbaum T, Nadal M, Winner U, Ars E, Estivill X, Lazaro C. Mitotic recombination effects homozygosity for NF1 germline mutations in neurofibromas. *Nat Genet* 2001;**28**:294–6.
69 **Bahuau M**, Pelet A, Vidaud D, Lamireau T, LeBail B, Munnich A, Vidaud M, Lyonnet S, Lacombe D. GDNF as a candidate modifier in a type 1 neurofibromatosis (NF1) enteric phenotype. *J Med Genet* 2001;**38**:638–43.
70 **Reilly K**, Christy E, Loisel D, Ledger J, Bronson R, Jacks T. The role of modifier genes in NF1-associated tumours in mice. Presented at NNFF International Consortium for the Molecular Bioloby of NF1 and NF2, Aspen, Colorado, USA, 1992.
71 **Riccardi V**. *Neurofibromatosis: phenotype, natural history and pathogenesis*, 2nd ed. Baltimore: John Hopkins University Press, 1992.
72 **Friedman J**, Birch P. Type 1 neurofibromatosis: a descriptive analysis of the disorder in 1,728 patients. *Am J Med Genet* 1997;**70**:138–43.
73 **Lewis R**, Riccardi V. von Recklinghausen neurofibromatosis: prevalence of iris hamartoma. *Ophthalmology* 1981;**88**:348–54.
74 **Holt J**, Kuhns M. Macrocranium and macrocephaly in neurofibromatosis. *Skeletal Radiol* 1976;**1**:25–8.
75 **Ferner R**, Hughes R, Weinman J. Intellectual impairment in neurofibromatosis 1. *J Neurol Sci* 1996;**138**:125–33.
76 **Ozonoff S**. Cognitive impairment on neurofibromatosis type 1. *Am J Med Genet* 1999;**89**:45–52.

J Neurosurg 96:223–228, 2002

Vestibular schwannoma growth in patients with neurofibromatosis Type 2: a longitudinal study

VICTOR-FELIX MAUTNER, M.D., MICHAEL E. BASER, PH.D., SARANG D. THAKKAR, M.D., URS M. FEIGEN, M.D., J. M. FRIEDMAN, M.D., PH.D., AND LAN KLUWE, PH.D.

Departments of Neurology and Radiology, Klinikum Nord Ochsenzoll, Hamburg, Germany; Los Angeles, California; Department of Medical Genetics, University of British Columbia, Vancouver, Canada; and Department of Neurosurgery, University Hospital Eppendorf, Hamburg, Germany

Object. The factors that determine the growth rates of vestibular schwannomas (VSs) in patients with neurofibromatosis Type 2 (NF2) are unknown. The authors undertook this study to determine if clinical factors or type of constitutional *NF2* mutation were associated with VS growth rates in cases of NF2.

Methods. The authors reviewed serial gadolinium-enhanced magnetic resonance (MR) images of the head and full spine of 37 patients with sporadic NF2 who had been observed over periods ranging from 0.2 to 8 years (median 3.9 years) at a specialized referral clinic for NF2. A box model was used to calculate VS volumes so that tumor growth rates could be estimated. Temperature-gradient gel electrophoresis was used to screen for constitutional *NF2* mutations. The VS growth rates tended to decrease with increasing patient age at onset of signs or symptoms ($r^2 = 0.23$, $p = 0.003$) and at the time the baseline gadolinium-enhanced MR image was obtained ($r^2 = 0.38$, $p < 0.001$). The authors did not find significant associations between VS growth rates and the number of non-VS cerebral or spinal tumors or different types of constitutional *NF2* mutations.

Conclusions. There is considerable variability in growth rates of VSs in patients with NF2, but they tend to be higher in patients who are younger at onset of signs or symptoms.

KEY WORDS • **natural history** • **neurogenetics** • **neurofibromatosis Type 2** • **vestibular schwannoma**

NEUROFIBROMATOSIS Type 2 is an autosomal-dominant disorder that occurs with a symptomatic prevalence of 1 in 210,000 persons.[13] It is characterized by the development of benign nervous system tumors (VSs, other cranial and spinal tumors, and peripheral nerve tumors), as well as ocular and cutaneous abnormalities.[12,24,27] Tumors associated with NF2 are caused by inactivation of both alleles of the *NF2* tumor-suppressor gene by mutation or allele loss (Table 1).[29,34] The NF2 protein (termed "merlin" or "schwannomin") is highly homologous to proteins in the moesin-ezrin-radixin family that link glycophorin membrane proteins to the actin cytoskeleton.[29,34] Merlin-binding proteins have been identified, but the mechanism of the tumor-suppressor function of merlin is unknown.[7,16]

Unilateral sporadic VSs are also caused by inactivation of the *NF2* gene, but result from somatic mutations or loss of alleles. The prevalence of sporadic VSs is approximately 20 times greater than that of NF2 and, although there is a finite possibility that a person could experience independent bilateral sporadic VSs, patients in whom unilateral VSs develop at older ages and who do not meet the clinical diagnostic criteria for NF2[17] are highly unlikely to have NF2.[35] The growth rates of unilateral sporadic VSs have been studied,[6,10,26,33] but these findings may not be generalizable to NF2-associated VSs. The NF2-associated VSs are more lobular and less vascular than unilateral sporadic VSs[31] and have higher proliferation indices than the sporadic forms of these tumors.[2] Differences in the proliferation potential of heritable and sporadic VSs may be due to differences in mutational spectra or to allelic differences in tissues surrounding the tumors, which in NF2 patients have only one functional *NF2* allele.[2]

The severity of NF2 is assessed by examining a composite of clinical characteristics, primarily the number of non-VS cerebral tumors and spinal tumors, and the patient's age at onset of signs or symptoms.[27] Generally, nonsense and frameshift constitutional *NF2* mutations are associated with severe disease, splice-site mutations with variable disease severity, and missense mutations with mild disease.[14,18,19,28,30] More rapid tumor growth is an obvious possible cause for earlier age at onset and more severe disease, but in one small longitudinal study the researchers found higher tumor growth rates in older patients with NF2,[1] a conclusion that contradicts the impression of many clinicians. All studies of genotype–phenotype correlations in NF2 have been cross sectional. In this longitudinal study, we evaluated VS growth rates in patients with NF2 and examined possible associations with clinical and molecular factors.

Abbreviations used in this paper: $\log_{10}$ = logarithm to the base 10; MR = magnetic resonance; NF2 = neurofibromatosis Type 2; SE_b = standard error of the regression coefficient b; TDT = tumor doubling time; VS = vestibular schwannoma.

TABLE 1

*List of definitions**

Term	Definition
codon	nucleotide triplet that specifies an amino acid or a signal for terminating the synthesis of a polypeptide; a stop codon terminates the synthesis of a polypeptide
exon	segment of gene that is decoded to provide a messenger RNA or mature RNA product
frameshift mutation	mutation that alters the normal translational reading frame of a DNA sequence
in-frame deletion	deletion of a multiple of three nucleotides that puts the reading frame back in phase
intron	noncoding DNA that separates neighboring exons in a gene
missense mutation	nucleotide substitution that results in an amino acid change
nonsense mutation	mutation that occurs within a codon and changes it into a stop codon
splice-site mutation	mutation in the splice junction (exon–intron boundary) that destroys signals for exon–intron splicing†
translational reading frame	mechanism that moves a ribosome three nucleotides at a time during translation

* Based on definitions provided by Strachan and Read.

† A splice junction may be a splice acceptor site (junction between the end of an intron and the start of the next exon) or a splice donor site (junction between the end of an exon and the start of the downstream intron).

TABLE 2

Neuroradiological abnormalities in 37 patients with new NF2 *mutations*

Abnormality	No. of Patients (%)
cranial nerve tumors*	
olfactory	1 (3)
optic (schwannoma or meningioma)	5 (14)
oculomotor	4 (11)
trochlear	1 (3)
trigeminal	
unilat	16 (43)
bilat	6 (16)
vestibulocochlear	
unilat	2 (5)
bilat	35 (94)
hypoglossal	3 (8)
any nonvestibulocochlear cranial nerve tumor	26 (70)
intracranial meningioma	23 (62)
spinal tumor (all locations)†	35 (94)
cervical	30 (81)
thoracic	28 (76)
lumbar	31 (84)

* There were no tumors of the sixth, seventh, ninth, 10th, or 11th cranial nerves.

† Locations of spinal tumors are not mutually exclusive. A patient could be counted as harboring cervical, thoracic, and lumbar spinal tumors.

Clinical Material and Methods

Patient Population

Eighty-eight patients with NF2 were followed up at the Neurology Department, Klinikum Nord Ochsenzoll, Hamburg, Germany, a specialized referral clinic for NF2, during the period from 1988 through 1998. Eleven cases of inherited NF2 were excluded because the known family history of NF2 may have affected the patient's age at which the diagnosis of NF2 was made or the age at apparent clinical onset of NF2. Three patients who were known to have the somatic mosaic form of NF2 were also excluded. Of the remaining 74 patients with sporadic NF2, longitudinal gadolinium-enhanced MR imaging was available in 37 patients and unavailable in the other 37. These two groups had similar distributions of measured clinical characteristics and types of constitutional *NF2* mutations. All patients or their parents provided informed consent, and all patients met the clinical diagnostic criteria for definite NF2[17] or had identified constitutional *NF2* mutations.

Mutation Analysis

Deoxyribonucleic acid was extracted from peripheral lymphocytes or directly from blood by using a blood polymerase chain reaction kit according to the manufacturer's instructions (QIAmp Blood Kit; Qiagen, Hilden, Germany). Exons 1 through 15 of the NF2 coding region were scanned with temperature-gradient gel electrophoresis.[19] No mutations have been reported to date in exons 16 or 17 (M Baser, unpublished data).

Brain and Spine Imaging and Image Analysis

We evaluated VS growth rates by retrospectively analyzing full head and spine gadolinium-enhanced MR images that were obtained initially (the baseline measurement) and subsequently, usually annually. A 1.5-tesla MR magnet (Magnetom 63 SP; Siemens, Erlangen, Germany) was used. The same MR magnet and software were used throughout the study period (1988–1998). Sagittal and coronal 4-mm slices were examined. Both T_1- and T_2-weighted sagittal images were obtained, and T_1-weighted coronal and sagittal images were obtained before and after administration of gadolinium. Cervical spine images were obtained using a Helmholtz neck coil, and thoracic and lumbar spine images by using a circularly polarized surface coil. Tumors less than 4 mm in diameter were excluded to avoid nonspecific findings. All gadolinium-enhanced MR images were assessed independently by two radiologists, and the mean of each pair of measurements in the two sets of readings was used. Volumes of VSs were calculated on the basis of maximum extensions in anteroposterior, mediolateral, and superoinferior planes from two dimensions on film. We did not analyze computerized tomography scans or MR images obtained without gadolinium.

Statistical Analysis

Preoperative VS volume measurements were available for 64 VSs in 37 patients; two patients had unilateral VSs and eight other patients had undergone VS excision before two sequential gadolinium-enhanced MR images were obtained. Growth rates were expressed as TDT in years to account for possible differences in growth rates related to the baseline VS volume. Average growth rate (presented in cm^3/year) was calculated using linear regression over the entire period of observation. The TDT was calculated as follows: (2 × baseline VS volume)/average VS growth rate per year.

For eight VSs, the average tumor growth rate presented in cubic centimeters per year was 0 and the TDT could not

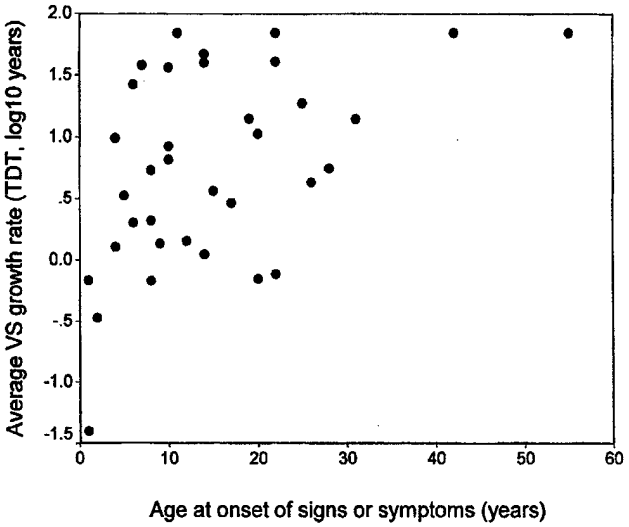

FIG. 1. Scattergram comparison of VS growth rate and patient age at onset of signs or symptoms ($r^2 = 0.23$, $p = 0.003$). Tumor doubling times of 70 years are arbitrarily assigned values.

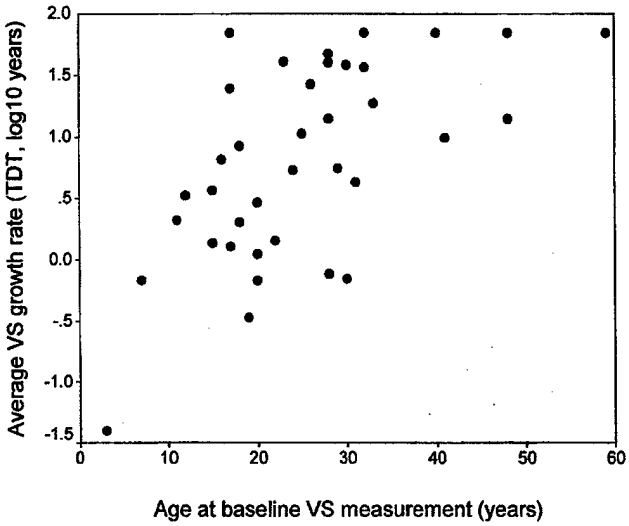

FIG. 2. Scattergram comparison of VS growth rate and patient age at time of baseline VS measurement ($r^2 = 0.38$, $p < 0.001$). Tumor doubling times of 70 years are arbitrarily assigned values.

be calculated. We assigned an arbitrary TDT of 70 years to these tumors and to three VSs with negative growth rates. The highest TDT for a single VS in the study was 53 years, and only three VSs demonstrated TDTs greater than 30 years; the results were very similar when an arbitrary TDT of 50 years instead of 70 years was assigned. In patients with bilateral VSs, growth rates and volumes from both sides were averaged in some analyses because there were no significant differences between the relationship of left- and right-sided growth rates and volumes to covariates. A $\log_{10}$ transformation was used for the TDTs because the doubling times ranged from 0.03 to 70 years and were non-normally distributed.

The covariates studied were sex, age at onset of signs or symptoms of NF2, age when the baseline gadolinium-enhanced MR image was obtained, number of intracranial meningiomas, number of spinal tumors, and type of constitutional *NF2* mutation. All covariates were considered fixed. The number of NF2 tumors increases with patient age, but in no patients did new non-VS tumors develop that grew to 4 mm or larger in diameter (the inclusion criterion) during the follow-up period. The two-tailed Fisher exact test, Pearson correlation coefficient, and linear regression were used for tests of association. The Mann–Whitney U-test was used to test between-group differences in TDTs. Probability values lower than 0.05 were considered to be statistically significant.

Results

Seventeen (46%) of the 37 patients were female. The median age at onset of signs or symptoms of NF2 was 12 years. The age at onset was highly correlated with the age at which the gadolinium-enhanced MR image was obtained ($r^2 = 0.59$, $p < 0.001$), which averaged 13 years later. The median length of observation with enhanced imaging was 3.9 years (range 0.2–8 years), with a median of five serial imaging sessions. Spinal tumors were found in 35 patients (94%); in five patients (14%) the tumors were located in the thoracic or lumbar spine, but not in the cervical spine (Table 2). Intracranial meningiomas were present in 62% of patients. Trigeminal nerve tumors were the most common non-VS cranial nerve tumor (59% of patients).

As expected, the shapes of the VS growth curves were highly variable and included linear, sigmoid, logarithmic, and irregular curves. Using a linear model to calculate TDTs, VS growth rates decreased (that is, $\log_{10}$ TDTs increased) with increasing patient age at onset of signs or symptoms and at the baseline imaging session (Figs. 1 and 2). The linear regression equations relating tumor growth rate to patient age were the following: mean TDT in $\log_{10}$ years = 0.26 + 0.03 (patient age at onset of signs or symptoms in years; $SE_b = 0.01$ years, $r^2 = 0.23$, $p = 0.003$); and mean TDT in $\log_{10}$ years = −0.24 + 0.04 (age at baseline imaging in years; $SE_b = 0.01$ years, $r^2 = 0.38$, p , 0.001).

Twenty-seven patients with 48 VSs underwent four or more volume measurements, and sigmoid curves could be fit to 22 VSs (46%) in 17 of these patients. A sigmoid growth curve was not more likely to occur with longer periods of observation.

Individual VS growth rates were highly variable, ranging from no growth to a TDT of 0.03 years. The patient in Case 62, 3 years old at the time the baseline gadolinium-enhanced MR images were obtained, was the youngest patient in the study and his tumor displayed unusually high growth rates. His left- and right-sided VSs grew at TDTs of 0.03 and 0.05 years, respectively, causing death 3 months after the baseline measurements were obtained. These VS growth rates were 10 times greater than any others in the study, but the associations of tumor growth rates with patient age were very similar when this patient was excluded from the analysis.

Left- and right-sided VS growth rates, but not baseline VS volumes, were highly correlated (Figs. 3 and 4). The linear regression equations that describe the associations between right-sided VS and left-sided VS growth rates and volumes were the following: right-sided VS TDT in $\log_{10}$ years = 0.24 + 0.66 (left-sided VS TDT in $\log_{10}$ years;

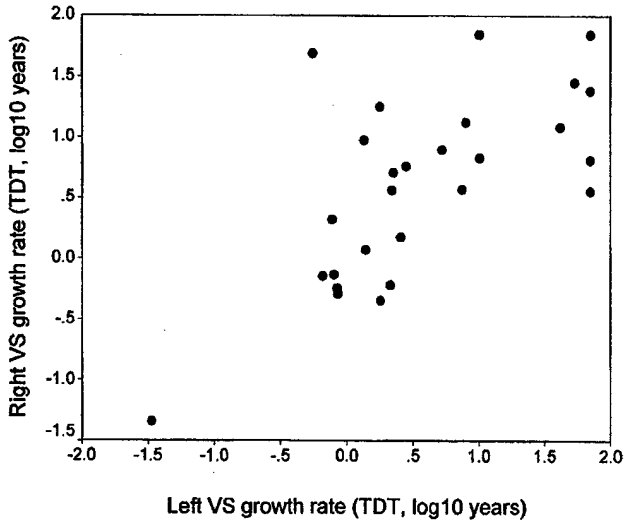

FIG. 3. Scattergram comparison of growth rates of left- and right-sided VSs ($r^2 = 0.48$, $p < 0.001$). Tumor doubling times of 70 years are arbitrarily assigned values.

$SE_b = 0.14$, $r^2 = 0.48$, $p < 0.001$); and right-sided VS baseline volume in cubic centimeters = 5.3 + 0.16 (left-sided VS baseline volume in cubic centimeters; $SE_b = 0.1$, $r^2 = 0.09$, $p = 0.11$).

The VS growth rates and baseline VS volumes did not vary significantly with the number of intracranial meningiomas or spinal tumors.

Constitutional *NF2* mutations were identified in 23 patients (62%), and included eight frameshift mutations, seven nonsense mutations, four splice donor site mutations, three splice acceptor site mutations, and one in-frame deletion (Table 3). The median VS growth rate of patients with splice-site mutations was 2.6-fold lower than that of patients with nonsense or frameshift mutations, but the variability of growth rates was very high and this difference was not statistically significant ($p = 1$; Table 4).

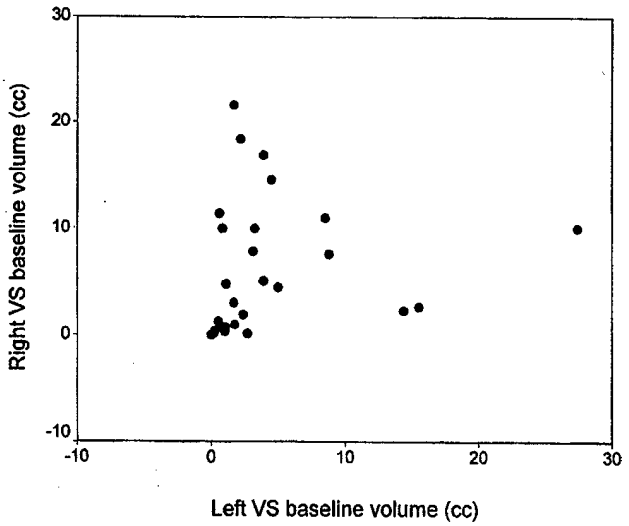

FIG. 4. Scattergram of left- and right-sided baseline VS volumes ($r^2 = 0.09$, $p = 0.11$). cc = cubic centimeter.

TABLE 3

Identified constitutional NF2 *mutations in 23 patients with NF2**

Case No.	Altered Exon	Altered Codon	Nucleotide Change	Consequence
51	1	12	35–36 del GC	frameshift
68	2	56	166 del C	frameshift
35	2	57	169 C → T	nonsense
5	3	111	331 C → T	nonsense
18	3	118	352–354 del TTC	in-frame deletion
27	5		agTA → atTA	splice acceptor site
44	5		agTA → aaTA	splice acceptor site
55	6	196	586 C → T	nonsense
40	7		+5 g → c	splice donor site
57	7		agGG → ggGG	splice acceptor site
28	8		AGgt → GGgt	splice donor site
24	8	239	717 del G	frameshift
3	8	262	784 C → T	nonsense
4	8	262	784 C → T	nonsense
17	10	303	908–909 del AC	frameshift
15	11	349	1047–1053 del CTGAACGC	frameshift
45	11	360	1079 G → T	nonsense
46	12	410	1229 del A	frameshift
14	12	428	1282 C → T	nonsense
12	14		AAgt → AAct	splice donor site
52	14	490	1469 del C	frameshift
8	15		AGgt → ATgt	splice donor site
42	15	527	1580 del A	frameshift

* Some mutations have been previously reported in studies by Kluwe and colleagues (1996 and 1998). Abbreviations: del = delete; + = gain of.

Discussion

The main findings in this study included the clear tendency for VS growth rates to be higher among younger patients with NF2 and the high correlation of left- and right-sided VS growth rates in patients with bilateral tumors. The presentation of NF2 in children is markedly different from that in adults because the presenting sign or symptom in children is usually unrelated to the VSs.[11,23,25] Individuals who are diagnosed with NF2 at younger ages have an increased risk of mortality.[3] Our finding that VS growth rates are higher in younger patients contradicts the finding of Abaza and colleagues,[1] but is consistent with those of Baser, et al.,[4] perhaps because our study and that conducted by Baser, et al., were based on VSs that had never been treated surgically, whereas Abaza and colleagues included measurements on postoperative VSs. This could lead to a bias toward tumors in older patients and/or tumors displaying more rapid growth.[4]

The high correlation of VS growth rates, but not volumes, in patients with bilateral VSs indicates that the left- and right-sided VSs have grown at similar rates for different lengths of time. This interpretation is consistent with stochastic inactivation of the second *NF2* allele in the two Schwann cells that give rise to the left- and right-sided VSs. Further support for the involvement of stochastic processes comes from a study of monozygotic twins with NF2, who have the same general disease severity but differ with respect to specific disease features and timing of their occurrence.[5] The high variability in VS growth rates from year to year in the same individual also is consistent with the in-

fluence of stochastic factors or complex interactions on VS growth rates.

Although we did not observe an association between type of constitutional *NF2* mutation and VS growth rates, this study population is too small to draw conclusions about whether such correlations exist. Cross-sectional genotype–phenotype correlation studies have led to consistent findings of associations between clinical indices of NF2 disease severity and type of constitutional *NF2* mutation.[14,18,19,28,30] Genes other than *NF2* may affect NF2 disease severity,[9] schwannoma tumorigenesis,[8,22] and meningioma tumorigenesis.[21] Such modifying genes might also influence VS growth rates.

A possible source of bias in this study may arise from the fact that prevalent cases were selected and the patients were often given the diagnosis before referral to our clinic. Patients with faster-growing tumors would come to surgery sooner and may have been excluded from this study. Although we are unable to assess this bias, there is no evidence that the patients with NF2 who were included in this study differed from those who were referred but lacked longitudinal measurements, because the distributions of clinical characteristics and types of constitutional *NF2* mutations were similar in both groups.

Another possible source of bias may arise because box models were used to estimate VS volumes, rather than precise computer volumetrics; however, volume measurements based on three dimensions provide a relatively good approximation.[15,20] Spherical models have been used to estimate VS volumes when measurements are available in only two dimensions,[10] but VSs can vary widely in shape; many of the VSs in this study did not have similar measurements in all three dimensions, thus indicating nonspherical shapes.

Logarithmic models have been used to calculate TDTs for VSs and other tumor types, particularly when only two longitudinal measurements have been available,[10] but we could fit only a sigmoid growth curve to approximately half of the VSs for which we had four or more volume measurements. It has been suggested that linear models of VS growth are less appropriate as the length of observation increases,[20] but we did not find such an association in this study.

Conclusions

Growth rates of VSs associated with NF2 tend to be higher in younger patients than in older ones. Larger and longer longitudinal studies are needed to elucidate more fully the clinical and genetic predictors of VS growth in NF2.

Authorship

Drs. Baser and Mautner contributed equally to this study.

Acknowledgments

We thank the patients with NF2 and their families for participating in the study, and Drs. Harry Joe and Jeff Gornbein for statistical advice.

TABLE 4

Indices of disease severity by constitutional NF2 *mutation type in 37 patients with sporadic NF2*

Type of Constitutional *NF2* Mutation	No. of Patients	Median TDT in Years (range)*	Patient Age at Onset of Signs/Symptoms (yrs)†	Percentage of Patients W/ Other Tumors: Intracranial Meningiomas	Percentage of Patients W/ Other Tumors: Spinal Tumors
nonsense or frameshift	15	5.4 (0.7–70)	13.3 ± 1.5	67	93
splice-site	7	14.0 (0.3–40.9)	14.9 ± 4.7	57	100
in-frame deletion	1	38.3	7.0	100	100
unidentified	14	6.6 (0.04–70)	17.9 ± 4.1	57	93

* Difference in median TDT between patients with nonsense or frameshift mutations and those with splice-site mutations ($p = 1$, Mann–Whitney U-test).

† Values are shown as means ± standard error of mean where applicable.

References

1. Abaza MM, Makariou E, Armstrong M, et al: Growth rate characteristics of acoustic neuromas associated with neurofibromatosis type 2. **Laryngoscope 106:**694–699, 1996
2. Antinheimo J, Haapasalo H, Seppäla M, et al: Proliferative potential of sporadic and neurofibromatosis 2-associated schwannomas as studied by MIB-1 (Ki-67) and PCNA labeling. **J Neuropathol Exp Neurol 54:**776–782, 1995
3. Baser ME, Friedman JM, Evans DGR: Predictors of survival in neurofibromatosis 2. **Am J Hum Genet 65 (Suppl):**A314, 1999 (Abstract)
4. Baser ME, Makariou EV, Parry DM: Predictors of vestibular schwannoma growth in patients with neurofibromatosis Type 2. **J Neurosurg 96:**217–222, 2002
5. Baser ME, Ragge NK, Riccardi VM, et al: Phenotypic variability in monozygotic twins with neurofibromatosis 2. **Am J Med Genet 64:**563–567, 1996
6. Bederson JB, von Ammon K, Wichmann WW, et al: Conservative treatment of patients with acoustic tumors. **Neurosurgery 28:**646–651, 1991
7. Bretscher A, Chambers D, Nguyen R, et al: ERM-Merlin and EBP50 protein families in plasma membrane organization and function. **Annu Rev Cell Dev Biol 16:**113–143, 2000
8. Bruder CE, Ichimura K, Tingby O, et al: A group of schwannomas with interstitial deletions on 22q located outside the *NF2* locus shows no detectable mutations in the *NF2* gene. **Hum Genet 104:**418–424, 1999
9. Bruder CEG, Ichimura K, Blennow E, et al: Severe phenotype of the neurofibromatosis type 2 in a patient with a 7.4 MB constitutional deletion on chromosome 22: possible localization of a neurofibromatosis type 2 modifier gene? **Genes Chromosomes Cancer 25:**184–190, 1999
10. Charabi S, Thomsen J, Mantoni M, et al: Acoustic neuroma (vestibular schwannoma): growth and surgical and nonsurgical consequences of the wait-and-see policy. **Otolaryngol Head Neck Surg 113:**5–14, 1995
11. Evans DGR, Birch JM, Ramsden RT: Paediatric presentation of type 2 neurofibromatosis. **Arch Dis Child 81:**496–499, 1999
12. Evans DGR, Huson SM, Donnai D, et al: A clinical study of type 2 neurofibromatosis. **Q J Med 84:**603–618, 1992
13. Evans DGR, Huson SM, Donnai D, et al: A genetic study of type 2 neurofibromatosis in the United Kingdom. I. Prevalence, mutation rate, fitness, and confirmation of maternal transmission effect on severity. **J Med Genet 29:**841–846, 1992

14. Evans DGR, Trueman L, Wallace A, et al: Genotype/phenotype correlations in type 2 neurofibromatosis (NF2): evidence for more severe disease associated with truncating mutations. **J Med Genet 35:**450–455, 1998
15. Fiirgaard B, Pedersen CB, Lundorf E: The size of acoustic neuromas: CT and MRI. **Neuroradiology 39:**599–601, 1997
16. Gutmann DH: The neurofibromatoses: when less is more. **Hum Mol Genet 10:**747–755, 2001
17. Gutmann DH, Aylsworth A, Carey JC, et al: The diagnostic evaluation and multidisciplinary management of neurofibromatosis 1 and neurofibromatosis 2. **JAMA 278:**51–57, 1997
18. Kluwe L, Beyer S, Baser ME, et al: Identification of NF2 germline mutations and comparison with neurofibromatosis 2 phenotypes. **Hum Genet 98:**534–538, 1996
19. Kluwe L, MacCollin M, Tatagiba M, et al: Phenotypic variability associated with 14 splice-site mutations in the *NF2* gene. **Am J Med Genet 77:**228–233, 1998
20. Laasonen EM, Troupp H: Volume growth rate of acoustic neurinomas. **Neuroradiology 28:**203–207, 1986
21. Leone PE, Bello MJ, de Campos JM, et al: NF2 gene mutations and allelic status of 1p, 14q, and 22q in sporadic meningiomas. **Oncogene 18:**2231–2239, 1999
22. Leone PE, Bello MJ, Mendiola M, et al: Allelic status of 1p, 14q, and 22q and NF2 gene mutations in sporadic schwannomas. **Int J Mol Med 1:**889–892, 1998
23. MacCollin M, Mautner VF: The diagnosis and management of neurofibromatosis 2 in childhood. **Semin Pediatr Neurol 5:** 243–252, 1998
24. Mautner VF, Lindenau M, Baser ME, et al: The neuroimaging and clinical spectrum of neurofibromatosis 2. **Neurosurgery 38:**880–886, 1996
25. Mautner VF, Tatagiba M, Guthoff R, et al: Neurofibromatosis 2 in the pediatric age group. **Neurosurgery 33:**92–96, 1993
26. Nedzelski JM, Schessel DA, Pfeiderer A, et al: Conservative management of acoustic neuromas. **Otolaryngol Clin North Am 25:**691–705, 1992
27. Parry DM, Eldridge R, Kaiser-Kupfer MI, et al: Neurofibromatosis 2 (NF2): clinical characteristics of 63 affected individuals and clinical evidence for heterogeneity. **Am J Med Genet 52:** 450–461, 1994
28. Parry DM, MacCollin MM, Kaiser-Kupfer MI, et al: Germ-line mutations in the neurofibromatosis 2 gene: correlations with disease severity and retinal abnormalities. **Am J Hum Genet 59:** 529–539, 1996
29. Rouleau GA, Merel P, Lutchman M, et al: Alteration in a new gene encoding a putative membrane-organizing protein causes neurofibromatosis type 2. **Nature 363:**515–521, 1993
30. Ruttledge MH, Andermann AA, Phelan CM, et al: Type of mutation in the neurofibromatosis type 2 gene *(NF2)* frequently determines severity of disease. **Am J Hum Genet 59:**331–342, 1996
31. Sobel RA: Vestibular (acoustic) schwannomas: histologic features in neurofibromatosis 2 and in unilateral cases. **J Neuropathol Exp Neurol 52:**106–113, 1993
32. Strachan T, Read AP: **Human Molecular Genetics.** Oxford: BIOS Scientific, 1996, pp 589–596
33. Strasnick B, Glasscock ME III, Haynes D, et al: The natural history of untreated acoustic neuromas. **Laryngoscope 104:** 1115–1119, 1994
34. Trofatter JA, MacCollin MM, Rutter JL, et al: A novel moesin-, ezrin-, radixin-like gene is a candidate for the neurofibromatosis 2 tumor suppressor. **Cell 72:**791–800, 1993
35. Wu CL, Thakker N, Neary W, et al: Differential diagnosis of type 2 neurofibromatosis: molecular discrimination of NF2 and sporadic vestibular schwannomas. **J Med Genet 35:**973–977, 1998

Manuscript received November 27, 2000.
Accepted in final form September 27, 2001.
This study was supported in part by Wilhelm-Sander-Stiftung No. 93.052.1 and No. 93.052.2 and by Hamburger Stiftung zur Förderung der Krebsbekämpfung No. 116, 127, 93.052.3.
This study was presented in part to the American College of Medical Genetics, February 27–March 1, 1998, Los Angeles, California; at the 47th Annual Meeting of the American Society of Human Genetics, October 28–November 1, 1997, Baltimore, Maryland (**Am J Hum Genet 63 [Suppl 4]:**A63, 1998); and to the National Neurofibromatosis Foundation International Consortium for the Molecular Biology of NF1 and NF2, June 7–10, 1998 and June 4–7, 2000, Aspen, Colorado.
Address reprint requests to: Michael E. Baser, Ph.D., 2257 Fox Hills Drive, Los Angeles, California 90064. email: baser@earthlink.net.

American Journal of Medical Genetics 125A:157–161 (2004)

Analysis of Neurofibromatosis 1 (NF1) Lesions by Body Segment

Chana Palmer,[1,2] Jacek Szudek,[1,3] Harry Joe,[4] Vincent M. Riccardi,[5] and J.M. Friedman[1]*

[1]*Department of Medical Genetics, The University of British Columbia, Vancouver, Canada*
[2]*Department of Genetics, Stanford University, Stanford, California*
[3]*Dalhousie Medical School, Halifax, Nova Scotia, Canada*
[4]*Department of Statistics, The University of British Columbia, Vancouver, Canada*
[5]*American Medical Consumers, La Crescenta, California*

Café-au-lait spots and neurofibromas are defining features of neurofibromatosis 1 (NF1), but they vary greatly in number, size, and clinical importance from patient to patient. The cause of this variability is unknown. We tested the hypotheses that development of these lesions is influenced by local or familial factors. The presence or absence of café-au-lait spots, cutaneous neurofibromas, and diffuse plexiform neurofibromas was recorded for each of 10 divisions of the body surface in 547 NF1 patients, including 117 affected individuals in 52 families. We used stratified Mantel-Haenszel tests to look for local associations between the presence of diffuse plexiform neurofibromas, cutaneous neurofibromas, and café-au-lait spots in individual body segments of NF1 patients. We used a random effects model to obtain intrafamilial correlation coefficients for the age-adjusted number of body divisions affected with each of the three lesions. No significant association was observed between the occurrence of cutaneous and diffuse plexiform neurofibromas, between café-au-lait spots and cutaneous neurofibromas, or between café-au-lait spots and plexiform neurofibromas in the same body segment. The correlation among relatives in the number of body segments affected with café-au-lait spots was 0.45 (95% confidence interval [CI] = 0.18–0.71), with cutaneous neurofibromas, 0.37 (95% CI = 0.15–0.55), and with plexiform neurofibromas, 0.35 (95% CI = 0.15–0.57). We conclude that the development of café-au-lait spots, cutaneous neurofibromas, and plexiform neurofibromas are spatially independent in NF1 patients but that the development of all three lesions is influenced by familial factors.

KEY WORDS: neurofibromatosis 1; familial correlation; café-au-lait spots; neurofibromas

INTRODUCTION

Neurofibromatosis 1 (NF1) is an autosomal dominant condition characterized by extremely variable expressivity. Café-au-lait spots and neurofibromas are the defining features. Neurofibromas are complex benign tumors arising in the fascicles of peripheral nerves [Korf, 1999]. Histologically, a local increase in endoneurial matrix of the fascicle is accompanied by a thickened perineurium, increased size and number of Schwann cells [Harkin and Reed, 1969; Woodruff, 1999], and increased numbers of mast cells and fibroblasts [Giorno et al., 1989]. Cutaneous neurofibromas are confined to a single fascicle within a nerve, while diffuse plexiform neurofibromas involve multiple fascicles [Burger and Scheithauer, 1994].

Cutaneous neurofibromas begin to appear in mid-childhood and eventually develop in almost all NF1 patients [Friedman and Riccardi, 1999; DeBella et al., 2000]. Cutaneous neurofibromas tend to increase in number and size with age. Some adults with NF1 have hundreds or thousands of these lesions; other NF1 patients develop only a few cutaneous neurofibromas throughout life.

Diffuse plexiform neurofibromas are almost always, if not always, congenital [Friedman and Riccardi, 1999]. Many are apparent on surface examination, although they often extend into deeper tissues. Some diffuse

Grant sponsor: United States Army Medical Research and Materiel Command; Grant number: NF960003.

*Correspondence to: J.M. Friedman, M.D., Ph.D., Department of Medical Genetics; The University of British Columbia; 6174 University Boulevard; Vancouver, BC V6T 1Z3; Canada.
E-mail: frid@interchange.ubc.ca

Received 17 January 2002; Accepted 11 April 2003
DOI 10.1002/ajmg.a.20354

plexiform neurofibromas involve only deeper tissues and are not apparent on physical examination. Plexiform neurofibromas tend to be larger than cutaneous neurofibromas, sometimes involving an entire limb or other part of the body. Plexiform neurofibromas may give rise to malignant peripheral nerve sheath tumors, but discrete cutaneous neurofibromas rarely, if ever, do.

Café-au-lait spots are pigmented macules. Histologically, they contain melanocytes with abnormally large pigment particles [Fitzpatrick, 1981]. Café-au-lait spots may be present at birth, and by 1 year of age almost all children with NF1 have six or more of these lesions [Friedman and Riccardi, 1999; DeBella et al., 2000]. The number and location of café-au-lait spots and neurofibromas are highly variable, even among NF1 patients of similar age. The cause of this variability is unknown. Here we test the hypotheses that the development of these lesions is influenced by local or familial factors.

SUBJECTS AND METHODS

Subjects

Five hundred and forty-seven NF1 patients, including 117 affected individuals in 52 families, who had information recorded on spatial distribution of skin lesions were available in the NF Institute Database [Riccardi, 1992]. All of these patients were evaluated by Dr. Vincent Riccardi, and all meet the NIH diagnostic criteria for NF1 [National Institutes of Health Consensus Development Conference, 1988; Gutmann et al., 1997]. For each patient, the presence of one or more café-au-lait spots, one or more cutaneous neurofibromas, and one or more diffuse plexiform neurofibromas was recorded for each of the ten divisions of the body surface shown in Figure 1.

Café-au-lait spots were defined as light brown macules with a greatest diameter of at least 5 mm. In addition to being larger than freckles, café-au-lait spots usually do not occur in clusters, whereas freckles almost always do in people with NF1. Discrete dermal neurofibromas were classified as either cutaneous or subcutaneous. Cutaneous neurofibromas lie in the skin and move with it; the skin can be moved over the top of subcutaneous neurofibromas, which lie deeper. Subcutaneous neurofibromas were not analysed in this study because they were too infrequent for statistical evaluation.

Analysis of Local Effect

We used two-layered Mantel-Haenszel tests [SPSS, 1998] to look for local associations between the presence of diffuse plexiform neurofibromas and cutaneous neurofibromas in individual body segments of each NF1 patient. We stratified simultaneously by the body segment being considered and by the number of other body segments with one or more cutaneous neurofibromas (a categorical variable with range 0–9). This stratification was used to adjust for the fact that an NF1 patient who has a larger total number of body segments with one or more neurofibromas is more likely to have at least one neurofibroma in any particular segment than an NF1 patient who has fewer total body segments affected. This approach, which takes all factors that affect the likelihood of developing neurofibromas into account, was used instead of stratifying by age alone because other clinical factors also affect the likelihood that an NF1 patient will have neurofibromas [Szudek et al., 2000a; Szudek et al., 2003].

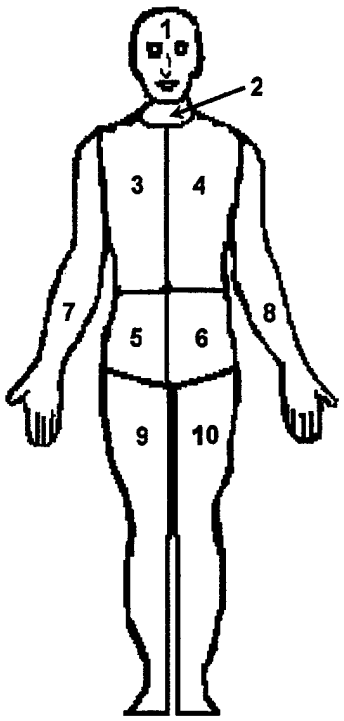

Fig. 1. Body segment scheme used by Neurofibromatosis Institute Database.

Confidence intervals for the summary odds ratio (OR) were obtained using a jackknife based on 20 different subgroups—a number that is sufficiently large to produce a stable estimate [Miller, 1974]. Homogeneity was assessed using the Breslow-Day test [SPSS, 1998]. Local associations between café-au-lait spots and cutaneous neurofibromas and between café-au-lait spots and plexiform neurofibromas were analyzed in the same manner.

Skin Surface Area

The body divisions used in this study cover varying amounts of skin surface area, so we checked for an association between surface area and the presence of one or more cutaneous neurofibromas in a segment. Using logistic regression, we set the segment area as the independent variable and the presence or absence of cutaneous neurofibromas as the dependent variable. We tested in a similar manner for associations between surface area and the presence of diffuse plexiform neurofibromas or café-au-lait spots in a segment. Since the median age of our patients was 13 years, we

approximated the surface area of the body segments by using standard percentages for 10–14 year-old individuals [McManus and Pruitt, 1996]. The proportions of total surface area assigned to each body segment were: head = 11%, neck = 2%, right upper torso = 12%, left upper torso = 12%, right lower torso = 4%, left lower torso = 4%, right arm = 9.5%, left arm = 9.5%, right leg = 18%, and left leg = 18%.

Total Number of Neurofibromas

In addition to data on whether each body segment was affected by one or more cutaneous neurofibromas, complete counts of cutaneous neurofibromas were available for 44 of the patients. The total number of neurofibromas in these patients ranged from none to several hundred and appeared to increase logarithmically with the number of affected segments. We used linear regression [SPSS, 1998] to test the relationship between log-transformed counts of the total number of cutaneous neurofibromas in an individual and the number of body segments that included one or more cutaneous neurofibromas. Counts of the total number of café-au-lait spots were not made, and few subjects had more than one plexiform neurofibroma, so these variables were not analyzed in this manner.

Familial Analysis

For the familial analysis, we stratified subjects into 5-year age intervals, calculated the deciles for the total number of segments affected with cutaneous neurofibromas in each stratum, and ranked each subject by decile for the stratum in which he or she lay. We then used random effects models to obtain maximum likelihood estimates and confidence intervals for intrafamilial correlation coefficients for rank [Spjotvoll, 1967; Donner et al., 1989]. Café-au-lait spots and plexiform neurofibromas were analyzed in the same manner.

RESULTS

We studied the distribution of café-au-lait spots, cutaneous neurofibromas, and diffuse plexiform neurofibromas in 10 segments of the body surface (Fig. 1) in each of 547 patients with NF1. Two hundred eighty-one (51.4%) of the subjects were female, and 266 (48.6%) were male. Four hundred twenty-six (77.9%) were white, 67 (12.2%) were Hispanic, 44 (8.0%) were black and 10 (1.8%) were of other or mixed origin. The mean age was 17.5 years, and the median age was 13 years. The youngest patient included was a newborn infant, and the oldest was 64.3 years of age.

Lesion Frequency by Body Segment

Table I shows the frequency of these lesions in each of the 10 body segments. Three hundred thirty-seven patients had one or more cutaneous neurofibromas, and 216 patients had at least one plexiform neurofibroma. Cutaneous and plexiform neurofibromas occurred with similar frequencies in all ten body segments. Café-au-lait spots were observed in almost all patients and had similar frequencies in all segments except the head, where these lesions were less frequent.

No Associations Between Lesion Types Within Individual Body Segments

Table II shows the ten body segments examined and the odds ratios for associations of each pair of lesions for each segment. No association was observed between the occurrence of cutaneous and diffuse plexiform neurofibromas in the same body segment. The summary odds ratio (OR) was 1.20 (95% confidence interval [CI] = 0.81–1.79). There was no evidence for heterogeneity across body segments ($P = 0.37$).

Similarly, there was no association between the presence of café-au-lait spots and either cutaneous or diffuse plexiform neurofibromas within a single body segment. There was significant ($P = 0.03$) heterogeneity in the occurrence of cutaneous neurofibromas and café-au-lait spots, with a positive association seen in the neck (OR = 2.94; 95% CI = 1.20–7.20). No evidence of heterogeneity across body segments was found for the occurrence of plexiform neurofibromas and café-au-lait spots ($P = 0.52$).

TABLE I. Number and Percentage of 547 NF1 Patients Who Have One or More Cutaneous Neurofibromas, Diffuse Plexiform Neurofibromas, or Café-au-lait Spots in Each of 10 Body Segments

	Cutaneous neurofibromas		Plexiform neurofibromas		Café-au-lait spots	
Segment	Total	(%)	Total	(%)	Total	(%)
1. Head	179	(33)	47	(8)	101	(18)
2. Neck	168	(31)	29	(5)	397	(73)
3. Right upper torso	259	(47)	32	(6)	532	(97)
4. Left upper torso	258	(47)	21	(4)	531	(97)
5. Right lower torso	285	(52)	55	(10)	537	(98)
6. Left lower torso	287	(52)	41	(7)	533	(97)
7. Right arm	206	(38)	21	(4)	514	(94)
8. Left arm	208	(38)	19	(3)	511	(93)
9. Right leg	219	(40)	54	(10)	527	(96)
10. Left leg	220	(40)	45	(8)	525	(96)
Total	337	(62)	216	(39)	543	(99)

TABLE II. Associations Between Cutaneous Neurofibromas, Diffuse Plexiform Neurofibromas, and Café-au-lait Spots by Body Segment in 547 NF1 Patients

	Cutaneous and plexiform neurofibromas		Cutaneous neurofibromas and café-au-lait spots		Café-au-lait spots and plexiform neurofibromas	
Segment	OR	(95% CI)	OR	(95% CI)	OR	(95% CI)
1. Head	0.95	(0.34–2.68)	1.34	(0.67–2.67)	1.26	(0.60–2.65)
2. Neck	2.39	(0.51–11.20)	2.59	(1.23–5.47)	2.42	(0.71–8.24)
3. Right upper torso	0.83	(0.23–3.02)	0.26	(0.01–10.34)		
4. Left upper torso	0.39	(0.06–2.49)	0.12	(0.01–7.07)	1.29	(0.02–83.37)
5. Right lower torso	0.85	(0.32–2.24)	0.98	(0.01–84.41)		
6. Left lower torso	0.91	(0.35–2.36)	1.13	(0.19–6.94)	0.06	(0.01–0.99)
7. Right arm	1.17	(0.09–14.43)	1.91	(0.29–12.67)		
8. Left arm	1.01	(0.18–5.60)	0.91	(0.18–4.65)	0.22	(0.02–1.97)
9. Right leg	3.91	(1.02–15.06)	0.20	(0.04–1.15)	0.35	(0.05–2.34)
10. Left leg	3.60	(0.99–13.08)	1.10	(0.24–5.00)	2.70	(0.17–44.12)
Summary	1.20	(0.81–1.79)	1.36	(0.91–2.03)	1.25	(0.74–2.12)

Odds ratios (OR) could not be calculated for the association of café-au-lait spots and plexiform neurofibibromas in the right upper torso, right lower torso, or right arm because there were no patients who had plexiform neurofibromas but did not have café-au-lait spots in these segments.

Log-Linear Relationship Between Segment Size and Number of Cutaneous Neurofibromas

The number of body segments affected with one or more cutaneous neurofibromas was strongly correlated with the total number of cutaneous neurofibromas in 44 NF1 patients in whom both total counts and data on the number of affected body segments were available ($r = 0.95$, $P < 0.001$). The relationship is log linear; the regression equation is:

$$\log(\text{total number of neurofibromas} + 1) = 0.23 \times (\text{number of segments affected}) + 0.014$$

We observed no significant association between the relative size of the body surface area in a segment and the presence of one or more cutaneous neurofibromas ($P = 0.18$) or of a diffuse plexiform neurofibroma ($P = 0.23$). In contrast, an association was found between the presence of one or more café-au-lait spot in a body segment and its surface area expressed as a percentage of the body's total ($P < 0.001$, OR = 1.030, 95% CI = 1.015–1.046).

All Three Lesions Are Correlated Among Relatives With NF1

We estimated intrafamilial correlations in the age-adjusted number of body segments that included one or more café-au-lait spots, one or more cutaneous neurofibromas, or one or more plexiform neurofibromas in 117 affected members of 52 families. We found significant intrafamilial correlations for the number of body segments affected by each of these clinical features. The intrafamilial correlation coefficient for the number of body segments affected with café-au-lait spots was 0.45 (95% CI = 0.18–0.71). The correlation among relatives with NF1 for the number of body segments affected with cutaneous neurofibromas was 0.37 (95% CI = 0.15–0.55). The correlation coefficient among relatives for the number of body segments affected with plexiform neurofibromas was 0.35 (95% CI = 0.15–0.57).

DISCUSSION

Lesions in Body Segments of Individual Patients

We found a very high correlation ($r = 0.95$) between the number of body segments in which one or more cutaneous neurofibromas was present and the total number of cutaneous neurofibromas in 44 patients in whom counts were available. Counting all cutaneous neurofibromas in an adult with NF1 is very tedious, and our observation provides the basis for using the number of body segments affected by cutaneous neurofibromas as a surrogate for the total number of cutaneous neurofibromas in clinical trials and studies of genotype–phenotype correlations. It seems likely that a similar relationship exists between the number of body segments affected with café-au-lait spots or plexiform neurofibromas and the severity of each of these disease features, but we did not have information on total counts of these lesions available to demonstrate this.

Since almost all, if not all, diffuse plexiform neurofibromas are of congenital origin [Friedman and Riccardi, 1999], we wanted to find out if they influence the subsequent development of cutaneous neurofibromas. Our findings indicate that the occurrence of cutaneous neurofibromas in NF1 patients is not strongly influenced by the local presence of a diffuse plexiform neurofibroma. In fact, we found that all three of the lesions studied (café-au-lait spots, cutaneous neurofibromas, and plexiform neurofibromas) occurred independently of each another in almost all of the body segments analyzed (Table II). We found a significant association between café-au-lait spots and cutaneous neurofibromas only in the neck. One possible reason the neck might be affected by both lesions is recurrent minor trauma to the skin associated with flexion, extension, and rotation of the head [Riccardi, 1990].

The independent occurrence of cutaneous neurofibromas, plexiform neurofibromas, and café-au-lait spots in most body regions is consistent with the possibility that somewhat different pathogenic mechanisms are involved in development of these three lesions. Families with *NF1* mutations who develop café-au-lait spots but no tumors have been reported [Abeliovich et al., 1995], an observation that is consistent with different pathogenic factors being involved in the development of café-au-lait spots and neurofibromas. In mouse models of NF1, cutaneous and plexiform neurofibromas can develop by different pathogenic pathways [Feigenbaum et al., 1996; Cichowski et al., 1999; Vogel et al., 1999].

Familial Correlations

The intrafamilial correlations we observed for cutaneous neurofibromas and café-au-lait spots in NF1 patients are consistent with the findings of a previous study [Easton et al., 1993]. The number of familial patients and the prevalences of all three lesions were similar in these two studies. Our study found a similar correlation for café-au-lait spots but higher correlation coefficients for cutaneous neurofibromas than Easton and his associates did. We also found a significant familial correlation for plexiform neurofibromas. Easton et al. [1993] analyzed this feature as a discrete (present/absent) trait and found no familial association.

We have also studied the familiality of café-au-lait spots, cutaneous neurofibromas, and plexiform neurofibromas as discrete traits in an independent series of NF1 patients [Szudek et al., 2000b; Szudek et al., 2002]. The results of that study are consistent with the current one and with the study of Easton and associates [1993] despite differences in design and methodology: We again found strong intrafamilial correlations for café-au-lait spots ($r = 0.43$, 95% CI = 0.29–0.57) and cutaneous neurofibromas ($r = 0.49$, 95% CI = 0.33–0.65). Like Easton et al. [1993] we did not find a correlation for the occurrence of plexiform neurofibromas considered as a discrete trait when all relatives were considered, but we did find a significant sib-sib correlation for the occurrence of this clinical feature ($r = 0.18$, 95% CI = 0.04–0.32). These observations provide further evidence for the importance of familial factors in the development of café-au-lait spots and neurofibromas in people with NF1.

The genetic basis for these familial associations has not been determined, but contributing factors may include effects of the mutant *NF1* allele itself, effects of the normal *NF1* allele, or modifying effects of other loci. The number of individuals included in our study was too small to permit comparison of the strength of the correlation among relatives of various classes, which would be necessary to distinguish these factors statistically. The moderate magnitudes of the intrafamilial correlation coefficients we found show that familial factors alone are insufficient to predict the degree to which a patient will be affected by these lesions.

ACKNOWLEDGMENTS

We thank Patricia Birch for her help with this study.

REFERENCES

Abeliovich D, Gelman-Kohan Z, Silverstein S, Lerer I, Chemke J, Merin S, Zlotogora J. 1995. Familial cafe au lait spots: A variant of neurofibromatosis type 1. J Med Genet 32:985–986.

Burger P, Scheithauer B. 1994. Tumors of the central nervous system. In: Atlas of tumor pathology. Fascicle 10. Washington, DC: Armed Forces Institute of Pathology.

Cichowski K, Shih TS, Schmitt E, Santiago S, Reilly K, McLaughlin ME, Bronson RT, Jacks T. 1999. Mouse models of tumor development in neurofibromatosis type 1. Science 286:2172–2176.

DeBella K, Szudek J, Friedman JM. 2000. Use of the national institutes of health criteria for diagnosis of neurofibromatosis 1 in children. Pediatrics 105:608–614.

Donner A, Wells G, Eliasziw M. 1989. On two approximations to the F-distribution: Application to testing for intraclass correlation in family studies. Canadian J Statistics 17:209–215.

Easton D, Ponder M, Huson S, Ponder B. 1993. An analysis of variation in expression of neurofibromatosis (NF) type I (NFI): Evidence for modifying genes. Am J Hum Genet 53:305–313.

Feigenbaum L, Fujita K, Collins FS, Jay G. 1996. Repression of the NF1 gene by Tax may expain the development of neurofibromas in human T-lymphotropic virus type 1 transgenic mice. J Virol 70:3280–3285.

Fitzpatrick TB. 1981. Melanin synthesis pathways in the pathogenesis of neurofibromatosis. Adv Neurol 29:209–211.

Friedman JM, Riccardi VM. 1999. Clinical and epidemiological features. In: Friedman JM, Gutmann DH, MacCollin M, Riccardi VM, editors. Clinical and epidemiological features. Baltimore: Johns Hopkins University Press. pp 29–86.

Giorno R, Lieber J, Claman HN. 1989. Ultrastructural evidence for mast cell activation in a case of neurofibromatosis. Neurofibromatosis 2:35–41.

Gutmann D, Aylsworth A, Carey J, Korf B, Marks J, Pyeritz R, Rubenstein A, Viskochil D. 1997. The diagnostic evaluation and multidisciplinary management of neurofibromatosis 1 and neurofibromatosis 2. JAMA 278:51–57.

Harkin J, Reed R. 1969. Tumors of the peripheral nervous system. Tumors of the peripheral nervous system. Washington, DC: Armed Forces Institute of Pathology. pp 67–100.

Korf BR. 1999. Plexiform neurofibromas. Am J Med Genet 89:31–37.

McManus WF, Pruitt BA Jr. 1996. Thermal injuries. In: Feliciano DV, Moore EE, Mattox KL, editors. Trauma, 3rd ed. Stamford, Connecticut: Appleton & Lange. pp 937–949.

Miller R. 1974. The jackknife—a review. Biometrika 61:1–15.

National Institutes of Health Consensus Development Conference. 1988. Neurofibromatosis: Conference statement. Arch Neurol 45:575–578.

Riccardi V. 1990. The potential role of trauma and mast cells in the pathogenesis of neurofibromas. In: Ishibashi Y, Hori Y, editors. The potential role of trauma and mast cells in the pathogenesis of neurofibromas. Elsevier, Amsterdam. pp 167–190.

Riccardi VM. 1992. Neurofibromatosis: Phenotype, natural history, and pathogenesis. Baltimore: The Johns Hopkins University Press.

Spjotvoll E. 1967. Optimum invariant tests in unbalanced variance component models. Ann Math Statist 38:422–428.

SPSS. 1998. SPSS for Windows . Ver. 9.0.0.

Szudek J, Birch P, Riccardi VM, Evans DG, Friedman JM. 2000a. Associations of clinical features in neurofibromatosis 1 (NF1). Genet Epidemiol 19:429–439.

Szudek J, Joe H, Friedman JM. 2000b. Familial aggregation of neurofibromatosis 1 (NF1) clinical features. Am J Hum Genet 67:211.

Szudek J, Joe H, Friedman JM. 2002. Analysis of intra-familial phenotypic correlation in neurofibromatosis 1 (NF1). Genet Epidemiol 23:150–164.

Szudek J, Evans D, Friedman JM. 2003. Logistic regresssive models of neurofibromatosis 1 (NF1) clinical features. Hum Genet 112:289–297.

Vogel KS, Klesse LJ, Velasco-Miguel S, Meyers K, Rushing EJ, Parada LF. 1999. Mouse tumor model for neurofibromatosis type 1. Science 286: 2176–2179.

Woodruff JM. 1999. Pathology of tumors of the peripheral nerve sheath in type 1 neurofibromatosis. Am J Med Genet 89:23–30.

Genetic Epidemiology 23:150–164 (2002)

Analysis of Intrafamilial Phenotypic Variation in Neurofibromatosis 1 (NF1)

J. Szudek,[1,2] H. Joe,[3] and J.M. Friedman[1]*

[1]Department of Medical Genetics, University of British Columbia, Vancouver, British Columbia, Canada
[2]Dalhousie Medical School, Halifax, Nova Scotia, Canada
[3]Department of Statistics, University of British Columbia, Vancouver, British Columbia, Canada

The relationship of genetic factors to variable expressivity in neurofibromatosis 1 (NF1) is poorly understood. We examined familial aggregation of NF1 features among different classes of affected relatives. Clinical information was obtained from the National NF Foundation International Database on 904 affected individuals in 373 families with 2 or more members with NF1. We used multivariate probit regression to measure the associations between various classes of relatives for each of 10 clinical features of NF1, while simultaneously adjusting for covariates including related features, age, and gender. Two distinct patterns were observed when we compared associations between first- and second-degree relatives, sibs, and parent-child pairs: Lisch nodules and café-au-lait spots had greater associations between first-degree relatives than between second-degree relatives, while subcutaneous neurofibromas, plexiform neurofibromas, café-au-lait spots, and intertriginous freckling had greater associations between sibs than between parents and children. In addition, Lisch nodules, subcutaneous neurofibromas, and cutaneous neurofibromas had greater associations between affected fathers and children than between affected mothers and children. These familial patterns suggest that unlinked modifying genes and the normal NF1 allele may both be involved in the development of particular clinical features of

Grant sponsor: Department of the Army, USAMRMC; Grant numbers: NF960003, NF990038; Grant sponsor: National Neurofibromatosis Foundation.
*Correspondence to: J.M. Friedman, M.D., Ph.D., Department of Medical Genetics, University of British Columbia, 6174 University Blvd., Vancouver, British Columbia V6T 1Z3, Canada.
E-mail: frid@interchange.ubc.ca
Received for publication 26 December 2001; Revision accepted 19 March 2002
Published online in Wiley InterScience (www.interscience.wiley.com). DOI: 10.1002/gepi.01129

NF1, but that the relative contributions vary for different features. Genet. Epidemiol. 23:150–164, 2002.

Key words: neurofibromatosis 1; familial correlation; multivariate probit regression

INTRODUCTION

Neurofibromatosis 1 (NF1) is an autosomal-dominant disease that affects about 1/3,500 people [Friedman, 1999]. NF1 can affect the skin, skeleton, and nervous system, and is characterized by highly variable expressivity [Friedman et al., 1999]. Many disease features are progressive, but the rate of progression and the occurrence of serious manifestations vary greatly from one patient to another [Friedman and Riccardi, 1999]. This variability and the confounding effect of age have hindered efforts to characterize the relationship of genetic factors at the *NF1* locus or other loci to disease variability.

More than 400 different constitutional *NF1* mutations have been reported [Fahsold et al., 2000; Korf, 1999; Messiaen et al., 2000]. In general, little evidence has been found of allele-phenotype correlations in NF1, although a more or less consistent phenotype occurs in association with deletions involving the entire *NF1* gene [Dorschner et al., 2000; Tonsgard et al., 1997]. Similar clinical features were observed among affected members of a few families with the NF1 variants Watson syndrome [Allanson et al., 1991], familial café-au-lait spots [Abeliovich et al., 1995], or familial spinal neurofibromas [Ars et al., 1998; Poyhonen et al., 1997; Pulst et al., 1991]. This observation is consistent with an allele-phenotype correlation, but no consistent kind of *NF1* mutation has been found in families with these or other phenotypic variants. Affected members of a single family with typical NF1 often have quite different disease phenotypes, despite sharing an identical mutant *NF1* allele. Clearly, variation in the mutant *NF1* allele itself does not account for all of the variability seen in most disease features.

Easton et al. [1993] studied the expressivity of NF1 in 175 affected members of 48 families, and found statistically significant correlations for the number of café-au-lait spots, the number of dermal discrete neurofibromas, and head circumference among affected relatives. Comparison of the strength of these correlations in relatives of different classes provided evidence for modifying genes influencing the number of café-au-lait spots.

We showed that several statistically significant associations exist between the occurrence of individual clinical features in 3,067 unrelated probands with NF1 [Szudek et al., 2000b; Szudek et al., unpublished findings]. We also found significant associations in the occurrence of Lisch nodules, optic glioma, learning disability, macrocephaly, and short stature in affected parent-child pairs [Szudek et al., 2000b], but made no attempt to adjust for the nonindependence of multiple relative-pairs from the same family or for associations among clinical features in individuals in this preliminary study. We now extend our analysis to measure correlations of NF1 features among relatives of various classes, using methods that take other clinical features, gender, and age into account, and adjust for the nonindependence of affected relatives. By comparing the correlations observed, we provide evidence that

genetic sources of variation are generally important in NF1 and vary for different clinical features.

SUBJECTS AND METHODS

Subjects

All patients in this study met the NIH diagnostic criteria for NF1 [Gutmann et al., 1997; NIH, 1988]. Data were obtained from the National NF Foundation International Database (NFDB) [Friedman et al., 1993]. The NFDB contains extensive demographic, clinical, and genetic data on NF1 patients from more than 20 participating clinical centers in North America, Europe, Japan, and Australia. All information is recorded using a standard format and consistent definitions of clinical features. The greatest strength of the NFDB is its large size. The limitations include the fact that data are contributed by staff members of specialized neurofibromatosis clinics, which probably produces an ascertainment bias.

At the time of this study, the available dataset included 373 families with two or more affected members, for a total of 904 individuals with NF1. Three hundred forty-six of these were nuclear families that included either an affected parent and one or more affected children or two or more affected sibs. Twenty-seven families were more extended, including a total of 74 second-degree affected relative-pairs. The family sizes ranged from 2–7 affected members. There were 272 families with 2, 65 with 3, 24 with 4, 6 with 5, 3 with 6, and 3 with 7 affected members included in the study.

For analysis of familiality, we selected 10 clinical features of NF1: café-au-lait spots, intertriginous freckling, Lisch nodules, cutaneous neurofibromas, subcutaneous neurofibromas, plexiform neurofibromas, seizures, scoliosis, optic glioma, and neoplasms other than neurofibromas or optic gliomas ("other neoplasms"). Most of these features were identified by physical examination, and all were treated as binary variables. Café-au-lait spots were coded as "present" if the subject had six or more spots. Cutaneous or subcutaneous neurofibromas were coded as "present" if the subject had two or more lesions of the same type. Plexiform neurofibroma was coded as "present" if the subject had one or more lesions. Lisch nodules were diagnosed or excluded by slit-lamp examination. The presence or absence of optic glioma was determined by cranial MRI or CT examination. Only patients with definite presence or absence of a feature were considered in models involving that feature. The complete dataset used in this study is available from the authors on request.

Statistical Methods

Familial correlations in each class of relatives were estimated for clinical features measured as binary (presence/absence) variables by means of a multivariate probit model [Ashford and Sowden, 1970; Joe, 1995; Mendell and Elston, 1974]. For a particular binary response variable, the covariates used for adjustment were chosen on the basis of a univariate probit or logistic stepwise regression, ignoring familial dependence. These covariates were then used in the multivariate probit model. We included age as a covariate in all analyses, because many NF1 features have a higher prevalence in older patients [DeBella et al., 2000]. We showed previously that clinical

features do not occur independently in NF1 patients, even after adjusting for the effect of age [Szudek et al., 2000b; Szudek et al., unpublished findings]. Therefore, we also included the binary variables representing the presence or absence of other associated features, as well as gender, as covariates to minimize confounding. In addition, we considered stature and head circumference as covariates after standardizing the measurements for each patient to age- and gender-specific population norms [Szudek et al., 2000a].

For the multivariate probit model, the binary response vector is $(Y_1,\ldots,Y_k)$ for a family of size k, Y_j is 1 if a latent variable $Z_j \leq \beta_0 + \beta'x$, where β_0 is an intercept and β is a vector of regression coefficients for the covariate vector x. $(Z_1,\ldots, Z_k)$ have a joint multivariate normal distribution with zero mean vector and correlation matrix R, where the (latent) correlation for a given pair depends on the relation type of the pair.

The estimates of the regression coefficients and latent correlation coefficients, together with an estimated covariance matrix and standard errors, were obtained by numerical maximum likelihood, using the quasi-Newton algorithm [Nash, 1990]. The multivariate normal rectangle probabilities for the multivariate probit model were computed using fast approximation methods [Joe, 1995]; the first-order approximation requires only bivariate normal rectangle probabilities, and the second-order approximation requires multivariate probabilities up to the fourth dimension. These approximations have made feasible the computations for the multivariate probit model; they are much more accurate than older methods, such as the approximation of Mendell and Elston [1974].

Univariate probit regressions were used to obtain appropriate functions for age (e.g., $e^{-\text{age}\neq 14}$) and initial estimates of regression coefficients for covariates representing related features, interactions between related features, and gender. Familial aggregation was assessed among sibs, parent-child pairs (including mother-child and father-child pairs separately), and second-degree relatives with a multivariate probit model.

Parameters and coefficients with 95% confidence intervals that excluded zero were deemed statistically significant. Standard errors and covariance matrices were used to test for differences between intrafamilial correlation coefficients for different comparisons. For example, to test for a difference between a sib-sib correlation and parent-child correlation, we used the following formula:

$$Z = \frac{r_{ss} - r_{pc}}{s} \text{ where } s = \sqrt{(SE_{r_{ss}})^2 + (SE_{r_{pc}})^2 - 2\,\text{cov}(r_{ss}, r_{pc})}.$$

Z-scores were converted into *P*-values according to the standard normal distribution. We used one-tailed tests to compare correlations between first-degree and second-degree relatives and between sib pairs and parent-child pairs, because we had a prior expectation that correlations between sibs would be at least as strong as those between parents and children [Easton et al., 1993; Szudek et al., 2000b]. We used two-tailed tests to compare mother-child correlations to father-child correlations.

RESULTS

We studied 904 individuals with NF1 from 373 families with two or more affected members. Ninety-one percent of the individuals studied were white, 2%

Asian, 1% Black, 1% Latin, and the remainder either of "other" or "unknown" ethnic origin. Table I shows the prevalences of each of the 10 NF1 clinical features in affected fathers, mothers, and their affected children in the NFDB study sample, and compares them to the prevalences in the sample used by Easton et al. [1993].

Familial aggregation among various classes of relatives was estimated using multivariate regression models. Table II shows the regression parameters and standard errors for the terms that were included in each model. The strength of association between the modelled feature and a covariate is measured by β. A unit increase in the value of the covariate means the modelled feature is $\exp(2\beta)$ times more likely to be present. For example, subjects with intertriginous freckling were $\exp(2 \times 0.52) = 2.8$ times more likely also to have café-au-lait spots than subjects of the same age and gender without intertriginous freckling. Also, subjects with intertriginous freckling *and* subcutaneous neurofibromas were $\exp(2 \times (0.52 - 0.18 + 0.62)) = 6.8$ times more likely also to have café-au-lait spots.

The parameter estimates for age were highly significant ($P < 0.001$) for Lisch nodules, subcutaneous neurofibromas, cutaneous neurofibromas, and intertriginous freckling; significant ($P < 0.05$) for café-au-lait spots, optic gliomas, and plexiform neurofibromas; and not significant ($P > 0.05$) for other neoplasms, seizures, or scoliosis. The parameter estimate for gender was not significant in any of the models.

Table III shows the number of sib, parent-child (including mother-child and father-child), and second-degree relative-pairs used in each model. Subjects were

TABLE I. Number and Percentage of Subjects From the NFDB and From Easton *et al.* [1993] With Various NF1 Features[a]

Feature	NFBD										Easton et al. [1993]	
	Affected fathers		Affected mothers		Affected children of affected fathers		Affected children of affected mothers		All affected relatives		All affected relatives	
	N	%	N	%	N	%	N	%	N	%	N	%
Lisch nodules	63	81	101	80	64	63	101	51	409	60		
Café-au-lait macules	67	68	125	73	115	79	181	74	657	75	129	88
Cutaneous neurofibromas	78	80	119	69	37	25	67	27	355	40	121	76
Optic glioma	4	13	2	4	8	14	14	15	45	15	9	5
Subcutaneous neurofibromas	60	61	99	59	31	21	58	23	291	33		
Intertriginous freckling	79	83	147	88	112	78	191	78	699	80		
Seizures	7	7	12	7	8	5	16	6	58	6	12	7
Plexiform neurofibromas	24	24	35	20	25	18	44	18	176	20	37	21
Scoliosis	7	8	8	6	29	22	32	14	96	12	27	16
Other neoplasms	4	4	11	6	4	3	7	3	33	4		

[a]Features not considered by Easton et al. [1993] are left blank.

TABLE II. Summary of Regressions in Multivariate Probit Models for 10 Clinical NF1 Features[a]

Modelled feature	Intercept and covariates	β	SE
Lisch nodules	β_0	0.65	0.08
	Age	−3.35	0.32
	Male gender	−0.01	0.08
	Café-au-lait spots	0.23	0.15
	Cutaneous neurofibromas	0.44	0.20
	Café-au-lait spots * cutaneous neurofibromas	−0.09	0.22
Café-au-lait spots	β_0	0.28	0.14
	Age	−0.66	0.25
	Male gender	0.03	0.09
	Intertriginous freckling	0.51	0.12
	Subcutaneous neurofibromas	−0.41	0.26
	Intertriginous freckling * subcutaneous neurofibromas	0.61	0.28
Cutaneous neurofibromass	β_0	−1.62	0.11
	Age	−5.56	0.36
	Male gender	0.01	0.10
	Subcutaneous neurofibromas	0.62	0.11
	Plexiform neurofibromas	0.36	0.12
Optic glioma	β_0	−1.02	0.13
	Age	0.72	0.57
	Male gender	0.06	0.17
	Plexiform neurofibromas	0.01	0.37
	Head circumference	0.19	0.07
	Neoplasms	0.55	0.49
Subcutaneous neurofibromas	β_0	−1.72	0.12
	Age	−3.78	0.35
	Male gender	−0.04	0.08
	Café-au-lait spots	0.43	0.11
	Cutaneous neurofibromas	0.73	0.13
	Plexiform neurofibromas	0.52	0.17
	Intertriginous freckling * plexiform neurofibromas	−0.24	0.23
Intertriginous freckling	β_0	0.49	0.15
	Age	−1.58	0.30
	Male gender	−0.23	0.12
	Café-au-lait spots	0.52	0.14
	Subcutaneous neurofibromas	−0.18	0.27
	Lisch nodules	0.55	0.14
	Café-au-lait spots * subcutaneous neurofibromas	0.62	0.33
Seizures	β_0	−1.43	0.11
	Age	−0.88	0.65
	Male gender	−0.04	0.15
Plexiform neurofibromas	β_0	−1.11	0.11
	Age	−0.88	0.38
	Male gender	0.07	0.09
	Subcutaneous neurofibromas	0.46	0.16
	Cutaneous neurofibromas	0.37	0.14
	Subcutaneous * cutaneous neurofibromas	−0.21	0.22

Table continues

TABLE II. Continued

Modelled feature	Intercept and covariates	β	SE
Scoliosis	β_0	−1.11	0.09
	Age	−0.57	0.34
	Male gender	−0.02	0.11
Other neoplasms	β_0	−0.95	0.23
	Age	−4.07	2.11
	Male gender	−0.06	0.21
	Lisch nodules	−0.55	0.25
	Optic glioma	0.32	0.31

[a]The first column lists the 10 modelled features. Columns 2–4 show the covariates and their regression parameter estimates (β) with standard errors (SE) used in each model. β_0 is the intercept in the model equation. Each regression accounts for covariates such as related features, interactions between related features, age, and gender. Interactions are depicted by features separated by an asterisk, and their values equal the product of the two interacting features.

TABLE III. Number of Relatives Used in Multivariate Probit Models for 10 Clinical NF1 Features

Modelled feature	Number of affected pairs included for feature			
	Sibs	Mother-child	Father-child	Second-degree relatives
Lisch nodules	192	159	79	35
Café-au-lait macules	248	210	129	69
Cutaneous neurofibromas	264	224	131	69
Optic glioma	55	37	26	4
Subcutaneous neurofibromas	253	220	131	69
Intertriginous freckling	179	148	75	35
Seizures	268	233	140	74
Plexiform neurofibromas	264	224	131	69
Scoliosis	228	191	131	53
Other neoplasms	47	33	20	3

included in a model only if the status ("presence" or "absence") of the modelled feature and all covariates was known.

Figure 1 shows the adjusted intrafamilial correlation coefficients and 95% confidence intervals for six clinical features among 746 affected first-degree relatives and among 148 affected second-degree relatives. The multivariate probit regression failed to converge on correlation coefficients between second-degree relatives for optic glioma, other neoplasms, seizures, or scoliosis because of the low frequency of these features and insufficient sample size. We did obtain correlation coefficients between first-degree relatives for these features, but none of these correlations was significantly different from zero. Statistically significant positive correlations between first-degree relatives were found for 5 of the 6 other features listed in Figure 1. Significant positive correlations between second-degree relatives were also found for 2 of these 6 features. Significant negative correlations were not observed for any of the features. Correlations were significantly greater among first-degree relatives than among second-degree relatives for Lisch nodules ($P = 0.0001$) and café-au-lait spots ($P = 0.0004$). Correlations among first-degree relatives were not statistically different

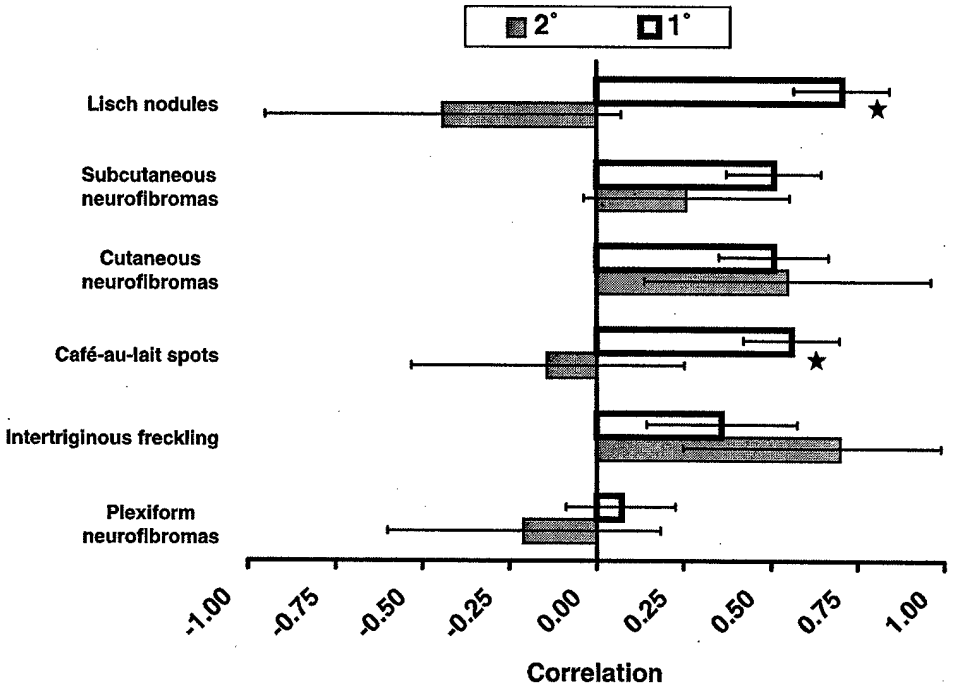

Fig. 1. Adjusted intrafamilial correlation coefficients and 95% confidence intervals for six clinical features among 746 affected first-degree relatives and 148 affected second-degree relatives. Star indicates a significant difference between correlation coefficients of the two classes being compared. The multivariate probit regression failed to converge on correlation coefficients between second-degree relatives for optic glioma, other neoplasms, seizures, or scoliosis because of the low frequency of these features and insufficient sample size. 2°, second degree; 1°, first degree.

from correlations among second-degree relatives for subcutaneous neurofibromas ($P=0.06$), cutaneous neurofibromas ($P=0.49$), intertriginous freckling ($P=0.07$), or plexiform neurofibromas ($P=0.11$).

Figure 2 shows the adjusted intrafamilial correlation coefficients and 95% confidence intervals for six features among 268 affected sib pairs and among 373 affected parent-child pairs. Again, the multivariate probit regression failed to converge on correlation coefficients between sibs or parent-child pairs for optic glioma, other neoplasms, seizures, or scoliosis. Statistically significant positive correlations between sibs were found for all six features in Figure 2. Significant positive correlations between parents and children were found for 4 of the 6 features. Significant negative correlations were not observed for any of the features. Correlations were significantly greater between sibs than between parents and children for subcutaneous neurofibromas ($P=0.04$), café-au-lait spots ($P=0.001$), intertriginous freckling ($P=0.03$), and plexiform neurofibromas ($P=0.02$). Correlations between sibs were not statistically different from the correlations between parents and children for Lisch nodules ($P=0.40$) or cutaneous neurofibromas ($P=0.29$).

Figure 3 shows the adjusted intrafamilial correlation coefficients and 95% confidence intervals for six features between 233 affected mother-child pairs and

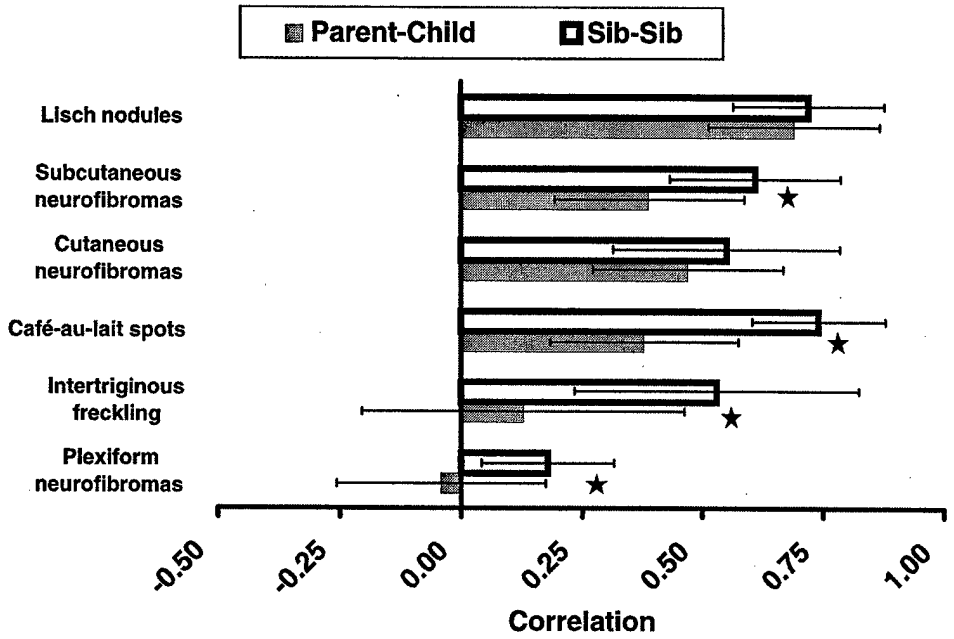

Fig. 2. Adjusted intrafamilial correlation coefficients and 95% confidence intervals for six features among 268 affected sib pairs and 373 affected parent-child pairs. Star indicates a significant difference between correlation coefficients of the two classes being compared. The multivariate probit regression failed to converge on correlation coefficients between sibs or parent-child pairs for optic glioma, other neoplasms, seizures, or scoliosis.

between 140 affected father-child pairs. Statistically significant positive correlations between mothers and children were found for 3 of the 6 features. Significant positive correlations between fathers and children were found for 4 of the 6 features. Significant negative correlations were not observed for any of the features in either relationship. Correlations between fathers and children were significantly greater than correlations between mothers and children for Lisch nodules ($P=0.001$), subcutaneous neurofibromas ($P=0.0001$), and cutaneous neurofibromas ($P=0.02$). Correlations did not differ significantly between father-child pairs and mother-child pairs for café-au-lait spots ($P=0.62$), intertriginous freckling ($P=0.71$), or plexiform neurofibromas ($P=0.17$).

DISCUSSION

Limitations of Our Data and Methods

We analyzed familial latent correlations for 10 NF1 clinical features while adjusting for other related features, age, and gender through statistical modelling. We were able to test for differences between correlations among various classes of relatives for 6 of the 10 features studied. Differences between various classes of relatives were found for each of these six features (Figs. 1–3).

The NFDB draws its information from specialized clinics, so we were concerned about the representativeness of our sample. However, frequencies of features found

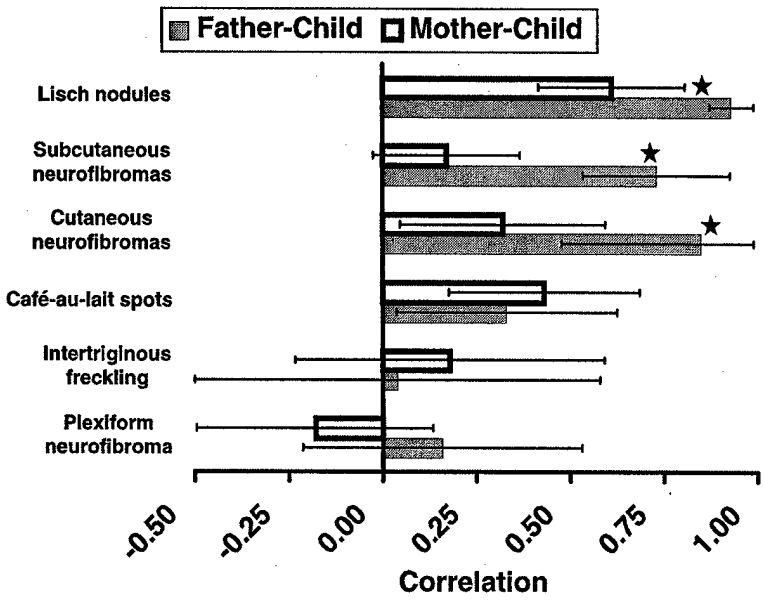

Fig. 3. Adjusted intrafamilial correlation coefficients and 95% confidence intervals for six features between 233 affected mother-child pairs and 140 affected father-child pairs. Star indicates significant difference between correlation coefficients of the two classes being compared. 2°, second degree; 1°, first degree.

among the familial cases used in this study (Table I) are comparable to those seen in another family study of variable NF1 expressivity [Easton et al., 1993] and in two available population-based studies of NF1 patients [Huson et al., 1989; Samuelsson and Axelsson, 1981].

Easton et al. [1993] studied 175 individuals with NF1 from 48 families, including 6 pairs of monozygotic twins, 76 pairs of sibs, 60 parent-offspring pairs, 54 second-degree relative pairs, and 43 third-degree relative pairs. These investigators examined eight NF1 clinical features and found significant intrafamilial correlations for three quantitative variables: number of café-au-lait spots, number of cutaneous neurofibromas, and head circumference. Easton et al. [1993] also analyzed five traits as binary variables, but these comparisons did not include adjustment for age. Furthermore, none of their analyses adjusted for the nonindependence of multiple relative-pairs from the same family or of various clinical features. Our sample size is five times larger, and we examined 10 clinical features, 6 of which are the same as those of Easton et al. [1993]. Also, we included associations between features as covariates in the familial analyses. Unlike Easton et al. [1993], we did not have counts of café-au-lait spots and dermal discrete neurofibromas, but the quantitative investigations of these features by Easton et al. [1993] complement our binary analyses nicely. Both studies found evidence of modifying genes on café-au-lait spots but not on dermal discrete neurofibromas.

All of the features we studied were treated as binary variables. Many of the clinical features of NF1 (and other diseases) are by nature binary, and ours is the first

study to examine correlations for binary traits among different familial relationships while accounting for continuous covariates such as age. Similar methods were used to study lens opacities [Anonymous, 1994] and liver cancer [Liang and Beaty, 1991] in individuals who did not have NF1, but we may be the first to study an autosomal-dominant disease in this manner.

Although this is by far the largest group of NF1 families ever studied, we only had 74 pairs of second-degree relatives. Models for most features used even fewer second-degree relatives because the data were incomplete. Subjects were included in a model only if the status of the modelled feature and of all covariates was known (Table III). These relatively small sample sizes are reflected in the wide 95% confidence intervals for the correlation coefficients among second-degree relatives (Fig. 1). Statistical techniques are less reliable for smaller sample sizes, so we must attach an additional note of caution to the point estimates for the correlation coefficients between second-degree relatives, particularly for Lisch nodules and intertriginous freckling, in which the analysis included only 35 pairs of second-degree relatives (Table III).

Several features had significantly positive correlations among second-degree relatives, but none of these correlations was significantly greater than that for the same feature among first-degree relatives (Fig. 1). Similarly, several features had significantly positive correlations between parents and children, but none of the correlations was greater than that for the same feature between sibs (Fig. 2). The absence of significant negative correlations supports the statistical validity of our approach. One would expect to observe negative, as well as positive, correlations by chance when making multiple comparisons.

The most important confounding factor in familial analyses of NF1 is age. Many disease features are more prevalent in older NF1 patients [Cnossen et al., 1998], and if not appropriately controlled, age might produce a correlation between affected relatives of similar age (e.g., sibs) or obscure a correlation between relatives of very different ages (e.g., parents and children). Our multivariate models minimize the confounding effect of age, but they may not eliminate it completely. The covariate representing age was significant in models for most features, but it is possible that a residual age effect is contributing to the observed differences between sib-sib and parent-child pairs for features such as subcutaneous neurofibromas and intertriginous freckling that become more prevalent with age (Fig. 2). Age is less likely to influence the intrafamilial correlations for café-au-lait spots or plexiform neurofibromas which, when considered as discrete variables, occur with a relatively stable frequency with age [DeBella et al., 2000; Friedman et al., 1999].

Patterns of Associations of Clinical Features Among Relatives

Lisch nodules and café-au-lait spots had significantly higher correlations among first-degree relatives than among second-degree relatives. Higher correlations for first- than second-degree relatives would be expected for effects produced by modifying genes at unlinked loci, but might also result from environmental factors that are more likely to be shared among closer relatives. Our observations are consistent with the effect of a modifying gene on the pathogenesis of Lisch nodules.

Easton et al. [1993] found a higher correlation for café-au-lait spots between monozygotic twins than between sibs, suggesting the effect of a genetic locus or loci in addition to *NF1*. Our findings of a strong correlation for café-au-lait spots in first-degree relatives but no correlation among second-degree relatives are consistent with this interpretation.

Lisch nodules and café-au-lait spots share an origin from neural crest-derived tissue, but this is also true of some other lesions characteristic of NF1, including neurofibromas of all types and intertriginous freckling [Bolande, 1981]. We previously reported an association between the occurrence of Lisch nodules and café-au-lait spots in individual NF1 patients [Szudek et al., 2000b], but intertriginous freckling was also associated, i.e., a feature that shows no indication of a stronger familial correlation among first-degree than second-degree relatives (Fig. 1).

Intertriginous freckling, subcutaneous neurofibromas, plexiform neurofibromas, and café-au-lait spots had higher correlations between sibs than between parents and children. Easton et al. [1993] found that concordance for dermal discrete neurofibromas (which include subcutaneous neurofibromas) between monozygotic twins was much higher than between sibs, an observation that suggests the involvement of a genetic factor. Affected sibs would be expected to share the same normal *NF1* allele by descent half of the time, but parent-child pairs rarely would. Effects of functional polymorphisms of the normal *NF1* allele might explain a higher correlation of these features among sib pairs than among parent-child pairs. Another possible explanation is that differences in environmental factors are more likely to be shared among sibs than between a parent and child.

Intertriginous freckling, subcutaneous neurofibromas, plexiform neurofibromas, and café-au-lait spots all share an origin from neural crest-derived cells. We found that café-au-lait spots and intertriginous freckling tended to occur together in individual NF1 patients, and so did cutaneous, subcutaneous, and plexiform neurofibromas, but associations were not seen between the features in these two groups [Szudek et al., unpublished findings]. In the present study, we did not find a stronger correlation for cutaneous neurofibromas in sibs than in parent-child pairs, as we did for subcutaneous and plexiform neurofibromas (Fig. 2).

Lisch nodules, subcutaneous neurofibromas, and cutaneous neurofibromas had higher correlations between affected fathers and children than between affected mothers and children (Fig. 3). Our sample included twice as many mother-child pairs as father-child pairs, so we were concerned about ascertainment bias, i.e., the possibility that only severely affected father-child pairs tended to be seen in the NF clinics that contributed data to the NNFF International Database. However, the frequencies of all features studied were similar in affected fathers and affected mothers (Table I).

Shared environment is unlikely to be the sole cause of associations between parents and children, due to large differences in age. It is also unlikely that shared environment is responsible for the difference in correlations between mother-child and father-child pairs. Likewise, a multifactorial influence with a more extreme threshold for males than for females cannot explain the observations for these features. Gender is not a significant predictive factor in any of our models (Table II), and feature frequencies among affected children of affected fathers are similar to those among affected children of affected mothers (Table I). Parent-of-origin effects

on severity of NF1 have been suggested [Hall, 1981; Miller and Hall, 1978], but most studies do not support this possibility [Huson et al., 1989; Riccardi and Wald, 1987]. Our findings are consistent with a parent-of-origin effect on the strength of the parent-child correlation rather than with a more severe phenotype in affected offspring of parents of one gender when compared to affected offspring of parents of the other gender. Similar parent-child aggregation patterns were reported for body mass index [Friedlander et al., 1988] and blood pressure [Hurwich et al., 1982], but they are unprecedented in NF1. We do not know of a genetic mechanism that can explain this phenomenon.

CONCLUSIONS

The patterns of familial correlations shown here suggest that genetic factors involved in determining the occurrence of various clinical features of NF1 vary, depending on the feature. In some instances, the effects of unlinked modifying genes may be most important. In other instances, the effects of the normal *NF1* allele may predominate. More than one genetic factor may be involved, and the relative importance of various genetic and nongenetic effects may vary for different features.

Some of the clinical variability that characterizes NF1 may result from allelic heterogeneity of the constitutional *NF1* mutation. Many NF1 patients have been genotyped, but little evidence of allele-phenotype correlation has been observed [Rasmussen and Friedman, 2000]. This may be because phenotypic differences resulting from *NF1* allelic heterogeneity are generally small in comparison to other sources of variability. It is also possible, however, that important *NF1* genotype-phenotype correlations exist but have not been recognized because of the complexity of the NF1 phenotype [Riccardi, 1999], its strong dependence on age [DeBella et al., 2000], the nonindependence of many clinical features [Szudek et al., 2000b; Szudek et al., unpublished findings], and the heterogeneity of pathogenic *NF1* mutations [Fahsold et al., 2000; Korf, 1999; Messiaen et al., 2000].

Our findings suggest that most NF1 clinical features have important genetic components. The patterns of variable expressivity are subtle, so data will be required on a very large number of patients and/or on very large families to identify modifying genes that affect the NF1 phenotype. Objective quantitative variables such as lesion counts would enable a more detailed analysis of familial segregation patterns and would require fewer patients than binary variables of the type used in the analyses reported here. Given the progressive nature of many NF1 disease features and the potentially confounding effects of age on analysis, it is essential that the data be representative of all age groups. A very dense map of single-nucleotide polymorphisms (SNPs) is now available in humans [Sachidanandam et al., 2001], so a random genome scan for NF1 modifying loci is theoretically possible. Improved understanding of neurofibromin's biochemical functions may permit the discovery of interacting proteins and of upstream and downstream effectors that are critical to the development of particular phenotypic features. This would greatly facilitate the identification of modifying loci.

The multivariate probit regression methods used in this study to estimate familial aggregation of NF1 clinical features, while adjusting for age, gender, and the presence of other clinical features, are likely to be useful for analysis of other genetic

diseases. Application of these methods to Mendelian conditions that have highly variable and age-dependent phenotypes, such as tuberous sclerosis complex [Cheadle et al., 2000], Gorlin syndrome [Wicking and Bale, 1997], and Stickler syndrome [Snead and Yates, 1999], seems especially promising.

ACKNOWLEDGMENTS

The NFDB is supported by the National Neurofibromatosis Foundation.

REFERENCES

Abeliovich D, Gelman-Kohan Z, Silverstein S, Lerer I, Chemke J, Merin S, Zlotogora J. 1995. Familial cafe au lait spots: a variant of neurofibromatosis type 1. J Med Genet 32:985–6.

Allanson J, Upadhaya M, Watson G, Partington M, MacKenzie A, Lahey D, MacLeod H, Sarfarazi M, Broadhead W, Harper P, Huson S. 1991. Watson syndrome: is it a subtype of type 1 neurofibromatosis? J Med Genet 28:752–6.

Anonymous. 1994. Familial aggregation of lens opacities: the Framingham Eye Study and the Framingham Offspring Eye Study. Am J Epidemiol 140:555–64.

Ars E, Kruyer H, Gaona A, Casquero P, Rosell J, Volpini V, Serra E, Lazaro C, Estivill X. 1998. A clinical variant of neurofibromatosis type 1: familial spinal neurofibromatosis with a frameshift mutation in the NF1 gene. Am J Hum Genet 62:834–41.

Ashford J, Sowden R. 1970. Multivariate probit analysis. Biometrics 26:535–546.

Bolande R. 1981. Neurofibromatosis—the quintessential neurocristopathy: pathogenic concepts and relationships. Adv Neurol 29:67–75.

Cheadle J, Reeve M, Sampson J, Kwiatkowsk ID. 2000. Molecular genetic advances in tuberous sclerosis. Hum Genet 107:97–114.

Cnossen M, de Goede-Bolder A, van den Broek K, Waasdorp C, Oranje A, Stroink H, Simonsz H, van den Ouweland A, Halley D, Niermeijer M. 1998. A prospective 10 year follow up study of patients with neurofibromatosis type 1. Arch Dis Child 78:408–12.

DeBella K, Szudek J, Friedman JM. 2000. Use of the National Institutes of Health criteria for diagnosis of neurofibromatosis 1 in children. Pediatrics 105:608–14.

Dorschner MO, Sybert VP, Weaver M, Pletcher BA, Stephens K. 2000. NF1 microdeletion breakpoints are clustered at flanking repetitive sequences. Hum Mol Genet 9:35–46.

Easton D, Ponder M, Huson S, Ponder B. 1993. An analysis of variation in expression of neurofibromatosis (NF) type I (NFI): evidence for modifying genes. Am J Hum Genet 53:305–13.

Fahsold R, Hoffmeyer S, Mischung C, Gille C, Ehlers C, Kucukceylan N, Abdel-Nour M, Gewies A, Peters H, Kaufmann D, Buske A, Tinschert S, Nurnberg P. 2000. Minor lesion mutational spectrum of the entire NF1 gene does not explain its high mutability but points to a functional domain upstream of the GAP-related domain. Am J Hum Genet 66:790–818.

Friedlander Y, Kark JD, Kaufmann NA, Berry EM, Stein Y. 1988. Familial aggregation of body mass index in ethnically diverse families in Jerusalem. The Jerusalem Lipid Research Clinic. Int J Obes 12:237–47.

Friedman JM. 1999. Epidemiology of neurofibromatosis type 1. Am J Med Genet 89:1–6.

Friedman JM, Greene C, Birch P, NNFF International Database. 1993. National Neurofibromatosis Foundation International Database. Am J Med Genet 45:88–91.

Friedman JM, Gutmann DH, MacCollin M, Riccardi VM. 1999. Neurofibromatosis: phenotype, natural history, and pathogenesis. Baltimore: Johns Hopkins University Press. p xiv, 381.

Friedman JM, Riccardi VM. 1999. Clinical and epidemiological features. In: Friedman JM, Gutmann DH, MacCollin M, Riccardi VM, editors. Neurofibromatosis: phenotype, natural history, and pathogenesis. Baltimore: Johns Hopkins University Press. p 29–86.

Gutmann DH, Aylsworth A, Carey JC, Korf B, Marks J, Pyeritz RE, Rubenstein A, Viskochil D. 1997. The diagnostic evaluation and multidisciplinary management of neurofibromatosis 1 and neurofibromatosis 2. JAMA 278:51–7.

Hall J. 1981. Possible maternal and hormonal factors in neurofibromatosis. Adv Neurol 29:125–31.

Hurwich BJ, Rosner B, Nubani N, Kass EH, Lewitter FI. 1982. Familial aggregation of blood pressure in a highly inbred community, Abu Ghosh, Israel. Am J Epidemiol 115:646–56.

Huson S, Compston D, Clark P, Harper P. 1989. A genetic study of von Recklinghausen neurofibromatosis in south east Wales: I. Prevalence, fitness, mutation rate, and effect of parental transmission on severity. J Med Genet 26:704–11.

Joe H. 1995. Approximations to multivariate normal rectangle probabilities based on conditional expectations. J Am Stat Assoc 90:957–64.

Korf B. 1999. NNFF International NF1 Genetic Analysis Consortium mutation summary data, National Neurofibromatosis Foundation. Available at http://www.nf.org/nf1gene/nf1gene.mutdata.summary.html.

Liang KY, Beaty TH. 1991. Measuring familial aggregation by using odds-ratio regression models. Genet Epidemiol 8:361–70.

Mendell N, Elston R. 1974. Multifactorial qualitative traits: genetic analysis and prediction of recurrence risks. Biometrics 30:41–57.

Messiaen LM, Callens T, Mortier G, Beysen D, Vandenbroucke I, Van Roy N, Speleman F, Paepe AD. 2000. Exhaustive mutation analysis of the NF1 gene allows identification of 95% of mutations and reveals a high frequency of unusual splicing defects. Hum Mutat 15:541–55.

Miller M, Hall J. 1978. Possible maternal effect on severity of neurofibromatosis. Lancet 2:1071–3.

Nash J. 1990. Compact numerical methods for computers: linear algebra and function minimisation. New York: Hilger.

NIH. 1988. Neurofibromatosis: conference statement. National Institutes of Health Consensus Development Conference. Arch Neurol 45:575–8.

Poyhonen M, Leisti E-L, Kytölä S, Leisti J. 1997. Hereditary spinal neurofibromatosis: a rare form of NF1? J Med Genet 34:184–7.

Pulst SM, Riccardi VM, Fain P, Korenberg JR. 1991. Familial spinal neurofibromatosis: clinical and DNA linkage analysis. Neurology 41:1923–7.

Rasmussen SA, Friedman JM. 2000. NF1 gene and neurofibromatosis 1. Am J Epidemiol 151:33–40.

Riccardi VM. 1999. Historical background and introduction. In: Friedman JM, Gutmann DH, MacCollin M, Riccardi VM, editors. Neurofibromatosis: phenotype, natural history, and pathogenesis. Baltimore: Johns Hopkins University Press. p 1–25.

Riccardi V, Wald J. 1987. Discounting an adverse maternal effect on severity of neurofibromatosis. Pediatrics 79:386–93.

Sachidanandam R, Weissman D, Schmidt S, Kakol J, Stein L, Marth G, Sherry S, Mullikin J, Mortimore B, Willey D, Hunt S, Cole C, Coggill P, Rice C, Ning Z, Rogers J, Bentley D, Kwok P, Mardis E, Yeh R, Schultz B, Cook L, Davenport R, Dante M, Fulton L, Hillier L, Waterston R, McPherson J, Gilman B, Schaffner S, Van Etten W, Reich D, Higgins J, Daly M, Blumenstiel B, Baldwin J, Stange-Thomann N, Zody M, Linton L, Lander E, Altshuler D. 2001. A map of human genome sequence variation containing 1.42 million single nucleotide polymorphisms. Nature 409:928–33.

Samuelsson B, Axelsson R. 1981. Neurofibromatosis: a clinical and genetic study of 96 cases in Gothenburg, Sweden. Acta Derm Venereol [Suppl] (Stockh) 95:67–71.

Snead M, Yates J. 1999. Clinical and molecular genetics of Stickler syndrome. J Med Genet 36:353–9.

Szudek J, Birch P, Friedman JM, NNFF International Database Participants. 2000a. Growth in North American white children with neurofibromatosis 1 (NF1). J Med Genet 37:933–8.

Szudek J, Birch P, Riccardi VM, Evans DG, Friedman JM. 2000b. Associations of clinical features in neurofibromatosis 1 (NF1). Genet Epidemiol 19:429–39.

Tonsgard J, Yalavarthi K, Cushner S, Short M, Lindgren V. 1997. Do NF1 gene deletions result in a characteristic phenotype? Am J Med Genet 73:80–86.

Wicking C, Bale A. 1997. Molecular basis of the nevoid basal cell carcinoma syndrome. Curr Opin Pediatr 9:630–5.

Genetic Epidemiology 24: 265–272 (2003)

Exploring the "Two-Hit Hypothesis" In NF2: Tests of Two-hit and Three-hit Models of Vestibular Schwannoma Development

Ryan Woods,[1] J. M. Friedman,[2*] D. Gareth R Evans,[3] Michael E. Baser,[4] and Harry Joe[1]

[1]*Department of Statistics, University of British Columbia, Vancouver, Canada*
[2]*Department of Medical Genetics, University of British Columbia, Vancouver, Canada*
[3]*St. Mary's Hospital, Manchester, United Kingdom*
[4]*Los Angeles, California*

Neurofibromatosis 2 (NF2) is a genetic disease that occurs in approximately 1 in 40,000 live births. Almost all affected individuals develop bilateral tumors of Schwann cells that surround the vestibular nerves; these tumors are known as vestibular schwannomas (VS). Evidence from molecular genetic studies suggests that at least two mutations are involved in formation of VS in patients with NF2. Several authors proposed probabilistic models for this process in other tumors, and showed that such models are consistent with incidence data. We evaluated two different probabilistic models for a "2-hit" hypothesis for VS development in NF2 patients, and we present results from fitting these models to incidence data. Molecular evidence does not exclude the possibility that additional hits are necessary for the development of VS, and we also assessed a "3-hit" model for tumor formation. The "3-hit" model fits the data marginally better than one of the "2-hit" models and much better than the other "2-hit" model. Our findings suggest that more than two mutations may be necessary for VS development in NF2 patients. *Genet Epidemiol* 24:265–272, 2003. © 2003 Wiley-Liss, Inc.

Key words: neurofibromatosis 2; vestibular schwannoma; Knudson's hypothesis; tumorigenesis

Grant sponsor: Department of the Army; Grant numbers: NF960003, NF990038; Grant sponsor: Vancouver Chapter, Acoustic Neuroma Association of Canada; Grant sponsor: Summer Student Grant; British Columbia Medical Services Foundation.
*Correspondence to: J.M. Friedman, M.D., Ph.D., Department of Medical Genetics, University of British Columbia, 6174 University Blvd., Room 300H, Vancouver, British Columbia V6T 1Z3, Canada. E-mail: frid@interchange.ubc.ca
Received for publication 3 June 2002; Revision accepted 5 November 2002
Published online in Wiley InterScience (www.interscience.com).
DOI: 10.1002/gepi.10238

INTRODUCTION

Probabilistic models for tumorigenesis have been used extensively in genetic epidemiology to generate and test hypotheses about the genetic mechanisms that are responsible for tumor development [Armitage and Doll, 1954; Hethcote and Knudson, 1978; Knudson, 1971; Moolgavkar and Knudson, 1981; Moolgavkar and Luebeck, 1992]. The common theme incorporated into most of these models is that a tumor cell is assumed to be the outcome of a sequence of irreversible events (mutations). These events progressively transform normal tissue cells into tumor cells. Chu [1987] provided a clear, nonmathematical introduction to these models.

Knudson [1971] and Knudson et al. [1975] proposed a two-stage model for cancer initiation to describe the incidence of both sporadic and hereditary retinoblastomas. According to this model, a tissue cell is transformed into a tumor cell after sustaining two irreversible mutations. This is often referred to as a "2-hit" model, where the term "hit" refers to mutations in a cell. The first of these mutations is assumed to occur in one of two ways: in hereditary cases, individuals inherit the first mutation; in sporadic cases, the first mutation occurs by chance in a somatic-cell progenitor of the tumor. The second mutation is assumed to occur by chance in a tumor-cell progenitor in both hereditary and sporadic cases.

Subsequent molecular genetic studies demonstrated that this model was correct in that both alleles of the *RB1* locus are almost always mutated in retinoblastoma [Knudson, 1996]. Moreover, one mutant *RB1* allele is inherited and the second allele is lost somatically in tumors in patients with hereditary retinoblastoma, whereas both alleles are lost somatically in sporadic retinoblastomas,

as predicted [Knudson, 1996]. Many other hereditary tumors, including those associated with Li-Fraumeni syndrome [Evans and Lozano, 1997], hereditary breast and ovarian cancer syndrome [Hofmann and Schlag, 2000], hereditary adenomatous polyposis [Aaltonen, 2000], and neurofibromatosis 1 [Parada, 2000], have been shown to involve a similar "2-hit" mechanism. Functional or actual loss of both alleles of these and other tumor supressor genes is now known to be an important pathogenic mechanism in most neoplasms [Fearon, 2001].

However, it is clear that the pathogenesis of many tumors involves more than just two "hits." Tumors often exhibit mutations or functional alteration of several different genetic loci, and none of these changes may be sufficient by itself to produce a malignant phenotype [Strachan and Read, 1999]. It is, therefore, of some interest to consider more complex epidemiological models than that originally formulated by Knudson [1996]. Moolgavkar and Venzon [1979] introduced an alternate mathematical formulation of the 2-hit model that incorporated both the growth and death of cells in the tissue at risk; this model is depicted in Fig. 1. This formulation is also convenient to extend to a 3-hit model; such a model (Fig. 2) would require that a tissue cell sustain three mutations to develop into a tumor cell.

Neurofibromatosis 2 (NF2) is a dominantly inherited tumor predisposition syndrome [MacCollin, 1999; MacCollin and Stemmer-Rachamimov, 1999]. Most affected patients develop bilateral vestibular schwannomas (VS), and many develop schwannomas of other nerves and meningiomas. Mutations of both alleles of the *NF2* locus have been demonstrated in tumors from patients with NF2 as well as in sporadic VS in patients who do not have NF2 [Evans et al., 2000]. In accordance with the hypothesis of Knudson [1996], a germline *NF2* mutation can be demonstrated in most, and is presumed to exist in all, patients with NF2 [Evans et al., 2000].

The purpose of this study is to fit a selection of multistage models for tumor-cell development to VS data from patients with NF2. VS are tumors of Schwann cells that surround the vestibular nerves;

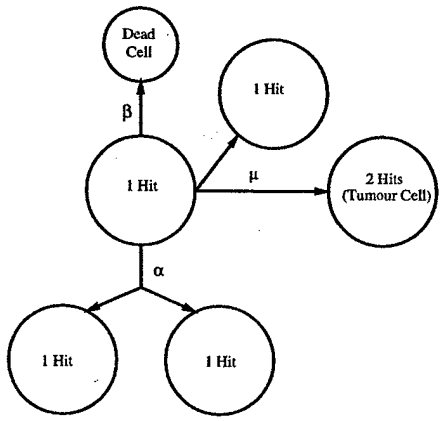

Fig. 1. Two-hit model for development of vestibular schwannomas in NF2 patients. All cells in the body have at least one mutation, inherited through the germline. Circles denote cells in a given stage of the model, and arrows denote possible transitions between stages of the model. α, β, and μ represent cell growth, death, and mutation rates, respectively.

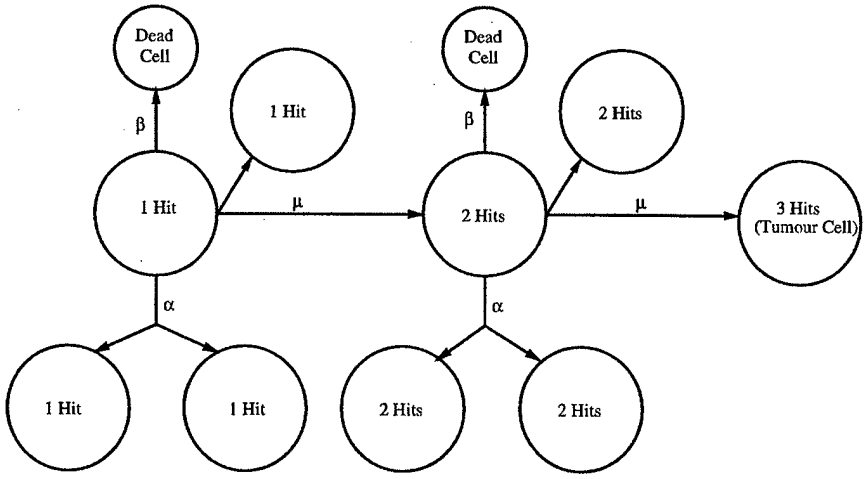

Fig. 2. Three-hit model for development of vestibular schwannomas in NF2 patients. All cells in the body have at least one mutation, inherited through the germline. Circles denote cells in a given stage of the model, and arrows denote possible transitions between stages of the model α, β, and μ represent cell growth, death, and mutation rates, respectively.

hence the tissue at risk for our study is the pool of Schwann cells that surround both vestibular nerves. We will examine the fit of two different 2-hit models and a 3-hit model to our patient data.

MODELS AND METHODS

DESCRIPTION OF DATA

The patient data used to fit the models were obtained from the United Kingdom NF2 Registry, which contains clinical and genetic information on a large number of NF2 patients ascertained through medical specialists throughout the United Kingdom. Information available for each patient included age at onset of first VS, whether the VS was unilateral or bilateral, and family history. The database contains 163 NF2 probands who had sufficient information for inclusion in this study. For the analyses that follow, we assume that this sample is representative of all NF2 patients. The tumor of interest is the VS, and the dependent variable that we model is the age at occurrence of the first tumor cell. We assume that the time between development of the first tumor cell and the age at which the first VS is detected is roughly constant and therefore does not affect model comparisons. Although all patients included in our analysis have bilateral VS, we model only the time to diagnosis of the first VS in these patients.

TWO-HIT MODEL OF MOOLGAVKAR AND VENZON [1979]

The two-mutation model for hereditary tumors presented by Moolgavkar and Venzon [1979] is appropriate for NF2 patients who have one mutant copy of the *NF2* gene present in all cells at birth. According to this model, a Schwann cell in an NF2 patient becomes a tumor cell when a second mutation occurs, inactivating the normal *NF2* gene. This model assumes that in a small interval of time, Δt, a Schwann cell divides into two Schwann cells with probability $\alpha\Delta t+o(\Delta t)$; dies with probability $\beta\Delta t+o(\Delta t)$; or mutates to form a tumor cell with probability $\mu\Delta t+o(\Delta t)$. The probability that more than one event occurs in this interval of time is $o(\Delta t)$. We will use the notation $\boldsymbol{\theta}$ to denote the vector of model parameters (α, β, μ). Additionally, it is assumed that cells behave independently of one another and that mutations occur during cell division. We also assume that Schwann cells with one mutation are phenotypically identical and have an identical rate of cellular proliferation as normal Schwann cells.

We will refer to two fundamental statistical quantities throughout this paper, namely the hazard function and the probability distribution function. Let $h(t|\boldsymbol{\theta})$ denote the hazard function for the random variable T; here $\boldsymbol{\theta}$ is used to denote the vector of parameters from a parametric model for T. This function represents the instantaneous risk of tumor at time t in a previously tumor-free tissue and is defined in the following fashion:

$$h(t|\boldsymbol{\theta}) = \lim_{\Delta t \to 0} \frac{\Pr(t \le T < t + \Delta t | T \ge t; \boldsymbol{\theta})}{\Delta t}. \quad (1)$$

The probability distribution function for the random variable T, denoted by $F(t|\boldsymbol{\theta})$, represents the probability that an individual will develop a tumor prior to or at time t. We can express $F(t|\boldsymbol{\theta})$ in terms of the hazard function given above:

$$F(t|\boldsymbol{\theta}) = 1 - \exp\left\{-\int_0^t h(u|\boldsymbol{\theta})du\right\}. \quad (2)$$

It is worth noting that the probability density function for T is given by $f(t|\boldsymbol{\theta}) = F'(t|\boldsymbol{\theta}) = h(t|\boldsymbol{\theta})\{1 - F(t|\boldsymbol{\theta})\}$.

For this model, Moolgavkar and Venzon [1979] showed that the hazard function for the random variable T, representing the age at occurrence of the somatic mutation (i.e., of the first tumor cell), is given by:

$$h(t|\boldsymbol{\theta}) = -\alpha\phi(1, 0, t) + (\alpha + \beta + \mu) - \beta(\phi(1, 0, t))^{-1},$$

where

$$\phi(1, 0, t) = \frac{C_1 - C_2\left[\frac{1-C_1}{1-C_2}\exp\{\alpha(C_1 - C_2)t\}\right]}{1 - \left[\frac{1-C_1}{1-C_2}\exp\{\alpha(C_1 - C_2)t\}\right]}. \quad (3)$$

and

$$\begin{aligned} C_1 &= \frac{1}{2\alpha}(\alpha + \beta + \mu) - \frac{1}{2\alpha}\sqrt{\alpha^2 - 2\alpha\beta + 2\alpha\mu + \beta^2 + 2\beta\mu + \mu^2}, \\ C_2 &= \frac{1}{2\alpha}(\alpha + \beta + \mu) + \frac{1}{2\alpha}\sqrt{\alpha^2 - 2\alpha\beta + 2\alpha\mu + \beta^2 + 2\beta\mu + \mu^2}, \end{aligned} \quad (4)$$

Note that $h(t|\boldsymbol{\theta})$ is the hazard function for T assuming a single initial tissue cell. If we assume that the tissue contains N cells initially, then the hazard function for the entire tissue, $h_N(t|\boldsymbol{\theta})$, is simply $Nh(t|\boldsymbol{\theta})$; this follows directly from the assumption that the cells behave independently

of one another. A likelihood for the data can be constructed in the customary fashion [Lawless, 1982], with patient i, having tumor onset time t_i, contributing $h_N(t_i|\theta)\{\{1-F_N(t_i|\theta)\}\}$ to the likelihood. The likelihood, as a function of θ, can be maximized by means of a quasi-Newton algorithm [Nash, 1990] to obtain maximum likelihood estimates (MLE) of the model parameters.

NONHOMOGENEOUS POISSON PROCESS

Another approach to modeling this two-mutation process is to make some additional assumptions regarding the division and death of tissue cells. If the tissue were assumed to grow according to a deterministic process, then the number of cells present in the tissue at any time t can be given by a function $X(t)$. If a reasonable functional form for $X(t)$ could be chosen and it is assumed that there is a small chance that any of the tissue cells mutate, then the generation of tumor cells can be modeled according to a nonhomogeneous Poisson process. If we assume that the rate at which tissue cells mutate is a constant μ, then the intensity of the process is simply $h(t|\mu) = \mu X(t)$, which is of course the hazard function for the age at occurrence of the somatic mutation. We will refer to this model as the "Poisson" model.

A likelihood for the data is easily constructed for this model, and the MLE for the mutation rate has a simple, closed form solution. Again, the contribution of patient i to the likelihood function is $f(t_i|\mu) = h(t_i|\mu)\{1-F(t_i|\mu)\}$, and the MLE for the mutation rate, estimated from a sample of n patients, is given by:

$$\hat{\mu} = \frac{n}{\sum_{i=1}^{n}\left(\int_0^{t_i} X(s)ds\right)}. \qquad (5)$$

It is important to note that the choice of the function $X(t)$ clearly influences the estimate of the communication rate. The integral in the expression for the estimate of the mutation rate may require numerical integration if the function chosen for $X(t)$ is not conveniently integrable.

THREE-HIT MODEL

Thus far we have assumed that tumorigenesis is a two-mutation process, and that a tumor cell is generated when a normal Schwann cell sustains two irreversible mutations. Here we explore a model that assumes that a tumor cell is the end result of a normal tissue cell sustaining three irreversible mutations; this model will be referred to as the "3-hit" model. In NF2 patients, the first of these mutations has already been sustained prior to birth, and the two subsequent mutations are assumed to occur by chance in the somatic tissue. We assume for simplicity that these two mutations occur at a constant, common mutation rate μ. We also assume that Schwann cells with one mutation or with two mutations have identical rates of cellular proliferation as normal Schwann cells. Moolgavkar and Luebeck [1990] presented a model that is appropriate for this process, and Heidenreich et al. [1997] discussed parameter identifiability issues with the model. It is possible to estimate a reduced number of model parameters without assuming equal mutation rates in the two stages of the model, but a different parameterization would require additional assumptions and may yield estimates that are difficult to interpret.

Again we denote the number of Schwann cells in our tissue of interest by $X(t)$; recall that these cells already carry a single mutation. As in the case of the Poisson model, we must specify a functional form for $X(t)$ to fit our model to patient data. We will refer to cells that have sustained a second but not a third mutation as intermediate cells, and cells that have sustained three mutations as tumor cells. In a small interval of time Δt, the probability that an intermediate cell is generated by the mutation of a tissue cell is $\mu X(t)\Delta t + o(\Delta t)$. The probability that more than one intermediate cell is generated in this fashion is $o(\Delta t)$. The growth, death, and mutation of the intermediate cells are assumed to follow a birth-death process. Again, in a small interval of time Δt, an intermediate cell divides into two intermediate cells with probability $\alpha\Delta t + o(\Delta t)$, dies with probability $\beta\Delta t + o(\Delta t)$, and divides into an intermediate cell and a tumor cell with probability $\mu\Delta t + o(\Delta t)$. The probability of more than one such event occurring in this time interval is $o(\Delta t)$. Moolgavkar and Luebeck [1990] showed that for such a model, the hazard function is given by:

$$h(t|\theta) = \mu^2 \int_0^t X(s)\,\exp\{g(\theta; t-s)\}ds, \qquad (6)$$

where

$$g(\theta; t-s) = 2\alpha C_1(t-s) + 2\log\left\{\frac{1-\frac{1-C_1}{1-C_2}}{1-\frac{1-C_1}{1-C_2}\exp\{\alpha(C_1-C_2)(t-s)\}}\right\} - (\alpha+\beta+\mu)(t-s), \qquad (7)$$

and C_1 and C_2 are defined as above.

TABLE I. Summary of assumptions used to estimate number of vestibular nerve Schwann cells for Poisson and 3-hit models, and references that support assumptions chosen

Factor	Range	Midvalue	References
Number of vestibular nerves	2	2	
Number of axons in each vestibular nerve	14,000–22,000	18,500	Rasmussen, 1940; Natural and Schuknecht, 1972; Bergstrom, 1973; Richter, 1980
Length	5–7 mm	6 mm	F.H. Linthicum, Jr., personal communication
Internode distance (distance covered by one Schwann cell)	0.5–1.0 mm	0.75 mm	Natout et al., 1987; Schalow, 1989; Vizoso, 1950

A likelihood for the data as a function of θ can be constructed in a similar fashion to the previous models, and estimates for the model parameters can be found by numerically maximizing the likelihood. The integral in Equation (6) can be calculated numerically.

RESULTS

To enable the fitting of both the Poisson and 3-hit models to patient data, we must include an estimate of the number of Schwann cells in the tissue as a function of age. We assume that this function is constant in the fitting of both of these models; thus for any time t, we assume $X(t)$=300,000. This number is calculated from the estimates summarized in Table I, as twice the product of the number of axons found in each vestibular nerve and the length of a nerve axon, divided by the internode distance. Using the midvalues in Table I, we get $2 \times 18{,}500 \times 6.0/0.75$=300,000 as the total number of Schwann cells in the pool that gives rise to a vestibular schwannoma.

We assume that this number of cells remains roughly constant [Vizoso, 1950] from about 24 weeks postconception, when it is first achieved, through adulthood. The mutations that give rise to a tumor must therefore occur during tissue maintenance, as rare cell divisions are triggered to replace tissue cells that die from time to time.

These assumptions mean that the value N for the 2-hit model will be 300,000, and that the maximum value the function $X(t)$ can take for the Poisson and 3-hit models is also 300,000. We will comment further on these assumptions in the Discussion.

Any integration required in the likelihood of the 3-hit model has been performed numerically with Romberg integration [Mathews, 1992]. Note that the integral in the expression for the Poisson likelihood is simplified in the case where $X(t)$ is constant and can be done analytically, and results in an exponential distribution for T.

TABLE II. Summary of parameter estimates from model fitting

Model: 2-hit model		
Value of log-likelihood: −669.0		
Akaike information criterion: −672.0		
Parameter	Estimate	SE
α	3.73×10^{-1}	1.39×10^{-1}
β	3.27×10^{-1}	1.39×10^{-1}
μ	3.76×10^{-8}	1.00×10^{-8}
Model: Poisson model		
Value of log-likelihood: −717.0		
Akaike information criterion: −718.0		
Parameter	Estimate	SE
μ	1.11×10^{-7}	0.09×10^{-7}
Model: 3-hit model		
Value of log-likelihood: −651.3		
Akaike information criterion: −654.3		
Parameter	Estimate	SE
α	8.26×10^{-1}	0.71×10^{-1}
β	8.21×10^{-1}	0.71×10^{-1}
μ	7.15×10^{-5}	0.59×10^{-5}

The MLEs for the 2-hit model parameters are presented with their estimated standard errors in Table II; the value of the log-likelihood evaluated at the MLE is also provided. The estimated model parameters can be input into the distribution function $F_N(t|\theta)$ and plotted by age to provide a comparison between the distribution produced by the model and the empirical distribution for the data. The estimated and empirical distributions are plotted in Fig. 3. The overall model fit is reasonable; however, the model-estimated incidence of tumor is much higher than the observed incidence for ages less than 20 years.

The estimate of the mutation rate from the Poisson model, its estimated standard error, and the value of the log-likelihood evaluated at the estimate are presented in Table II. The Poisson model-estimated distribution function for age at onset of the first tumor cell is plotted in Fig. 3 to allow for comparison with the empirical distribution function and the 2-hit model. The fit of the Poisson model to the data is quite poor.

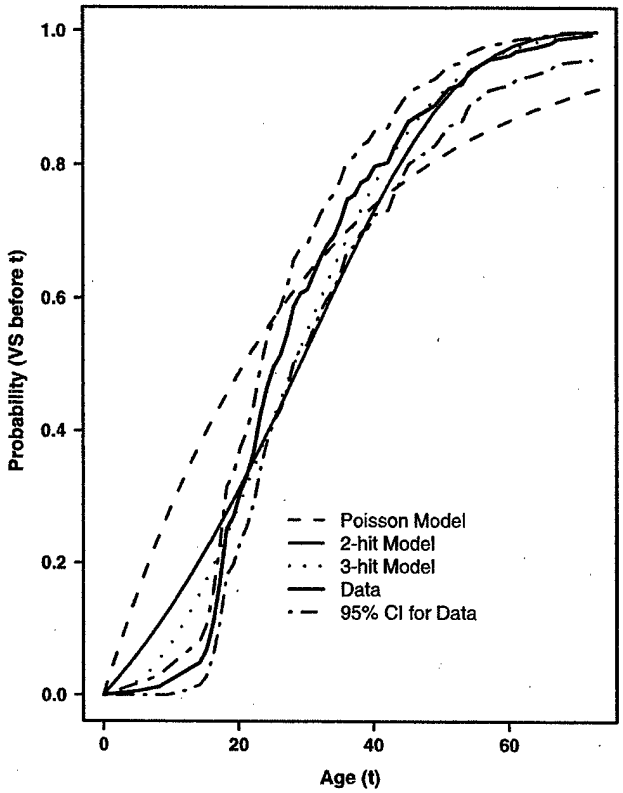

Fig. 3. Model-fitted distribution functions from three models and empirical distribution function for data. CI, confidence interval.

A similar display of model parameter estimates is provided in Table II for the 3-hit model. The model-estimated distribution function for the 3-hit model is also included in Fig. 3. The model-estimated distribution function fits the data fairly closely for the 3-hit model, except for ages less than 18.

An additional method of comparing the fit of the models to the data is to use the Akaike information criterion (AIC) [Sakamoto et al., 1986], which adds a penalty term for the number of model parameters to the log-likelihood. For our summaries, we define AIC to be $\log(\ell) - p$, where ℓ is the likelihood for the data and p is the number of model parameters. The ordering of the three models according to this criterion is consistent with the quality of model fit observed in Fig. 3: the 3-hit model provides the best fit to the data, the 2-hit model provides the next best fit, and the Poisson model provides the poorest fit.

DISCUSSION

The models we have described all make a common assumption regarding the process of mutation in the tissue: that mutations can only occur during cell divisions involved in the process of tissue maintenance once the tissue has reached its maximum size of 300,000 cells. This implies that cells do not sustain additional mutations in the period of time between conception and about 24 weeks postconception, when the pool of normal Schwann cells associated with the vestibular nerves reaches it definitive size [Vizoso, 1950]. This assumption is not true, and it should be possible to develop a model in which cells are at risk of mutating at any time from conception, through determination of the small pool of precursor cells that gives rise to the Schwann cells of the vestibular nerve, to the rapid expansion of this pool to its maximum size, and afterwards as these cells occasionally divide in the process of cell maintenance. Moolgavkar and Luebeck [1990] discussed a model in which the parameters are assumed to vary over time. Applying models of this kind to our data would be of interest, and will be the focus of further work.

Vestibular schwannomas arise through a process of mutation in one of the Schwann cells associated with the vestibular nerves. Our assumed value for the number of Schwann cells in

this normal tissue pool is 300,000; here we discuss the sensitivity of the results to this assumption. We refit all models assuming a range of values for this parameter, to determine the effect on estimates obtained for other model parameters and fitted distribution functions. We tried values between 200,000–400,000 for all models, and in all cases the effect on the fitted distribution functions was negligible. The values of the log-likelihoods evaluated at the parameter estimates were also unchanged by these perturbations of the assumed number of cells in the tissue. The actual values of the other parameter estimates did change with different assumed values for the number of cells in the tissue. For the Poisson model, the estimated mutation rates varied from 8.35^{-8} to 1.67×10^{-6} for 400,000 to 200,000 tissue cells. For the 2-hit model, the mutation rate varied between 2.82×10^{-8} to 5.65×10^{-8} for 400,000 to 200,000 tissue cells. Although the estimates for the cell division and death parameters also varied across fittings, the difference between these parameters, i.e., the net cell proliferation rate, remained roughly constant. For the 3-hit model, we saw mutation rate estimates in the range from 8.73×10^{-5} to 6.20×10^{-5} for 200,000 to 400,000 tissue cells. Again, the cell division and death rate estimates varied across fittings, but the difference between these two parameters remained roughly constant across the fittings.

In summary, we do not feel that our results are sensitive to modest perturbations of the assumed number of Schwann cells in the normal tissue pool from which a VS arises. The rate-limiting step in the development of VS in these models is the mutation rate. Although other events, including proliferation of the single mutated tumor cell to form a mass large enough to be detected clinically, are involved in tumor formation, we assumed that these processes do not vary among tumors. This assumption is incorrect but should not influence our conclusions as long as these processes are independent of the variables included in the model.

The Poisson model provides a poor fit to the data, but the 2-hit and 3-hit models fit the data well, except for ages less than 18 years. The 3-hit model provides a marginally better fit according to Figure 3 and the Akaike information criterion. The result for the Poisson model is not surprising, as it estimates only a single parameter from the data. Thus the Poisson model is much less flexible than the other two models. The slightly superior fit of the 3-hit model is compatible with the possibility that the pathogenesis of these tumors requires more than the two mutations of a Schwann cell. Other tumors, most notably colon cancer, have been shown to develop after a multistep pathogenesis. Moolgavkar and Luebeck [1992] used models similar to those described here to model the multistep pathogenesis of colon cancer accurately. Other authors also discussed the pathogenesis of colon cancer as a multistage process [Chung, 2000; Kinzler and Vogelstein, 1996]. The notion that more than two mutations are required to produce a schwannoma in NF2 is supported by molecular genetic studies [Lamszus et al., 2000; Bruder et al., 1999]. There is clearly a need for further molecular genetic studies to examine the effect of other genes on the development of NF2-associated tumors.

The methodology discussed here can also be applied to patient data for other NF2 tumors, such as meningiomas and epidymomas. As well, it would be interesting to examine the effect of incorporating genotype information into these models. Genotype-phenotype correlations have been observed in NF2, and the inclusion of a patient's genotype may result in a model that fits the data more closely.

ACKNOWLEDGMENTS

We thank Drs. Jean Moore and Fred Linthicum, Jr., for generously providing expertise and data on the neuroanatomy of the vestibular nerve.

REFERENCES

Aaltonen LA. 2000. Hereditary intestinal cancer. Semin Cancer Biol 10:289–98.

Armitage P, Doll R. 1954. The age distribution of cancer and a multistage theory of carcinogenesis. Br J Cancer 8:1–12.

Bergström B. 1973. Morphology of the vestibular nerve. II. The number of myelinated vestibular nerve fibers in man at various ages. Acta Otolaryngol (Stockh) 76:173–9.

Bruder CE, Ichimura K, Blennow E, Ikeuchi T, Yamaguchi T, Yuasa Y, Collins VP, Dumanski JP. 1999. Severe phenotype of neurofibromatosis type 2 in a patient with a 7.4-MB constitutional deletion on chromosome 22: possible location of a neurofibromatosis type 2 modifier gene? Genes Chromosomes Cancer 25:184–90.

Chu KC. 1987. A nonmathematical view of mathematical models for cancer. J Chronic Dis 40:163S–170S.

Chung DC. 2000. The genetic basis of colorectal cancer: insights into critical pathways of tumorigenesis. Gastroenterology 119:854–65.

Evans DG, Sainio M, Baser ME. 2000. Neurofibromatosis type 2. J Med Genet 37:897–904.

Evans SC, Lozano G. 1997. The Li-Fraumeni syndrome: an inherited susceptibility to cancer. Mol Med Today 3:390–5.

Fearon ER. 2001. Tumor-suppressor genes. In: Scriver CR, Beaudet AL, Sly WS, Valle D, editors. The metabolic & molecular bases of inherited disease, 8th ed. New York: McGraw-Hill. p 665–74.

Heidenreich WF, Luebeck EG, Moolgavkar SH. 1997. Some properties of the hazard function of the two-mutation clonal expansion model. Risk Anal 17:391–9.

Hethcote HW, Knudson AG. 1978. Model for the incidence of embryonal cancers: application to retinoblastoma. Proc Nat Acad Sci USA 75:2453–7.

Hofmann W, Schlag PM. 2000. BRCA1 and BRCA2–breast cancer susceptibility genes. J Cancer Res Clin Oncol 126:487–96.

Kinzler KW, Vogelstein B. 1996. Lessons from hereditary colorectal cancer. Cell 87:159–70.

Knudson AG. 1971. Mutation and cancer: statistical study of retinoblastoma. Proc Natl Acad Sci USA 68:820–3.

Knudson AG. 1996. Hereditary cancer: two hits revisited. J Cancer Res Clin Oncol 122:135–40.

Knudson AG, Hethcote HW, Brown BW. 1975. Mutation and childhood cancer: a probabilistic model for the incidence of retinoblastoma. Proc Natl Acad Sci 72:5116–20.

Lamszus K, Vahldiek F, Mautner VF, Schichor C, Tonn J, Stavrou D, Fillbrandt R, Westphal M, Kluwe L. 2000. Allelic losses in neurofibromatosis 2-associated meningiomas. J Neuropathol Exp Neurol 59:504–12.

Lawless JF 1982. Statistical models and methods for lifetime data. New York: Wiley.

MacCollin M. 1999. Neurofibromatosis 2: clinical aspects. In: Friedman JM, Gutmann DH, MacCollin M, Riccardi VM, editors. Neurofibromatosis: phenotype, natural history, and pathogenesis, 3rd ed. Baltimore: Johns Hopkins University Press. p 299–326.

MacCollin M, Stemmer-Rachaminov AO. 1999. Neurofibromatosis 2: associated tumors. In: Friedman JM, Gutmann DH, MacCollin M, Riccardi VM, editors. Neurofibromatosis: phenotype, natural history, and pathogenesis, 3rd ed. Baltimore: Johns Hopkins University Press. p 327–62.

Mathews JH. 1992. Numerical methods for mathematics, science, and engineering, 2nd ed. Englewood Cliffs, NJ: Prentice Hall.

Moolgavkar SH, Knudson AG. 1981. Mutation and cancer: a model for human carcinogenesis. J Natl Cancer Inst 66:1037–51.

Moolgavkar SH, Luebeck G. 1990. Two-event model for carcinogenesis: biological, mathematical, and statistical considerations. Risk Anal 10:323–41.

Moolgavkar SH, Luebeck G. 1992. Multistage carcinogenesis: population-based model for colon cancer. J Natl Cancer Inst 84:610–7.

Moolgavkar SH, Venzon DJ. 1979. Two-event models for carcinogenesis: incidence curves for childhood and adult tumors. Math Biosci 47:55–77.

Nash JC. 1990. Compact numerical methods for computers: linear algebra and function minimisation, 2nd ed. New York: Hilger.

Natout MA, Terr LI, Linthicum FH, House WF. 1987. Topography of vestibulocochlear nerve fibers in the posterior cranial fossa. Laryngoscope 97:954–8.

Naufal PM, Schuknecht HF. 1972. Vestibular, facial, and ocululomotor neuropathy in diabetes mellitus. Arch Otolaryngol 96:468–74.

Parada LF. 2000. Neurofibromatosis type 1. Biochim Biophys Acta 1471:13–9.

Rasmussen AT. 1940. Studies of the VIIIth cranial nerve of man. Laryngoscope 50:67–83.

Richter E. 1980. Quantitative study of human Scarpa's ganglion and vestibular sensory epithelia. Acta Otolaryngol (Stockh) 90:199–208.

Sakamoto Y, Ishiguro M, Kitagawa G. 1986. Akaike information criterion statistics. Tokyo: KTK Scientific Publishers.

Schalow G. 1989. Efferent and afferent fibers in human sacral ventral nerve roots: basic research and clinical implications. Electromyogr Clin Neurophysiol 29:33–53.

Strachan T, Read AP. 1999. Human molecular genetics, 2nd ed. New York: Wiley-Liss. p 427–44.

Vizoso AD. 1950. The relationship between internodal length and growth in human nerves. J Anat 82:342–53.

Genetic Epidemiology 23:245–259 (2002)

Intrafamilial Correlation of Clinical Manifestations in Neurofibromatosis 2 (NF2)

Y. Zhao,[1] R.A. Kumar,[2] M.E. Baser,[3] D.G.R. Evans,[4] A. Wallace,[4] L. Kluwe,[5] V.F. Mautner,[6] D.M. Parry,[7] G.A. Rouleau,[8] H. Joe,[1] and J.M. Friedman[2]*

[1]Department of Statistics, University of British Columbia, Vancouver, British Columbia, Canada
[2]Department of Medical Genetics, University of British Columbia, Vancouver, British Columbia, Canada
[3]Los Angeles, California
[4]Department of Medical Genetics, St. Mary's Hospital, Manchester, United Kingdom
[5]Department of Neurology, Klinikum Nord Ochsenzoll, Hamburg, Germany
[6]Department of Neurosurgery, University Hospital Eppendorf, Hamburg, Germany
[7]Genetic Epidemiology Branch, Division of Cancer Epidemiology and Genetics, National Cancer Institute, National Institutes of Health, Bethesda, Maryland
[8]Center for Research in Neuroscience, McGill University, Montreal, Quebec, Canada

Measuring correlation in clinical traits among relatives is important to our understanding of the causes of variable expressivity in Mendelian diseases. Random effects models are widely used to estimate intrafamilial correlations, but such models have limitations. We incorporated survival techniques into a random effects model so that it can be used to estimate intrafamilial correlations in continuous variables with right censoring, such as age at onset. We also describe a negative-binomial gamma mixture model to determine intrafamilial correlations of discrete (e.g., count) data. We demonstrate the utility of these methods by analyzing intrafamilial correlations among patients with neurofibromatosis 2 (NF2), an autosomal-dominant disease caused by mutations of the *NF2* tumor-suppressor gene. We estimated intrafamilial correlations in age at first symptom

*Correspondence to: J.M. Friedman, M.D., Ph.D., Department of Medical Genetics, University of British Columbia, 6174 University Blvd., Room 300H, Vancouver, British Columbia V6T 1Z3, Canada. E-mail: frid@interchange.ubc.ca
Received for publication 4 March 2002; Revision accepted 10 April 2002
Published online in Wiley InterScience (www.interscience.wiley.com). DOI: 10.1002/gepi.10181

of NF2, age at onset of hearing loss, and number of intracranial meningiomas in 390 NF2 nonprobands from 153 unrelated families. A significant intrafamilial correlation was observed for each of the three features: age at onset (0.35; 95% confidence interval (CI) 0.23–0.47), age at onset of hearing loss (0.51; 95% CI, 0.35–0.64), and number of meninginomas (0.29; 95% CI, 0.15–0.43). Significant correlations were also observed for age at first symptom within NF2 families with truncating mutations (0.41; 95% CI, 0.06–0.68) or splice-site mutations (0.29; 95% CI, 0.03–0.51), for age at onset of hearing loss within families with missense mutations (0.67; 95% CI, 0.18–0.89), and for number of meningiomas within families with splice-site mutations (0.39; 95% CI, 0.13–0.66). Our findings are consistent with effects of both allelic and nonallelic familial factors on the clinical variability of NF2. Genet. Epidemiol. 23:245–259, 2002.

Key words: intrafamilial correlation; random effects model; right censoring; negative-binomial gamma mixture model; neurofibromatosis 2

INTRODUCTION

Variable expressivity is common in Mendelian diseases, especially those that are transmitted as autosomal-dominant traits. Variable expressivity may be manifested in many different ways, including variation in age at onset, types and numbers of clinical features that develop, overall disease severity, rate of progression, length of course, or final outcome. Many different genetic and nongenetic causes of variable expressivity may exist and act alone or in combination [Scriver and Waters, 1999; Dipple and McCabe, 2000].

Random effects models are used to estimate intraclass and intrafamilial associations by dividing phenotypic variance into components that are attributable to different sources of variation. Although methods based on sums of squares are widely used to estimate these variance components, this approach is not applicable when censoring is present. Moreover, since the standard random effects model is based on normality assumptions, it is not appropriate when the data are discrete. In this paper, we extended the standard random effects model to overcome these limitations. We demonstrate the use of these extended models by analyzing the familiality of selected clinical features of neurofibromatosis 2 (NF2).

NF2 is a highly penetrant Mendelian disease that is transmitted as an autosomal-dominant trait. The incidence of NF2 at birth has been estimated to be between 1 in 33,000 and 1 in 40,000 [Evans et al., 1992a]. Age at presentation is usually between 11–30 years, although younger cases and diagnoses in the fourth and fifth decades also occur [Evans et al., 1992a; Parry et al., 1994]. The hallmark of NF2 is bilateral vestibular schwannomas (VSs), but meningiomas, nonvestibular schwannomas, and presenile cataracts are also common. NF2 symptoms are usually related to "tumor burden," i.e., the number, size, and location of tumors, and may include hearing loss, tinnitus, vertigo, seizures, facial weakness, and visual impairment [Evans et al., 1992c; Parry et al., 1994].

The responsible gene, *NF2*, has been identified and sequenced [Trofatter et al., 1993; Rouleau et al., 1993]. Pathogenic mutations have been found throughout the gene, and a different mutation occurs in almost every family. These mutations are of

various types, but most can be classified as nonsense, frameshift, splice-site, missense, or large deletions [MacCollin, 1999].

Clinical studies indicate that the phenotypic expression and natural history of NF2 tend to be similar within a family, and that more variability occurs between families [Evans et al., 1992a; Parry et al., 1994, 1996]. Previous studies demonstrated allele-phenotype correlations for certain *NF2* mutation classes. In general, constitutional truncating mutations (frameshift or nonsense) are associated with severe disease, missense mutations and large deletions with milder disease, and splice-site mutations with variable disease severity, although exceptions do occur [Kluwe et al., 1996, 1998; Parry et al., 1996; Ruttledge et al., 1996; Evans et al., 1998a].

Despite the general similarity in disease severity among affected relatives, substantial phenotypic differences may occur within families [Mautner et al., 1996; Baser et al., 1996b]. It is not known whether this variability occurs by chance or is caused by modifying genes at other loci [Bruder et al., 1999], coincident environmental exposures, or some combination of factors [Baser et al., 1996b].

We developed statistical methods to estimate the magnitude of intrafamilial correlations for continuous variables with censored observations and for count variables. We used these methods to test whether the phenotypic similarities found among relatives with NF2 can be explained entirely by the recognized *NF2* mutation class-phenotype correlation. We calculated intrafamilial correlation coefficients (τ) for three clinical features (age at first symptom, age at onset of hearing loss, and number of intracranial meningiomas) for a large series of NF2 patients and within subgroups of patients with truncating mutations, splice-site mutations, missense mutations, or large deletions of the *NF2* gene. We demonstrate significant intrafamilial correlations for each of these phenotypic features within the entire group of NF2 patients and in one or more subgroups of patients with a particular class of constitutional *NF2* mutations. Our findings suggest that familial factors beyond *NF2* mutation class are important in the pathogenesis of these features in some patients with NF2.

MATERIALS AND METHODS

Statistical Analysis

Random effects model for censored data

In a random effects model, the total variance for a variable can be separated into two components: variance between families (σ_B^2) and variance within a family (σ_W^2). Let k be the number of families in the study, n_i be the number of affected members in the ith family, and Y_{ij} be the value of the jth patient of the ith family. The statistical model is

$$Y_{ij} = \mu + A_i + \varepsilon_{ij},\ i = 1, \ldots k;\ j = 1, \ldots n_i,$$

where A_is are independent normal random variables with mean 0 and variance σ_B^2; ε_{ij}s are also independent random variables with mean 0 and variance σ_W^2. A_is and ε_{ij}s are mutually independent. In the above model, μ represents the overall mean of all the individuals; A_i is common to all the members from the same family, representing

the deviation of the mean of this particular family from the overall mean μ. The variance of A_i, σ_B^2, reflects the between-family variation, and the variance of ε_{ij}, σ_W^2, reflects the within-family variation. The total variance σ^2 is the sum of σ_B^2 and σ_W^2. When the feature is relatively homogenous within families, σ_W^2 will be small in comparison to the total variance. Therefore, the strength of intrafamilial resemblance can be measured by the ratio of the between-family variance to the total variance: $\tau=\sigma_B^2/(\sigma_B^2+\sigma_W^2)$, i.e., the intrafamilial correlation.

A widely used procedure for estimating variance components is to equate sums of squares to their expected values; this approach is not applicable when the variable under consideration is subject to right censoring. Therefore, we used maximum likelihood estimation (MLE) to incorporate survival techniques into a random effects model. Each family in the study contributes one term to the likelihood function. For an individual who has developed the age-dependent feature, we calculate the instantaneous likelihood that the feature occurs at the observed onset age; for an individual who does not have the feature, we calculate the likelihood that the feature occurs beyond the patient's current age. For the ith family, let T_i be the subgroup of all the individuals with the feature and C_i the subgroup of all individuals without the feature. y_{ij} is the age at onset of the feature if it is present; otherwise, y_{ij} is the patient's age at last examination. The contribution of the family to the likelihood is

$$P_i = f_{T_i}(y_{ij}, j \in T_i)\,\Pr(Y_{ij'} > y_{ij'}, j' \in C_i | Y_{ij} = y_{ij}, j \in T_i),$$

where f_{T_i} is the joint density of $\{ Y_{ij}, j \in T_i\}$, and the second term on the right-hand side is the conditional probability of $\{Y_{ij'} > y_{ij'}, j' \in C_i\}$ given $\{Y_{ij} = y_{ij}, j \in T_i\}$. P_i is parametrized as a function of μ, σ^2 and τ [Jobson, 1996]. The log-likelihood $\Sigma\log(P_i)$ can be maximized numerically with a quasi-Newton method (e.g., Nash, 1990) to obtain the maximum likelihood estimates of μ, σ^2 and τ together with an estimated covariance matrix.

We applied this method to data for two continuous variables available on NF2 patients: age at first symptom and age at onset of hearing loss. For age at first symptom, censoring is present when a patient is asymptomatic at the time of examination or death; for age at onset of hearing loss, censoring occurs when a patient does not have hearing loss at the time of examination or death.

Random effects model for discrete data

A random effects model based on a normal distribution is not realistic for a count variable with a high frequency of zeros, such as number of meningiomas in a patient with NF2. We considered using a Poisson distribution to model these data, but the mean and variance are equal in the Poisson distribution. In contrast, the within-family variation is greater than the mean in the NF2 meningioma data. We used a negative-binomial gamma mixture model, based on the assumption that the expected count may differ between families as well as within a single family. The similarity within families is represented by a factor with a gamma distribution. For any given family, the count in each member follows a negative-binomial distribution [Lawless, 1987] conditional on the familial factor.

Suppose in the ith family, Y_{ij} is the count in the jth member. We assume that the family factor Λ_i is an unobserved random variable having a gamma distribution with mean 1 and variance $1/\theta$. Conditionally on Λ_i, Y_{ij}s are independent and have a negative-binomial distribution with mean $\mu_{ij} = \mu_0\Lambda_i$, where μ_0 is the overall mean count across all the families. Given μ_{ij} and another parameter λ, the probability function of the negative-binomial distribution is fully specified as

$$\Pr(Y_{ij} = y) = \frac{\Gamma(\lambda + y)\mu_{ij}^y\lambda^\lambda}{\Gamma(\lambda)y!(\mu_{ij} + \lambda)^{\lambda+y}}.$$

Since the family factor Λ_i is a random variable, the count per patient varies from family to family. A large variance of Λ_i implies that the families are very different in their means. The correlation between two particular family members, τ, depends on θ, λ, and μ_0:

$$\tau = \frac{\mu_0^2\lambda}{\mu_0\theta\lambda + \mu_0^2(1 + \theta + \lambda)}.$$

The mean μ_{ij} can also be allowed to depend on covariates through a log link function. Let x_{ij} be a vector of covariates and β the vector of coefficients, then $\mu_{ij} = \Lambda_i \exp(x_{ij}\beta)$. The correlation between two particular family members is no longer a constant, but instead depends on their x-values. If the covariate values of two family members are x_{ij} and $x_{ij'}$, the correlation between them is:

$$\tau = \frac{\mu_j\mu_{j'}\lambda}{\sqrt{[\mu_j\theta\lambda + \mu_j^2(1 + \theta + \lambda)][\mu_{j'}\theta\lambda + \mu_{j'}^2(1 + \theta + \lambda)]}},$$

where $\mu_k = \exp(x_{ik}\beta)$, $k = j$ or j'.

Note that in the gamma negative-binomial model, the variance cannot be partitioned into additive components. The variance of the familial factor is $1/\theta$ and the conditional variance of the individual factor depends on the dispersion parameter $1/\lambda$. They are not additive because there is additional variation from the Poisson sampling that depends on the mean.

We used this negative-binomial gamma mixture model to assess familiality of meningioma count data in NF2 patients. The maximum likelihood estimates of θ, λ, and μ_0, together with an estimated covariance matrix, were obtained numerically using a quasi-Newton method [Nash, 1990], and the standard error of τ was derived by the delta method [Agresti, 1990]. It would be appropriate to include covariates such as age, but this information was unavailable for many patients in our data set. Therefore, no covariates were included in the analysis presented below.

Genotype-phenotype correlations

The constitutional *NF2* mutation was known in a subset of the families, and this permitted us to assess whether the *NF2* allele-phenotype correlation accounts for all of the intrafamilial correlation observed. Patients belonging to families with each of the following four kinds of *NF2* constitutional mutations were analyzed separately: 1) truncating mutations (frameshift or nonsense), 2) splice-site or splice effect mutations, 3) missense mutations, and 4) large deletions.

TABLE I. Number of NF2 Families and Patients Included for Each of the Clinical Features Examined

Mutation type and clincal feature	Number of families	Number of patients
All mutation types		
Age at first symptom	150	373
Age of onset of hearing loss	114	261
Number of intracranial meningiomas	122	259
Truncating (nonsense or frameshift)		
Age at first symptom	37	58
Age of onset of hearing loss	25	39
Number of intracranial meningiomas	30	44
Splice-site		
Age at first symptom	32	101
Age at onset of hearing loss	23	60
Number of intracranial meningiomas	27	79
Missense		
Age at first symptom	12	50
Age at onset of hearing loss	9	38
Number of intracranial meningiomas	10	23
Large deletions		
Age at first symptom	13	42
Age at onset of hearing loss	11	34
Number of intracranial meningiomas	12	36

Intrafamilial correlation coefficients were calculated within subsets of families who shared similar constitutional *NF2* mutation types. To demonstrate the *NF2* genotype-phenotype correlations, we also compared the means of each pair of mutation subgroups simultaneously. The Bonferroni method [Seber, 1977] was used to control the type I error in these multiple comparisons. The z-score was calculated for the difference between each pair of means, but only those with P-value $< \alpha/k$ were considered to be statistically significant, where α was chosen as 0.05, and k is the total number of pairs tested (6 in this instance).

Patients

Three hundred and ninety patients from 153 families were ascertained from both published and unpublished sources (Supplemental information can be found at http://www.interscience.wiley.com/jpages/0741-0395/suppmat/index.html). All patients included met the Manchester clinical diagnostic criteria for NF2 [Evans et al., 1992b], had an identified constitutional *NF2* mutation, or both. Probands were excluded from the table and from all statistical analyses to avoid ascertainment bias. All other affected individuals were included if clinical information was available for at least 1 of the 3 manifestations studied: age at first symptom, age at onset of hearing loss, or number of intracranial meningiomas. These variables were examined because they were the most reliably reported features across the various data sources used for the study. Meningiomas were identified by cranial CT or MRI scan. Only intracranial meningiomas were considered in this study. The total numbers of families and patients used to examine each clinical feature are given in Table I.

Age at first symptom of NF2 and age at onset of hearing loss are both subject to right censoring. Censoring can occur either because the manifestation was not present at the time of last evaluation, or because the manifestation was not present when the subject died. Death accounts for a small proportion of censored cases in this data set.

RESULTS

Among the 390 NF2 patients included in this study, 300 (76.9%) had bilateral VSs, 31 (7.9%) had a unilateral VS, 26 (6.7%) had no VS, and in 33 cases (8.5%) the VS status was unknown.

Age at First Symptom

Three hundred and seventy-three patients from 150 families were included in the study of age at first symptom. Seventy-two (19%) patients were asymptomatic at time of last examination or death, and were therefore treated as right-censored cases in this analysis. Among the symptomatic patients, age at first symptom ranged from 1–62 years.

To assess the assumption of normality for age at first symptom, we examined normal probability plots for all subjects together and for subjects in each mutation subclass. These plots did not show extreme skewness, except in the subclass of patients with large deletion mutations, where the distribution was skewed to the right. The random effects model was also fit in this subgroup, using log-transformed age at first symptom. The estimate of τ was about the same, so only the results of the model using untransformed values of age are reported here.

Table II shows the means, standard deviations, and intrafamilial correlations calculated for affected members of all families included in this study, as well as for members of families with each of four types of constitutional *NF2* mutations: truncating mutations, splice-site mutations, missense mutations, and large deletions. The value of τ within each subgroup of mutations except large deletions was similar in magnitude to that seen when all families were analyzed together. For all *NF2* mutations considered together, the intrafamilial correlation coefficient for age at first symptom was 0.35, and the lower 95% confidence limit was 0.23. The 95%

TABLE II. Mean, Standard Deviation, and Intrafamilial Correlation of Age at First Symptom in 373 NF2 Patients From 150 Families[a]

Mutation type	Censoring rate	Mean	Standard deviation	Intrafamilial correlation (τ)
All mutation types	19%	24.9 (23.1, 26.8)	13.1 (12.0, 14.2)	0.35 (0.23, 0.47)
Truncating (nonsense or frameshift)	15%	18.7 (15.6, 21.9)	9.5 (7.6, 11.5)	0.41 (0.06, 0.68)
Splice-site	19%	25.1 (21.6, 28.5)	12.1 (10.0, 14.2)	0.29 (0.03, 0.51)
Missense	20%	29.3 (24.1, 34.6)	11.9 (8.9, 14.9)	0.32 (0, 0.61)
Large deletions	14%	24.5 (20.0, 29.0)	11.3 (8.7, 14.0)	0.10 (0, 0.34)

[a]Approximate 95% confidence intervals of point estimates are given in parentheses.

confidence intervals for τ were always wider in the subgroups, as expected with smaller sample sizes. Nevertheless, in two of the subgroups (truncating mutations and splice-site mutations), the lower limit of the 95% confidence interval of τ excluded 0.

We conducted pairwise tests to assess differences between mean ages at first symptom in the subgroups, and tested nominal statistical significance using the Bonferroni method. The mean age at first symptom in the subgroup with truncating mutations was significantly different from the mean age at first symptom in the splice-site and missense subgroups, whereas the differences between all other pairs were not statistically significant. Patients with truncating mutations had an earlier mean age at first symptom (18.7 years) and less variation (standard deviation, 9.5 years). The pattern of age at first symptom is shown more clearly in the Kaplan-Meier estimates of the proportion of asymptomatic patients at various ages for each mutation type (Fig. 1).

Age at Onset of Hearing Loss

Of 261 NF2 patients from 114 families for whom hearing status was known, 192 individuals (74%) had lost their hearing at the time of examination. The age at onset of hearing loss among these patients ranged from 3–62 years. Sixty-nine (26%) of the 261 patients did not have hearing loss at the time of last examination or death, and were treated as right-censored in the analysis.

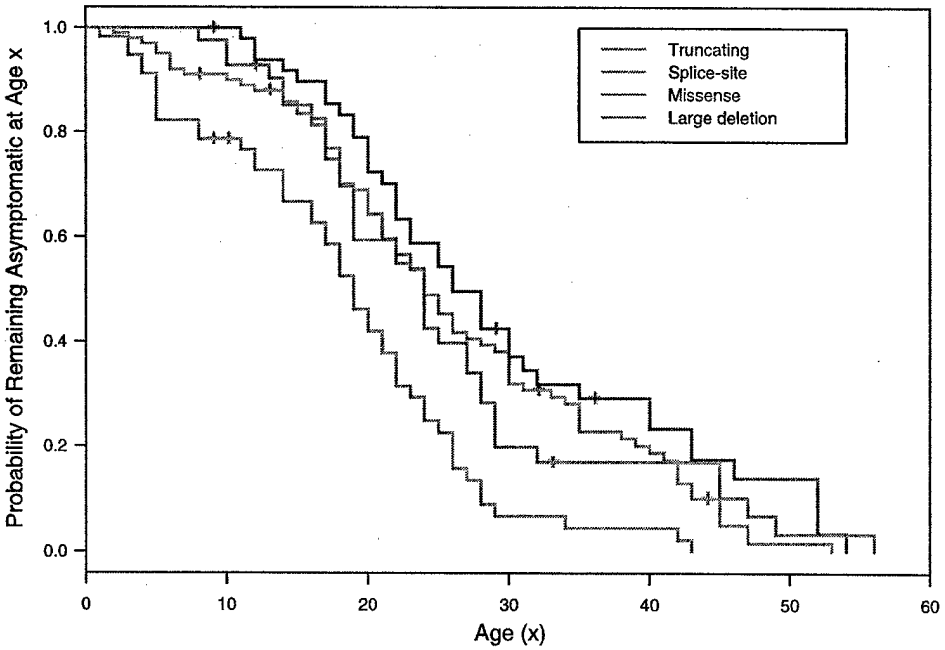

Fig. 1. Kaplan-Meier estimates of probability of remaining asymptomatic at a given age. [Color figure can be viewed in the online issue, which is available at www.interscience.wiley.com]

TABLE III. Mean, Standard Deviation, and Intrafamilial Correlation of Age at Onset of Hearing Loss for 261 NF2 Patients From 114 Families[a]

Mutation type	Censoring rate	Mean	Standard deviation	Intrafamilial correlation (τ)
All mutation types	26%	29.6 (27.2, 32.1)	13.3 (11.8, 14.9)	0.51 (0.35, 0.64)
Truncating (nonsense or frameshift)	23%	22.2 (19.3, 25.1)	7.4 (5.5, 9.4)	0.41 (0, 0.76)
Splice-site	40%	31.6 (27.4, 35.9)	11.7 (8.9, 14.5)	0.29 (0, 0.62)
Missense	24%	36.9 (27.4, 46.4)	14.9 (8.1, 21.7)	0.67 (0.18, 0.89)
Large deletions	26%	28.9 (22.2, 35.6)	13.0 (9.2, 16.8)	0.19 (0, 0.55)

[a]Approximate 95% confidence intervals of the point estimates are given in parentheses.

To assess the assumption of normality for age at onset of hearing loss, we examined normal probability plots for all patients together and for each mutation subclass. The distribution for all cases together was not skewed, but right skewness was observed for all subclasses except truncating mutations. A logarithmic transformation provided a better fit for the subgroups that had a skewed distribution, but the estimates of τ remained almost the same as without the transformation. For this reason, we only report results for the analysis without transformation of age.

The means, standard deviations, and intrafamilial correlations for age at onset of hearing loss are reported in Table III, and the Kaplan-Meier estimates are plotted in Figure 2. A strong intrafamilial correlation was seen for age at hearing loss when all patients were considered together ($\tau = 0.51$; 95% CI, 0.35–0.64). Within the subgroups defined by constitutional *NF2* mutation type, those with missense mutations had a somewhat higher intrafamilial correlation than the other subgroups, and it was only in this subgroup that the 95% confidence interval of the correlation coefficient excluded zero.

Pairwise tests showed that the mean age at onset of hearing loss for patients with truncating mutations was significantly lower than that of patients with splice-site or missense mutations. The means of the other subgroups did not differ significantly from each other.

Number of Intracranial Meningiomas

Two hundred and fifty-nine NF2 patients from 122 families were used in the study of intracranial meningiomas. The distribution of number of meningiomas is summarized in Table IV by mutation type, and estimates of the model parameters and intrafamilial correlations are reported in Table V.

The mean number of intracranial meningiomas per patient was 1.01 (95% CI, 0.70–1.32). A significant intrafamilial correlation for number of meningiomas was observed for all NF2 patients combined ($\tau = 0.29$; 95% CI, 0.15–0.43).

NF2 patients with truncating mutations had the highest mean number of meningiomas, i.e., 1.92 (95% CI, 1.02–2.82), but this was associated with relatively high within-family variance. The magnitude of the intrafamilial correlation coefficient was small in this subgroup.

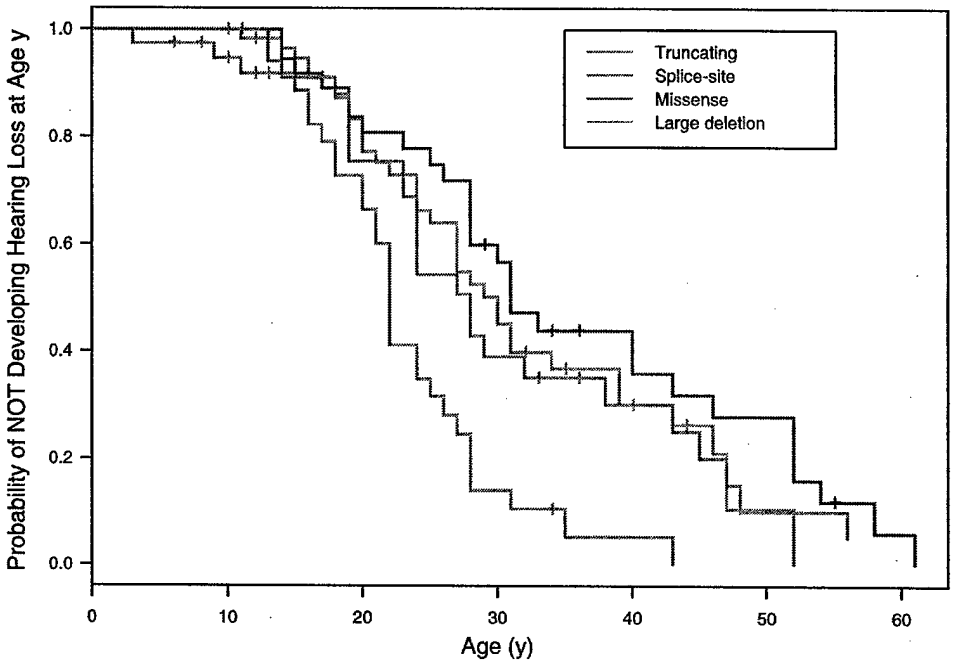

Fig. 2. Kaplan-Meier estimates of probability of *not* developing hearing loss by a given age. [Color figure can be viewed in the online issue, which is available at www.interscience.wiley.com]

TABLE IV. Distribution of Number of Meningiomas in 259 NF2 Patients From 122 Families

	Frequency of number of meningiomas										
Mutation type	0	1	2	3	4	5	6	7	9	10	19
All mutation types	164	50	19	8	6	5	2	1	2	1	1
	63.3%	19.3%	7.3%	3.1%	2.3%	1.9%	0.8%	0.4%	0.8%	0.4%	0.4%
Truncating[a]	18	9	4	4	4	1	1	1	1	1	0
	40.9%	20.5%	9.1%	9.1%	9.1%	2.3%	2.3%	2.3%	2.3%	2.3%	
Splice-site	50	19	6	1	1	1	0	0	1	0	0
	63.3%	24.1%	7.6%	1.3%	1.3%	1.3%			1.3%		
Missense	16	6	0	1	0	0	0	0	0	0	0
	70.0%	26.1%		4.3%							
Large deletions	25	4	6	0	0	0	0	0	0	0	1
	69.4%	11.1%	16.7%								2.8%

[a]Nonsense and frameshift.

The mean number of intracranial meningiomas among NF2 patients with splice-site mutations was 0.72 (95% CI, 0.29–1.15). In contrast to the situation with truncating mutations, the within-family variation was small, and the between-family variation was large for NF2 patients with splice-site mutations. The point estimate of

TABLE V. Parameter Estimates and Intrafamilial Correlation Coefficients for Number of Meningiomas[a]

Mutation type	$1/\theta$[b]	$1/\lambda$[c]	Mean (μ_0)	Intrafamilial correlation (τ)
All mutation types	1.24 (0.53, 1.95)	0.93 (0.32, 1.54)	1.01 (0.70, 1.32)	0.29 (0.15, 0.43)
Truncating (nonsense and frameshift)	0.29 (0.00, 0.58)	1.19 (0.17, 2.21)	1.92 (1.02, 2.82)	0.12 (0.00, 0.25)
Splice-site	1.43 (0.14, 2.72)	0.34 (0, 0.89)	0.72 (0.29, 1.15)	0.39 (0.13, 0.66)
Missense	0.28 (0, 0.69)	0.47 (0, 2.45)	0.42 (0.09, 0.75)	0.08 (0, 0.23)
Large deletions	1.25 (0, 3.94)	2.37 (0, 5.96)	0.96 (0, 2.02)	0.16 (0, 0.45)

[a]Approximate 95% confidence intervals for the point estimates are given in parentheses.
[b]$1/\theta$, variance between families.
[c]$1/\lambda$, negative binomial dispersion parameter.

the intrafamilial correlation coefficient was higher in this subgroup than in any of the other mutation subgroups, and the 95% confidence interval excluded zero.

The mean number of intracranial meningiomas among NF2 patients with missense mutations was 0.42 (95% CI, 0.09–0.75), the lowest among the four mutation subgroups because 16 of the 23 patients in this subgroup had no meningiomas. The variation both between families and within a family was similar in magnitude to the mean, and the intrafamilial correlation coefficient was small.

The mean number of intracrainal meningiomas among NF2 patients with large deletions was 0.96 (95% CI, 0–2.02). The within- and between-family variances were both large, mainly because of one patient (patient 201 in family 1648) who developed 19 meningiomas by age 18 [Bruder et al., 2001]. More than 2/3 of individuals with this mutation type had no meningiomas, and all of the others had either one or two meningiomas, including patient 201's two affected relatives. When this family was excluded from the analysis, the mean number of meningiomas among the remaining patients with large deletions was 0.39, both within- and between-family variation were much smaller, and the intrafamilial correlation was even lower (0.06).

DISCUSSION

Statistical Methods

The statistical methods used here should be of use in intrafamilial correlation studies of other genetic diseases. Random effects models are commonly used to analyze intraclass and intrafamilial correlations in continuous traits, and we extended this method to include right-censored data. The maximum likelihood method we describe can also accommodate two other types of censoring frequently associated with age-related traits: left censoring (e.g., the event occurred before time of examination) and interval censoring (e.g., the event occurred between two examinations). A mixed-effects model can be used to adjust the correlations calculated by this method for covariates [Searle et al., 1992].

The negative-binomial gamma mixture model we developed for count traits is also likely to be useful for other genetic diseases. A Poisson mixture model is sometimes used with count data [Foulley et al., 1987], but the Poisson distribution

is constrained because the variance is equal to the mean. A mixture model based on the negative-binomial distribution allows more flexibility, and is therefore more appropriate for count variables with overdispersion relative to the Poisson distribution [Tempelman and Gianola, 1996].

Intrafamilial Correlations in NF2

Phenotypic variability is observed in individuals with NF2, both within and between families. We employed a random effects model incorporating survival techniques to estimate intrafamilial correlations in two continuous variables that are right-censored: age at first symptom, and age at onset of hearing loss. We used a negative-binomial gamma mixture model to estimate intrafamilial correlations for a discrete variable, i.e., number of intracranial meningiomas. Our results demonstrate that relatives with NF2 are more similar to each other than to unrelated affected individuals with respect to each of these clinical features. These observations are consistent with anecdotal clinical experience [Evans et al., 2000]. Parry et al. [1996] adjusted for intrafamilial correlation in their genotype-phenotype analysis, but the intrafamilial correlation of NF2 phenotypes has not previously been tested statistically.

Intrafamilial correlations, such as those observed in this study, may have a variety of causes. Effects of the mutant allele, of other shared genes, of shared environmental factors, or of a combination of genetic and environmental factors may produce such correlations. Distinguishing between these possibilities requires analysis of phenotypic correlations among affected family members of various classes, such as monozygotic twins, sibs, parent-child pairs, and more distant relatives.

Since all affected individuals in the same family can be presumed to carry the same constitutional alteration of the *NF2* locus, the nature of the *NF2* mutation itself might account for the familiality we observed. This possibility is supported by the associations observed in cross-sectional studies between allele class and disease severity in NF2 [Kluwe et al., 1996, 1998; Parry et al., 1996; Ruttledge et al., 1996; Evans et al., 1998a]. Our study includes data on patients who are also included in these earlier studies, and as expected, we found similar effects.

We also observed intrafamilial correlations of similar or greater magnitude for each of the features studied in subgroups of patients who all had the same type of constitutional *NF2* mutation. While it is possible that specific allelic differences within each mutation class account for these intrafamilial correlations, our findings could also reflect the effects of modifying genes. Recent reports of putative modifying loci for *NF2* are consistent with this interpretation [Bruder et al., 1999; Goutebroze et al., 2000]. Several genes other than *NF2* have been implicated in meningioma development, including loci on chromosomes 1, 3, 6, 7, and 22 [Sanson et al., 1993; Sulman et al., 1998; Comtesse et al., 1999], but the contribution of these loci to the interfamilial variability observed in NF2 pedigrees is unknown.

Our studies are subject to several limitations. We used data from a variety of sources, and differences in referral patterns, diagnostic acumen, and criteria for diagnosis probably exist among the centers. Age at first symptom and age at onset of hearing loss were taken from published data (including updated data provided by the

authors) and unpublished data. The definitions of these ages may vary from source to source. In many cases, age at first symptom and age at onset of hearing loss were assigned retrospectively and thus may be subject to recall errors. All these factors could affect the accuracy of our results.

Although this study was based on the largest collection of clinical data available on NF2 patients, consideration of separate mutation types was limited by small sample sizes. Consequently, our estimates of τ for the subgroups are associated with wide confidence intervals. Some of the correlations that did not appear to be significant in this study might be important, but require larger samples for demonstration. A likelihood ratio test could be performed to assess whether intrafamilial correlations vary significantly with mutation type. This would be useful in a study that included more patients, but a likelihood ratio test would not show significant differences because of the small sample size of each subgroup in the present study.

The penetrance of NF2 and the prevalence of individual tumor types generally increase with age [Mautner et al., 1993; MacCollin and Mautner, 1998]. Time from onset of symptoms may also influence the number of meningiomas in an NF2 patient, so it would be appropriate to model this time variable as an additional source of variation that is independent of the familial factor. Unfortunately, we did not know the age at which meningioma status was determined for many of the patients in this study, so we could not include age as a covariate in our analysis.

Statistical techniques provide powerful means of studying genetic and nongenetic aspects of diseases such as NF2. Methods are needed to estimate intrafamilial correlations for other kinds of non-normally distributed traits, such as ordered categorical data (e.g., severity of disease) and continuous data that are not normally distributed (e.g., disease progression rate). Each of these data types requires a different statistical model to capture specific distributional features. Models that allow a wide range of dependent structures, so that various genetic and environmental components of phenotypic variation can be assessed at the same time, are especially desirable.

REFERENCES

Agresti A. 1990. Categorical data analysis. New York: John Wiley and Sons.

Baser ME, Mautner VF, Ragge NK, Nechiporuk A, Riccardi VM, Klein J, Sainz J, Pulst SM. 1996a. Presymptomatic diagnosis of neurofibromatosis 2 using linked genetic markers, neuroimaging, and ocular examinations. Neurology 47:1269–77.

Baser ME, Ragge NK, Riccardi VM, Janus T, Gantz B, Pulst SM. 1996b. Phenotypic variability in monozygotic twins with neurofibromatosis 2. Am J Med Genet 64:563–7.

Bijlsma EK, Merel P, Fleury P, van Asperen CJ, Westerveld A, Delattre O, Thomas G, Hulsebos TJ. 1995. Family with neurofibromatosis type 2 and autosomal dominant hearing loss: identification of carriers of the mutated NF2 gene. Hum Genet 96:1–5.

Bruder CE, Ichimura K, Blennow E, Ikeuchi T, Yamaguchi T, Yuasa Y, Collins VP, Dumanski JP. 1999. Severe phenotype of neurofibromatosis type 2 in a patient with a 7.4-MB constitutional deletion on chromosome 22: possible localization of a neurofibromatosis type 2 modifier gene? Genes Chromosomes Cancer 25:184–90.

Bruder CE, Hirvela C, Tapia-Paez I, Fransson I, Segraves R, Hamilton G, Zhang XX, Evans DG, Wallace AJ, Baser ME, Zucman-Rossi J, Hergersberg M, Boltshauser E, Papi L, Rouleau GA, Poptodorov G, Jordanova A, Rask-Andersen H, Kluwe L, Mautner V, Sainio U, Hung G, Mathiesen T, Moller

C, Pulst SM, Harder H, Heiberg A, Honda M, Niimura M, Sahlen S, Blennow E, Albertson DG, Pinkel D, Dumanski JP. 2001. High resolution deletion analysis of constitutional DNA from neurofibromatosis type 2 (NF2) patients using microarray-CGH. Hum Mol Genet 10:271–82.

Comtesse N, Heckel D, Racz A, Brass N, Glass B, Meese E. 1999. Five novel immunogenic antigens in meningioma: cloning, expression analysis, and chromosomal mapping. Clin Cancer Res 5:3560–8.

De Klein A, Riegman PH, Bijlsma EK, Heldoorn A, Muijtjens M, den Bakker MA, Avezaat CJ, Zwarthoff EC. 1998. A G→A transition creates a branch point sequence and activation of a cryptic exon, resulting in the hereditary disorder neurofibromatosis 2. Hum Mol Genet 7:393–398.

Dipple KM, McCabe RB. 2000. Phenotypes of patients with "simple" mendelian disorders are complex traits: thresholds, modifiers, and systems dynamics. Am J Hum Genet 66:1729–1735.

Evans DG, Huson SM, Donnai D, Neary W, Blair V, Teare D, Newton V, Strachan T, Ramsden R, Harris R. 1992a. A genetic study of type 2 neurofibromatosis in the United Kingdom. I. Prevalence, mutation rate, fitness, and confirmation of maternal transmission effect on severity. J Med Genet 29:841–6.

Evans DG, Huson SM, Donnai D, Neary W, Blair V, Newton V, Strachan T, Harris R. 1992b. A genetic study of type 2 neurofibromatosis in the United Kingdom. II. Guidelines for genetic counselling. J Med Genet 29:847–52.

Evans DG, Huson SM, Donnai D, Neary W, Blair V, Newton V, Harris R. 1992c. A clinical study of type 2 neurofibromatosis. Q J Med 84:603–18

Evans DG, Trueman L, Wallace A, Collins S, Strachan T. 1998a. Genotype/phenotype correlations in type 2 neurofibromatosis (NF2): evidence for more severe disease associated with truncating mutations. J Med Genet 35:450–5.

Evans DG, Wallace AJ, Wu CL, Trueman L, Ramsden RT, Strachan T. 1998b. Somatic mosaicism: a common cause of classic disease in tumor-prone syndromes? Lessons from type 2 neurofibromatosis. Am J Hum Genet 63:727–36.

Evans DG, Sainio M, Baser ME. 2000. Neurofibromatosis type 2. J Med Genet 37:897–904.

Foulley JL, Gianola D, Im S. 1987. Genetic evaluation of traits distributed as Poisson-binomial with reference to reproductive characters. Theor Appl Genet 73:870–7.

Goutebroze L, Brault E, Muchardt C, Camonis J, Thomas G. 2000. Cloning and characterization of SCHIP-1, a novel protein interacting specifically with spliced isoforms and naturally occurring mutant NF2 proteins. Mol Cell Biol 20:1699–712.

Hung G, Faudoa R, Baser ME, Xue Z, Kluwe L, Slattery W, Brackman D, Lim D. 2000. Neurofibromatosis 2 phenotypes and germ-line NF2 mutations determined by an RNA mismatch method and loss of heterozygosity analysis in NF2 schwannomas. Cancer Genet Cytogenet 118:167–8.

Jacoby LB, MacCollin M, Parry DM, Kluwe L, Lynch J, Jones D. 1999. Allelic expression of the NF2 gene in neurofibromtosis 2 and schwannomatosis. Neurogenetics 2:101–8.

Jobson JD. 1996. Applied multivariate data analysis. New York: Springer-Verlag.

Kluwe L, Bayer S, Baser ME, Hazim W, Haase W, Funsterer C, Mautner VF. 1996. Identification of *NF2* germ-line mutations and comparison with neurofibromatosis 2 phenotypes. Hum Genet 98:534–8.

Kluwe L, MacCollin M, Tatagiba M, Thomas S, Hazim W, Haase W, Mautner VF. 1998. Phenotypic variability associated with 14 splice-site mutations in the *NF2* gene. Am J Med Genet 77:228–33.

Lawless JF. 1987. Negative binomial and mixed Poisson regression. Can J Stat 15:209–25.

Lopez-Correa C, Zucman-Rossi J, Brems H, Thomas G, Legius E. 2000. *NF2* gene deletion in a family with a mild phenotype. J Med Genet 37:75–7.

MacCollin M. 1999. Neurofibromatosis, phenotype, natural history, and pathogenesis, 3rd ed. Baltimore and London: Johns Hopkins University Press.

MacCollin M, Mautner VF. 1998. The diagnosis and management of neurofibromatosis 2 in childhood. Semin Pediatr Neurol 5:243–52.

MacCollin M, Mohney T, Trofatter J, Wertelecki W, Ramesh V, Gusella J. 1993. DNA diagnosis of neurofibromatosis 2. Altered coding sequence of the merlin tumor suppressor in an extended pedigree. JAMA 270:2316–20.

Mautner VF, Tatagiba M, Guthoff R, Samii M, Pulst SM. 1993. Neurofibromatosis 2 in the pediatric age group. Neurosurgery 33:92–6.

Mautner V, Baser M, Kluwe L. 1996. Phenotypic variability in two families with novel splice-site and frameshift *NF2* mutations. Hum Genet 98:203–6.

Merel P, Hoang-Xuan K, Sanson M, Bijlsma E, Rouleau G, Laurent-Puig P, Pulst S, Baser M, Lenoir G, Sterkers JM, Philippon J, Resche F, Mautner VF, Fischer G, Hulsebos T, Aurias A, Delattre O, Thomas G. 1995. Screening for germ-line mutations in the *NF2* gene. Genes Chromosomes Cancer 12:117–27.

Nash JC. 1990. Compact numerical methods for computers: linear algebra and function minimisation, 2nd ed. New York: Hilger.

Parry DM, Elridge R, Kaiser-Kupfer MI, Bouzas EA, Pikus A, Patronas N. 1994. Neurofibromatosis 2 (NF2): clinical characteristics of 63 affected individuals and clinical evidence for heterogeneity. Am J Med Genet 52:450–46.

Parry DM, MacCollin MM, Kaiser-Kupfer MI, Pulaski K, Nicholson HS, Bolesta M, Eldridge R, Gusella JF. 1996. Germ-line mutations in the neurofibromatosis 2 gene: correlations with disease severity and retinal abnormalities. Am J Hum Genet 59:529–39.

Rouleau GA, Merel P, Lutchman M, Sanson M, Zucman J, Marineau C, Hoang-Xuan K, Demczuk S, Desmaze C, Plougastel B, Pulst SM, Lenoir G, Blusma E, Fashold R, Dumanski J, de Jong P, Parry D, Eldrige R, Aurias A, Delattre O, Thomas G. 1993. Alteration in a new gene encoding a putative membrane-organizing protein causes neurofibromatosis type 2. Nature 363:515–21.

Ruttledge MH, Andermann AA, Phelan CM, Claudio JO, Han FY, Chretien N, Rangaratnam S, MacCollin M, Short P, Parry D, Vichels V, Riccardi VM, Weksburg R, Kitamura K, Bradburn JM, Hall BD, Propping P, Rouleau GA. 1996. Type of mutation in the neurofibromatosis type 2 gene (NF2) frequently determines severity of disease. Am J Hum Genet 59:331–42.

Sainio M, Strachan T, Blomstedt G, Salonen O, Setala K, Palotie A, Palo J, Pyyko I, Peltonen L, Jaaskelainen J. 1995. Presymptomatic DNA and MRI diagnosis of neurofibromatosis 2 with mild clinical course in an extended pedigree. Neurology 45:1314–22.

Sainio M, Jaaskelainen J, Pihlaja H, Carpen O. 2000. Mild familial neurofibromatosis 2 associates with expression of merlin with altered COOH-terminus. Neurology 54:1132–8.

Sanson M, Marineau C, Desmaze C, Lutchman M, Ruttledge M, Baron C, Narod S, Delattre O, Lenoir G, Thomas G, Aurias A, Rouleau GA. 1993. Germline deletion in a neurofibromatosis type 2 kindred inactivates the NF2 gene and a candidate meningioma locus. Hum Mol Genet 8:1215–20.

Scoles DR, Baser ME, Pulst SM. 1996. A missense mutation in the neurofibromatosis 2 gene occurs in patients with mild and severe phenotypes. Neurology 47:544–6.

Scriver CR, Waters PJ. 1999. Monogenic traits are not simple: lessons from phenylketonuria. Trends Genet 15:267–72.

Searle SR, Casella, G, McCulloch CE. 1992. Variance components. New York: John Wiley and Sons.

Seber G. 1977. Linear regression analysis. New York: John Wiley and Sons.

Sulman EP, Dumanski JP, White PS, Zhao H, Maris JM, Mathiesen T, Bruder C, Cnaan A, Brodeur GM. 1998. Identification of a consistent region of allelic loss on 1p32 in meningiomas: correlation with increased morbidity. Cancer Res 58:3226–30.

Tempelman RJ, Gianola D. 1996. A mixed effects model for overdispersed count data in animal breeding. Biometrics 52:265–79.

Trofatter JA, MacCollin MM, Rutter JL, Murrell JR, Duyao MP, Parry DM, Eldridge R, Kley N, Menon AG, Pulaski K, Haase VH, Ambrose CM, Munroe D, Bove C, Haines JL, Martuza RL, MacDonald ME, Seizinger BR, Short MP, Buckler AJ, Gusella JF. 1993. A novel Moesin-, ezrin-, radixin-like gene is a candidate for the neurofibromatosis 2 tumor suppressor. Cell 72:791–800 [published erratum appears in Cell 1993;75:826].

Wertelecki W, Rouleau GA, Superneau DW, Forehand LW, Williams JP, Haines JL, Gusella JF. 1988. Neurofibromatosis 2: clinical and DNA linkage studies of a large kindred. N Engl J Med 319: 278–83.

Zucman-Rossi J, Legoix P, Der Sarkissian H, Cheret G, Sor F, Bernardi A, Cazes A, Giraud S, Ollagnon E, Lenoir G, Thomas G. 1998. NF2 gene in neurofibromatosis type 2 patients. Hum Mol Genet 7:2095–101.